# Non-targeted analysis of new psychoactive substances using mass spectrometric techniques

by

Daniel J. Pasin, MRACI

A thesis submitted for the

Degree of Doctor of Philosophy (Science)

University of Technology Sydney

2018

# Certificate of authorship and originality

I certify that the work in this thesis has not previously been submitted for a degree nor has it been submitted as part of the requirements for a degree except as fully acknowledged within the text.

I also certify that the thesis has been written by me. Any help that I have received in my research work and the preparation of the thesis itself has been acknowledged. In addition, I certify that all the information sources and literature used are indicated in the thesis. This research is supported by an Australian Government Research Training Program Scholarship.

Production Note:
Signature removed prior to publication.

Daniel J. Pasin, MRACI
26/02/2018

# Acknowledgements

Firstly, I would like to extend my deepest thanks to my primary supervisor, Associate Professor Shanlin Fu. You have been my primary supervisor for both my honours and PhD degrees and over these last 5 years, you have been nothing but supportive, patient and encouraging. I could always rely on you to provide timely feedback and you were always happy to endorse me for post-PhD opportunities. It has been a great pleasure to complete my PhD research under your supervision.

I would also like to thank my co-supervisors, Dr. Adam Cawley and Dr. Sergei Bidny. Without your external collaboration, the success of this project could not be possible. Furthermore, I wish to acknowledge the staff at the Australian Racing Forensic Laboratory (ARFL) and Forensic Toxicology Laboratory at NSW FASS for your assistance in this project. Furthermore, I would like to thank them for the financial support throughout this project including the purchase of reference materials and providing an external scholarship top-up.

Thank you to all the UTS academic and professional staff for your assistance throughout my project even though I was not in the laboratory much - I know Ron Shimmon will miss me dearly. I would also like to thank the Centre of Forensic Science and Professor Claude Roux for allowing me so many opportunities to present my research at domestic and international conferences. This has subsequently provided me invaluable contacts that will be no doubt be beneficial in the future.

To the UTS friends that I have made over the last couple of years, thank you for making my time during my PhD and living in Sydney enjoyable - I always know that I have somewhere to stay if I am in Europe. I would also like to thank Morgan “Mo” Philp for being a great colleague putting up with me at conferences and my general nonsense.

Lastly, I want to express my deepest gratitude to my family for supporting me throughout my PhD journey both emotionally and financially. You have always encouraged me to do my best and it has allowed me to achieve something that I never thought possible and love you all dearly.

# Table of contents

# List of figures

# List of tables

# List of abbreviations

| | |
|---|---|
| .csv | Comma-separated value file |
| $[M+H]^+$ | Protonated precursor ion |
| $[M-H]^-$ | Deprotonated precursor ion |
| ADBICA | *N*-(1-amino-3,3-dimethyl-1-oxo-2-butanyl)-1-pentyl-1*H*-indole-3-carboxamide |
| 25B-NBOMe/25B | 2-(4-bromo-2,5-dimethoxyphenyl)-*N*-[(2 methoxyphenyl)methyl]ethanamine |
| 25C-NBOMe/25C | 2-(4-chloro-2,5-dimethoxyphenyl)-*N*-[(2-methoxyphenyl)methyl]ethanamine |
| 25D-NBOMe/25D | 2-(4-methyl-2,5-dimethoxyphenyl)-*N*-[(2-methoxyphenyl)methyl]ethanamine |
| 25E-NBOMe/25E | 2-(4-ethyl-2,5-dimethoxyphenyl)-*N*-[(2-methoxyphenyl)methyl]ethanamine |
| 25G-NBOMe | 2-(3,4-dimethyl-2,5-dimethoxyphenyl)-*N*-[(2-methoxyphenyl)methyl]ethanamine |
| 25H-NBOMe/25H | 2-(2,5-dimethoxyphenyl)-*N*-[(2-methoxyphenyl)methyl]ethanamine |
| 25I-NBF | ***N***-(2-fluorobenzyl)-2-(4-iodo-2,5-dimethoxyphenyl)ethanamine |
| 25I-NBMD | *N*-(2,3-methylenedioxybenzyl)-2-(4-iodo-2,5-dimethoxyphenyl)ethanamine |
| 25I-NBOMe/25I | 2-(4-iodo-2,5-dimethoxyphenyl)-*N*-[(2-methoxyphenyl)methyl]ethanamine |
| 25N-NBOMe/25N | 2-(4-nitro-2,5-dimethoxyphenyl)-*N*-[(2-methoxyphenyl)methyl]ethanamine |
| 25P-NBOMe | 2-(4-propyl-2,5-dimethoxyphenyl)-*N*-[(2-methoxyphenyl)methyl]ethanamine |
| 25T2-NBOMe/25T2 | 2-(4-ethylthio-2,5-dimethoxyphenyl)-*N*-[(2-methoxyphenyl)methyl]ethanamine |
| 25T4-NBOMe | 2-(4-isoproprylthio-2,5-dimethoxyphenyl)-*N*-[(2-methoxyphenyl)methyl]ethanamine |
| 25T7-NBOMe | 2-(4-propylthio-2,5-dimethoxyphenyl)-*N*-[(2-methoxyphenyl)methyl]ethanamine |
| 25T-NBOMe | 2-(4-methylthio-2,5-dimethoxyphenyl)-*N*-[(2-methoxyphenyl)methyl]ethanamine |
| 25X-NBOMe | 2-(2,5-dimethoxyphenyl)-*N*-(2-methoxybenzyl) derivatives |
| 2C-B | 4-bromo-2,5-dimethoxyphenethylamine |
| 2C-B-Fly | 2-(4-bromo-2,3,6,7-tetrahydrofuro[2,3-f][1]benzofuran-8-yl)ethanamine |
| 2C-C | 4-chloro-2,5-dimethoxyphenethylamine |
| 2C-D | 2,5-dimethoxy-4-methylphenethylamine |
| 2C-E | 4-ethyl-2,5-dimethoxyphenethylamine |

| | |
|---|---|
| 2C-G | 2,5-dimethoxy-3,4-dimethylphenethylamine |
| 2C-H | 2,5-dimethoxyphenethylamine |
| 2C-I | 4-iodo-2,5-dimethoxyphenethylamine |
| 2C-P | 2,5-dimethoxy-4-propylphenethylamine |
| 2C-T | 2,5-dimethoxy-4-methylthiophenethylamine |
| 2C-T-2 | 2,5-dimethoxy-4-ethylthiophenethylamine |
| 2C-T-4 | 2,5-dimethoxy-4-isopropylthiophenethylamine |
| 2C-T-7 | 2,5-dimethoxy-4-propylthiophenethylamine |
| 2C-X | 2,5-dimethoxyphenethylamines derivatives |
| 3,4-DMMC | 3,4-dimethylmethcathinone |
| 4-EEC | 4-ethylethcathinone |
| 4-EMC | 4-ethylmethcathinone |
| 4-MEC | 4-methylethcathinone |
| 4-MMC | 4-methylmethcathinone |
| 5F-AB-PINACA | *N*-(1-amino-3-methyl-1-oxo-2-butanyl)-1-(5-fluoropentyl)-1*H*-indazole-3-carboxamide |
| 5F-ADBICA | *N*-(1-amino-3,3-dimethyl-1-oxo-2-butanyl)-1-(5-fluoropentyl)-1*H*-indole-3-carboxamide |
| 5F-APICA | *N*-(1-adamantanyl)-1-(5-fluoropentyl)-1*H*-indole-3-carboxamide |
| 5F-CUMYL-PINACA | 1-(5-fluoropentyl)-*N*-(2-phenyl-2-propanyl)-1*H*-indazole-3-carboxamide |
| 5F-MMB-PICA | Methyl *N*-{[1-(5-fluoropentyl)-1*H*-3-indolyl]carbonyl}valinate |
| 5F-MMB-PINACA | Methyl *N*-{[1-(5-fluoropentyl)-1*H*-3-indazolyl]carbonyl}valinate |
| 5F-PB-22 | 8-quinolinyl 1-(5-fluoropentyl)-1*H*-indole-3-carboxylate |
| 5-HT | 5-hydroxytryptamine |
| AB-CHMINACA | *N*-(1-amino-3-methyl-1-oxo-2-butanyl)-1-(cyclohexylmethyl)-1*H*-indazole-3-carboxamide |
| AB-FUBINACA | *N*-(1-amino-3-methyl-1-oxo-2-butanyl)-1-(4-fluorobenzyl)-1*H*-indazole-3-carboxamide |
| AB-PINACA | *N*-(1-amino-3-methyl-1-oxo-2-butanyl)-1-pentyl-1*H*-indazole-3-carboxamide |
| ADB-CHMINACA | *N*-(1-amino-3,3-dimethyl-1-oxo-2-butanyl)-1-(cyclohexylmethyl)-1*H*-indazole-3-carboxamide |
| ADB-FUBINACA | *N*-(1-amino-3,3-dimethyl-1-oxo-2-butanyl)-1-(4-fluorobenzyl)-1*H*-indazole-3-carboxamide |
| AJS | Agilent Jet Stream |
| AM-1241 | (2-iodo-5-nitrophenyl){1-[(1-methyl-2-piperidinyl)methyl]-1*H*-3-indolyl}methanone |
| AM-1248 | 1-adamantanyl{1-[(1-methyl-2-piperidinyl)methyl]-1*H*-3-indolyl}methanone |

| | |
|---|---|
| AM-2201 | [1-(5-fluoropentyl)-1*H*-3-indolyl](1-naphthyl)methanone |
| AM-2233 | (2-iodophenyl){1-[(1-methyl-2-piperidinyl)methyl]-1*H*-3-indolyl}methanone |
| AM-694 | [1-(5-fluoropentyl)-1*H*-3-indolyl](2-iodophenyl)methanone |
| ANU | Australian National University |
| AORC | Association of official racing chemists |
| APCI | Atmospheric pressure chemical ionisation |
| APICA | *N*-(1-adamantanyl)-1-pentyl-1*H*-indole-3-carboxamide |
| AR | Analytical reagent |
| ARFL | Australian Racing Forensic Laboratory |
| BB-22 | 8-quinolinyl 1-(cyclohexylmethyl)-1*H*-indole-3-carboxylate |
| bbCID | Broadband collision-induced dissociation |
| Bromo-DragonFly | 1-(8-bromobenzo[1,2-*b*; 4,5-*b*']difuran-4-yl)-2-aminopropane |
| BZP | Benzylpiperazine |
| CA | California |
| CB | Cannabinoid receptor |
| CBD | Cannabidiol |
| cc | Cubic centimetres |
| CDC | Centre for Disease Control |
| CE | Capillary electrophoresis (separation technique) |
| CE | Collision energy (mass spectrometry) |
| CID | Collision-induced dissociation |
| cm | Centimetre |
| CMF | Charge-migration fragmentation |
| CO | Carbon monoxide |
| CRF | Charge-retention |
| CRM | Certified reference material |
| Da | Dalton |
| DART | Direct analysis in real time |
| DBE | Double bond equivalents |
| DDA | Data-dependent acquisition |
| DEA | Drug Enforcement Administration |
| DESI | Desorption electrospray ionisation |
| DIA | Data-independent acquisition |
| DOB | 4-bromo-2,5-dimethoxyamphetamine |
| DOET | 4-ethyl-2,5-dimethoxyamphetamine |
| DOH/2,5-DMA | 2,5-dimethoxyamphetamine |
| DOI | 4-iodo-2,5-dimethoxyamphetamine |
| DOM | 2,5-dimethoxy-4-methylamphetamine |

| | |
|---|---|
| DOT | 2,5-dimethoxy-4-methylthioamphetamine |
| DOX | 2,5-dimethoxyamphetamines derivatives |
| ECC | Extracted compound chromatogram |
| EE | Even electron |
| EI | Electron ionisation |
| EIC | Extracted ion chromatogram |
| EMCDDA | European Monitoring Centre for Drugs and Drug Addiction |
| ESI+ | Positive electrospray ionisation |
| EU | European Union |
| eV | Electron volt |
| EWS | Early Warning System |
| FbF | Find by Formula |
| FIA | Flow injection analysis |
| FUB-144 | [1-(4-fluorobenzyl)-1*H*-3-indolyl](2,2,3,3-tetramethylcyclopropyl)methanone |
| FUB-NPB-22 | 8-quinolinyl 1-(4-fluorobenzyl)-1*H*-indazole-3-carboxylate |
| FWHM | Full width at half maximum |
| GC-MS | Gas chromatography – mass spectrometry |
| GHz | Gigahertz |
| GUI | Graphical user interface |
| $H_2O$ | Water |
| HCD | Higher energy collision dissociation |
| HESI | Heated electrospray ionisation |
| HPLC | High-performance liquid chromatography |
| HRAM | High-resolution accurate mass |
| HRMS | High-resolution mass spectrometry |
| Hz | Hertz |
| IDA | Information-dependent acquisition |
| IL | Illinois |
| IS | Internal standard |
| IUPAC | International Union of Pure and Applied Chemists |
| JWH | John William Huffman |
| JWH-007 | (2-methyl-1-pentyl-1*H*-3-indolyl)(1-naphthyl)methanone |
| JWH-015 | (2-methyl-1-propyl-1*H*-3-indolyl)(1-naphthyl)methanone |
| JWH-016 | (1-butyl-2-methyl-1*H*-3-indolyl)(1-naphthyl)methanone |
| JWH-018 | 1-naphthyl(1-pentyl-1*H*-3-indolyl)methanone |
| JWH-019 | (1-hexyl-1*H*-3-indolyl)(1-naphthyl)methanone |
| JWH-020 | (1-heptyl-1*H*-3-indolyl)(1-naphthyl)methanone |
| JWH-030 | 1-naphthyl(1-pentyl-1*H*-3-pyrrolyl)methanone |

| | |
|---|---|
| JWH-073 | (1-butyl-1*H*-3-indolyl)(1-naphthyl)methanone |
| JWH-081 | (4-methoxy-1-naphthyl)(1-pentyl-1*H*-3-indolyl)methanone |
| JWH-098 | (4-methoxy-1-naphthyl)(2-methyl-1-pentyl-1*H*-3-indolyl)methanone |
| JWH-122 | (4-methyl-1-naphthyl)(1-pentyl-1*H*-3-indolyl)methanone |
| JWH-200 | {1-[2-(4-morpholinyl)ethyl]-1*H*-3-indolyl}(1-naphthyl)methanone |
| JWH-203 | 2-(2-chlorophenyl)-1-(1-pentyl-1*H*-3-indolyl)ethanone |
| JWH-210 | (4-ethyl-1-naphthyl)(1-pentyl-1*H*-3-indolyl)methanone |
| JWH-250 | 2-(2-methoxyphenyl)-1-(1-pentyl-1*H*-3-indolyl)ethanone |
| JWH-307 | [5-(2-fluorophenyl)-1-pentyl-1*H*-3-pyrrolyl](1-naphtyl)methanone |
| KMD | Kendrick mass defect |
| kV | Kilovolt |
| L | Litre |
| LC-MS | Liquid chromatography – mass spectrometry |
| LLE | Liquid-liquid extraction |
| LLOQ | Lower limit of quantification |
| LOD | Limit of detection |
| LRMS | Low-resolution mass spectrometry |
| M | Moles per litre; mol/L |
| *m/z* | Mass-to-charge ratio |
| $M^{+\bullet}$ | Radical cation |
| $M^{+\bullet\bullet}$ | Diradical cation |
| MA | Massachusetts |
| MAE | Microwave-assisted extraction |
| MALDI | Matrix-assisted laser desorption ionisation |
| mDa | Millidalton |
| MDF | Mass defect filtering |
| MDMA | 3,4-methylenedioxymethamphetamine |
| MDMB-CHMICA | Methyl *N*-{[1-(cyclohexylmethyl)-1*H*-3-indolyl]carbonyl}-3-methylvalinate |
| MDMB-FUBINACA | Methyl *N*-{[1-(4-fluorobenzyl)-1*H*-3-indazolyl]carbonyl}-3-methylvalinate |
| MDMB-PINACA | Methyl *N*-[(1-pentyl-1*H*-3-indazolyl)carbonyl]-3-methylvalinate |
| MDMC | 2,3-methylenedioxymethcathinone |
| MDPBP | 3,4-methylenedioxy-α-pyrrolidinobutiophenone |
| MDPPP | 3,4-methylenedioxy-α-pyrrolidinopropiophenone |
| MDPV | 3,4-methylenedioxypyrovalerone |

| | |
|---|---|
| MFE | Molecular feature extraction |
| MFG | Molecular formula generator |
| mg | Milligram |
| MI | Michigan |
| mL | Millilitre |
| mM | Millimoles per litre; mmol/L |
| mm | Millimetre |
| MMB-FUBINACA | Methyl *N*-{[1-(4-fluorobenzyl)-1*H*-3-indazolyl]carbonyl}valinate |
| MO | Missouri |
| MPBP | 4-methyl-α-pyrrodinobutiophenone |
| MS | Mass spectrometry |
| MS/MS or $MS^2$ | Tandem mass spectrometry |
| MSC | Molecular Structure Correlator |
| $MS^n$ | Multistage tandem-mass spectrometry |
| MΩ | Megaohm |
| $N_2$ | Nitrogen gas |
| NaCl | Sodium chloride |
| ng | Nanogram |
| $NH_3$ | Ammonia |
| NJ | New Jersey |
| NL | Neutral loss |
| NLF | Neutral loss filtering |
| NMI | National Measurement Institute |
| NMR | Nuclear magnetic resonance |
| NPS | New psychoactive substances |
| NSW | New South Wales |
| OE | Odd electron |
| OH | Ohio |
| PA | Pennsylvania |
| PCA | Principal component analysis |
| PCDL | Personal compound database and library |
| PET | Positron emission tomography |
| PFAC | Perfluoroalkyl compounds |
| PiHKAL | Phenethylamines I have known and loved |
| PLE | Pressurised liquid extraction |
| pNLC | Precursor neutral loss chromatogram |
| ppm | Parts per million |
| PPP | Pyrrolidinopropiophenone |
| PTR | Proton transfer reaction |
| QLD | Queensland |
| QqQ | Triple quadrupole |

| | |
|---|---|
| QTOF | Quadrupole time-of-flight |
| $R^2$ | Coefficient of determination |
| rpm | Revolutions per minute |
| s | Seconds |
| S/N | Signal-to-noise ratio |
| SA | South Australia |
| SALLE | Salting-out assisted liquid-liquid extraction |
| SCX | Strong cation exchange |
| SIEVE® | Statistical Iterative Exploratory Visualization Environment |
| SPE | Solid-phase extraction |
| SRI | Selective reagent ionisation |
| STA | Systematic toxicological analysis |
| SWATH® | Sequential window acquisition of all theoretical spectra |
| SWGDRUG | Scientific Working Group for the Analysis of Seized Drugs |
| TCC | Total compound chromatogram |
| TCMP | Tetramethylcyclopropyl |
| THC | $\Delta^9$-tetrahydrocannabinol |
| TIC | Total ion chromatogram |
| TiHKAL | Tryptamines I have known and loved |
| TOF | Time-of-flight |
| TX | Texas |
| UK | United Kingdom |
| UNODC | United Nations Office of Drugs and Crime |
| UR-144 | (1-pentyl-1*H*-3-indolyl)(2,2,3,3-tetramethylcyclopropyl)methanone |
| USA | United States of America |
| V | Volt |
| VBA | Visual Basic for Applications |
| XLR-11 | [1-(5-fluoropentyl)-1*H*-3-indolyl](2,2,3,3-tetramethylcyclopropyl)methanone |
| α-PVP | α-pyrrolidinovalerophenone |
| Δ | Mass error |
| µg | Microgram |
| µL | Microlitre |

# Publications and conference proceedings

*Refereed journal publications directly related to this project*

1. **Pasin, D.**, Cawley, A., Bidny, S., Fu, S. (2017) Current applications of high-resolution mass spectrometry for the analysis of new psychoactive substances: a critical review. Analytical and Bioanalytical Chemistry, doi: 10.1007/s00216-017-0441-4.
2. **Pasin, D.**, Cawley, A., Bidny, S., Fu, S. (2017) Characterisation of hallucinogenic phenethylamines using high-resolution mass spectrometry for non-targeted screening purposes. Drug Testing and Analysis, doi: 10.1002/dta.2171.
3. Cawley, A., **Pasin, D.**, Ganbat, N., Ennis, L., Smart, C., Greer, C., Keledjian, J., Fu, S., Chen, A. (2016) The potential for complementary targeted/non-targeted screening of novel psychoactive substances in equine urine using liquid chromatography-high resolution accurate mass spectrometry. Analytical Methods. 8(8): 1789-97, doi: 10.1039/C6ay00156d

*Refereed journal publications from other related research activities*

1. Bidny, S., Gago, K., Chung, P., Albertyn, D., **Pasin, D**. (2017) Simultaneous screening and quantification of basic, neutral and acidic drugs in blood using UPLC-QTOF-MS. Journal of Analytical Toxicology. 41(3): 181-95, doi: 10.1093/jat/bkw118.
2. **Pasin, D.**, Bidny, S., Fu, S. (2015). Analysis of new designer drugs in post-mortem blood using high-resolution mass spectrometry. Journal of Analytical Toxicology. 39(3): 163-71, doi: 10.1093/jat/bku144

*Refereed conference proceedings (presenting author underlined)*

1. **Pasin, D.**, Cawley, A., Bidny, S., Fu, S. Evaluating the use of Kendrick Mass Defect Analysis for rapid discovery of new psychoactive substances in non-targeted screening approaches. 55th Meeting of The International Association of Forensic Toxicologists. Boca Raton, United States of America. Jan 6-11, 2018.
2. **Pasin, D.**, Cawley, A., Bidny, S., Fu, S. Characterization of Cannabinoids Using High-Resolution Mass Spectrometry for Non-Targeted Screening. 21st Triennial Meeting of the International Association of Forensic Science. Toronto, Canada. Aug 21-25, 2017.
3. **Pasin, D.**, Cawley, A., Bidny, S., Fu, S. Non-targeted screening of new psychoactive substances using liquid chromatography-high resolution mass spectrometry. *Royal Australian Chemical Institute Centenary Congress.* Melbourne, Australia. July 23-28, 2017
4. **Pasin, D.**, Cawley, A., Bidny, S., Fu, S. The use of collision-induced fragmentation pathways of hallucinogenic phenethylamines for the detection and identification of novel analogues. Australian and New Zealand Forensic Science Society 23rd International Symposium on the Forensic Sciences. Auckland, New Zealand. Sept 18-22, 2016.
5. **Pasin, D.**, Cawley, A., Bidny, S., Fu, S. The application of mass defect filtering in data mining of high-resolution mass spectrometry data for non-targeted screening strategies of new psychoactive substances. 54th Meeting of The International Association of Forensic Toxicologists. Brisbane, Australia. Aug 28-Sept 1, 2015
6. **Pasin, D.**, Fu, S., Cawley, A. An investigation into the collision induced dissociation pathways of synthetic cathinones using high-resolution mass

spectrometry for non-targeted screening purposes. 7th European Academy of Forensic Science Conference. Prague, Czech Republic. Sept 6-11, 2015.

7. **Pasin, D.**, Fu, S., Cawley, A. Preliminary investigation into the use of mass defect filtering for data reduction and non-targeted screening strategies for new psychoactive substances (NPS) using high-resolution mass spectrometry. 7th European Academy of Forensic Science Conference. Prague, Czech Republic. Sept 6-11, 2015.
8. **Pasin, D.**, Fu, S., Cawley, A. Collision-induced dissociation pathways of hallucinogenic phenethylamines (2C-X) and their N-(2-methoxybenzyl) derivatives (NBOMe) using high-resolution mass spectrometry for non-targeted screening purposes. 53rd Meeting of The International Association of Forensic Toxicologists. Florence, Italy. Aug 30-Sept 4, 2015 (poster).
9. Cawley, A., **Pasin, D.**, Ganbat, N., Ennis, L., Smart, C., Greer, C., Keledjian, J., Fu, S., Chen, A. Validation of non-targeted high-resolution accurate mass spectrometry analysis in forensic toxicology: A case study in NBOMe detection. 53rd Meeting of The International Association of Forensic Toxicologists. Florence, Italy. Aug 30-Sept 4, 2015.
10. Cawley, A., Ganbat, N., Ennis, L., **Pasin, D.**, Smart, C., Keledjian, J., Fu, S., Chen, A., Mariani, M., Jones, D. The potential of complementary targeted/untargeted high-resolution accurate mass screening strategies for advanced sports anti-doping. Royal Australian Chemical Institute National Congress. Adelaide, Australia. Dec 7-12, 2014.
11. **Pasin, D.**, Bidny, S., Fu, S. Detection and quantification of 40 new designer drugs in post-mortem blood using high-resolution mass spectrometry. Australian and New Zealand Forensic Science Society 22nd International Symposium on the

Forensic Sciences. Adelaide, Australia. Aug 31-Sept 4, 2014.

12. **Pasin, D.**, Bidny, S., Fu, S. Analysis of new designer drugs in post-mortem blood using high resolution mass spectrometry. Forensic and Clinical Toxicology Association Inc. Meeting. Sydney, Australia. Dec 2-4, 2013.
13. Bidny, S., Kelly, G., Gago, K., David, M., Duong, T., **Pasin, D**. The application of high-resolution mass spectrometry and ultra-performance liquid chromatography in forensic toxicology for the simultaneous screening and quantification of basic, neutral and acidic drugs in blood. Forensic and Clinical Toxicology Association Inc. Meeting. Sydney, Australia. Dec 2-4, 2013.

# Abstract

The proliferation of new psychoactive substances (NPS) has become problematic for forensic drug chemistry and analytical toxicology laboratories that rely on the use of targeted screening methods for the detection of analytes. In order to detect novel NPS derivatives, non-targeted or general unknown screening workflows need to be implemented. Recently, high-resolution mass spectrometry (HRMS) has become the workhorse for general drug screening due to its ability to collect full scan MS and MS/MS data, which can be retrospectively interrogated and has been identified as a potential tool for non-targeted screening.

Top-down screening approaches involving the selection of abundant precursor ions is difficult in toxicological analyses particular when analytes of interest exist at low concentrations. Mass defect-based top-down screening approaches were developed and evaluated for the detection of low concentration analogues. Application of mass defect filtering (MDF) on fortified and authentic samples revealed that the efficacy of this technique was dependent on sample complexity, chromatographic resolution and, more critically, software availability and/or capability. An in-house Microsoft Office Excel-based KMD analysis software was developed using the Visual Basic for Applications (VBA) programming language. Briefly, the software workflow involves the importation of single or multiple comma-separated value (.csv) files, followed by the calculation of KMD values for each mass-to-charge (*m/z*) entry normalized to – $CH_2$. The data can then be filtered by *m/z* range, intensity, mass defect and even/odd mass. KMD values which match the user-defined values (up to 8 different values can be monitored simultaneously) are highlighted and isolated for easy visualization. These *m/z* values can then be extracted using the corresponding native data processing

software to observe the presence of distinct chromatographic peaks for the selected *m/z* values. The program was capable of rapidly interrogating numerical MS data from multiple files acquired by major HRMS platform vendors. In addition, differential analysis software was also evaluated for the detection of anomalous signals not present in control samples, however, this technique requires representative control matrices in addition to supplementary data processing software that is not always provided by HRMS vendors or requires separate purchase.

Bottom-up screening strategies involve the monitoring of common product ions and neutral losses (NLs) for particular subclasses, where aligning chromatographic peaks for multiple product ions or NLs may indicate the possible presence of a novel NPS analogue. Collision-induced dissociation (CID) studies were performed on synthetic cathinone, hallucinogenic phenethylamine and synthetic cannabinoid derivatives to determine key product ions and NLs. 2C-X and DOX derivatives had common losses of $NH_3$, $CH_6N$ and $C_2H_9N$ and common product ions at *m/*z 164.0837, 149.0603 and 134.0732 for 2C-X derivatives and *m/z* 178.0994, 163.0754, 147.0804 and 135.0810 for DOX derivatives. The 25X-NBOMe derivatives had characteristic product ion spectra with abundant ions at *m/z* 121.0654 and 91.0548, together with minor NLs corresponding to 2-methylanisole and 2-methoxybenzylamine and $C_9H_{14}NO$.

Product ion pairs *m/z* 117.0573/105.0699, 131.0730/105.0699, 145.0886/119.0855, 159.1043/133.1012 149.0635/123.0605 and 161.0835/135.0804 were indicative of different substituted traditional cathinone derivatives. Methylenedioxycathinone-type cathinones did not exhibit common product ions but instead exhibited NLs of 18.0106 ($H_2O$), 48.0211 ($CH_4O_2$) and 76.0160 Da ($C_2H_4O_3$). The presence of *m/z* 98.0964, 112.1121 or 126.1277 and a NL of 71.0735 Da was indicative of synthetic cathinones that contain a pyrrolidine ring such as the α-pyrrolidinophenone-type and

methylenedioxy-α-pyrrolidinophenone-type cathinones. Product ions *m/z* 105.0699 and 119.0855 were indicative of unsubstituted and methylphenyl α-pyrrolidinophenone-type cathinones, respectively. While *m/z* 149.0233 was indicative of methylenedioxy-α-pyrrolidinophenone-type cathinones.

Naphthoylindole derived synthetic cannabinoids exhibited major product ions at *m/z* 155.0491, 169.0648, 183.0804 and *m/z* 185.0597 while 2-iodobenzoylindole and TMCP derivatives exhibited the product ion *m/z* 230.9301 and *m/z* 125.0961, respectively. Product ions corresponding to the linker-core-tail were observed at *m/z* 214.1226 (PICA), 232.1132 (5F-PICA), 215.1179 (PINACA), 233.1085 (5F-PINACA), 240.1383 (CHMICA), 241.1335 (CHMINACA), 252.0819 (FUBICA) and 253.0772 (FUBINACA). Furthermore, the presence of *m/z* 144.0444, 158.0600 and 145.0402 were indicative of the indole, 2-methylindole and indazole acylium cations.

These strategies were applied retrospectively to authentic forensic casework samples that were confirmed to contain NPS analogues at relatively low concentrations. All analytes of interest were detected using a combination of top-down and bottom-up screening strategies. Overall, these strategies offer a vendor-agnostic approach for the detection of NPS analogues that can be implemented immediately for samples of interest.

# *CHAPTER 1:*

# *INTRODUCTION*

## 1.1 A brief overview of new psychoactive substances

New (or novel) psychoactive substances (NPS), designer drugs and legal highs are all terms used to refer to new emerging recreational drugs which are designed primarily to circumvent the legislative measures that have been established for conventional drugs of abuse such as cocaine, heroin and *N*-methylamphetamine [1-4]. However, more recently the term NPS has become widely adopted with certain jurisdictions using NPS in their legislative framework. In particular, New South Wales (NSW, Australia) have recently implemented the Drugs and Poisons Legislation Amendment (New Psychoactive and Other Substances) Act 2013 and the Psychoactive Substances Act 2013 has been adopted in New Zealand [5, 6]. The European Monitoring Centre for Drugs and Drug Addiction (EMCDDA) defines NPS as follows:

***"….****a new narcotic or psychotropic drug, in pure form or in preparation, that is not controlled by the 1961 United Nations Single Convention on Narcotic Drugs or the 1971 United Nations Convention on Psychotropic Substances, but which may pose a public health threat comparable to that posed by substances listed in these conventions (Council Decision 2005/387/JHA)."* [7]

To summarise, the modification or alteration of pre-existing psychoactive substances to produce new compounds that are intended to exert similar pharmacological effects as conventional drugs that are able to circumvent state and/or federal legislation. According to the latest European Drug Report, more than 500 NPS analogues were reported to the European Union (EU) Early Warning System (EWS) over the last decade with the number of new analogues reported in the last five years comprising approximately 80% of the total number [8]. The highest number of new analogues reported for the first time was in 2014 with 101 analogues (~20%). The NPS market

has been traditionally dominated by synthetic cannabinoids with 157 of the 467 analogues (34%) reported between 2009 and 2015, however, psychedelic tryptamines, piperazines and hallucinogenic phenethylamines were predominant between 2005 and 2007. In addition to synthetic cannabinoids, synthetic cathinones also dominate the NPS market with 93 analogues (20%) reported between 2009 and 2015 and higher numbers of analogues reported compared to synthetic cannabinoids in 2010 and 2015 [8, 9]. Recently, other NPS classes have become prevalent including the highly-potent synthetic opioids [8].

### 1.1.1 Synthetic cathinones

Synthetic cathinones or β-keto amphetamines are compounds that are derived from naturally occurring cathinone (*S*-(-)-2-amino-1-phenylpropan-1-one) present in the khat plant (*Catha Edulis)*. Cathinone serves as the scaffold for synthetically modified variants such as 4-methylmethcathinone (mephedrone), 3,4-methylenedioxypyrovalerone (MDPV) and 3,4-methylenedioxymethcathinone (methylone) [10-13]. Synthetic cathinones have been identified as the main active ingredients in a range of products, which have been marketed as “bath salts”, “plant food” and “jewellery cleaner”. Structurally all cathinones share the β-keto phenethylamine moiety with substitutions typically made at the *meta*- or *para*-positions relative to the alkylamine chain, however, *ortho*- substitutions are also prevalent. Furthermore, substitutions can be made at the amine group to form secondary and tertiary amines and at the α-carbon [14-16]. The majority of synthetic cathinones can be classified into four different subclasses such as traditional cathinones (Figure 1.1a), 3,4-methylenedioxy-type (Figure 1.1b), α-pyrrolidinophenone-type (Figure 1.1c) and methylenedioxy-α-pyrrolidinophenone-type (Figure 1.1d) cathinones. The general pharmacodynamics of synthetic cathinones

involves either the stimulation of release or the reuptake inhibition of the monoamine neurotransmitters, dopamine, norepinephrine and 5-hydroxytryptamine (5-$HT_{2A}$, serotonin). All cathinones have been observed to inhibit norepinephrine transporters with varying dopamine and serotonin transporter inhibition [17-22]. A review by Ellefsen *et al*. [23] indicated that ring substituted derivatives such as mephedrone and methylone exhibited monoamine transporter inhibition for all neurotransmitters similar to 3,4-methylenedioxymethamphetamine (MDMA).

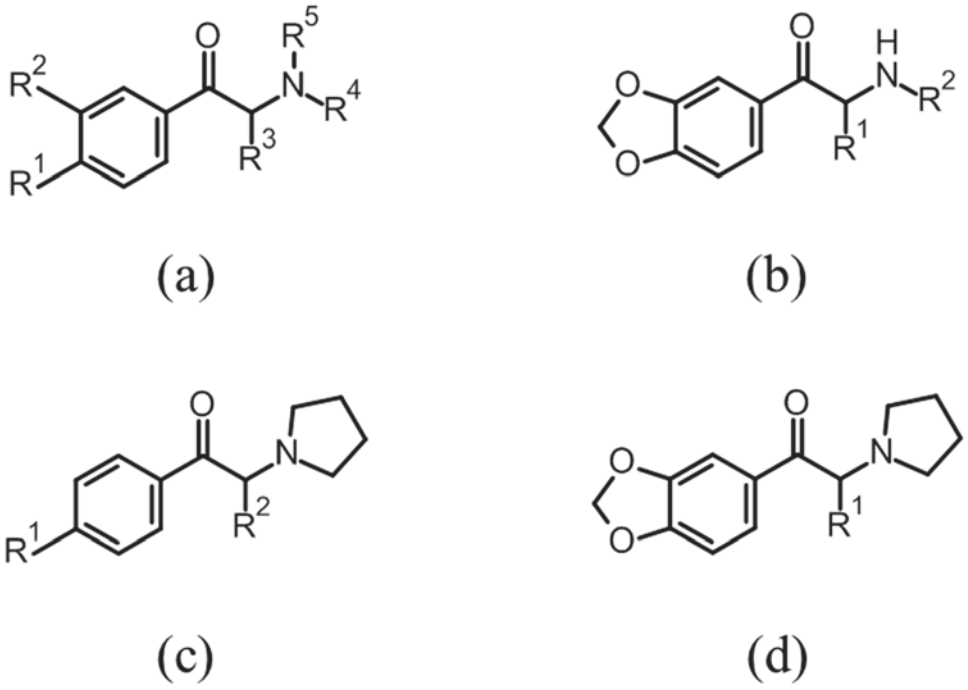


**Figure 1.1** General structure for traditional (a), 3,4-methylenedioxy-type (b), α-pyrrolidinophenone-type (c) and methylenedioxy-α-pyrrolidinophenone-type (d) cathinones.

### 1.1.2 Hallucinogenic phenethylamines

Hallucinogenic phenethylamines have recently become popular due to their potent serotonergic activity, giving users a sense of euphoria and intense hallucinogenic

episodes [24-26]. Their popularity is also attributed to literature such as the notable book published by Alexander Shulgin and Ann Shulgin, PiHKAL (***P**henethylamines **i** **H**ave **K**nown **A**nd **L**oved*) which outlines the synthesis of almost 200 ring-substituted phenethylamine derivatives and anecdotal information on the effects at certain doses from self-administration [27]. The most prevalent are the 2,5-dimethoxyphenethylamines, colloquially known as "2C's" or "2C-X", where "2C" refers to the 2 carbons atoms between the benzene ring and amine group and "X" refers to a letter or number corresponding to a possible substituent, e.g. 'B' (bromo), 'C' (chloro), and 'I' (iodo). Typically, these compounds are modified at the *para*-position by the addition of halogens, alkyl and thioalkyl groups [28]. In addition to the 2C's, PiHKAL also outlines the synthesis of 2,5-dimethoxyamphetamines or "DOX" derivatives which are structurally similar to the 2C's and only differ by the addition of an α-methyl group (Figure 1.2) [27, 29, 30].

Recently, more concerning derivatives of the ring-substituted phenethylamine class are the *N*-(2-methoxybenzyl) or 25X-NBOMe derivatives of the 2C-X compounds [31]. These compounds were first synthesized by Glennon *et al.* [32] and extensively studied by Ralf Heim [33] and Martin Hansen [34] as selective serotonin 2A ($5\text{-HT}_{2A}$) agonists.

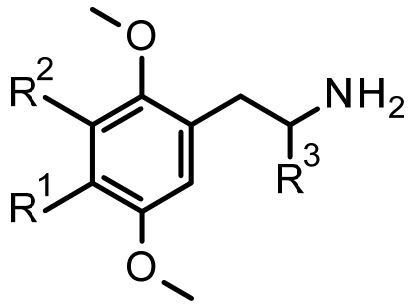


**Figure 1.2** General structure for 2C-X ($R^3 = H$) and DOX ($R^3 = CH_3$) hallucinogenic phenethylamines.

Generally, 25X-NBOMe derivatives were synthesised through reductive alkylation of selected 2C-X derivatives with 2-methoxybenzaldehyde (Figure 1.3) [31, 33]. The potency of these compounds has been demonstrated in literature, detailing the severe hallucinogenic episodes experienced by users of 25X-NBOMe derivatives, some of which have led to deaths as a result of their own actions [35-38].

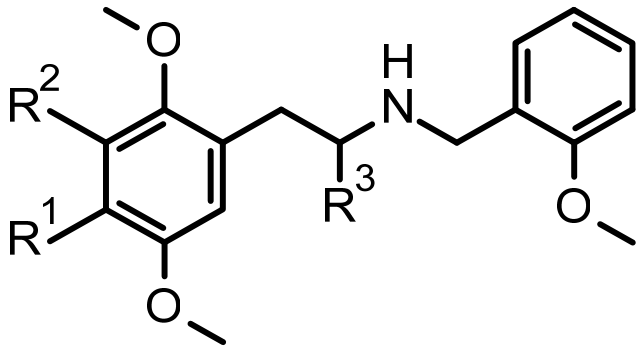


**Figure 1.3** General structure for 25X-NBOMe derivatives.

### 1.1.3 Synthetic cannabinoids

Natural cannabinoids such as $\Delta^9$-tetrahydrocannabinol (THC) and cannabidiol (CBD) are found in the foliage of *Cannabis sativa*, *Cannabis indica* and *Cannabis ruderalis* plants. THC has been characterised as a partial cannabinoid receptor (CB) agonist at the $CB_1$ and $CB_2$ receptors, providing users with a sense of euphoria when smoked, eaten or vaporised [39, 40]. Due to the current legislation around cannabis, there has been an emergence of products containing synthetic cannabinoids that are not covered under pre-existing legislative measures. Synthetic cannabinoids are specifically designed to be $CB_1$ and $CB_2$ receptor agonists. Some synthetic cannabinoids share the classical cannabinoid structure such as the HU-series, however, many analogues consist of an aminoalkylindole backbone. These derivatives are often synthesized for

pharmaceutical purposes due to the potential for $CB_2$ receptor agonists to inhibit tumour growth for various cancer types. Subsequently, these compounds often do not make it to the pharmaceutical market due to increased vulnerability for drug abuse, however, their synthetic procedures are often accessible via the internet. Synthetic cannabinoids are structurally diverse and have been categorised as either first-, second- or third-generation depending on whether their emergence occurred pre- or post-legislative changes in Europe and the United States of America (USA) [41, 42]. First-generation synthetic cannabinoids, such as the naphthoylindoles (Figure 1.4a) synthesised by John William Huffman (JWH), were prevalent in Spice and K2 products until the initial bans in 2009 (Europe) and 2010 (USA).

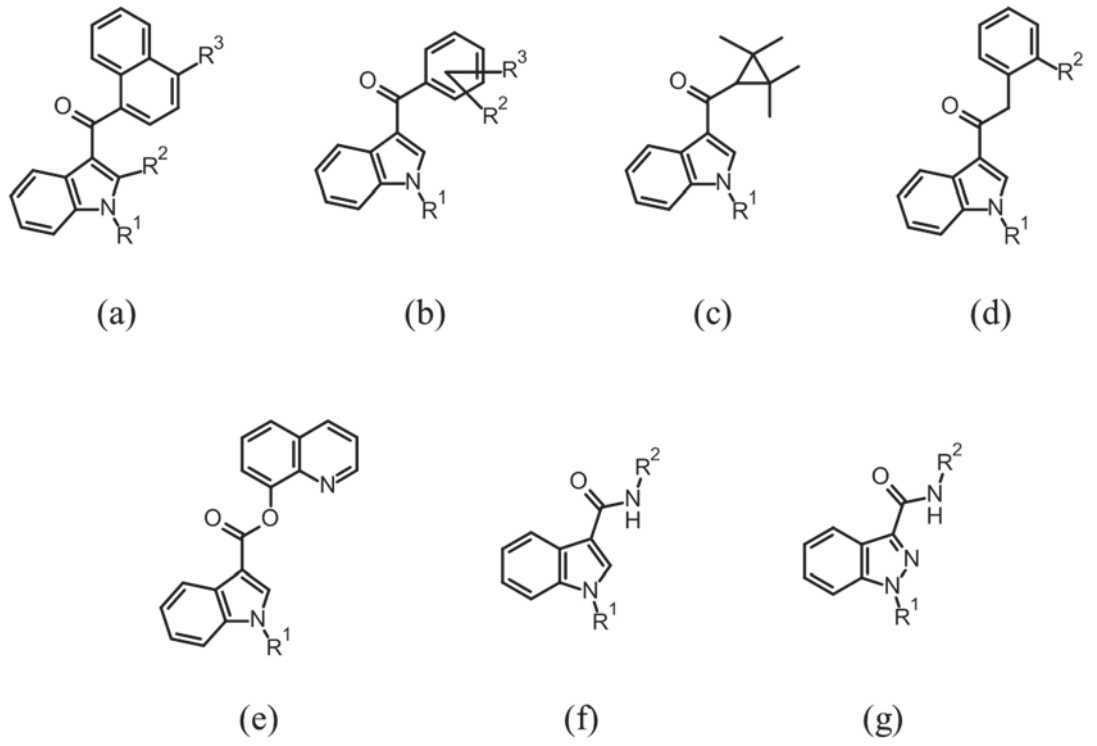


**Figure 1.4** General structures for naphthoylindole (a), benzoylindole (b), 2,2,3,3-tetramethylcyclopropylindole (c), phenacetylindole (d), quinolinylindole (e), 3-carboxamide-indole (f) and 3-carboxamide-indazole (g) synthetic cannabinoids.

These bans saw a reduction in the presence of first-generation synthetic cannabinoids in herbal incense products which were replaced with second-generation synthetic cannabinoids such as benzoylindoles (Figure 1.4b), 2,2,3,3-tetramethylcyclopropyl (Figure 1.4c) and phenacetylindoles (Figure 1.4d). More recently, there has been emergence of third-generation synthetic cannabinoids containing quinolinyl (Figure 1.4e), 3-carboxamide-indole (Figure 1.4f) and 3-carboxamide-indazole (Figure 1.4g) synthetic cannabinoids.

### 1.1.4 Other NPS derivatives

In addition to the aforementioned NPS classes, there have been other NPS classes that have entered the market but have subsequently disappeared or have been less prevalent due to lack of popularity such as psychedelic tryptamines and piperazine derivatives. Furthermore, there has been the proliferation of other NPS classes such as synthetic opioids.

#### *1.1.4.1 Psychedelic tryptamines*

Psychedelic tryptamines are substituted tryptamines (Figure 1.5a) which are structurally related to the serotonin neurotransmitter (Figure 1.5b) and are derived from the psychoactive compounds psilocybin (Figure 1.5c) and psilocin (Figure 1.5d) which are found in the psychedelic mushrooms *Psilocybe semilanceata, Psilocybe azurenscens* and *Psilocybe cyanescens* [43, 44]. Due to their structural similarity to serotonin, psychedelic tryptamines are 5-$HT_{2A}$ agonists, resulting in users experiencing severe hallucinatory effects. Many tryptamine derivatives were synthesized by Alexander Shulgin that were subsequently reported in his sequel to PiHKAL called TiHKAL: The Continuation, where TiHKAL is an abbreviation for **T**ryptamines **i** **H**ave **K**nown and **L**oved [45].

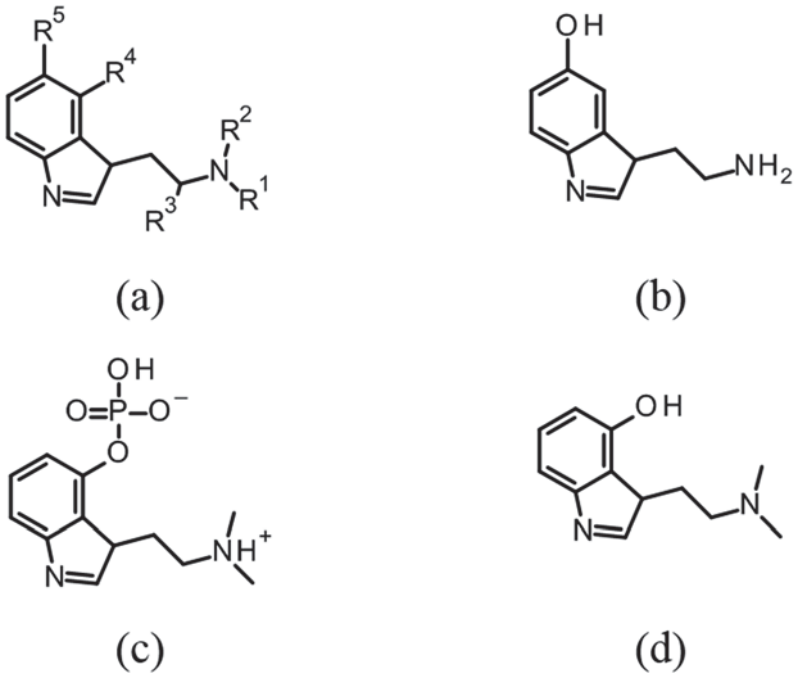


**Figure 1.5** General structure of psychedelic tryptamine (a) and structures of serotonin (b), psilocybin (c) and psilocin (d).

### *1.1.4.2 Piperazines*

Benzylpiperazine (Figure 1.6a) and phenylpiperazine (Figure 1.6b) derivatives have been the least abundant and least popular since their appearance on the drug market after their psychoactive properties were identified. Initially used in veterinary medicine as an anti-parasitic, piperazines have also been investigated for their use as vasodilators and to inhibit the growth of cancerous tumours [46, 47]. With effects similar to MDMA, these drugs were often used in nightclub scenes as "party pills" and seen as legal and safe alternatives, however, studies have shown that these compounds have similar if not the same associated risks as *N*-methylamphetamine and MDMA [48]. New Zealand was one country which had a large increase in piperazine use (primarily benzylpiperazine; BZP) at the turn of the 21$^{st}$ century due to reduced MDMA supply at the time [49-51]. As a consequence there was a large demand for an alternative to MDMA and BZP subsequently filled the market gap.

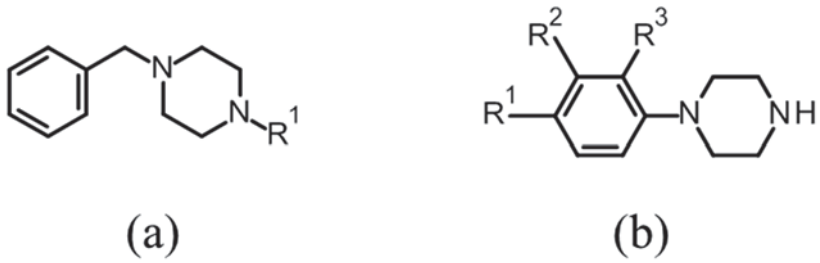


**Figure 1.6** General structures for benzylpiperazine (a) and phenylpiperazine (b) derivatives.

### *1.1.4.3 Synthetic opioids*

More recently there has been an emergence of synthetic opioids such as the fentanyl derivatives (Figure 1.7a) which often have potencies significantly higher than morphine [52]. One of the most potent of these is carfentanil (Figure 1.7b), a μ-opioid receptor agonist, with a clinical potency 10,000 times greater than that of morphine and 100 times greater than fentanyl (Figure 1.7c) [53, 54]. It was also implicated in the 2002 Moscow Theatre Siege which saw the death of 125 people. [53]. According to the Centre for Disease Control (CDC) in the USA, there were approximately 5000 fentanyl-related deaths in 2014 [53]. The large number of overdoses is largely attributed to the fact fentanyl derivatives may act as a diluent for heroin [52] with users not adjusting dosages.

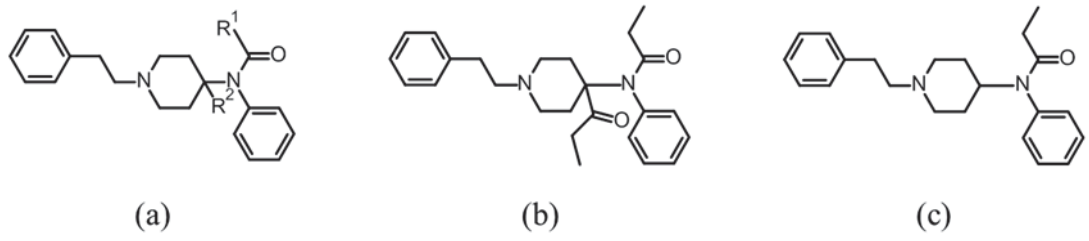


**Figure 1.7** Structures of fentanyl derivatives (a), carfentanil (b) and fentanyl (c).

### 1.1.5 References


1. German CL, Fleckenstein AE, Hanson GR. Bath salts and synthetic cathinones: An emerging designer drug phenomenon. *Life Sci*. 2014;97:2-8.
2. King LA, Kicman AT. A brief history of 'new psychoactive substances'. *Drug Test Anal*. 2011;3:401-3.
3. Spiller HA, Ryan ML, Weston RG, Jansen J. Clinical experience with and analytical confirmation of "bath salts" and "legal highs" (synthetic cathinones) in the United States. *Clin Toxicol*. 2011;49:499-505.
4. Bruno R, Matthews AJ, Dunn M, Alati R, McIlwraith F, Hickey S, Burns L, Sindicich N. Emerging psychoactive substance use among regular ecstasy users in Australia. *Drug Alcohol Depend*. 2012;124:19-25.
5. New South Wales Police Force (2013). New Psychoactive Substances. Accessed in April 2014. http://www.police.nsw.gov.au/community_issues/drugs/new_psychoactive_substances
6. New Zealand Government (2013). Psychoactive Substances Act. Accessed in April 2014. http://www.legislation.govt.nz/act/public/2013/0053/latest/DLM5042921.html?src=qs
7. Zuba D. Identification of cathinones and other active components of 'legal highs' by mass spectrometric methods. *TrAC, Trends Anal Chem*. 2012;32:15-30.
8. European Monitoring Centre for Drugs and Drug Abuse. European Drug Report 2016. Accessed in October 2016. http://www.emcdda.europa.eu/edr2016
9. European Monitoring Centre for Drugs and Drug Abuse. European Drug Report 2013. Accessed in November 2016. http://www.emcdda.europa.eu/publications/edr/trends-developments/2013
10. Baumann MH, Partilla JS, Lehner KR. Psychoactive "bath salts": Not so soothing. *Eur J Pharmacol*. 2013;698:1-5.
11. Prosser J, Nelson L. The Toxicology of Bath Salts: A Review of Synthetic Cathinones. *J Med Toxicol*. 2012;8:33-42.
12. Wieland DM, Halter MJ, Levine C. Bath salts: they are not what you think. *Journal of Psychosocial Nursing*. 2012;50:17-21.
13. Winder GS, Stern N, Hosanagar A. Are "Bath Salts" the next generation of stimulant abuse? *J Subst Abuse Treat*. 2013;44:42-5.
14. Swortwood M, Boland D, DeCaprio A. Determination of 32 cathinone derivatives and other designer drugs in serum by comprehensive LC-QQQ-MS/MS analysis. *Anal Bioanal Chem*. 2013;405:1383-97.
15. Sørensen LK. Determination of cathinones and related ephedrines in forensic whole-blood samples by liquid-chromatography–electrospray tandem mass spectrometry. *J Chromatogr B*. 2011;879:727-36.
16. Coppola M, Mondola R. Synthetic cathinones: Chemistry, pharmacology and toxicology of a new class of designer drugs of abuse marketed as "bath salts" or "plant food". *Toxicol Lett*. 2012;211:144-9.
17. Coppola M, Mondola R. 3,4-Methylenedioxypyrovalerone (MDPV): Chemistry, pharmacology and toxicology of a new designer drug of abuse marketed online. *Toxicol Lett*. 2012;208:12-5.
18. Maurer HH, Kraemer T, Springer D, Staack RF. Chemistry, Pharmacology, Toxicology, and Hepatic Metabolism of Designer Drugs of the Amphetamine (Ecstasy), Piperazine, and Pyrrolidinophenone Types: A Synopsis. *Ther Drug*

*Monit*. 2004;26:127-31.
19. Fantegrossi WE, Reissig CJ, Katz EB, Yarosh HL, Rice KC, Winter JC. Hallucinogen-like effects of N,N-dipropyltryptamine (DPT): Possible mediation by serotonin 5-HT1A and 5-HT2A receptors in rodents. *Pharmacol, Biochem Behav*. 2008;88:358-65.
20. Schifano F, Albanese A, Fergus S, Stair JL, Deluca P, Corazza O, Davey Z, Corkery J, Siemann H, Scherbaum N, Farre M, Torrens M, Demetrovics Z, Ghodse AH, Psychonaut Web M, Re DRG. Mephedrone (4-methylmethcathinone; 'meow meow'): chemical, pharmacological and clinical issues. *Psychopharmacology*. 2010;214:593-602.
21. Halberstadt AL, Geyer MA. Multiple receptors contribute to the behavioral effects of indoleamine hallucinogens. *Neuropharmacology*. 2011;61:364-81.
22. Halberstadt AL. Recent advances in the neuropsychopharmacology of serotonergic hallucinogens. *Behav Brain Res*. 2014.
23. Ellefsen KN, Concheiro M, Huestis MA. Synthetic cathinone pharmacokinetics, analytical methods, and toxicological findings from human performance and postmortem cases. *Drug Metab Rev*. 2016;48:1-29.
24. Cole MD, Lea C, Oxley N. 4-Bromo-2,5-dimethoxyphenethylamine (2C-B): a review of the public domain literature. *Sci Justice*. 2002;42:223-4.
25. de Boer D, Bosman I. A new trend in drugs-of-abuse; the 2C-series of phenethylamine designer drugs. *Pharm World Sci*. 2004;26:110-3.
26. Dean B, Stellpflug S, Burnett A, Engebretsen K. 2C or Not 2C: Phenethylamine Designer Drug Review. *J Med Toxicol*. 2013;9:172-8.
27. Shulgin AT, Shulgin A. Phenethylamines I have Known and Loved: A Chemical Love Story. Berkley: Transform Press; 1991.
28. Glennon RA, Young R, Benington F, Morin RD. Behavioral and serotonin receptor properties of 4-substituted derivatives of the hallucinogen 1-(2, 5-dimethoxyphenyl)-2-aminopropane. *J Med Chem*. 1982;25:1163-8.
29. Halberstadt AL, Powell SB, Geyer MA. Role of the 5-HT2A receptor in the locomotor hyperactivity produced by phenylalkylamine hallucinogens in mice. *Neuropharmacology*. 2013;70:218-27.
30. Collins M. Some new psychoactive substances: precursor chemicals and synthesis-driven end-products. *Drug Test Anal*. 2011;3:404-16.
31. Casale J, Hays P. Characterization of eleven 2,5-dimethoxy-N-(2-methoxybenzyl) phenethylamine (NBOMe) derivatives and differentiation from their 3-and 4-methoxybenzyl analogues Part–1. *Microgram J*. 2012;9.
32. Glennon RA, Dukat M, el-Bermawy M, Law H, De los Angeles J, Teitler M, King A, Herrick-Davis K. Influence of amine substituents on 5-HT2A versus 5-HT2C binding of phenylalkyl- and indolylalkylamines. *J Med Chem*. 1994;37:1929-35.
33. Heim R (2003), Synthese und Pharmakologie potenter 5-$HT_{2A}$-Rezeptoragonisten mit N-2-Methoxybenzyl-Partialstruktur, PhD thesis, Freie Universität Berlin.
34. Hansen M (2010), Design and Synthesis of Selective Serotonin Receptor Agonists for Positron Emission Tomography Imaging of the Brain, PhD thesis, Faculty of Pharmaceutical Sciences, University of Copenhagen.
35. Hill SL, Doris T, Gurung S, Katebe S, Lomas A, Dunn M, Blain P, Thomas SHL. Severe clinical toxicity associated with analytically confirmed recreational use of 25I–NBOMe: case series. *Clin Toxicol*. 2013;51:487-92.
36. Poklis JL, Devers KG, Arbefeville EF, Pearson JM, Houston E, Poklis A.

Postmortem detection of 25I-NBOMe [2-(4-iodo-2,5-dimethoxyphenyl)-N-[(2-methoxyphenyl)methyl]ethanamine] in fluids and tissues determined by high performance liquid chromatography with tandem mass spectrometry from a traumatic death. *Forensic Sci Int*. 2014;234:e14-e20.

37. Rose SR, Poklis JL, Poklis A. A case of 25I-NBOMe (25-I) intoxication: a new potent 5-HT2A agonist designer drug. *Clin Toxicol*. 2013;51:174-7.
38. Stellpflug S, Kealey S, Hegarty C, Janis G. 2-(4-Iodo-2,5-dimethoxyphenyl)-N-[(2-methoxyphenyl)methyl]ethanamine (25I-NBOMe): Clinical Case with Unique Confirmatory Testing. *J Med Toxicol*. 2014;10:45-50.
39. Marshell R, Kearney-Ramos T, Brents LK, Hyatt WS, Tai S, Prather PL, Fantegrossi WE. In vivo effects of synthetic cannabinoids JWH-018 and JWH-073 and phytocannabinoid Δ9-THC in mice: Inhalation versus intraperitoneal injection. *Pharmacol, Biochem Behav*. 2014;124:40-7.
40. Seely KA, Lapoint J, Moran JH, Fattore L. Spice drugs are more than harmless herbal blends: A review of the pharmacology and toxicology of synthetic cannabinoids. *Prog Neuropsychopharmacol Biol Psychiatry*. 2012;39:234-43.
41. Shanks KG, Behonick GS, Dahn T, Terrell A. Identification of Novel Third-Generation Synthetic Cannabinoids in Products by Ultra-Performance Liquid Chromatography and Time-of-Flight Mass Spectrometry. *J Anal Toxicol*. 2013;37:517-25.
42. Shanks KG, Dahn T, Behonick G, Terrell A. Analysis of first and second generation legal highs for synthetic cannabinoids and synthetic stimulants by ultra-performance liquid chromatography and time of flight mass spectrometry. *J Anal Toxicol*. 2012;36:360-71.
43. Arunotayanun W, Dalley JW, Huang X-P, Setola V, Treble R, Iversen L, Roth BL, Gibbons S. An analysis of the synthetic tryptamines AMT and 5-MeO-DALT: Emerging 'Novel Psychoactive Drugs'. *Bioorg Med Chem Lett*. 2013;23:3411-5.
44. Pichini S, Marchei E, García-Algar O, Gomez A, Di Giovannandrea R, Pacifici R. Ultra-high-pressure liquid chromatography tandem mass spectrometry determination of hallucinogenic drugs in hair of psychedelic plants and mushrooms consumers. *J Pharm Biomed Anal*. 2014;100:284-9.
45. Shulgin AT, Shulgin A. Tryptamines I have Known and Loved: The Continuation. Berkley: Transform Press; 1997.
46. Stanaszek R, Zuba D. 1-(3-chlorophenyl) piperazine (mCPP)–a new designer drug that is still a legal substance. *Probl Forensic Sci*. 2006;66:220-8.
47. Byrska B, Zuba D, Stanaszek R. Determination of piperazine derivatives in "legal highs". *Probl Forensic Sci*. 2010;82:101.
48. Tsutsumi H, Katagi M, Miki A, Shima N, Kamata T, Nishikawa M, Nakajima K, Tsuchihashi H. Development of simultaneous gas chromatography–mass spectrometric and liquid chromatography–electrospray ionization mass spectrometric determination method for the new designer drugs, N-benzylpiperazine (BZP), 1-(3-trifluoromethylphenyl)piperazine (TFMPP) and their main metabolites in urine. *J Chromatogr B*. 2005;819:315-22.
49. Cohen BMZ, Butler R. BZP-party pills: A review of research on benzylpiperazine as a recreational drug. *Int J Drug Policy*. 2011;22:95-101.
50. Wilkins C, Sweetsur P, Parker K. The impact of the prohibition of benzylpiperazine (BZP) "legal highs" on the availability, price and strength of BZP in New Zealand. *Drug Alcohol Depend*. 2014;144:47-52.
51. Wilkins C, Sweetsur P. The impact of the prohibition of benzylpiperazine (BZP)

'legal highs' on the prevalence of BZP, new legal highs and other drug use in New Zealand. *Drug Alcohol Depend*. 2013;127:72-80.
52. Suzuki J, El-Haddad S. A review: Fentanyl and non-pharmaceutical fentanyls. *Drug Alcohol Depend*. 2017;171:107-16.
53. Casale JF, Mallette JR, Guest EM. Analysis of illicit carfentanil: Emergence of the death dragon. *Forensic Chem*. 2017;3:74-80.
54. Yong Z, Gao X, Ma W, Dong H, Gong Z, Su R. Nalmefene reverses carfentanil-induced loss of righting reflex and respiratory depression in rats. *Eur J Pharmacol*. 2014;738:153-7.

## 1.2 PUBLICATION: Current applications of high-resolution mass spectrometry for the analysis of new psychoactive substances: a critical review (doi: 10.1007/s00216-017-0441-4)

### 1.2.1 Foreword

The following section is a critical review that was accepted for publication in the journal *Analytical and Bioanalytical Chemistry* and intended to be published in the critical review special issue in October 2017. It addresses the current applications of HRMS for the analysis of NPS in forensic drug chemistry and analytical toxicology with a critical overview of the current state of non-targeted screening. Permission has been granted by Springer via RightsLink for inclusion in this thesis (Licence no.: 4142740077664). This manuscript was authored by Mr. Daniel Pasin, Dr. Adam Cawley, Dr. Sergei Bidny and Associate Professor Shanlin Fu. The literature search and manuscript preparation were performed by D Pasin, with manuscript edits provided by A Cawley, S Bidny and S Fu. NOTE: Figure and table caption numbers have been adjusted to align with the chronology of this thesis and may not reflect those published in the online article.

# Current applications of high-resolution mass spectrometry for the analysis of new psychoactive substances: a critical review

Daniel Pasin[1], Adam Cawley[2], Sergei Bidny[3], Shanlin Fu[1*]

[1] Centre for Forensic Science, University of Technology Sydney, Broadway NSW 2007, Australia

[2] Australian Racing Forensic Laboratory, Racing NSW, Sydney NSW 2000, Australia

[3] Forensic Toxicology Laboratory, NSW Forensic and Analytical Science Service, Lidcombe, NSW 2141, Australia

*Author to whom correspondence should be addressed:

Shanlin Fu

University of Technology Sydney

15 Broadway, Sydney NSW 2007, Australia

Email : Shanlin.Fu@uts.edu.au

### 1.2.2 Abstract

The proliferation of new psychoactive substances (NPS) in recent years has resulted in the development of numerous analytical methods for the detection and identification of known and unknown NPS derivatives. High-resolution mass spectrometry (HRMS) has been identified as the method of choice for broad screening of NPS in a wide range of analytical contexts due to its ability to measure accurate masses using data-independent acquisition (DIA) techniques. Additionally, it has shown promise for non-targeted screening strategies that have been developed in order to detect and identify novel analogues without the need for certified reference materials (CRMs) or comprehensive mass spectral libraries. This paper reviews the applications of HRMS for the analysis of NPS in forensic drug chemistry and analytical toxicology. It provides an overview of the sample preparation procedures in addition to data acquisition, instrumental analysis and data processing techniques. Furthermore, it will give an overview of the current state of non-targeted screening strategies with discussion on future directions and perspectives of this technique.

### 1.2.3 Keywords

new psychoactive substances, high-resolution mass spectrometry, non-targeted screening.

### 1.2.4 Introduction

New psychoactive substances (NPS), designer drugs and "legal highs" are terms used to describe emerging novel compounds that are designed to exert similar pharmacological effects as traditional recreational drugs but intended to circumvent legislative measures [1-5]. Ultimately, most analogues eventually become controlled because of their unknown toxicological and pharmacological effects [6]. A dynamic situation exists between law-makers and clandestine laboratory operators that has caused rapid proliferation of novel analogues in recent years and, as such, makes the detection of these new derivatives potentially demanding in different contexts such as forensic drug chemistry and analytical toxicology. According to the latest European Drug Report, more than 500 NPS analogues were reported to the European Union (EU) Early Warning System (EWS) over the last decade with the number of new analogues reported in the last five years comprising approximately 80% of the total number [7]. The highest number of new analogues reported for the first time was in 2014 with 101 analogues (~20%). The NPS market has been traditionally dominated by synthetic cannabinoids with 157 of the 467 analogues (34%) reported between 2009 and 2015, however, psychedelic tryptamines, piperazines and hallucinogenic phenethylamines were predominant between 2005 and 2007. In addition to synthetic cannabinoids, synthetic cathinones also dominate the NPS market with 93 analogues (20%) reported between 2009 and 2015 and higher numbers of analogues reported compared to synthetic cannabinoids in 2010 and 2015 [7, 8]. More recently there has been an emergence of synthetic opioid and designer benzodiazepine derivatives which have exhibited much higher potencies than their traditional counterparts [9, 10]. These trends, in addition to the lack of available certified reference materials (CRMs) for novel analogues, highlights the fact that traditional targeted screening techniques are

inadequate in handling the rapid proliferation of NPS subsequently allowing them to potentially go undetected in routine screening analyses [11].

Traditionally, the analysis of NPS has been performed using conventional gas chromatography – mass spectrometry (GC-MS) or liquid chromatography – tandem mass spectrometry (LC-MS/MS) using triple quadrupole (QqQ) mass analyzers for screening and quantification of NPS. More recently, high-resolution mass spectrometry (HRMS) has grown in popularity due to its ability to measure accurate masses and operate in data-independent acquisition (DIA) modes [12]. This acquisition technique provides comprehensive full scan MS and MS/MS that can be retrospectively interrogated for new analytes of interest without the need for re-extraction and re-analysis in the application of non-targeted/untargeted screening.

This review will focus on the use of HRMS for the analysis of NPS, particularly highlighting the different techniques used for sample preparation, instrumental analysis, data acquisition and data processing in a range of matrices in different analytical contexts such as forensic drug chemistry and analytical toxicology. Since there is scope for HRMS to be utilized for non-targeted screening, an overview of the current applications of this technique will be provided with discussion on its potential future directions.

### 1.2.5 Analysis of NPS using HRMS

A literature search was performed using public domain repositories such as PubMed and ScienceDirect with the search term “new psychoactive” in combination with one or more of the following: “high-resolution”, “mass spectrometry”, “time-of-flight” and “orbitrap”. A total of 95 articles published between 2010 and early 2017 with 68 original research articles related to the analysis of NPS using HRMS were selected for

inclusion in this review. The first publication describing the use of HRMS for the analysis of NPS was in 2010 regarding the metabolism of 3,4-methylenedioxypyrovalerone (MPDV) published by Meyer *et al*. [13] and was followed by an increasing number of publications each year with a total of 25 publications identified in 2016, double the number published in 2015 (Figure A.1 in Appendix A). The increasing use of HRMS has been highlighted by several reviews, mostly focusing on the role of this technique in forensic and clinical toxicology [14-16]. Recently, Maurer and Meyer [17] reviewed the use of HRMS in toxicology and attributed its increased popularity to factors such as the ability to differentiate compounds with identical nominal masses but different accurate masses and the ease at which new compounds can be added to already existing screening procedures. Furthermore, they highlighted limitations such as instrument cost, the complexity of data processing software and the requirement of skilled operators. Finally, Meyer and Maurer [15] reviewed literature pertaining to the use of LC coupled to low- and high-resolution instrumentation for screening of NPS in biological matrices. They concluded that low-resolution mass spectrometry is still the standard technique for quantitative analysis due to ease of operation and reasonable cost, however, HRMS is likely to become the gold standard for non-targeted screening in coming years, provided that instrument prices are reduced and data mining software becomes more user-friendly.

### 1.2.6 Overview of the role HRMS in different analytical contexts

HRMS is a versatile analytical technique that can be applied in different configurations with interchangeable ionization sources and sophisticated data acquisition capabilities. Applications may range from the generation of molecular formulae from accurate masses to the development of screening and quantitative methods and further to non-

targeted screening strategies. Consequently, HRMS has become an important technique in drug testing for therapeutic, medico-legal and law enforcement purposes.

The analysis of seized materials in forensic drug chemistry is performed in accordance with the recommendations outlined by Scientific Working Group for the Analysis of Seized Drugs (SWGDRUG) [18]. Traditionally, this includes a combination of conventional analytical techniques such as GC-MS, Fourier-transform infrared (FTIR) spectroscopy and nuclear magnetic resonance (NMR) spectroscopy for confirmation and structural elucidation [11]. Recently, HRMS has been employed to confirm the proposed identity from GC-MS library matches by generating molecular formulae from acquired accurate masses. Unfortunately, in most cases involving NPS, commercial GC-MS libraries do not contain novel analogues. In this case, HRMS is often used to perform tandem MS (MS/MS) experiments to evaluate the collision-induced dissociation (CID) pathways for putative structural elucidation followed by confirmation using NMR spectroscopy. The aforementioned strategies have also been adopted for the analysis of purchased materials from "headshops" or from online vendors to determine the composition of "legal high" products available on the market. In both cases, the objective of these analyses is focused on the identification of active components and is qualitative rather than quantitative, however, determination of the purity of the material may be a requirement and can be determined by GC-MS or quantitative NMR.

In analytical toxicology, systematic toxicological analysis (STA) provides the identity and, in most circumstances, the concentrations of compounds present in biological matrices. For clinical toxicology, these analyses are typically qualitative and are intended to provide clinicians with information that is used to develop appropriate treatment plans for patients suspected of being intoxicated by particular substances.

Ojanperä *et al.* [16] reviewed the role of HRMS and stated that emergency clinical toxicological analyses are often restricted to two hours for sample transportation, analysis and reporting and subsequently limiting the analytical techniques that can be used. Simultaneously, Wu *et al*. [19] highlighted that unknown compounds pose serious challenges for clinicians regarding the treatment of patients. In addition, they also indicated that traditional targeted methods are limited in their ability to detect and identify novel analogues and suggested that HRMS may be a solution to this problem by providing a comprehensive screening tool.

For forensic toxicology, the same principals apply as clinical toxicology, however, the focus is shifted towards the requirements for results to be admissible and justifiable in a court of law [16]. Unlike clinical toxicology, forensic toxicology samples are typically subjected to a confirmation step following screening procedures and require fully validated quantitative procedures. Consequently, the detection and putative identification of novel analogues using non-targeted strategies bears no evidential weight since identification is limited by the requirement for the use of CRMs or mass spectral libraries.

Finally, the use of HRMS in metabolism studies has increased in recent years particularly because of the sophisticated software tools available [14]. Peters [20] reviewed the recent developments of LC-MS for metabolism studies of NPS identifying that the main advantage of HRMS is the elimination of interferences that have the same nominal mass but different accurate masses. HRMS; however, may not necessarily contribute more value to structural assignments of metabolites with intact product ions. The toxicokinetics of NPS have been comprehensively reviewed by Meyer [6] and Ellefsen *et al*. [21].

The role and application of HRMS is variable in different contexts, however, the general workflow is typically the same, which includes: sample preparation, instrumental analysis, data acquisition and data processing.

### 1.2.7 Sample preparation

Sample preparation procedures are often a requirement prior to instrumental analysis to extract analytes of interest out of complex matrices to provide cleaner extracts for the purpose of maintaining instrument capability. The sample preparation techniques reported have varied between matrix and within matrix type depending on the level of sensitivity and specificity required for particular assays.

#### *1.2.7.1 Seized materials and purchased legal highs*

These materials often exist in a wide variety of forms including powders or crystalline solids, herbal materials and blotter papers. Powders and crystalline solids were largely prepared using solvent extraction or dilution typically with methanol or acetonitrile for MS analyses utilizing LC or GC separation. Schevyrin *et al*. [22-24] dissolved smoke mixtures in methanol followed by an additional filtration step with a cellulose membrane. The extraction of blotter papers has been achieved by soaking the paper in methanol for 6 hours [25-27].

#### *1.2.7.2 Biological matrices*

For blood, sample preparation procedures included protein precipitation, liquid-liquid extraction (LLE), salting-out assisted liquid-liquid extraction (SALLE) and microwave-assisted extraction (MAE) [28-32]. Glicksberg *et al*. [28] reported the use of protein precipitation with acetonitrile followed by solid-phase extraction (SPE) for the extraction of synthetic cathinones from blood plasma and urine. Extraction efficiencies of greater than 80% and 90% were reported for plasma and urine,

respectively. The use of acetonitrile as a solvent for LLE [30] and SALLE [31] procedures has shown promise for the extraction of synthetic cathinones and synthetic cannabinoids with average recoveries greater than 80%.

The analysis of NPS in urine has typically been limited to the detection of parent molecules after extraction by SPE or LLE without the use of enzymatic or acid hydrolysis. Concheiro *et al.* [33, 34] utilized SPE for the extraction of synthetic cathinones and other NPS from 100 μL of urine using strong cation exchange (SCX) cartridges. They observed recoveries for most analytes to be greater than 90%. Archer *et al*. [35-37] has reported the use of LLE and SPE for the analysis of urine samples obtained from street urinals. In addition, SPE has been commonly used for the extraction of wastewater samples for epidemiological studies [38-40]. Bäckberg *et al*. [41] reported the use of a dilute and shoot method for the detection of MDMB-CHMICA in the urine of patients with non-fatal intoxications. The parent molecule; however, was not detected in urine but could be quantified in serum. Enzymatic hydrolysis with β-glucuronidase has been performed in a limited number of cases prior to SPE. [42, 43]. Sundström *et al*. [43] developed a NPS screening method in urine which included various hydroxylated and carboxylated synthetic cannabinoids metabolites which were positively detected in authentic urine samples.

The analysis of hair has been investigated in a limited number of studies with sample preparation procedures including MAE [32] and solvent extraction following ball mill pulverization [44]. Montesano *et al.* [45] evaluated the use of pressurized liquid extraction (PLE) for the extraction of various NPS analogues from cut hair following external decontamination. They investigated the use of different extraction temperatures and solvents and found that recoveries were typically higher with water and methanol (90:10 v/v) at 125ºC, however, potential thermo-degradation should be

considered when extracting at such high temperatures.

### 1.2.8 Instrumental analysis techniques

Over the years, many instrumental techniques have been investigated and evaluated for the analysis of NPS in different matrices in a variety of contexts. In most cases, conventional chromatographic methods such as reversed-phase LC and GC are commonly used particularly in toxicological assays where chromatographic separation is often necessary for complex biological matrices. Additionally, the use of direct sampling techniques has also been reported, particularly in forensic drug chemistry. Figure A.2 summarizes the frequency of chromatographic and direct sampling techniques. These techniques are typically coupled or interfaced with hybrid quadrupole time-of-flight (QTOF) mass spectrometers. However, the use of TOF instruments, high-resolution ion trap instruments such as the Thermo Fisher Scientific (Bremen, Germany) hybrid quadrupole-Orbitrap (Q Exactive™) and hybrid linear ion trap-Orbitrap (LTQ Orbitrap XL™) mass analyzers are also common. Figure A.3 summarizes the frequency of different HRMS platforms.

#### *1.2.8.1 Conventional separation techniques coupled to HRMS*

LC has been the most commonly adopted conventional separation technique coupled to HRMS for the analysis of NPS due to the well-recognized fact that analytes of interest do not need to be volatile and do not require derivatization [15, 28, 30, 33, 39, 42, 43, 46-48]. Subsequently, the use of GC coupled to HRMS for the analysis of NPS has been limited. Ojanperä *et al*. [49] reported the use of GC-QTOF-MS with atmospheric pressure chemical ionization (APCI) for the detection and quantification of a small of number of NPS in sheep blood without derivatization. Few studies have involved the use of both LC and GC coupled to HRMS. Schevyrin *et al*. [22-24]

published a series of articles reporting the detection of several synthetic cannabinoids for the first time in smoke mixtures from Russia and Belarus using both LC and GC coupled to QTOF-MS. The combination of both chromatography methods was used in lieu of these compounds having spectra in commercial libraries for GC-MS. Furthermore, the use of capillary electrophoresis (CE) coupled to QTOF-MS has been only reported once for the analysis of NPS in serum and hair by Woźniakiewicz *et al*. [32] with its limited use likely due to inconsistent migration times and reduced sensitivity compared to conventional LC and GC [50].

#### *1.2.8.2 Direct sample analysis techniques coupled to HRMS*

Recently, there has been a significant growth in the use of direct sampling analysis techniques, particularly in the analysis of seized materials. The advantage of this technique is the ability to rapidly analyze samples without chromatographic separation and with minimal to no sample preparation. Direct sampling techniques have been performed using an LC system where the sample is injected into the carrier flow that is delivered directly into the MS bypassing the chromatographic column. This technique is known as flow injection analysis (FIA) and has been reported on a single occasion by Alechaga *et al*. [51] for rapid, wide-range screening of NPS in "legal highs". Although this technique is rapid, it still requires minimal sample preparation such as dissolution of the sample in an appropriate solvent.

In addition, the use of matrix-assisted laser desorption ionization (MALDI) and desorption electrospray ionization (DESI) coupled to HRMS has been reported for the analysis of NPS [52-54]. Ostermann *et al*. [52] analyzed NPS CRMs and authentic samples using MALDI coupled to an LTQ-Orbitrap. It was indicated that sample preparation and analysis (MS and MS/MS) could be performed in approximately 4 min providing a rapid analytical technique. MALDI offers relatively simplistic sample

preparation and easy-to-interpret mass spectra, however, considerations need to be made regarding matrix selection and laser power to generate optimal results. More novel techniques such as proton transfer reaction (PTR) [55] and selective reagent ionization (SRI) [56, 57] coupled to QTOF-MS have been reported, however, their use has been limited.

The most commonly adopted ambient ionization technique is direct analysis in real-time (DART) mass spectrometry which is capable of rapidly analyzing samples without sample preparation. Briefly, DART-MS consists of two orifices (the outlet of the ion source and the inlet of the MS), samples are placed in between these orifices and their molecules interact with metastable ions created by the ion source which in turn produce monoisotopic ions $[M+H]^+$ or $[M-H]^-$ for basic and acidic molecules, respectively [58]. DART-MS has traditionally been coupled to TOF instruments particularly the JEOL AccuTOF™ DART (Tokyo, Japan), however, they have also been coupled with QTOF and Orbitrap mass analyzers. While this technique has been largely adopted for the analysis of seized materials, it has not found applications in analytical toxicology.

Poklis *et al.* [59] were the first to publish work that utilized DART coupled to HRMS for the analysis of purchased legal highs using an AccuTOF™ DART. They analyzed two products purchased on the internet, “Raving Dragon Novelty Bath Salts” and “Raving Dragon Voodoo Dust”, and found them to contain methylone and pentedrone, respectively. This study also highlighted the adaptive nature of the drug market and how it responds to legislative changes. The first product, purchased in February 2011 was found to contain methylone which was uncontrolled at the time. This product was removed from the market in October of the same year due to subsequent scheduling of mephedrone, methylone and MDPV and replaced with the second product in February

2012. This product was found to contain pentedrone which was not scheduled under the Controlled Substances Act (United States).

Musah *et al*. [60] reported the use of an AccuTOF™ DART with in-source CID to analyze pure synthetic cathinone standards or mixtures of cathinones with adulterants/cutting agents without sample preparation. Precursor ions for all cathinones and adulterants were detected and components of the mixtures could be identified by looking at the individual pure cathinone MS/MS spectra for each component. In addition, mixtures containing multiple cathinones could also be differentiated. They highlighted that due to the rapid analysis time samples containing synthetic cathinones and cutting agents could be triaged and this could be a viable option for reducing routine casework backlogs and provide the necessary information to make decisions on further confirmatory testing methods.

DART-MS has been also investigated for the analysis of synthetic cannabinoids in seized herbal materials. Habala *et al*. [58] analyzed 8 samples using a DART source coupled to an LTQ Orbitrap XL™ mass analyzer. The samples were analyzed using different methods including direct analysis of the solid herbal material and methanolic extracts. They positively identified six synthetic cannabinoids in the seized samples with identification achieved by comparing the MS/MS data with those reported in literature in addition to GC-MS data compared with the SWGDRUG library. A drawback of directly analyzing herbal material is often the inhomogeneity of the samples and it is recommended that sampling be conducted in replicate and at different locations within the seized exhibit. It was also discovered that the leaves have a greater concentration than the stems of plant material. This study highlights the viability of DART-MS for the analysis of herbal materials that does not rely on solvent selection and chromatographic methods for separation.

Comprehensive screening of NPS using DART-MS has also been reported by Gwak *et al*. [61] who developed a method to screen for 35 NPS using DART coupled to a hybrid QTOF-MS. The panel comprised of mostly synthetic cathinones and synthetic cannabinoids with a single phenethylamine derivative (25I-NBOMe) and all analytes were detected with mass errors within ± 5 ppm. The panel of selected analytes; however, contained many isomeric compounds that could not be differentiated by full scan MS since there is no separation component in DART-QTOF-MS. They also highlighted that the use of a QTOF mass analyzer instead of the most commonly used AccuTOF™ provides the ability to simultaneously collect full scan MS and MS/MS data. They also compared the product ion spectra of the selected analytes generated using DART and ESI and found that the relative intensities were similar to those provided by ESI, allowing for comparison of DART-MS data with spectral libraries developed using ESI. In addition, they also assessed the limit of detection for the DART-QTOF-MS and found that all analytes had LODs between 300 to 340 pg. This screening method was successfully applied to authentic samples with identification based on comparison with spectral libraries, however, they could not detect both compounds in one of the samples due to the data-dependent acquisition (DDA) method. It was stated that the "Auto MS/MS" function selects only the most abundant peak for CID, however, to our knowledge, multiple precursors can be selected using this function that would allow MS/MS spectra to be produced for both analytes.

Although this technique is rapid and high-throughput, there are certain limitations that should be considered. Firstly, since there is no chromatographic separation, isomeric compounds cannot be differentiated if their precursor and product ions are identical such as the positional isomers of 4-methylmethcathinone (mephedrone). Secondly, complex spectra containing analytes of interest, carrier flow components and

interferences are produced due to the fact that all ions are recorded within the very short time frame that can be difficult to interpret particularly for MS/MS.

### 1.2.9 Data acquisition

HRMS offers powerful data acquisition techniques compared to those employed by low-resolution mass analyzers and has the capability of being operated in a number of acquisition modes. The simplest data acquisition technique, which is a generic feature for all HRMS platforms, is full scan MS mode which measures all intact masses that reach the detector. This provides accurate *m/z* values that can be used to generate chemical formulae with high mass accuracy (< 5 ppm mass error). Archer *et al*. [37] employed only full scan MS for the analysis of NPS in pooled urine samples indicating that if there was the possible presence of a substance that the residue could be re-analysed using MS/MS or MS/MS/MS ($MS^3$). Although, it is unclear as to why they used only full scan MS considering they were using a LTQ Orbitrap XL™ which is capable of collecting MS and MS/MS data simultaneously, removing the need for re-analysis. Determination of chemical formulae and double bond equivalents (or degree of unsaturation; DBE) based on accurate mass can provide important information, however, it does not provide information on chemical structure, therefore, MS/MS is used for CID to provide putative structural elucidation. MS/MS can be either tandem-in-space such as QTOF mass analyzers or tandem-in-time such as linear ion Orbitrap instruments. In addition, MS/MS can be operated in either DDA or DIA modes.

#### *1.2.9.1 Data-dependent MS/MS acquisition*

DDA operates by taking an initial MS survey scan and then MS/MS events are triggered if precursor ions in the preceding scan meet predefined criteria such as an intensity threshold for *n*-selected precursor ions. This acquisition mode can be

operated in an "untargeted" manner where MS/MS events are triggered based on the abundance of precursor ions in the preceding MS scan. A limitation of this technique is that it is possible for MS/MS events to be triggered by abundant and irrelevant compounds such as background or contamination ions that may necessitate reanalysis if analytes of interest did not trigger an MS/MS event. Andrés-Costa *et al.*[38] reported the use of information-dependent acquisition (IDA) with an inclusion list for the quantification of NPS in wastewater using a Sciex TripleTOF (Framingham, MA, USA). Precursor ions that exceeded 1000 counts and were within an ion tolerance of 10 mDa were selected for MS/MS at a collision energy of 40 eV. They suggested that data can be acquired for multiple CEs in separate injections for lower intensity precursor ions or by adding IDA functions at different collision energies for higher intensity ions. The lowest calibration level for each analyte was determined by the concentration that gave an intensity ≥ 10,000 counts to ensure that MS/MS was triggered for lower concentrations and with achievable identification. To increase the coverage of precursor ions subjected to MS/MS it may be reasoned that the number of MS/MS events per scan can simply be increased, however, the cycle time (MS scan + *n*MS/MS scans) should be considered in conjunction with chromatographic peak widths.

Additionally, DDA can be operated in a targeted precursor selection mode whereby MS/MS events are triggered when pre-selected mass-to-charge (*m/z*) ratios in inclusions lists are detected in the preceding MS scan [28, 45, 49]. These inclusion lists are typically populated with precursor ion data and, if known, retention times obtained from CRMs. Inclusion of retention time for a particular *m/z* value will only trigger MS/MS events for a specified retention time window. Furthermore, masses can be specified for MS/MS exclusion, such as common background and interference ions.

Concheiro *et al*. [33, 34] reported the use of data-dependent MS/MS (ddMS$^2$) with an inclusion list using a Q Exactive™. Detected precursor ions above the optimized threshold (up to 10 per cycle) were filtered by the quadrupole, fragmented by higher energy collision dissociation (HCD) followed by collection in the C-trap and analysed by the Orbitrap. Targeted DDA ensures that only analytes of interest trigger MS/MS events making the data analysis procedure significantly easier. A limitation of this acquisition technique; however, is that it does not allow for retrospective data interrogation of new compounds if they were not subjected to MS/MS, therefore, samples would need to be extracted and reanalyzed which may not be possible if they are no longer available.

Fortunately, complementary targeted and untargeted DDA can be performed in a single analysis. This technique operates by conducting an MS scan followed by targeted MS/MS using an inclusion list and then untargeted MS/MS on *n*-selected precursors. González-mariño *et al.* [40] reported the use of a DDA acquisition mode for screening of NPS that involved MS/MS events for the top 5 most abundant precursor ions in the MS scan. Additionally, the DDA method also had an inclusion list of precursor ions for analytes that did not have reference standards available. They also performed targeted screening using MS data from synthetic cannabinoid and cathinone reference standards.

More recently in 2016, Qian *et al*. [62] detected and identified four new synthetic cannabinoids (ADB-BINACA, AB-FUBICA, ADB-FUBICA and AB-BICA) in a seized sample from a dismantled clandestine laboratory in China. DDA acquisition was performed with an MS scan succeeded by an MS/MS scan with a sweeping collision energy (25 ± 15 V in this case) to generate product ion spectra.

### *1.2.9.2 Data-independent MS/MS acquisition*

DIA techniques subject all precursor ions detected in the MS scan to CID, providing full scan MS/MS. DIA is typically achieved by the rapid alternation between low and high energy channels. Most vendors offer DIA techniques such as $MS^E$ (Waters Corporation, Milford, MA, USA), All Ions MS/MS (Agilent Technologies, Santa Clara, CA, USA), broadband CID (bbCID; Bruker, Billerica, MA, USA). More novel DIA techniques such as sequential window acquisition of all theoretical mass spectra (SWATH®; Sciex) have been developed which involves sequential CID of mass range increments. Kinyua *et al*. [63, 64] reported the use of All Ion MS/MS in two separate studies for qualitative screening of NPS in biological matrices. The data was acquired using three scan segments with different collision energies (0, 15 and 35 eV) to provide the precursor ion (0 eV) and product ions at low and high collision energies (15 and 35 eV, respectively). Sundström *et al.* [43] developed and validated a broad screening and quantification method for synthetic cannabinoids and cathinones using bbCID, with reliable identification when compared to a database of 277 compounds

Baz-Lomba *et al.* [39] conducted screening of psychoactive substances including a limited number of NPS in wastewater samples using $MS^E$. A MS scan was acquired using a collision energy of 6 eV in the first low energy function followed by a collision energy ramp from 15 to 50 eV in the second high energy function. Similarly, Pasin *et al.* [31] analyzed 37 NPS (mostly cathinones) in post-mortem blood using a first function collision energy of 6 eV and a second function collision energy ramp of 10-40 eV to produce fragment-rich product ion spectra. The major advantage of DIA techniques is that it offers full retrospective data interrogation capabilities with the acquisition of full scan data for both MS and MS/MS [44]. The main limitation of DIA is that due to multiple precursor ions simultaneously subjected to CID in the same

MS/MS event, spectra containing product ions for all precursor ions are generated ('chimeric spectra'). These spectra can be difficult to interpret if the product ions cannot be associated with the correct precursor ion [65].

#### *1.2.9.3 $MS^n$ acquisition*

An advantage of tandem-in-time MS/MS techniques is that higher order or multi-stage MS/MS experiments ($MS^n$) can be performed. This involves an initial CID experiment on the precursor ion followed by a subsequent CID on a selected product ion. This is possible in tandem-in-time instruments because trapped ions are subjected to a collision energy and selectively ejected with the process repeated to the $n^{th}$ degree. $MS^2$ is the most commonly used acquisition technique in routine analyses, however, $MS^n$ is often used for elucidation of product ions. While there have been no $MS^n$ studies reported using ion-trap instruments, "pseudo-$MS^3$" experiments using QTOF instruments for structural elucidation have been performed by applying high source voltages to induce in-source CID followed by CID using the collision cell [25-27, 66, 67]. This technique was applied to the structural elucidation of new synthetic cannabinoid derivatives, AM(N)-2201, BIM-018 and BIM-2201. Pseudo-$MS^3$ experiments were used to investigate the CID pathway of the common product ion *m/z* 233.1085 for both AM(N)-2201 and BIM-2201 by using a fragmentor voltage of 260 V to induce in-source CID followed by targeted MS/MS [23].

### 1.2.10 Data processing techniques

Data processing techniques used for the detection and identification of analytes can vary from instrument-to-instrument due to the independent nature of software supplied by instrument vendors. In addition, the objective of an analysis can dictate what workflow is utilized in particular contexts (i.e. targeted vs. non-targeted). These

techniques; however, can be generally categorized into *known* and *unknown* data processing techniques (Figure 1.8). Known data processing techniques can be achieved through the use of CRMs (*targeted screening*) and compound libraries (*suspect screening*). Non-targeted screening will be discussed as a separate section.

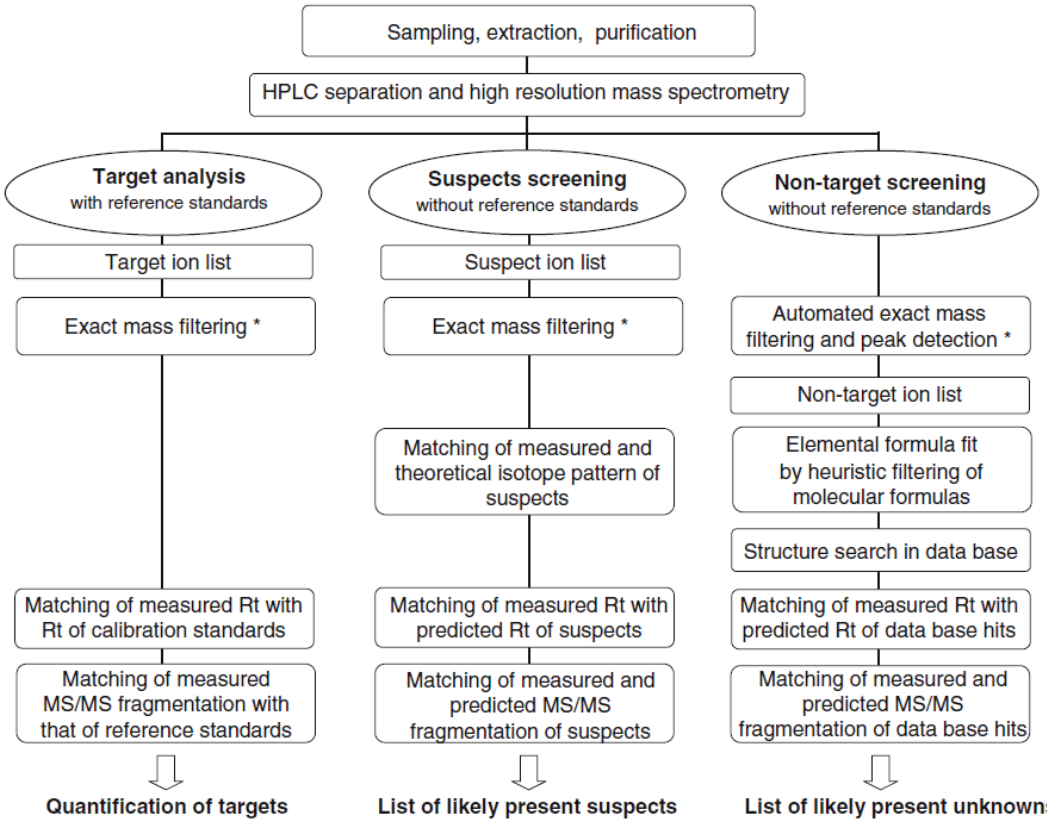


**Figure 1.8** Comparison of systematic workflows for (i) quantitative target analysis with reference standards, (ii) suspects screening without reference standards, and (iii) non-target screening of unknowns in environmental samples by using LC–high resolution (tandem) mass spectrometry.*Note that the m/z range of the extraction window for the exact mass filtering depends on the mass accuracy and the resolving power of the mass spectrometer used. Reproduced from [67] with permission of Springer.

### *1.2.10.1 Targeted screening*

Targeted screening strategies involve the automated interrogation of acquired sample data with data collected from CRMs such as retention time, precursor and product ion

m/z and can be used for analyte confirmation and quantification [63, 68]. Targeted screening methods have been commonly developed in analytical toxicology for the analysis of biological matrices such as blood [30, 31], urine [33, 34, 47, 64] or a combination of both [28]. For qualitative screening, methods can be updated easily with new CRMs, however, a limitation of developing broad in-house libraries that encompass a large number of candidate analytes is the cost of purchasing all necessary CRMs. In addition, the suppliers of CRMs may be located in overseas countries which can result in delays due to permit authorizations and shipping times by which time the analytes may have declined in popularity and disappeared off the market. Furthermore, since many of these compounds are becoming controlled they may be embargoed by enforcement agencies such as the USA Drug Enforcement Administration (DEA) and require additional fees for purchase.

*1.2.10.2* Suspect screening

An alternative approach to developing targeted screening methods is the use of suspect screening which involves the interrogation of acquired sample data using "suspect" compound-specific information in the absence of appropriate CRMs [69]. For a suspected compound, the chemical formula is known and, therefore, the accurate monoisotopic mass ($[M+H]^+$/$[M-H]^-$) can be determined and in turn extracted [63]. Putative identification using suspect screening can then be confirmed by acquiring the appropriate CRM, if available. For the analysis of NPS, most suspect screening methods reported have involved the comparison of acquired sample data with mass spectral libraries for detection and identification. These libraries are often comprehensive, providing better coverage of NPS analogues than conventional targeted methods. Libraries can be typically obtained from instrument vendors or other third party commercial library developers that are curated and regularly updated for

new compounds. Suspect screening has been used in isolation and as a complementary technique with targeted screening for greater analyte coverage [40]. Heikman *et al*. [70] reported the use of complementary targeted and suspect screening with an in-house database containing 500 compounds, CRMs were available for 280 of these compounds with the remainder comprising of rare NPS and their known and predicted metabolites. Some studies have stated that databases or libraries have been used to process data but provided no information on which databases were used or how many compounds were in these databases. The use of the SWGDRUG database has been reported on two occasions for the analysis of synthetic cannabinoids, however, this database is for LRMS EI-MS data only [58, 71]. Other commercial libraries such as the NIST/EPA/NIH NIST 08 and the department of Forensic Science of the Commonwealth of Virginia 2012 custom Druglist have been reported [59]. Custom databases populated with data from different sources have been developed and utilized in two studies [51, 72], however, most databases described encompass many categories of drugs and not just NPS so it is unclear how comprehensive they actually are or the number of NPS derivatives is simply not reported.

Ford and Berg [73] screened almost 100 samples including herbal blends, cigarettes, liquids and powders/pills obtained over a year period (2014-2015) in the United Kingdom using two different mass spectral libraries. The samples were analyzed using the data-independent $MS^E$ acquisition mode and compared to a synthetic cannabinoid mass spectral library with over 100 first, second and third-generation derivatives. In addition, the acquired mass spectra were also compared to a comprehensive general screening that contains over 1300 compounds including approximately 10% NPS. Identification was based on mass accuracy (± 5 ppm) of the precursor and product (qualifier) ion, an average isotopic match within 20% compared to the theoretical ratio

and retention time within ± 0.3 min. The most comprehensive database developed to date was reported by Kinyua *et al*. [63] who built an in-house library using the personal compound database and library (PCDL) manager with over 1500 entries using information from literature including from the European Monitoring Centre for Drugs and Drug Addiction (EMCDDA) and United Nations Office of Drugs and Crime (UNODC). Development of libraries typically relies on primary source information such as those acquired from CRMs and secondary sources such as information published in literature, thus, limiting databases to known compounds. In addition, commercial libraries are often updated with new analogues, however, it is unrealistic to believe that libraries are updated as soon as novel analogues are detected and therefore there will be a delay in detection capabilities.

### 1.2.11 Non-targeted/untargeted screening strategies

The recent proliferation of NPS has initiated considerable interest into the development of so-called "non-targeted" or "untargeted" screening strategies in order to detect and putatively identify novel compounds without the use of CRMs or mass spectral libraries. The use of the term "non-targeted screening" or "non-targeted analysis"; however, has adopted different definitions over the years with an obvious lack of consistency in the use of this concept. Oberacher and Arnhard [65] reviewed the use of non-targeted LC-MS strategies in forensic toxicology indicating that non-targeted analyses can be achieved by applying DDA or DIA techniques and comparing the collected data with mass spectral libraries. In addition, Lung *et al*. [72] reported the use of non-targeted analysis for the detection of NPS in clinical toxicology with DIA and suspect screening. The efficacy of non-targeted screening, in part, relies on the adoption of appropriate data acquisition techniques, however, data acquisition constitutes only one part of the non-targeted screening workflow [74]. The use of mass

spectral libraries for identification of compounds has been advantageous previously, however, with the rapid proliferation of NPS analogues these libraries can no longer be relied upon for detection of novel analogues. This is due to the fact that there can be a considerable delay between the time a novel analogue has been identified and its subsequent entry into a mass spectral library. Therefore, to keep up with the rapidly changing NPS market, more innovative workflows need to be developed and implemented for the detection and identification of NPS.

Non-targeted analysis has been more accurately defined as the detection and identification of compounds in a sample in the absence of prior information or when the molecular content of a sample is unknown [75]. This has been widely used in food and environmental analysis [68, 76]. More prominently, however, non-targeted screening has been used in metabolomics for the detection of biomarkers present in samples after treatment with particular stimuli and the strategies developed have been used as a model or have been adopted for non-targeted analyses in other areas. Metabolomics-based non-targeted strategies are typically designed to identify all compounds in treatment samples and compare them to the control samples to observe changes in the global metabolic profile and to determine potential biomarkers associated with the treatment. In this case, all compounds in either the control or treatment sample can be potentially relevant. The main issue with this *unbiased* approach, particularly in clinical and forensic toxicology, is the relevance of compounds identified. On the other hand, the concept of *biased* non-targeted screening was described by Ibañez *et al*. [75] which involves the discovery of new compounds *related* to known NPS. It should be noted that in this scenario, detection involves the discovery of compounds (components) using data processing techniques and not the detection of ions by the MS. In addition, non-targeted analysis needs to operate under

the assumption that a novel analogue will be extracted using currently employed sample preparation techniques and is ionisable under routine instrumental analysis. Furthermore, the strategies presented herein are mostly for the detection of parent molecules in chemical or biological samples, however, it is possible for these strategies to be extended to the detection metabolites of analogues which scarcely exist as the parent molecule in biological samples (e.g. synthetic cannabinoids). It should also be considered that the detection of analogues which are often present at low or sub-ng/mL levels in biological fluids, such as synthetic cannabinoids and synthetic opioids, may be limited by HRMS sensitivity.

Generally, biased non-targeted screening is a two-step process that involves the discovery or detection of a component followed by putative identification. Component discovery has been identified as the most problematic step, which can be categorized into two different approaches, *top-down* or *bottom-up* (Figure 1.9).

*1.2.11.1 Top-down non-targeted screening*

A top-down approach is best described as the most commonly employed non-targeted approach involving interrogation of mass spectral data by the selection of abundant peaks from the visual inspection of a total ion current (TIC) chromatogram. After the selection of a peak, the molecular formula can be generated from the accurate mass precursor ion along with other structural information such as DBE.

Kneisel *et al.* [77] analyzed different herbal product mixtures by GC-MS and found an abundant peak that could not be identified by the current database at the time, however, it was observed that this compound had product ions similar to those formed by JWH-250.

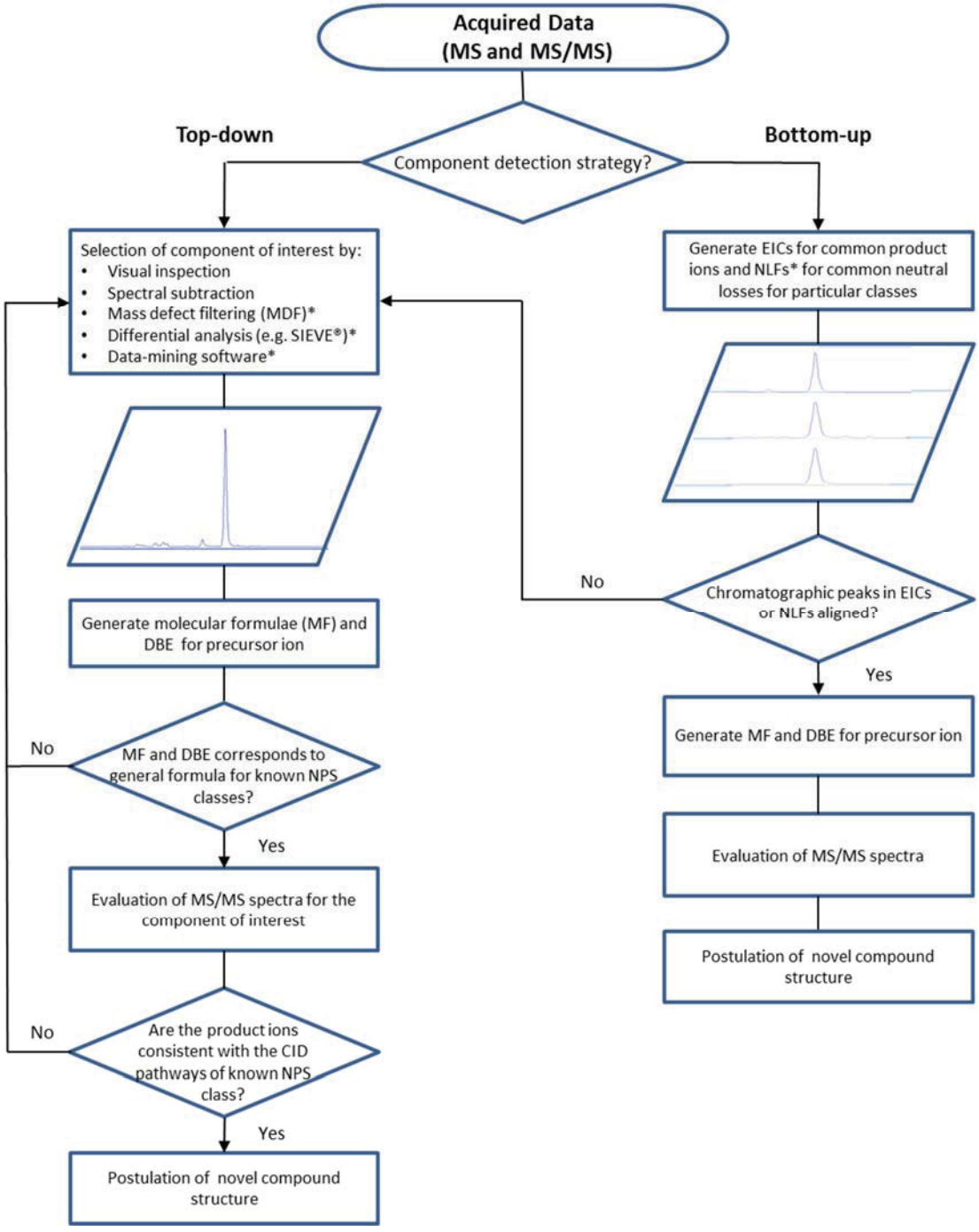


**Figure 1.9** Comparison of top-down and bottom-up non-targeted screening workflows using HRMS. The * denotes that specialised software is required.

It was postulated that the compound was an α-methyl derivative of JWH-250 (a phenylacetylindole synthetic cannabinoids) that had a molecular ion 14 mass units higher than JWH-250. Both the α-methyl derivative and suspect compound had the same fragments under EI-MS, however, when treated with derivatising agents the

respective methyl and silyl derivatives were not formed indicating a lack of the 2-methoxyphenacetyl moiety.

LC-QTOF-MS analyses showed that the product ion at *m/z* 135.1168 corresponded to $[C_{10}H_{15}]^+$ compared to the α-methylphenacetyl fragment (*m/z* 135.0810, $[C_9H_{15}O]^+$). This product ion corresponded to an adamantoyl moiety which was determined with the assistance of NMR studies and the compound was identified as 3-(1-adamantoyl)-1-pentylindole, now known as AB-001. An obvious limitation to top-down screening using the visual inspection of TICs is that it is only appropriate for samples that produce simple TICs with minimal abundant peaks that can be quickly located. Therefore, this technique is not well suited to toxicological samples with complex TICs containing compounds of interest not visually obvious and abundant, potentially overlapping with endogenous components and background ions. Furthermore, the main limitation of a top-down approach is assessing the relevance of candidate peaks with respect to the compound class of interest. For instance, does the generated molecular formula, DBE and MS/MS data correlate with the compound class of interest? As a result, this approach can be a time-intensive and laborious process when multiple candidate peaks are required for interrogation.

The use of an innovative data filtering approach has been reported in an attempt to improve the efficacy of top-down approaches. Grabenauer *et al*. [78] reported the use of *mass defect filtering* (MDF) for the analysis of synthetic cannabinoids in herbal products (Figure 1.10) and was able to detect JWH-250 that was not visible in the TIC. MDF, a technique commonly used in metabolomics, filters out mass spectral data based on a defined mass defect window and is effective when a class of related compounds have narrow mass defect ranges [79].

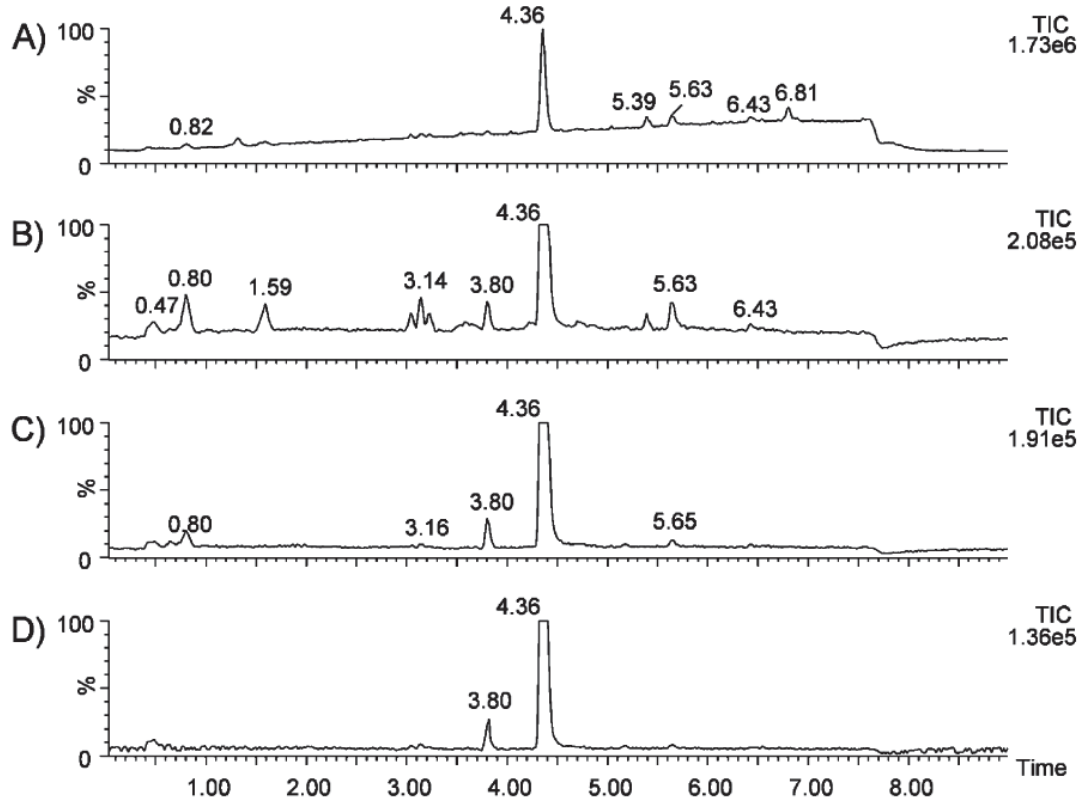


**Figure 1.10** Total ion chromatogram of "K2-Summit" with no filtering (A) and with a mass defect filter centered at 0.1859 with a window of ±50 mDa (B), ± 20 mDa (C), and ±10 mDa (D). Reprinted with permission from [74]. Copyright 2012 American Chemical Society.

In this case, MDF was applied to samples with simple TICs, however, to our knowledge it has not been applied in an analytical toxicological context to assess its efficacy on complex sample TICs. Furthermore, it is likely that many candidate peaks are endogenous components so it is crucial that potentially exogenous peaks are prioritized for interrogation to prevent the interrogation of "false-positive" components. The removal of endogenous or background peaks can be achieved by the use of data processing algorithms to subtract TIC data of a representative pooled matrix or solvent blank from an authentic sample [80, 81]. It may be difficult; however, to obtain such a representative pooled sample that accounts for variations in endogenous component profiles in the population. A more innovative approach to identify exogenous components was reported by Cawley *et al*. [82], who described the

use of *differential analysis* software for the detection of phenethylamine-type NPS in equine urine using SIEVE® (Thermo Fisher Scientific) for doping control (Figure 1.11). The premise of this technique is that it involves the binary comparison of *m/z* data from representative matrix blanks and authentic samples to determine exogenous components and is a technique used mostly in metabolomics.

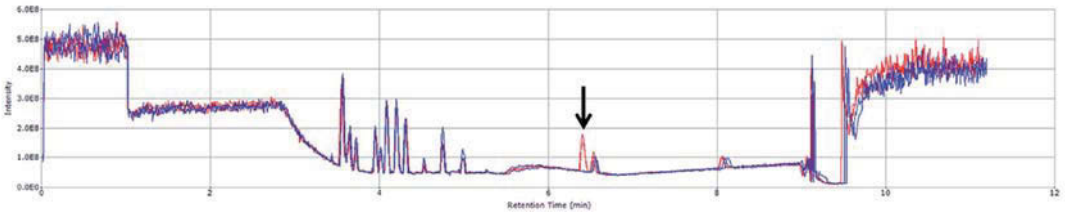


**Figure 1.11** SIEVE® total ion chromatogram (TIC) alignment showing the presence of 25B (annotated with ↓) spiked at 100 ng mL-1 in equine urine by comparison to a blank equine urine sample. [80] Published by The Royal Society of Chemistry.

Finally, most vendors provide data mining software such as Molecular Feature Extraction (MFE, Agilent Technologies), Find by Formula (FbF, Agilent Technologies), Chromalynx XS (Waters Corporation), Trace Finder (Thermo Fisher Scientific) and Peak View (Sciex). The use of software-assisted peak detection approaches have typically been limited to suspect screening [38, 47, 63, 64, 73, 83-85].

*1.2.11.2 Bottom-up non-targeted screening*

A *bottom-up* approach is an alternative technique involving the interrogation of acquired data using characteristic class-specific mass spectral information such as common product ions and neutral losses. Since this technique uses class-specific information it reduces the likelihood that "false-positive" components will be interrogated. Grabenaurer *et al*. [78] introduced the concept of *precursor ion*

*searching,* explaining that structurally related compounds can have the same product ions and that novel analogues could be detected by searching for the precursor ions of common product ions. Recently, Pasin *et al*. [86] reported the characterization of hallucinogenic phenethylamines using HRMS for non-targeted screening, identifying that common product ions and neutral losses could be monitored using basic data processing techniques such as *product ion searching* and *neutral loss filtering* (NLF). Figure 1.12 illustrates the use of NLF with precursor neutral loss chromatograms (pNLCs). Over the years, there has been considerable analysis of NPS analogues using HRMS, however, only some have reported the CID pathways [22-24, 46, 71, 84-88]. Furthermore, metabolism studies generally offer information on the CID pathways of NPS analogues since it is a conventional practice to determine the CID pathways of the parent molecule in order to identify the locations of metabolic transformations [48, 89-97]. As mentioned previously, the efficacy of bottom-up approaches largely relies on the acquisition of MS/MS data and it has been suggested that DIA techniques should be used rather than DDA [86].

The major limitation of this approach is that it requires data processing software capable of generating numerous EICs for characteristic product ions, if monitoring all potential NPS classes. Additionally, it is possible in the future that novel analogues could potentially have different product ions due to innovative structural modifications. In this case, the use of NLFs may account for novel analogues that have unknown product ions but exhibit known neutral losses. NLF, however, is a technique that is not widely incorporated into standard data processing software and has inconsistent functionality from vendor-to-vendor.

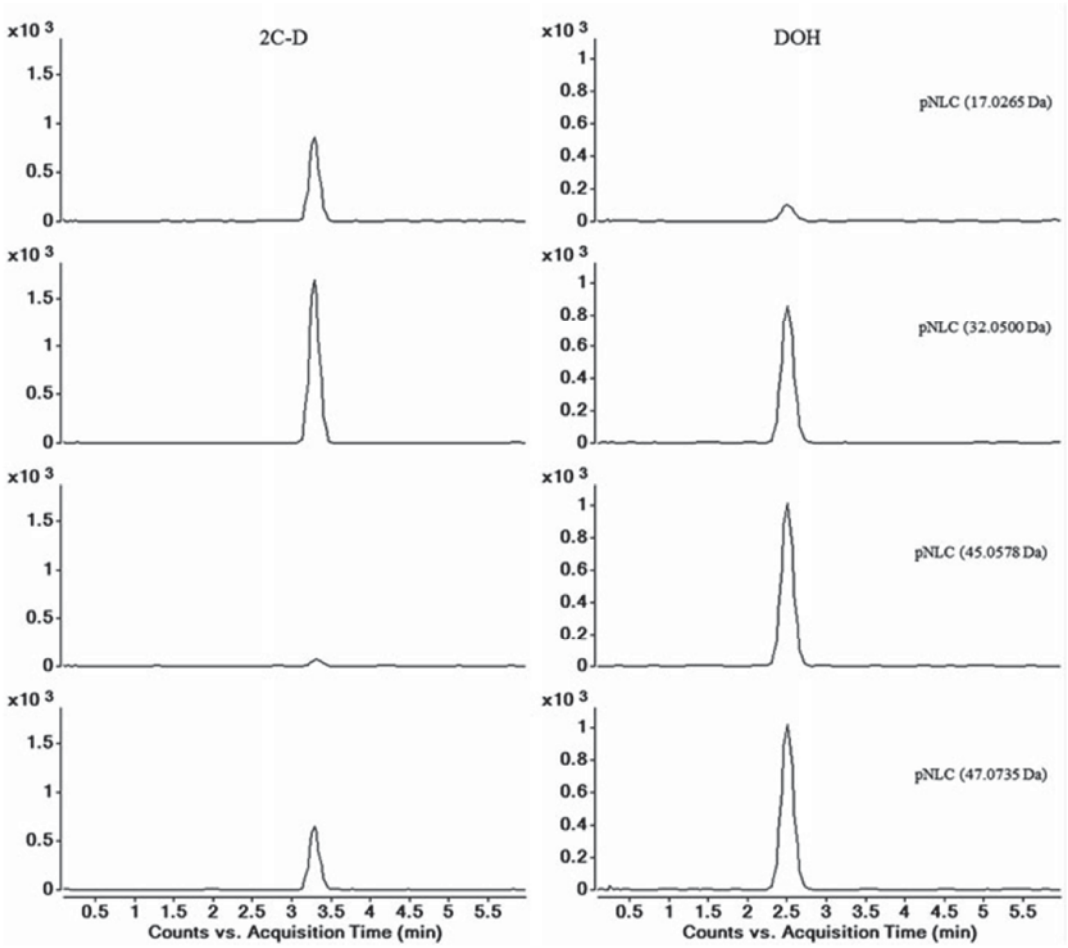


**Figure 1.12** Precursor neutral loss chromatograms (pNLCs) of 17.0265, 32.0500, 45.0576 and 47.0735 Da for 2C–D and DOH at 20 eV. Reproduced from [84] with permission of Springer**.**

### *1.2.11.3 Component identification*

Once a component of interest has been selected, a putative structure can be postulated from the molecular formula, DBE and interpretation of MS/MS spectra using known CID pathways [82, 93, 95]. This assessment of MS/MS spectra requires experienced analysts who are familiar with the CID pathways of NPS. Furthermore, *in silico* fragmentation can be performed to assess whether the postulated structure's experimental and theoretical fragmentation correlate. This has been performed using software such as Mass Frontier™ (Thermo Fisher Scientific) [82, 98] and Molecular Structure Correlator (MSC; Agilent Technologies) [47].

### 1.2.12 Conclusions and perspectives

The use of HRMS in forensic drug chemistry and analytical toxicology has gained popularity over recent years, providing a highly versatile analytical platform for targeted, suspect and non-targeted screening. It is evident that HRMS will ultimately become the gold standard for the analysis of samples suspected of containing NPS due to the ability to acquire full scan MS and MS/MS that can then be retrospectively interrogated. Future developments in HRMS sensitivity will also allow it to be applied to samples containing analogues, which are typically present at low concentrations in biological fluids such as synthetic cannabinoids and synthetic opioids. Presently, there is no single data processing technique that can be adopted for the reliable detection of novel analogues in non-targeted screening, however, the combination of reported techniques can be effective for the discovery of novel analogues. These reported techniques may include the activity-based untargeted screening approaches such as that developed by Cannaert *et al*. [99] for synthetic cannabinoids. It is envisaged that non-targeted screening will become a high-throughput and routinely employed technique. At this stage, due to the current capabilities of vendor software, the use of this technique should be intelligence-led and reserved for samples suspected of containing NPS. Accordingly, non-targeted screening approaches will need to be updated to accommodate the advances in data processing software. The development of software-dependent top-down workflows requires analysts that are familiar and competent in the use of specific software packages. Furthermore, these workflows typically cannot be translated to other software platforms due to the exclusive nature of data processing software. Currently, bottom-up workflows offer a globally compatible and software-agnostic option since the generation of EICs for common product ions does not require specialized software. This approach; however, requires

the knowledge of common product ions for NPS classes that will need to be updated to include common product ions for novel derivatives. This approach can provide potential intelligence on NPS misuse on local and international levels.

### 1.2.13 References


1. Collins M. Some new psychoactive substances: precursor chemicals and synthesis-driven end-products. *Drug Test Anal*. 2011;3:404-16.
2. Gibbons S. 'Legal Highs' - novel and emerging psychoactive drugs: a chemical overview for the toxicologist. *Clin Toxicol*. 2012;50:15-24.
3. Hill SL, Thomas SHL. Clinical toxicology of newer recreational drugs. *Clin Toxicol*. 2011;49:705-19.
4. Jerrard DA. "Designer drugs" - a current perspective. *J Emerg Med*. 1990;8:733-41.
5. Zawilska JB. "Legal highs" - new players in the old drama. *Curr Drug Abuse Rev*. 2011;4:122-30.
6. Meyer MR. New psychoactive substances: an overview on recent publications on their toxicodynamics and toxicokinetics. *Arch Toxicol*. 2016;90:2421-44.
7. European Monitoring Centre for Drugs and Drug Abuse. European Drug Report 2016. Accessed in October 2016. http://www.emcdda.europa.eu/edr2016
8. European Monitoring Centre for Drugs and Drug Abuse. European Drug Report 2013. Accessed in November 2016. http://www.emcdda.europa.eu/publications/edr/trends-developments/2013
9. Høiseth G, Tuv SS, Karinen R. Blood concentrations of new designer benzodiazepines in forensic cases. *Forensic Sci Int*. 2016;268:35-8.
10. Suzuki J, El-Haddad S. A review: Fentanyl and non-pharmaceutical fentanyls. *Drug Alcohol Depend*. 2017;171:107-16.
11. Archer RP, Treble R, Williams K. Reference materials for new psychoactive substances. *Drug Test Anal*. 2011;3:505-14.
12. Remane D, Wissenbach DK, Peters FT. Recent advances of liquid chromatography-(tandem) mass spectrometry in clinical and forensic toxicology - an update. *Clin Biochem*. 2016;49:1051-71.
13. Meyer MR, Du P, Schuster F, Maurer HH. Studies on the metabolism of the alpha-pyrrolidinophenone designer drug methylenedioxy-pyrovalerone (MDPV) in rat and human urine and human liver microsomes using GC-MS and LC-high-resolution MS and its detectability in urine by GC-MS. *J Mass Spectrom*. 2010;45:1426-42.
14. Meyer MR, Maurer HH. Current applications of high-resolution mass spectrometry in drug metabolism studies. *Anal Bioanal Chem*. 2012;403:1221-31.
15. Meyer MR, Maurer HH. Review: LC coupled to low- and high-resolution mass spectrometry for new psychoactive substance screening in biological matrices - Where do we stand today? *Anal Chim Acta*. 2016;927:13-20.
16. Ojanperä I, Kolmonen M, Pelander A. Current use of high-resolution mass spectrometry in drug screening relevant to clinical and forensic toxicology and doping control. *Anal Bioanal Chem*. 2012;403:1203-20.
17. Maurer HH, Meyer MR. High-resolution mass spectrometry in toxicology:

current status and future perspectives. *Arch Toxicol*. 2016;90:2161-72.
18. . Scientific Working Group for the Analysis of Seized Drugs Recommendations. Accessed in December 2016. http://www.swgdrug.org/approved
19. Wu AH, Gerona R, Armenian P, French D, Petrie M, Lynch KL. Role of liquid chromatography-high-resolution mass spectrometry (LC-HR/MS) in clinical toxicology. *Clin Toxicol*. 2012;50:733-42.
20. Peters FT. Recent developments in urinalysis of metabolites of new psychoactive substances using LC-MS. *Bioanalysis*. 2014;6:2083-107.
21. Ellefsen KN, Concheiro M, Huestis MA. Synthetic cathinone pharmacokinetics, analytical methods, and toxicological findings from human performance and postmortem cases. *Drug Metab Rev*. 2016;48:1-29.
22. Shevyrin V, Melkozerov V, Eltsov O, Shafran Y, Morzherin Y. Synthetic cannabinoid 3-benzyl-5-[1-(2-pyrrolidin-1-ylethyl)-1H-indol-3-yl]-1,2,4-oxadiazole. The first detection in illicit market of new psychoactive substances. *Forensic Sci Int*. 2016;259:95-100.
23. Shevyrin V, Melkozerov V, Nevero A, Eltsov O, Morzherin Y, Shafran Y. 3-Naphthoylindazoles and 2-naphthoylbenzoimidazoles as novel chemical groups of synthetic cannabinoids: chemical structure elucidation, analytical characteristics and identification of the first representatives in smoke mixtures. *Forensic Sci Int*. 2014;242:72-80.
24. Shevyrin V, Melkozerov V, Nevero A, Eltsov O, Shafran Y, Morzherin Y, Lebedev AT. Identification and analytical characteristics of synthetic cannabinoids with an indazole-3-carboxamide structure bearing a N-1-methoxycarbonylalkyl group. *Anal Bioanal Chem*. 2015;407:6301-15.
25. Sekuła K, Zuba D. Structural elucidation and identification of a new derivative of phenethylamine using quadrupole time-of-flight mass spectrometry. *Rapid Commun Mass Spectrom*. 2013;27:2081-90.
26. Zuba D, Sekuła K. Analytical characterization of three hallucinogenic N-(2-methoxy)benzyl derivatives of the 2C-series of phenethylamine drugs. *Drug Test Anal*. 2013;5:634-45.
27. Zuba D, Sekuła K, Buczek A. 25C-NBOMe – New potent hallucinogenic substance identified on the drug market. *Forensic Sci Int*. 2013;227:7-14.
28. Glicksberg L, Bryand K, Kerrigan S. Identification and quantification of synthetic cathinones in blood and urine using liquid chromatography-quadrupole/time of flight (LC-Q/TOF) mass spectrometry. *J Chromatogr B*. 2016;1035:91-103.
29. Soh YN, Elliott S. An investigation of the stability of emerging new psychoactive substances. *Drug Test Anal*. 2014;6:696-704.
30. Montesano C, Vannutelli G, Gregori A, Ripani L, Compagnone D, Curini R, Sergi M. Broad screening and identification of novel psychoactive substances in plasma by high-performance liquid chromatography-high-resolution mass spectrometry and post-run library matching. *J Anal Toxicol*. 2016;40:519-28.
31. Pasin D, Bidny S, Fu S. Analysis of new designer drugs in post-mortem blood using high-resolution mass spectrometry. *J Anal Toxicol*. 2015;39:163-71.
32. Woźniakiewicz A, Wietecha-Posłuszny R, Woźniakiewicz M, Bryczek E, Kościelniak P. A quick method for determination of psychoactive agents in serum and hair by using capillary electrophoresis and mass spectrometry. *J Pharm Biomed Anal*. 2015;111:177-85.
33. Concheiro M, Anizan S, Ellefsen K, Huestis MA. Simultaneous quantification of 28 synthetic cathinones and metabolites in urine by liquid chromatography-

high resolution mass spectrometry. *Anal Bioanal Chem*. 2013;405:9437-48.
34. Concheiro M, Castaneto M, Kronstrand R, Huestis MA. Simultaneous determination of 40 novel psychoactive stimulants in urine by liquid chromatography-high resolution mass spectrometry and library matching. *J Chromatogr A*. 2015;1397:32-42.
35. Archer JR, Dargan PI, Hudson S, Wood DM. Analysis of anonymous pooled urine from portable urinals in central London confirms the significant use of novel psychoactive substances. *QJM*. 2013;106:147-52.
36. Archer JR, Hudson S, Jackson O, Yamamoto T, Lovett C, Lee HM, Rao S, Hunter L, Dargan PI, Wood DM. Analysis of anonymized pooled urine in nine UK cities: variation in classical recreational drug, novel psychoactive substance and anabolic steroid use. *QJM*. 2015;108:929-33.
37. Archer JR, Dargan PI, Lee HM, Hudson S, Wood DM. Trend analysis of anonymised pooled urine from portable street urinals in central London identifies variation in the use of novel psychoactive substances. *Clin Toxicol*. 2014;52:160-5.
38. Andrés-Costa MJ, Andreu V, Picó Y. Analysis of psychoactive substances in water by information dependent acquisition on a hybrid quadrupole time-of-flight mass spectrometer. *J Chromatogr A*. 2016;1461:98-106.
39. Baz-Lomba JA, Reid MJ, Thomas KV. Target and suspect screening of psychoactive substances in sewage-based samples by UHPLC-QTOF. *Anal Chim Acta*. 2016;914:81-90.
40. González-Mariño I, Gracia-Lor E, Bagnati R, Martins CP, Zuccato E, Castiglioni S. Screening new psychoactive substances in urban wastewater using high resolution mass spectrometry. *Anal Bioanal Chem*. 2016;408:4297-309.
41. Bäckberg M, Tworek L, Beck O, Helander A. Analytically Confirmed Intoxications Involving MDMB-CHMICA from the STRIDA Project. *J Med Toxicol*. 2017;13:52-60.
42. Sundström M, Pelander A, Simojoki K, Ojanperä I. Patterns of drug abuse among drug users with regular and irregular attendance for treatment as detected by comprehensive UHPLC-HR-TOF-MS. *Drug Test Anal*. 2016;8:39-45.
43. Sundström M, Pelander A, Angerer V, Hutter M, Kneisel S, Ojanperä I. A high-sensitivity ultra-high performance liquid chromatography/high-resolution time-of-flight mass spectrometry (UHPLC-HR-TOFMS) method for screening synthetic cannabinoids and other drugs of abuse in urine. *Anal Bioanal Chem*. 2013;405:8463-74.
44. Frison G, Frasson S, Zancanaro F, Tedeschi G, Zamengo L. Detection of 3-methylmethcathinone and its metabolites 3-methylephedrine and 3-methylnorephedrine in pubic hair samples by liquid chromatography-high resolution/high accuracy Orbitrap mass spectrometry. *Forensic Sci Int*. 2016;265:131-7.
45. Montesano C, Vannutelli G, Massa M, Simeoni MC, Gregori A, Ripani L, Compagnone D, Curini R, Sergi M. Multi-class analysis of new psychoactive substances and metabolites in hair by pressurized liquid extraction coupled to HPLC-HRMS. *Drug Test Anal*. 2016. doi:10.1002/dta.2043
46. Fornal E. Identification of substituted cathinones: 3,4-Methylenedioxy derivatives by high performance liquid chromatography–quadrupole time of flight mass spectrometry. *J Pharm Biomed Anal*. 2013;81–82:13-9.
47. Paul M, Ippisch J, Herrmann C, Guber S, Schultis W. Analysis of new designer drugs and common drugs of abuse in urine by a combined targeted and

untargeted LC-HR-QTOFMS approach. *Anal Bioanal Chem*. 2014;406:4425-41.
48. Zaitsu K, Nakayama H, Yamanaka M, Hisatsune K, Taki K, Asano T, Kamata T, Katagai M, Hayashi Y, Kusano M, Tsuchihashi H, Ishii A. High-resolution mass spectrometric determination of the synthetic cannabinoids MAM-2201, AM-2201, AM-2232, and their metabolites in postmortem plasma and urine by LC/Q-TOFMS. *Int J Legal Med*. 2015;129:1233-45.
49. Ojanperä I, Mesihää S, Rasanen I, Pelander A, Ketola RA. Simultaneous identification and quantification of new psychoactive substances in blood by GC-APCI-QTOFMS coupled to nitrogen chemiluminescence detection without authentic reference standards. *Anal Bioanal Chem*. 2016;408:3395-400.
50. Baciu T, Botello I, Borrull F, Calull M, Aguilar C. Capillary electrophoresis and related techniques in the determination of drugs of abuse and their metabolites. *TrAC, Trends Anal Chem*. 2015;74:89-108.
51. Alechaga E, Moyano E, Galceran MT. Wide-range screening of psychoactive substances by FIA-HRMS: identification strategies. *Anal Bioanal Chem*. 2015;407:4567-80.
52. Ostermann KM, Luf A, Lutsch NM, Dieplinger R, Mechtler TP, Metz TF, Schmid R, Kasper DC. MALDI Orbitrap mass spectrometry for fast and simplified analysis of novel street and designer drugs. *Clin Chem Acta*. 2014;433:254-8.
53. Stojanovska N, Kelly T, Tahtouh M, Beavis A, Fu S. Analysis of amphetamine-type substances and piperazine analogues using desorption electrospray ionisation mass spectrometry. *Rapid Commun Mass Spectrom*. 2014;28:731-40.
54. Stojanovska N, Tahtouh M, Kelly T, Beavis A, Fu S. Presumptive analysis of 4-methylmethcathinone (mephedrone) using desorption electrospray ionisation - mass spectrometry (DESI-MS). *Aust J Forensic Sci*. 2014;46:411-23.
55. Botch-Jones S, Foss J, Barajas D, Kero F, Young C, Weisenseel J. The detection of NBOMe designer drugs on blotter paper by high resolution time-of-flight mass spectrometry (TOFMS) with and without chromatography. *Forensic Sci Int*. 2016;267:89-95.
56. Acton WJ, Lanza M, Agarwal B, Jürschik S, Sulzer P, Breiev K, Jordan A, Hartungen E, Hanel G, Märk L, Mayhew CA, Märk TD. Headspace analysis of new psychoactive substances using a selective reagent ionisation-time of flight-mass spectrometer. *Int J Mass Spectrom*. 2014;360:28-38.
57. Lanza M, Acton WJ, Sulzer P, Breiev K, Jürschik S, Jordan A, Hartungen E, Hanel G, Märk L, Märk TD, Mayhew CA. Selective reagent ionisation-time of flight-mass spectrometry: a rapid technology for the novel analysis of blends of new psychoactive substances. *J Mass Spectrom*. 2015;50:427-31.
58. Habala L, Valentová J, Pechová I, Fuknová M, Devinsky F. DART - LTQ ORBITRAP as an expedient tool for the identification of synthetic cannabinoids. *Leg Med*. 2016;20:27-31.
59. Poklis JL, Wolf CE, ElJordi OI, Liu K, Zhang S, Poklis A. Analysis of the first- and second-generation Raving Dragon Novelty Bath Salts containing methylone and pentedrone. *J For Sci*. 2015;60:S234-40.
60. Musah RA, Cody RB, Domin MA, Lesiak AD, Dane AJ, Shepard JR. DART-MS in-source collision induced dissociation and high mass accuracy for new psychoactive substance determinations. *Forensic Sci Int*. 2014;244:42-9.
61. Gwak S, Almirall JR. Rapid screening of 35 new psychoactive substances by ion mobility spectrometry (IMS) and direct analysis in real time (DART) coupled to

quadrupole time-of-flight mass spectrometry (QTOF-MS). *Drug Test Anal*. 2015;7:884-93.
62. Qian Z, Hua Z, Liu C, Jia W. Four types of cannabimimetic indazole and indole derivatives, ADB-BINACA, AB-FUBICA, ADB-FUBICA, and AB-BICA, identified as new psychoactive substances. *Forensic Toxicol*. 2016;34:133-43.
63. Kinyua J, Negreira N, Ibáñez M, Bijlsma L, Hernández F, Covaci A, van Nuijs ALN. A data-independent acquisition workflow for qualitative screening of new psychoactive substances in biological samples. *Anal Bioanal Chem*. 2015;407:8773-85.
64. Kinyua J, Negreira N, Miserez B, Causanilles A, Emke E, Gremeaux L, de Voogt P, Ramsey J, Covaci A, van Nuijs ALN. Qualitative screening of new psychoactive substances in pooled urine samples from Belgium and United Kingdom. *Sci Total Environ*. 2016;573:1527-35.
65. Oberacher H, Arnhard K. Current status of non-targeted liquid chromatography-tandem mass spectrometry in forensic toxicology. *TrAC, Trends Anal Chem*. 2016;84:94-105.
66. Zuba D, Sekuła K. Identification and characterization of 2,5-dimethoxy-3,4-dimethyl-β-phenethylamine (2C-G) – A new designer drug. *Drug Test Anal*. 2013;5:549-59.
67. Zuba D, Sekuła K, Buczek A. Identification and characterization of 2,5-dimethoxy-4-nitro-β-phenethylamine (2C-N) – A new member of 2C-series of designer drug. *Forensic Sci Int*. 2012;222:298-305.
68. Schymanski EL, Singer HP, Slobodnik J, Ipolyi IM, Oswald P, Krauss M, Schulze T, Haglund P, Letzel T, Grosse S, Thomaidis NS, Bletsou A, Zwiener C, Ibáñez M, Portolés T, de Boer R, Reid MJ, Onghena M, Kunkel U, Schulz W, Guillon A, Noyon N, Leroy G, Bados P, Bogialli S, Stipaničev D, Rostkowski P, Hollender J. Non-target screening with high-resolution mass spectrometry: critical review using a collaborative trial on water analysis. *Anal Bioanal Chem*. 2015;407:6237-55.
69. Krauss M, Singer H, Hollender J. LC-high resolution MS in environmental analysis: from target screening to the identification of unknowns. *Anal Bioanal Chem*. 2010;397:943-51.
70. Heikman P, Sundström M, Pelander A, Ojanperä I. New psychoactive substances as part of polydrug abuse within opioid maintenance treatment revealed by comprehensive high-resolution mass spectrometric urine drug screening. *Hum Psychopharmacol*. 2016;31:44-52.
71. Langer N, Lindigkeit R, Schiebel H-M, Papke U, Ernst L, Beuerle T. Identification and quantification of synthetic cannabinoids in "spice-like" herbal mixtures: Update of the German situation for the spring of 2016. *Forensic Sci Int*. 2016;269:31-41.
72. Lung D, Wilson N, Chatenet FT, LaCroix C, Gerona R. Non-targeted screening for novel psychoactive substances among agitated emergency department patients. *Clin Toxicol*. 2016;54:319-23.
73. Ford LT, Berg JD. Analysis of legal high materials by UPLC-MS/TOF as part of a toxicology vigilance system. What are the most popular novel psychoactive substances in the UK? *Ann Clin Biochem*. 2016;54:219-29.
74. Reid MJ, Baz-Lomba JA, Ryu Y, Thomas KV. Using biomarkers in wastewater to monitor community drug use: a conceptual approach for dealing with new psychoactive substances. *Sci Total Environ*. 2014;487:651-8.
75. Ibáñez M, Sancho JV, Bijlsma L, van Nuijs ALN, Covaci A, Hernández F.

Comprehensive analytical strategies based on high-resolution time-of-flight mass spectrometry to identify new psychoactive substances. *TrAC, Trends Anal Chem*. 2014;57:107-17.
76. Knolhoff AM, Croley TR. Non-targeted screening approaches for contaminants and adulterants in food using liquid chromatography hyphenated to high resolution mass spectrometry. *J Chromatogr A*. 2016;1428:86-96.
77. Kneisel S, Westphal F, Bisel P, Brecht V, Broecker S, Auwärter V. Identification and structural characterization of the synthetic cannabinoid 3-(1-adamantoyl)-1-pentylindole as an additive in 'herbal incense'. *J Mass Spectrom*. 2012;47:195-200.
78. Grabenauer M, Krol WL, Wiley JL, Thomas BF. Analysis of synthetic cannabinoids using high-resolution mass spectrometry and mass defect filtering: implications for nontargeted screening of designer drugs. *Anal Chem*. 2012;84:5574-81.
79. Sleno L. The use of mass defect in modern mass spectrometry. *J Mass Spectrom*. 2012;47:226-36.
80. Broecker S, Herre S, Wüst B, Zweigenbaum J, Pragst F. Development and practical application of a library of CID accurate mass spectra of more than 2,500 toxic compounds for systematic toxicological analysis by LC–QTOF-MS with data-dependent acquisition. *Anal Bioanal Chem*. 2011;400:101-17.
81. Broecker S, Pragst F, Bakdash A, Herre S, Tsokos M. Combined use of liquid chromatography–hybrid quadrupole time-of-flight mass spectrometry (LC–QTOF-MS) and high performance liquid chromatography with photodiode array detector (HPLC–DAD) in systematic toxicological analysis. *Forensic Sci Int*. 2011;212:215-26.
82. Cawley A, Pasin D, Ganbat N, Ennis L, Smart C, Greer C, Keledjian J, Fu S, Chen A. The potential for complementary targeted/non-targeted screening of novel psychoactive substances in equine urine using liquid chromatography-high resolution accurate mass spectrometry. *Anal Methods*. 2016;8:1789-97.
83. Ibáñez M, Bijlsma L, van Nuijs ALN, Sancho JV, Haro G, Covaci A, Hernández F. Quadrupole-time-of-flight mass spectrometry screening for synthetic cannabinoids in herbal blends. *J Mass Spectrom*. 2013;48:685-94.
84. Fornal E. Formation of odd-electron product ions in collision-induced fragmentation of electrospray-generated protonated cathinone derivatives: aryl α-primary amino ketones. *Rapid Commun Mass Spectrom*. 2013;27:1858-66.
85. Fornal E. Study of collision-induced dissociation of electrospray-generated protonated cathinones. *Drug Test Anal*. 2014;6:705-15.
86. Pasin D, Cawley A, Bidny S, Fu S. Characterisation of hallucinogenic phenethylamines using high-resolution mass spectrometry for non-targeted screening purposes. *Drug Test Anal*. 2017. doi:10.1002/dta.2171
87. Fornal E, Stachniuk A, Wojtyla A. LC-Q/TOF mass spectrometry data driven identification and spectroscopic characterisation of a new 3,4-methylenedioxy-N-benzyl cathinone (BMDP). *J Pharm Biomed Anal*. 2013;72:139-44.
88. Strano Rossi S, Odoardi S, Gregori A, Peluso G, Ripani L, Ortar G, Serpelloni G, Romolo FS. An analytical approach to the forensic identification of different classes of new psychoactive substances (NPSs) in seized materials. *Rapid Commun Mass Spectrom*. 2014;28:1904-16.
89. Andersson M, Diao X, Wohlfarth A, Scheidweiler KB, Huestis MA. Metabolic profiling of new synthetic cannabinoids AMB and 5F-AMB by human hepatocyte and liver microsome incubations and high-resolution mass

spectrometry. *Rapid Commun Mass Spectrom*. 2016;30:1067-78.
90. Diao X, Wohlfarth A, Pang S, Scheidweiler KB, Huestis MA. High-resolution mass spectrometry for characterizing the metabolism of synthetic cannabinoid THJ-018 and its 5-fluoro analog THJ-2201 after incubation in human hepatocytes. *Clin Chem*. 2016;62:157-69.
91. Ellefsen KN, Wohlfarth A, Swortwood MJ, Diao X, Concheiro M, Huestis MA. 4-Methoxy-alpha-PVP: in silico prediction, metabolic stability, and metabolite identification by human hepatocyte incubation and high-resolution mass spectrometry. *Forensic Toxicol*. 2016;34:61-75.
92. Swortwood MJ, Ellefsen KN, Wohlfarth A, Diao X, Concheiro-Guisan M, Kronstrand R, Huestis MA. First metabolic profile of PV8, a novel synthetic cathinone, in human hepatocytes and urine by high-resolution mass spectrometry. *Anal Bioanal Chem*. 2016;408:4845-56.
93. Watanabe S, Kuzhiumparambil U, Winiarski Z, Fu S. Biotransformation of synthetic cannabinoids JWH-018, JWH-073 and AM2201 by Cunninghamella elegans. *Forensic Sci Int*. 2016;261:33-42.
94. Wohlfarth A, Pang S, Zhu M, Gandhi AS, Scheidweiler KB, Liu HF, Huestis MA. First metabolic profile of XLR-11, a novel synthetic cannabinoid, obtained by using human hepatocytes and high-resolution mass spectrometry. *Clin Chem*. 2013;59:1638-48.
95. Watanabe S, Kuzhiumparambil U, Nguyen MA, Cameron J, Fu S. Metabolic profile of synthetic cannabinoids 5F-PB-22, PB-22, XLR-11 and UR-144 by Cunninghamella elegans. *AAPS J*. 2017. doi:10.1208/s12248-017-0078-4
96. Caspar AT, Helfer AG, Michely JA, Auwärter V, Brandt SD, Meyer MR, Maurer HH. Studies on the metabolism and toxicological detection of the new psychoactive designer drug 2-(4-iodo-2,5-dimethoxyphenyl)-N-[(2-methoxyphenyl)methyl]ethanamine (25I-NBOMe) in human and rat urine using GC-MS, LC-MS(n), and LC-HR-MS/MS. *Anal Bioanal Chem*. 2015;407:6697-719.
97. Franz F, Angerer V, Moosmann B, Auwärter V. Phase I metabolism of the highly potent synthetic cannabinoid MDMB-CHMICA and detection in human urine samples. *Drug Test Anal*. 2016. doi:10.1002/dta.2049
98. Lobo Vicente J, Chassaigne H, Holland MV, Reniero F, Kolář K, Tirendi S, Vandecasteele I, Vinckier I, Guillou C. Systematic analytical characterization of new psychoactive substances: A case study. *Forensic Sci Int*. 2016;265:107-15.
99. Cannaert A, Storme J, Franz F, Auwärter V, Stove CP. Detection and Activity Profiling of Synthetic Cannabinoids and Their Metabolites with a Newly Developed Bioassay. *Anal Chem*. 2016;88:11476-85.

## 1.3 Aims of the project

With unknown pharmacokinetic and pharmacodynamics properties, the proliferation of NPS analogues can pose significant health risks to recreational drug users. This may lead to increased hospitalisations and/or fatalities where the identity of compounds is required to elicit correct medical treatments or to assist in coronial proceedings. Furthermore, there is potential for these compounds to be exploited or abused in sport where new compounds may not be covered in current anti-doping assays. It is therefore paramount that drug-testing laboratories adopt holistic non-targeted screening strategies for the detection and putative identification of novel analogues.

The aim of this project is to develop strategies for the detection of NPS analogues using HRMS that can be applied to routine casework. More specifically these aims are to:

1. Evaluate the use of mass defect-related strategies for the rapid detection of NPS analogues for top-down detection strategies;
2. Evaluate the use of differential analysis software for the detection of exogenous components in top-down screening;
3. Investigate the CID pathways of known NPS such as synthetic cathinones, hallucinogenic phenethylamines and synthetic cannabinoids to determine key or common product ions and neutral losses (NLs) for bottom-up screening strategies and;
4. Apply the developed top-down and bottom-up screening strategies to authentic forensic casework samples to evaluate their efficacy for NPS detection.

# *CHAPTER 2:*

# *TOP-DOWN SCREENING*

# *STRATEGIES*

## 2.1 Rationale

Top-down screening approaches involve the systematic identification of chromatographic peaks where abundant peaks are selected from the visual inspection of TICs. Molecular formulae can then be generated for precursor ions and a structure can be postulated if MS/MS data was acquired. This process can be considerably time-consuming and likely to result in the interrogation of "false positive" candidates such as endogenous or background compounds. Furthermore, toxicologically relevant compounds may exist at low concentrations and not be visible upon visual inspection. This is also complicated by the fact that HRMS acquires substantially more data than conventional LRMS instrumentation and, therefore, may require intermediate data processing steps prior to the selection of candidate peaks to reduce the likelihood of interrogating irrelevant compounds. This chapter investigates the use of intermediate data-processing steps such as mass defect-based detection strategies and differential analysis to isolate and prioritise candidate chromatographic peaks for top-down screening strategies.

## 2.2 Mass defect filtering (MDF)

### 2.2.1 Introduction

The ability for HRMS instrumentation to distinguish between compounds with the same nominal mass but different exact mass is due to its ability to measure mass defects. The mass defect is the fractional portion of an exact mass and arises due to differences in nuclear binding energies for different elements relative to carbon-12 (mass defect of zero) [1]. Mass defects for common elements are shown in Table 2.1. Elements such as hydrogen and nitrogen have positive mass defects relative to their nominal mass which is the sum of protons and neutrons while electronegative elements such as halogens typically have negative mass defects. Subsequently, when a compound undergoes substitution it will increase (or decrease) the integer mass but will also have a net increase or decrease for the mass defect relative to the initial compound (Table 2.2).

**Table 2.1** Exact masses and mass defect of common elements.

| Element | Exact Mass [Da] | Mass defect [Da] |
|---|---|---|
| Hydrogen | 1.0078 | 0.0078 |
| Nitrogen | 14.0030 | 0.0030 |
| Carbon | 12.0000 | 0.0000 |
| Fluorine | 18.9984 | -0.0016 |
| Oxygen | 15.9949 | -0.0051 |
| Sulfur | 31.9721 | -0.0279 |
| Chlorine | 34.9688 | -0.0312 |
| Bromine | 78.9183 | -0.0817 |
| Iodine | 126.9044 | -0.0956 |

For example, subsequent alkylations will positively shift mass defects by 0.0157 Da for each -$CH_2$ unit added. Other substitutions resulting in positive mass defect shifts include the addition of methoxy, benzyl and pyrroldinyl substituents. It should also be noted that mass defect does not always increase with increasing integer mass since the addition of halogens, thiols, nitro and methylenedioxy groups can have net decreases on mass defect.

**Table 2.2** Mass and mass defect shifts for common NPS substitutions.

| Substitution | Formula change | Mass shift [Da] | Mass defect shift [Da] |
|---|---|---|---|
| Methyl | $+CH_2$ | 14.0157 | +0.0157 |
| Methoxy | $+OCH_2$ | 30.0106 | +0.0106 |
| Phenyl | $+C_6H_4$ | 76.0313 | +0.0313 |
| Benzyl | $+C_7H_6$ | 90.0470 | +0.0470 |
| 2-methoxybenzyl | $+CH(C_6H_4)OCH_3$ | 120.0575 | +0.0575 |
| Pyrrolidino | $+C_4H_7N$ | 69.0578 | +0.0578 |
| Nitro | $-H+NO_2$ | 45.9929 | -0.0071 |
| Fluoro | -H+F | 17.9906 | -0.0094 |
| Methylenedioxy | $+CO_2$ | 43.9898 | -0.0102 |
| Methylthio | $+SCH_2$ | 45.9877 | -0.0123 |
| Chloro | -H+Cl | 33.9610 | -0.0390 |
| Bromo | -H+Br | 77.9105 | -0.0895 |
| Iodo | -H+I | 125.8967 | -0.1034 |

Since substitutions have relatively minor net changes on the overall mass defect compared to the initial compound, it is reasoned that compounds which share similar core structures will have clustered mass defects [1, 2]. This theory has resulted in the use of MDF strategies to interrogate complex HRMS data for the discovery of structurally related compounds in non-targeted screening, specifically in metabolomics [3-6]. In these studies, the MDF is typically centred on the parent

molecule's mass defect with a filter tolerance that accounts for mass defect shifts from known bio-transformations. The advantage of using MDFs compared to nominal mass range filters is the fact that it significantly reduces the amount of data required for interrogation by isolating relevant *m/z* values within the MDF tolerance without restricting the presence of higher mass analogues (Figure 2.1). The use of MDF, however, requires the knowledge of mass defect ranges for compound classes of interest. Grabenauer *et al*. [2] determined the mass defect ranges of indole-derived synthetic cannabinoids (JWH series) and used a MDF centred on 0.1859 Da with a symmetric tolerance of ± 0.050 Da (50 mDa), indicating that this filter would capture up to 85% of known indole-derived analogues. The MDF was then applied to herbal products containing abundant synthetic cannabinoids, however, an additional compound (JWH-250) was detected that could not be observed in the TIC. From this, publication, the technique appeared to be promising, however, its use on complex toxicological samples for the detection of NPS has not been evaluated.

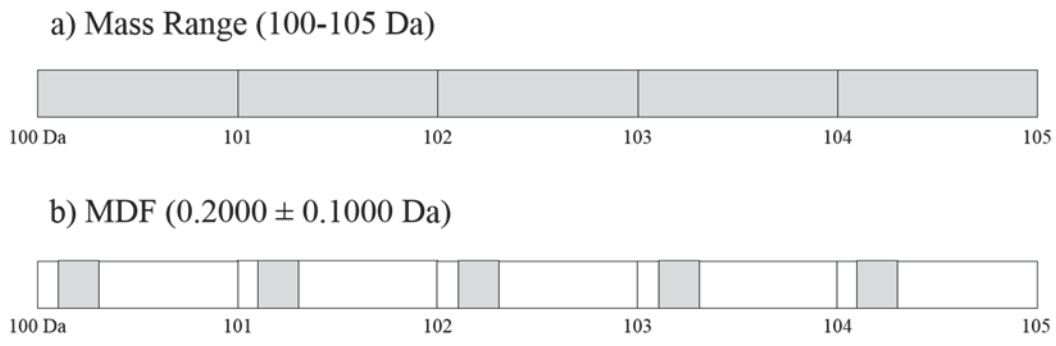


**Figure 2.1** Comparison of HRMS data (grey) when using (a) a mass range of 100-105 Da and (b) a MDF of 0.2000 ± 0.1000 Da.

## 2.2.2 Methods and materials

### *2.2.2.1 Mass defect ranges of NPS*

Catalogue searches of CRM suppliers such as Cayman Chemical (Ann Arbor, MI, USA), Lipomed AG (Arlsheim, Switzerland) and Chiron (Trondheim, Norway) for synthetic cathinones ($n$ = 50), hallucinogenic phenethylamines ($n$ = 36) and synthetic cannabinoids ($n$ = 56) were performed. Mass defect calculation was performed by calculating the monoisotopic mass ($[M+H]^+$) from the chemical formulae and subtracting the integer mass from the exact mass where the integer mass is the integer portion of the exact mass (i.e. the integer mass of *m/z* 276.1599 would be 276).

### *2.2.2.2 Chemicals and reagents*

MDPV and 2-(2,5-dimethoxyphenyl)-*N*-[(2-methoxyphenyl)methyl]ethanamine (25H-NBOMe) hydrochloride salts were manufactured by Lipomed AG and purchased as 1 mg/mL methanolic ampoules from PM Separations (Capalaba, QLD, Australia). The internal standard (IS), desipramine-$d_3$, was purchased from Grace (Deerfield, IL, USA). General laboratory reagents and solvents for sample preparation were of HPLC grade and were purchased from Thermo Fisher Scientific (Fair Lawn, NJ, USA). LC-MS grade acetonitrile was purchased from Burdick and Jackson (Muskegon, MI, USA). AR grade ammonium formate and formic acid were purchased from Sigma Aldrich (Castle Hill, NSW, Australia). Ultrapure grade water (18.2 MΩ.cm) was obtained from a Sartorius arium® pro ultra-pure water system (Goettingen, Germany).

### *2.2.2.3 Specimen collection*

Equine urine and plasma samples were obtained from three thoroughbred gelding horses following approval from the Racing NSW Animal Care and Ethics Committee (RP72). Human urine was obtained from a volunteer with approval from the Australian

National University (ANU) Human Research Ethics Committee as part of a parallel research program.

#### *2.2.2.4 Preparation of stock solutions*

Stock solutions (200 μg/mL) of MDPV and 25H-NBOMe were prepared by diluting 1 mg/mL analyte solution (1 mL) with methanol in a 5-mL volumetric flask

#### *2.2.2.5 Preparation of working solutions*

Working solutions of MDPV (10 μg/mL) and 25H-NBOMe (100 μg/mL) were prepared by diluting 250 μL and 25 μL of 200 μg/mL stock solution, respectively, with methanol in a 5-mL volumetric flask. A desipramine-$d_3$ working solution (3 μg/mL) was prepared by diluting 300 μL of 50 μg/mL stock in methanol using a 5-mL volumetric flask.

#### *2.2.2.6 Preparation of fortified biological samples*

Equine and human urine samples (3 mL) were adjusted to pH 5.3 and individually fortified with MDPV (30 μL), 25H-NBOMe (3 μL) and IS (50 μL) working solutions to achieve a final concentrations of 0.1 μg/mL and 0.05 μg/mL, for analytes and IS, respectively. Equine plasma samples (2 mL) were treated with trichloroacetic acid (300 μL), adjusted to pH 3, individually fortified with analyte and IS working solution to also achieve concentrations of 0.1 μg/mL and 0.05 μg/mL. The plasma samples were then centrifuged at 2500 rpm (1118 × *g*) for 10 min and the supernatant was collected. In addition to fortified matrices, unfortified matrices were also extracted and analysed. Samples were extracted according to Australian Racing Forensic Laboratory (ARFL, Sydney, NSW, Australia) accredited sample preparation procedures. Urine and plasma extracts were then loaded onto UCT mixed-mode $C_8$/strong cation exchange XTRACKT® (200 mg, 3 cc) solid phase extraction (SPE) columns (Bristol, PA, USA)

following conditioning with methanol (2 mL) and water (2 mL). The sorbents were then washed with acetic acid (0.1 M, 3 mL) and water (3 mL). The tubes were dried briefly prior to elution with a solution (3 mL) of ethyl acetate: aqueous ammonia (35 % v/v): methanol (97:3:0.3 % v/v/v). The eluates were treated with methanol:HCl (0.1 M, 1 drop) and then evaporated to dryness under nitrogen ($N_2$) gas at 60 $^oC$. The resulting residues were then reconstituted in methanol (50 µL) and ammonium acetate (10 mM, pH 4, 100µL) and transferred to plastic 200 µL conical limited volume sample vials for LC-QTOF-MS analysis.

*2.2.2.7 Instrumental analysis*

Chromatographic separation was achieved using an Agilent Technologies 1290 Infinity series ultra-performance liquid chromatograph (UPLC), consisting of an Inifinity II high speed pump (G4220A), thermostat (FC/ALS G1330B), column compartment (G1316C, 25$^oC$) and autosampler compartment (G4226A, 8$^oC$) coupled to an Agilent Technologies 6510 quadrupole time-of-flight mass spectrometer (QTOF-MS) fitted with a dual electrospray ionization (ESI) source. Instrument control and data acquisition was performed using Agilent Technologies MassHunter LC-MS Data Acquisition Software (Version B.05.01). A sample volume of 1 µL was injected onto an Agilent Technologies Poroshell 120 C18 column (2.1 x 75 mm, 2.7 µm particle size) using a gradient elution with a flow rate of 0.4 mL/min with a total run time of 17 min. Mobile phase A consisted of 20 mM ammonium formate and mobile phase B consisted of acetonitrile containing 0.1% (% v/v) formic acid. Initial mobile phase composition was 87% A which was held for 0.5 min and then decreased linearly to 50% A over 9.5 min. It was then decreased to 5% A over 0.75 min, held for 1.5 min and then returned to the initial conditions over 0.25 min with a final hold time of 2.5 min and post-run equilibration time of 2 min. The QTOF-MS was operated in

positive electrospray ionisation (ESI+) in scan mode using Extended Dynamic Range (2 GHz) over an acquisition range of *m/z* 50-1000 with capillary and fragmentor voltages set to 3500 V and 180 V, respectively.

#### *2.2.2.8 Data processing*

All data was processed using Agilent Technologies MassHunter LC-MS Qualitative Analysis Software (B.06.00). The data mining algorithm, MFE, was applied to all samples using the 'small molecules (chromatographic)' extraction algorithm over the entire retention time range with a *m/z* range 150-500 and a peak filter threshold ≥ 1000 counts. MFE deconvolutes mass spectral data by identifying *m/z* values which produce a chromatographic peak and designates them as a compound. For each compound an extracted compound chromatogram (ECC) is generated, these ECC are combined to generate a total compound chromatogram (TCC). The resulting compound list can be filtered using parameters such as retention time, m/z range, intensity and mass defect. Traditionally, compounds in the filtered list are identified by performing database searches for precursor m/z values or by comparison of acquired MS/MS data with mass spectral libraries, however, in this scenario the TCC is used as a mass defect filtered chromatogram.

### 2.2.3 Results and discussion

In order to identify an appropriate MDF to encompass multiple classes of NPS, the mass defect ranges for different NPS classes were determined. Figure 2.2 illustrates the proportion of analogues in mass defect ranges of 20 mDa increments over a range of 0.0000-0.3400 Da.

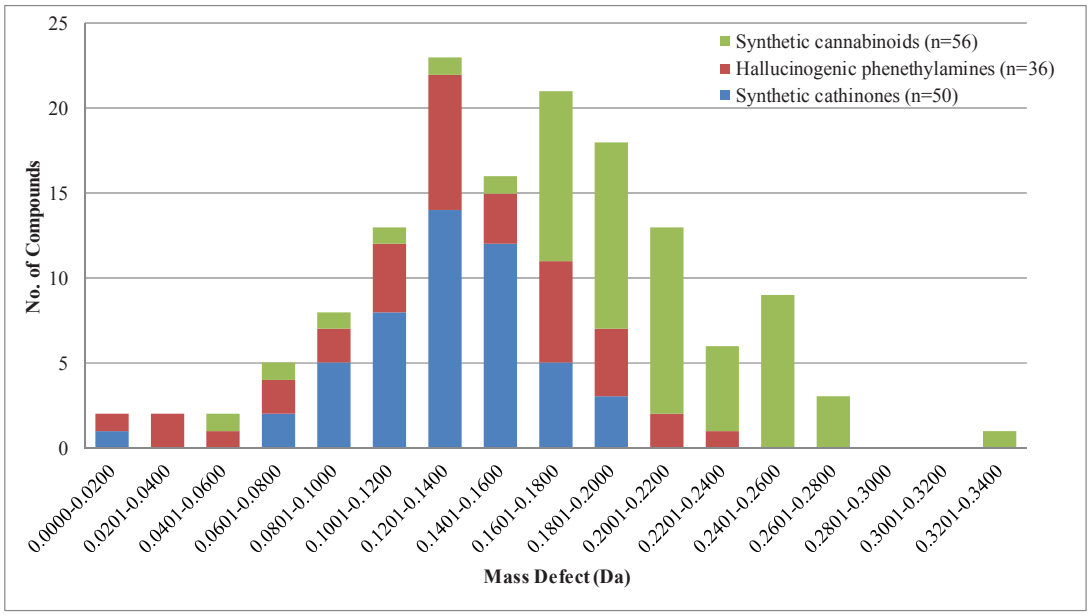


**Figure 2.2** Summary of mass defects for selected synthetic cathinones (blue), hallucinogenic phenethylamines (red) and synthetic cannabinoids (green).

Over half of the identified analogues had mass defects between 0.1201-0.2000 Da with the highest of proportion of analogues having mass defects situated between 0.1201 and 0.1400 Da, comprised mostly of synthetic cathinones ($n$ = 14) and hallucinogenic phenethylamines ($n$ = 8). Mass defects for synthetic cannabinoids were typically higher due to increased molecular weight and subsequently higher hydrogen content. Mass defects below 0.0800 Da were typically associated with analogues containing chlorine, bromine or iodine due to the considerable negative mass defect shifts of associated with the addition of halogens. The mass defect ranges encompassing 50% of analogues from selected classes (including and excluding halogens) were compared using box and whisker plots representing the minimum, 25$^{th}$ percentile, median, 75$^{th}$ percentile and maximum (Figure 2.3). In addition, the mass defect ranges encompassing 80% of analogues (including and excluding halogens) in the same manner using the 10$^{th}$ and 90$^{th}$ percentiles. The median mass defects for synthetic cathinones and hallucinogenic phenethylamines (halogen inclusive) were almost

identical with 0.1388 and 0.1368 Da, respectively, with overlapping mass defect ranges, while synthetic cannabinoids had a higher median mass defect of 0.2014 Da and offset mass defect ranges.

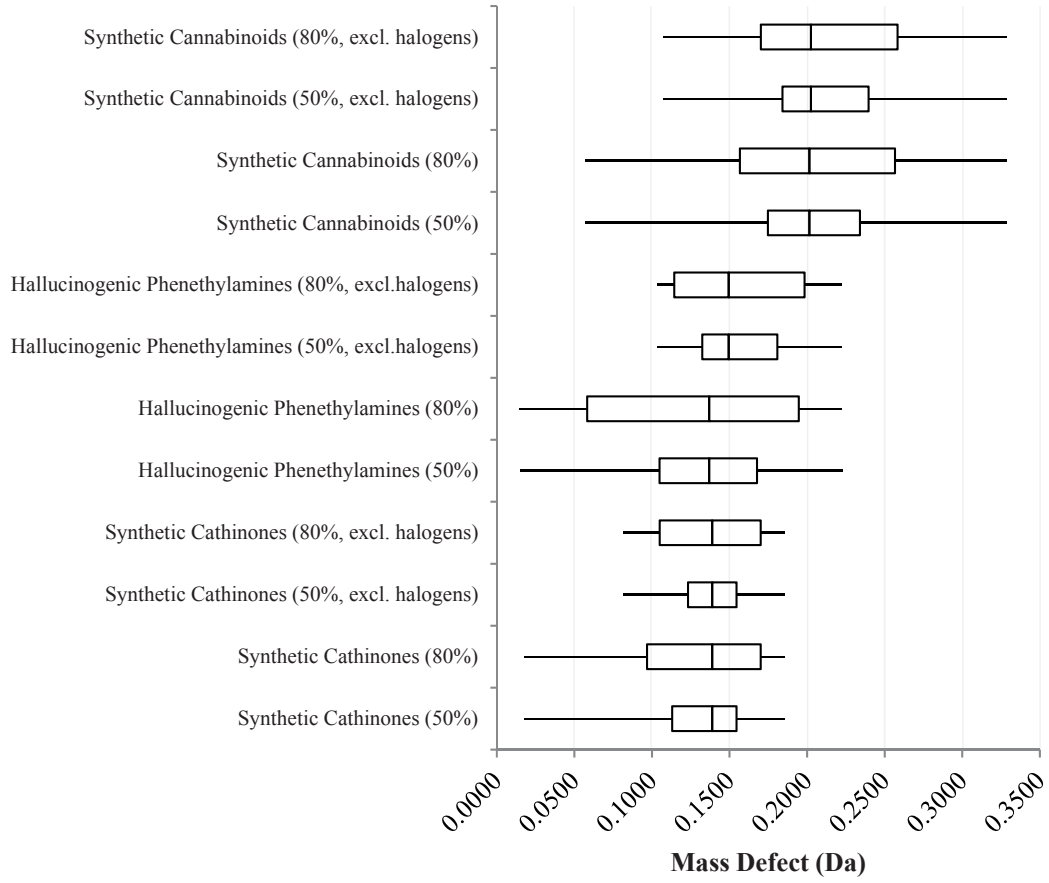


**Figure 2.3** Comparison of mass defect ranges for NPS classes with and without halogen analogues. The box plot represents the range of mass defects for 50% and 80% of selected analytes. The whiskers represent the minimum and maximum mass defect values.

Exclusion of halogenated compounds resulted in a minimal median change for synthetic cathinones and synthetic cannabinoids (Table 2.3). The median value for halogen excluded hallucinogenic phenethylamines had a positive increase of 12 mDa, which is likely due to the large proportion of analogues containing chlorine, bromine and iodine compared to synthetic cathinones and synthetic cannabinoids. The mass

defect ranges that encompassed 50% of analogues for individual classes (including and excluding halogens) were typically narrow with < 63 mDa widths. Synthetic cathinones had the narrowest widths (< 42 mDa) likely due to the number of isomeric analogues around the median value.

**Table 2.3** Median mass defect values, mass defect range and range widths for 50% and 80% of selected analytes including and excluding halogens.

| Class | Median [Da] | Mass defect range [Da, 50%] | Width [mDa] | Mass defect range [Da, 80%] | Width [mDa] |
|---|---|---|---|---|---|
| Synthetic cannabinoids | 0.2014 | 0.1747-0.2340 | 59.3 | 0.1567-0.2566 | 99.9 |
| Synthetic cannabinoids (excl. halogens) | 0.2025 | 0.1841-0.2396 | 55.5 | 0.1702-0.2583 | 88.1 |
| Hallucinogenic phenethylamines | 0.1368 | 0.1049-0.1676 | 62.7 | 0.0582-0.1946 | 136.4 |
| Hallucinogenic phenethylamines (excl. halogens) | 0.1494 | 0.1324-0.1808 | 48.4 | 0.1144-0.1983 | 83.9 |
| Synthetic cathinones | 0.1388 | 0.1130-0.1545 | 41.5 | 0.0968-0.1701 | 73.3 |
| Synthetic cathinones (excl. halogens) | 0.1388 | 0.1232-0.1545 | 31.3 | 0.1050-0.1701 | 65.1 |

When 80% of analogues were considered, the mass defect range widths increased by approximately 40 mDa for majority of classes and were typically less than 100 mDa, however, halogen-inclusive hallucinogenic phenethylamines increased by over 70 mDa. The overall mass defect ranges and proposed MDFs encompassing 50%, 80% and 100% of analogues are summarised in Table 2.4. Using MDFs such as those that would encompass 50% of potential NPS analogues could be effective due to the narrow widths (116.4-129.1 mDa), therefore, filtering out the majority of acquired data. The application of MDF, however, is intended to encompass as many analogues as possible, therefore, an MDF that can only encompass 50% of potential analogues is not favourable. Conversely, MDFs that provide coverage of all selected NPS analogues have much larger range widths (246.8-313.8 mDa), subsequently decreasing

the specificity of the filter. Therefore, a compromise between analogue coverage and filter specificity needs to be reached. The use of a MDF that encompasses 80% of analogues may be appropriate due to sufficient coverage and < 200 mDa filter widths.

**Table 2.4** Overall mass defect ranges for 50%, 80% and 100% of selected analogues including and excluding halogens.

| Proportion of analogues [%] | Incl./excl. halogens | Mass defect range [Da] | Width [mDa] | Centre ± tolerance [Da] |
|---|---|---|---|---|
| 50 | Incl. | 0.1049-0.2340 | 129.1 | 0.1695 ± 0.0646 |
| | Excl. | 0.1232-0.2396 | 116.4 | 0.1814 ± 0.0582 |
| 80 | Incl. | 0.0582-0.2566 | 198.4 | 0.1574 ± 0.0992 |
| | Excl. | 0.1144-0.2583 | 143.9 | 0.1864 ± 0.0720 |
| 100 | Incl. | 0.0147-0.3285 | 313.8 | 0.1716 ± 0.1569 |
| | Excl. | 0.0817-0.3285 | 246.8 | 0.2051 ± 0.1234 |

MFE was applied post-acquisition to equine plasma, equine urine and human urine samples that were fortified individually with MDPV and 25H-NBOMe at a concentration of 100 ng/mL and extracted using SPE. The TICs for the blank (Figure 2.4a) and fortified equine plasma were simple, with MDPV (Figure 2.4b) and 25H-NBOMe (Figure 2.4c) visible at 3.97 and 6.26 min, respectively. The TCCs generated from the application of MFE over *m/z* 150-450 using a MDF centred at 0.1574 Da with a symmetrical tolerance of ± 0.0992 Da (Figure 2.4d-f) had significantly reduced background noise compared to the TICs increasing the signal-to-noise ratio of the analytes and other peaks. The samples were also fortified with a desipramine-$d_3$ (*m/z* 270.2044) IS which was faintly visible in the TICs, however, it was visible at 7.24 min in the TCCs.

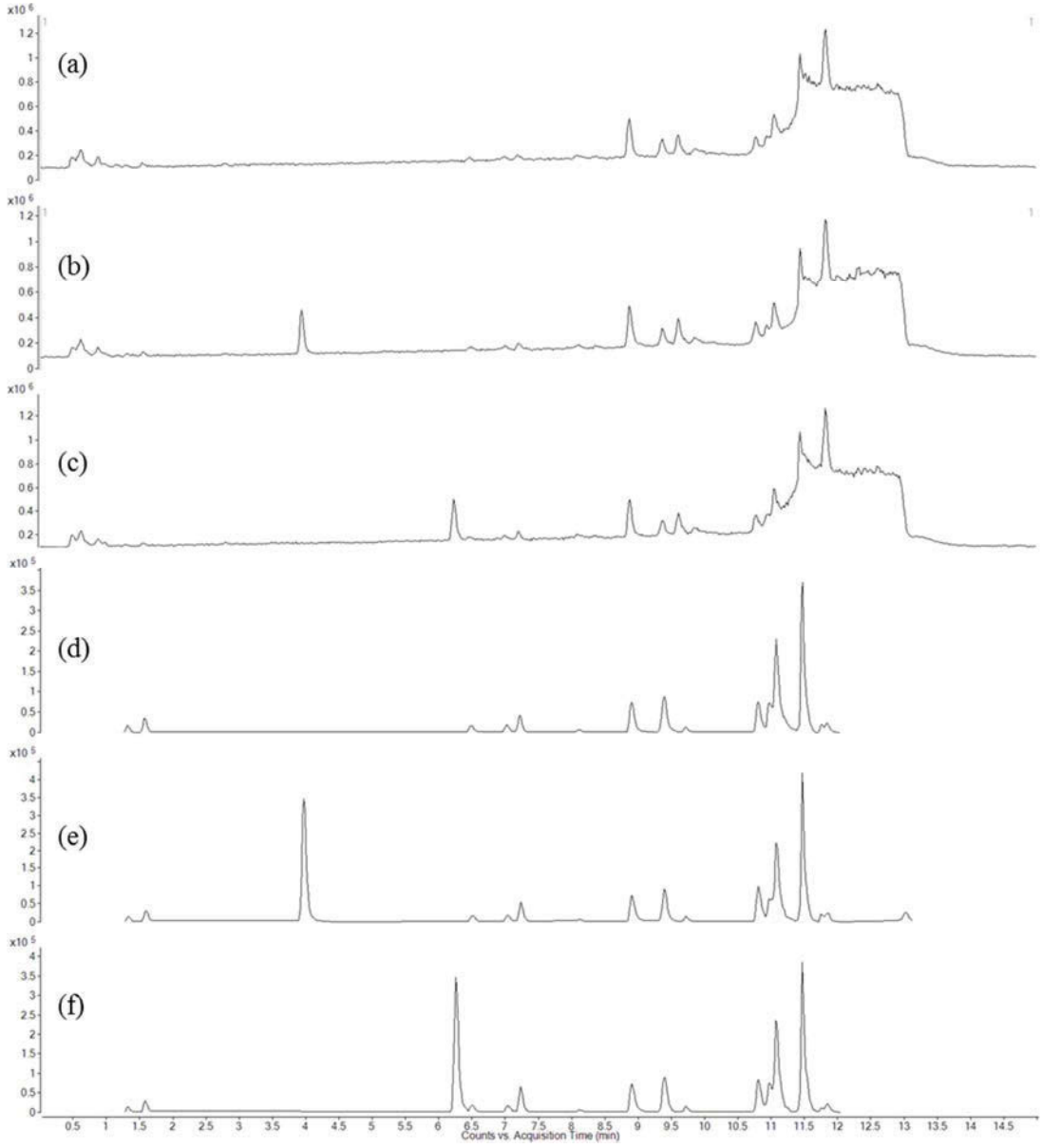


**Figure 2.4** TICs for blank equine plasma (a) and equine plasma fortified with 100 ng/mL MDPV (b) and 25H-NBOMe (c) and TCCs for blank plasma (d) and MDPV (e) and 25H-NBOMe (f) fortified plasma using a 0.1574 ± 0.0992 Da MDF with a *m/z* range 150-500.

In this example, MDF worked in a satisfactory manner due to the cleanliness of the sample TICs, significant analyte concentration and the use of a chromatographic method that has significant chromatographic resolution with a known NPS elution range of approximately 9 min.

The efficacy of MDF was briefly evaluated on authentic toxicological samples to determine whether it could be applied as a post-acquisition data processing technique on pre-existing screening methods. Unfortunately, when the same MFE method (Section 2.2.2.8) was applied to authentic human urine (Figure 2.5a) acquired using the same column and mobile phase composition but with a significantly shorter gradient, the TCC (Figure 2.5b) did not offer additional insight into the presence of NPS analogues due to comparable TCC and TIC. Additionally, authentic human urine was acquired using the same gradient as authentic urine sample but instead used a different C18 column and a mobile phase composition (A: 10 mM ammonium acetate and B: acetonitrile containing 0.1 % acetic acid). In this case, the TIC (Figure 2.5c) was significantly unresolved with no discernible peaks visible and subsequent application of MFE improved resolution of the TCC to a minor extent (Figure 2.5d).

It is evident that the efficacy of MDF is highly dependent on factors such as sample complexity and chromatographic resolution. Traditional targeted screening methods using HRMS often have narrow elution ranges to increase sample throughput. These methods are therefore not amenable to the application of particular post-acquisition non-targeted screening strategies since narrow elution ranges will result in overlapping peaks making low concentration analytes virtually undetectable using manual peak selection.

Furthermore, in analytical toxicology, complex samples are often encountered that are likely to result in the acquisition of significantly more data, increasing the probability that other compounds or background ions will have mass defects in the same range as NPS.

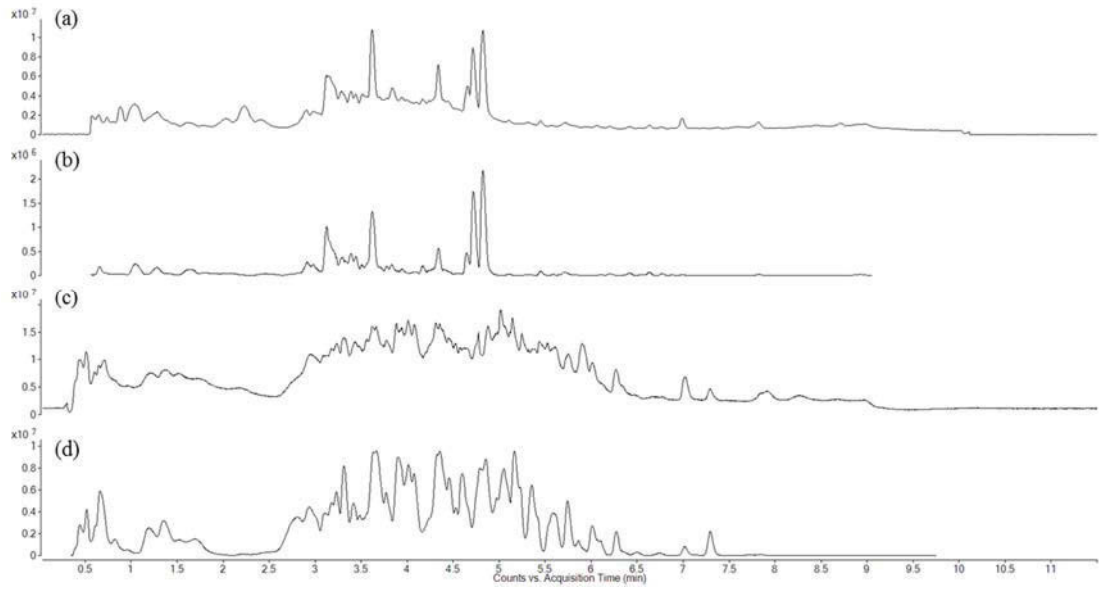


**Figure 2.5** Authentic human urine TIC (a) and TCC (b) acquired using a Poroshell 120 C18 column with mobile phase composition A: 20 mM ammonium formate and B: acetonitrile containing 0.1% formic acid. Authentic human urine TIC (c) and TCC (d) acquired using a Phenomenex Gemini C18 column (50 × 2 mm, 5 µm) with mobile composition A: 10 mM ammonium acetate and B: acetonitrile containing 0.1% acetic acid. Chromatographic conditions for both samples involved a flow rate of 0.5 mL/min and an initial mobile phase composition was 99% A which was held for 2 min, decreased linearly to 20% A over 6.5 min then returned to the initial conditions over 2 min.

It should also be considered that NPS analogues are not the only compounds in biological samples to have mass defects within the specified mass defect ranges and therefore the application of MDF is likely to result in TCCs that contain endogenous compounds. As an example, the mass defect profiles of whole blood samples ($n$ = 12) were generated by plotting a frequency distribution of mass defects from all acquired accurate masses over a 9 min retention time range (1-10 min) using ranges *m/z* 50-1000 (Figure 2.6a) and *m/z* 150-500 (Figure 2.6b). The frequency of mass defects acquired over the entire mass range is relatively consistent over the mass unit (0.0000-0.9999) with the frequency maxima observed between 0.1000 and 0.3000 Da. Application of a mass filter of *m/z* 150-500 resulted in a reduction of the frequencies of mass defects > 0.5000 which is to be expected as larger mass *m/z* values are likely to have higher mass defects. With the highest frequency of mass defects still observed

between 0.1000-0.3000 Da, therefore, subsequent application of MDFs encompassing any proportion of NPS analogues in whole blood would reduce the amount of acquired *m/z* values, however, the resulting data would still encompass a significant amount of endogenous *m/z* values. In addition to the aforementioned limitations, the major limitation of MDF is that it is not always offered in vendor data processing software and, if included, may not have consistent functionality from vendor-to-vendor. For example, MDF is often used in metabolomics data processing, it is designed as a data mining tool to detect potential metabolic candidates and not typically used to generate TCCs for peak selection. Additionally, it is used to monitor very narrow mass defect windows relative to the parent molecule and not used to monitor large defect ranges that encompass whole classes of analogues. Consequently, it is a technique that has not been utilised by laboratories for the detection NPS supported by the lack of publications using this technique in analytical toxicology since Grabenaurer's initial publication in 2012.

### 2.2.4 Conclusion

The mass defect ranges of commonly encountered NPS classes were established with a MDF of 0.1574 ± 0.0992 Da encompassing 80% of selected analogues. Evaluation of a post-acquisition MDF highlighted that its efficacy was mostly dependent on sample complexity and chromatographic resolution with a major limitation being the inconsistent functionality of vendor-supplied MDF applications. Future developments in data processing software may allow for the use of MDF in routine screening with improved efficacy for the detection of structurally-related unknowns. This may involve the ability to apply multiple MDFs simultaneously or sequentially in order to examine narrower mass defect ranges, potentially improving this technique's selectivity. While not currently possible in MassHunter, application of MDF to matrix

subtracted TICs may improve the detection of low concentration analytes that are masked by abundant matrix components.

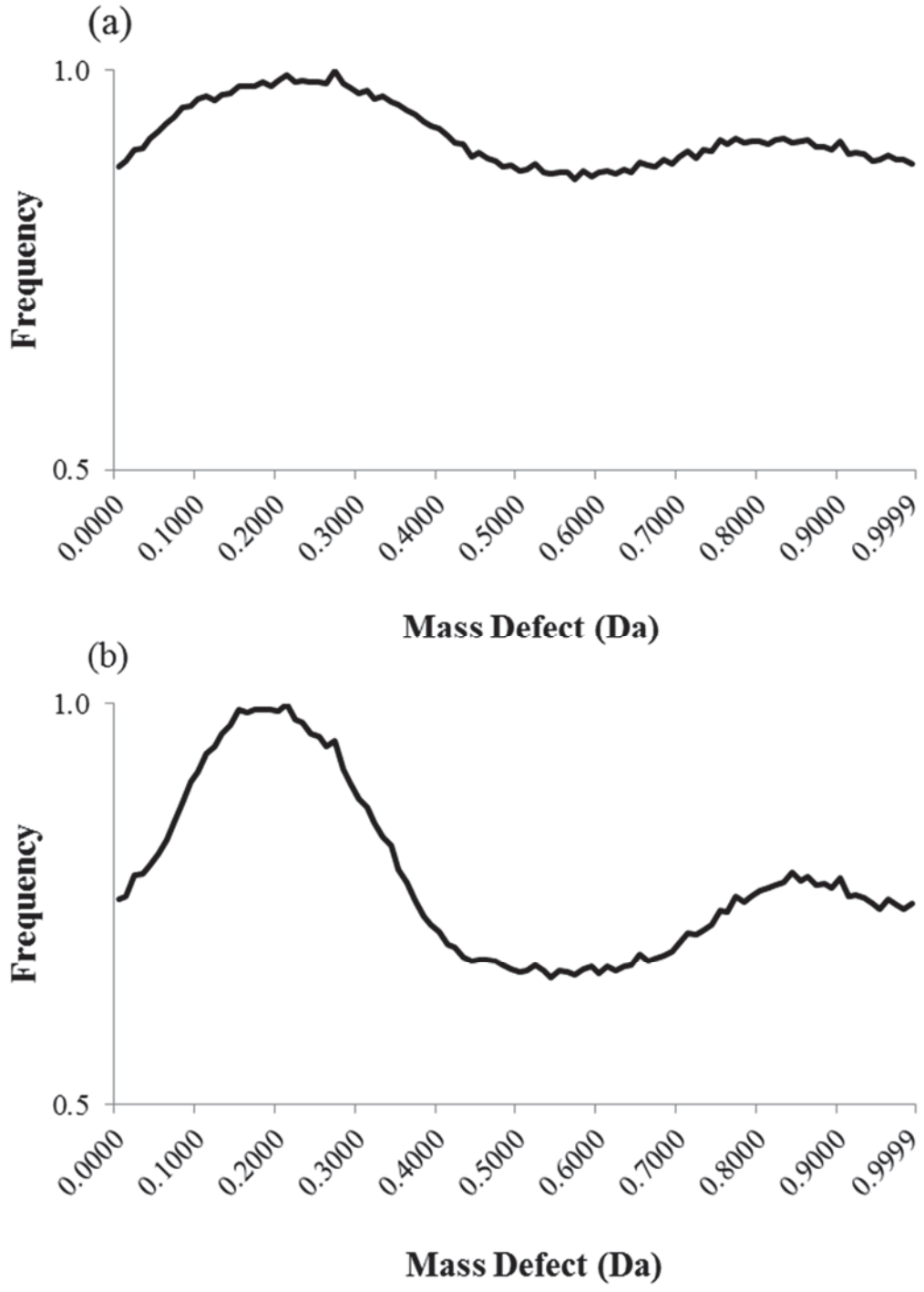


**Figure 2.6** Frequency distribution of mass defects for all *m/z* values detected over a *m/z* range of 50-1000 (a) and *m/z* 150-500 (b) in authentic whole blood samples.

## 2.3 Kendrick mass defect (KMD)

### 2.3.1 Introduction

An alternative concept proposed for simplifying complex mass spectral data is the use of Kendrick mass scales [1, 7]. It has been demonstrated that compounds which differ by the same molecular subunit (i.e. $CH_2$) have the same Kendrick mass defect (KMD), where Kendrick mass is derived by multiplying the accurate mass of the molecule by the ratio of the molecular subunit's nominal mass and accurate mass (Equation 1). For example, hydrocarbons which differ by $CH_2$ subunits can be converted to their respective Kendrick mass by multiplying the accurate mass by the ratio of 14.0000 Da and 14.0157 Da (Equation 2). For the purposes of this thesis this ratio has been defined as the 'Kendrick normalisation factor'. KMD is then calculated by subtracting the integer Kendrick mass from the exact Kendrick mass (Equation 3), where the integer Kendrick mass is simply the integer value of the exact Kendrick mass.

$$\text{Kendrick mass} = \text{IUPAC mass} \times \frac{\text{Nominal subunit mass}}{\text{Accurate subunit mass}} \quad (1)$$

$$\text{Kendrick mass } (CH_2) = \text{IUPAC mass} \times \frac{14.0000}{14.0157} \quad (2)$$

$$\text{KMD} = \text{Exact Kendrick mass} - \text{Integer Kendrick mass} \quad (3)$$

For example, application of Equation 2 to two $CH_2$ homologues with masses 163.0993 177.1149 Da produces Kendrick masses of 162.9166 and 176.9166 Da, respectively. Subtracting the integer Kendrick masses (Equation 3) of 162 and 176 Da from the Kendrick mass results in 0.9166 for both homologues. KMD has been applied to

various areas of analytical chemistry for the detection of $CH_2$ homologues [8-13], however, other normalisation factors have been used [14, 15]. Recently, Baduel *et al*. [16] used a normalisation factor of $CF_2$ (50/49.9968) for the detection of per- and polyfluoroalkyl compounds (PFACs) in concrete samples. In these cases, data is typically visualised using two-dimensional "Kendrick plots" where the nominal Kendrick mass is on the *x*-axis with the KMD on the *y*-axis. Peaks which have the same KMD value will line-up on the horizontal axis.

Since many NPS are $CH_2$ homologues of each other, KMD analysis may have the potential to detect NPS analogues in complex HRMS data. Unfortunately, current vendor data processing software does not offer the ability to interrogate HRMS data using specific KMD values and is limited to the generation of Kendrick plots. However, all that is required to apply KMD analysis to samples is a list of *m/z* values that were detected in a particular analysis. This can be achieved by utilising generic mass spectral averaging algorithms in native data processing software that can generate mass spectra containing all the detected *m/z* values and intensities over a selected chromatographic period.

### 2.3.2 Methods and materials

#### *2.3.2.1 KMD values of NPS*

The Kendrick mass of NPS analogues identified in Section 2.2.2.1 was calculated by multiplying $[M+H]^+$ values by 14.0000/14.0157. KMD values were then calculated according to Equation 3.

#### *2.3.2.2 KMD analysis software*

In order to apply KMD analysis to the peak lists obtained from authentic samples in a rapid and automated manner, a custom-built program was developed. This was

achieved by using the Visual Basic for Applications (VBA) programming environment in Microsoft Office Excel. The program utilised the macro function which executed a series of basic Excel actions automatically.

#### *2.3.2.3 Analysis of fortified samples*

The samples previously analysed in Section 2.2 were used to develop and evaluate a program to interrogate numerical mass spectral data for reference KMD values of NPS classes.

#### *2.3.2.4 Data analysis*

Acquired data was processed using Agilent Technologies MassHunter Qualitative Analysis Software (B.06.00). All nine data files were opened and processed simultaneously over a retention time range of 0.5-10 min using the 'Range Select' function. Averaged mass spectra were then generated using the 'Extract MS Spectrum' function. The spectra were then exported as a Microsoft Office Excel comma-separate value (.csv) files containing *m/z* values and corresponding intensities.

For the KMD analysis, the .csv files were imported and processed using a $CH_2$ normalisation factor with a KMD tolerance of 0.001 Da and an intensity threshold > 1000 counts. A total of eight KMD values were monitored including traditional cathinones (0.9232 Da), methylenedioxycathinones (0.8637 Da), α-pyrrolidinopropiophenone (0.9095 Da), methylenedioxy-α-pyrrolidinopropiophenone (0.8502 Da), alkyl 2C-X derivatives (0.9136 Da), thioalkyl 2C-X (0.8501 Da), alkyl NBOMe (0.8366 Da) and thioalkyl NBOMe (0.7727 Da) derivatives. The monoisotopic mass for desipramine-$d_3$ (*m/z* 270.2044) was monitored as an IS to evaluate the accuracy of the results.

### 2.3.3 Results and discussion

#### *2.3.3.1 KMD values of NPS classes*

The key KMD values for homologous series of NPS analogues have been listed in Table 2.5. Homologous series with identical KMD values were observed for synthetic cathinones and hallucinogenic phenethylamine subclasses. This is not surprising considering that analogues for both of these classes maintain their core structure and are typically alkyl-substituted. Furthermore, due to substitutions at different positions on the core structures, many isomeric analogues arise resulting in the identical KMD values. In contrast, homologous series are rarely observed for synthetic cannabinoids (except for some JWH analogues) due to significant structural dissimilarities between different analogues.

Synthetic cathinones can be categorised into four different KMD values corresponding to traditional (0.9232 Da), methylenedioxy-type (0.8637 Da), α-pyrrolidinophenone-type (0.9095 Da) and methylenedioxy-α-pyrrolidinophenone-type (0.8502 Da) cathinones. Unfortunately, due to some cathinone analogues containing fluorine (0.8936 Da), chlorine (0.8524 Da), bromine (0.7464 Da) and methoxy (0.9002 Da) substituents they could not be included into those categories. Hallucinogenic phenethylamines such as alkyl derivatives of 2C-X, including alkyl DOX derivatives, and alkyl 25X-NBOMe derivatives had KMD values of 0.9136 Da and 0.8366 Da, respectively. Similarly, multiple KMD values exist for the various derivatives which include halogens.

**Table 2.5** KMD values for common NPS subclasses based on $CH_2$ normalisation.

| Class | Subclass | Kendrick Mass Defect [Da] |
|---|---|---|
| Synthetic cathinones | Traditional | 0.9232 |
| | Methylenedioxy-type | 0.8637 |
| | α-pyrrolidinophenone-type | 0.9095 |
| | Methylenedioxy-α-pyrrolidinophenone-type | 0.8501 |
| Hallucinogenic phenethylamines | Alkyl 2C-X derivatives | 0.9136 |
| | Thioalkyl 2C-X derivatives | 0.8501 |
| | Bromo 2C-X derivatives | 0.7368 |
| | Chloro 2C-X derivatives | 0.8366 |
| | Iodo-2C-X derivatives | 0.6692 |
| | Alkyl NBOMe derivatives | 0.8366 |
| | Thioalkyl NBOMe derivatives | 0.7727 |
| | Bromo NBOMe derivatives | 0.6598 |
| | Chloro NBOMe derivatives | 0.7596 |
| | Iodo NBOMe derivatives | 0.5922 |

### *2.3.3.2 KMD analysis program*

A program (tentatively titled 'DefectDetect') was successfully developed in MS Office Excel to rapidly interrogate numerical mass spectrometry data. In order to enhance the user-friendliness of the program, it was given a graphical user interface (GUI) to provide an authentic "program-feel" consisting of a main menu (Figure 2.7) that appears on opening the macro-enabled Excel workbook.

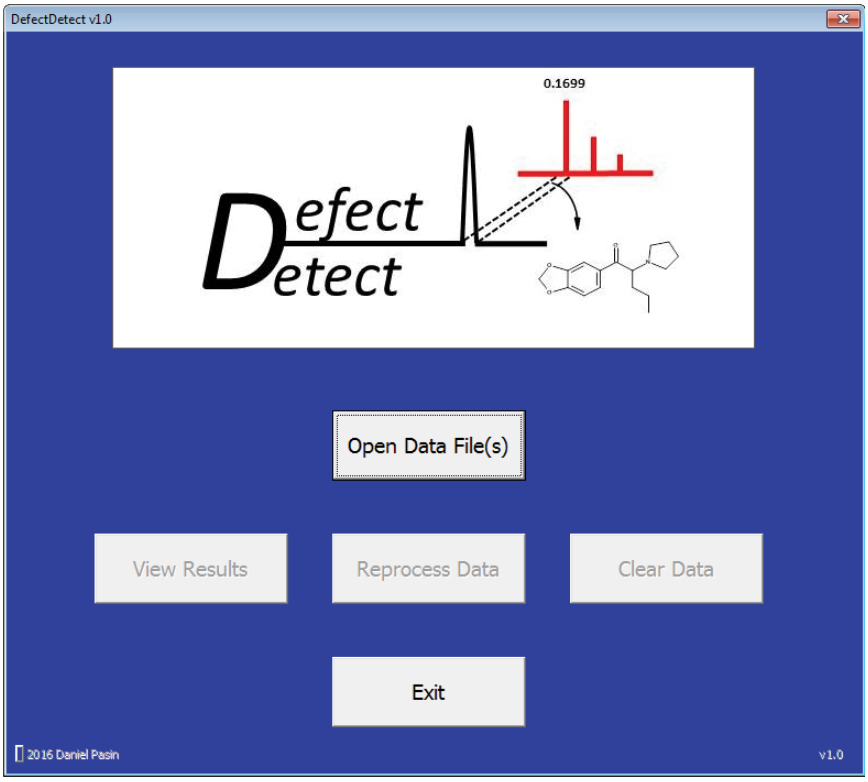


**Figure 2.7** Main menu of the DefectDetect KMD analysis software.

The main menu has an intuitive workflow (Figure 2.8) involving; (1) opening single or multiple data files, (2) viewing results from a previous analysis, (3) reprocessing data files with different parameters, (4) clearing previous results to open different data files and, (5) exiting the program. Activation of the "Open Data File(s)" button initiates the file import process where single or multiple .csv files can be selected for analysis. Each .csv file is then imported into separate Excel worksheets that are then renamed with the .csv file name. Additionally, the name of the .csv file is printed into the first row of the worksheet for further identification. A series of background calculations are performed with the values used to filter and analyse the data including:

**Even *m/z*** – this calculation determines whether m/z values are even or odd by performing an evenness test with a Boolean result (true/false) where false indicates that the m/z value is odd;

**Mass defect** – determined by subtracting the integer *m/z* value from the accurate *m/z* value;

**Kendrick mass** – determined by multiplying the *m/z* value with the user-defined Kendrick normalisation factor. This calculation is used only as an intermediate step to determine KMD, and;

**KMD** – Subtracting the integer Kendrick mass value from the accurate value.

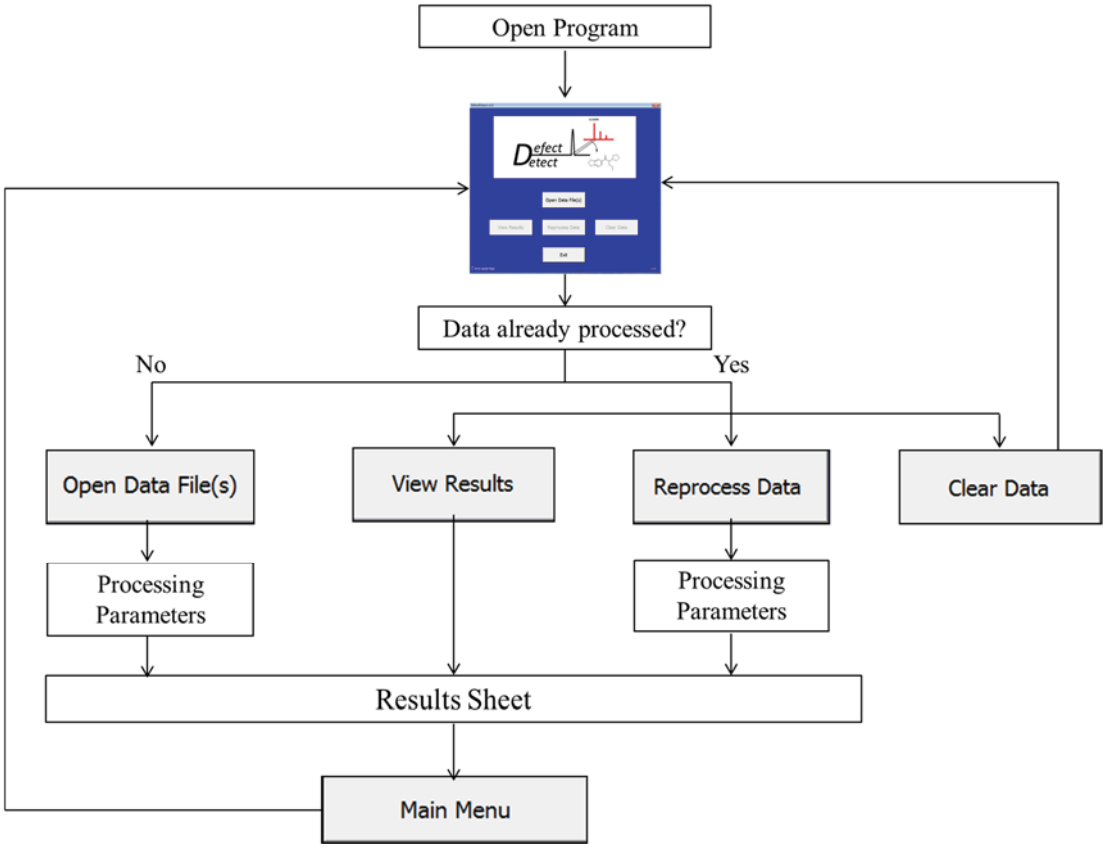


**Figure 2.8** Schematic of the DefectDetect workflow.

After the data importation, the processing parameters dialog opens and user-defined criteria can be specified (Figure 2.9). The processing parameters have been separated into different steps including the selection of KMD parameters and specifying how the results are filtered, sorted and displayed. Additionally, an IS can be specified.

Furthermore, a KMD calculator was also included for the determination of KMD values with different normalisation values for convenience.

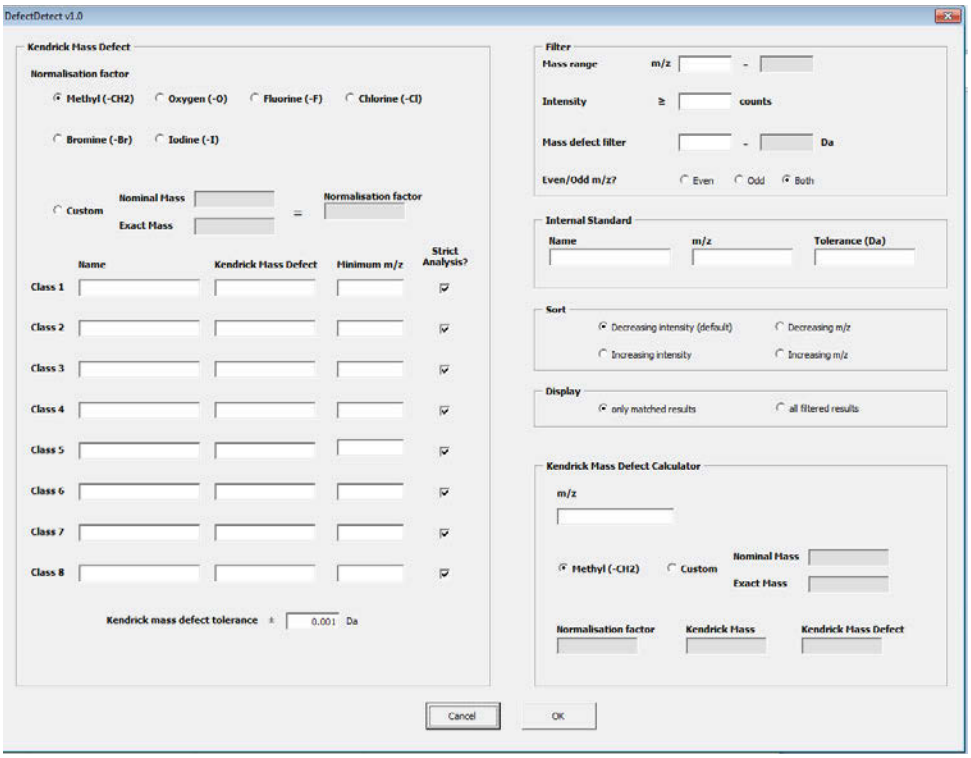


**Figure 2.9** DefectDetect data processing parameters.

The selection of KMD criteria (Figure 2.10) is the major part of the data processing workflow and involves the selection of a;

**Kendrick normalisation factor** – The normalisation factor specified is used in the calculation of nominal Kendrick mass and KMD in the file import process. In addition to the most commonly used normalisation of $CH_2$, some other default normalisations have been provided such as the addition of oxygen and halogens. Furthermore, custom normalisation factors can be specified using the nominal and accurate masses for other molecular subunit differences.

**KMD value** – Up to eight KMD values can be monitored simultaneously in a single analysis. Matched values are highlighted using eight different colours corresponding to the different KMD values. The values can be assigned names for reference after processing.

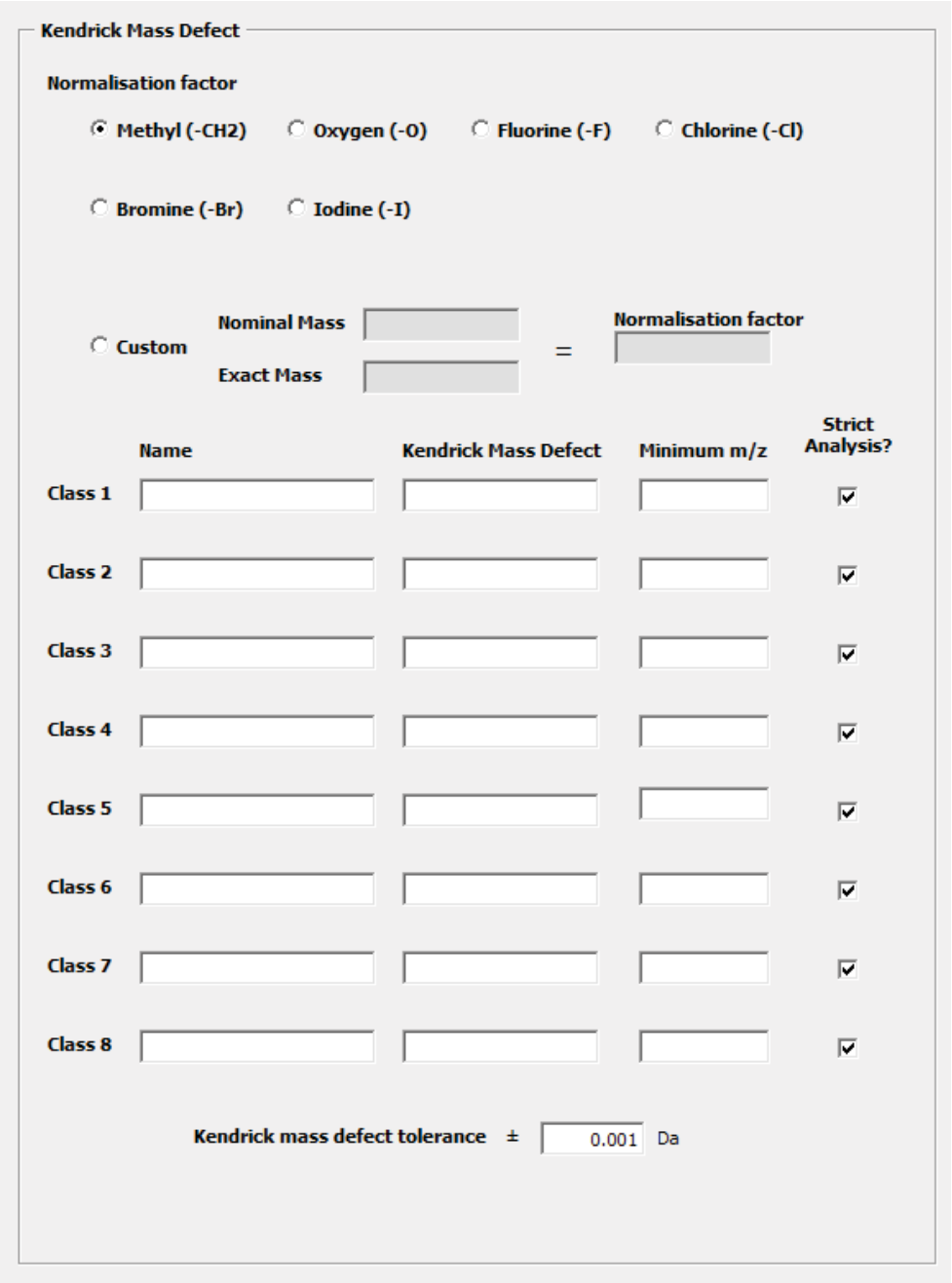


**Figure 2.10** KMD processing parameters.

Furthermore, if the 'Strict Analysis?' box is checked, the minimum mass specifies the reference mass at which molecule subunit nominal mass additions begin. For example, if a minimum mass of 150 is specified with a $CH_2$ normalisation it will only highlight rows which have the correct KMD value at masses 150, 164, 178, etc. If the box is unchecked it will highlight any specified KMD value, regardless of the nominal mass, and;

**KMD tolerance –** A symmetrical (±) KMD tolerance in Da can be specified to account for variations in accurate mass measurements of HRMS instrumentation.

Several filtering steps can be applied to reduce the number of candidate *m/z* values required for interrogation (Figure 2.11). These filter steps functions and include:

**Mass range** – filters *m/z* values outside of the user-defined upper and lower limits;

**Intensity threshold** – filters *m/z* below the specified intensity value;

**Mass defect filter** – *m/z* values can be filtered based on upper and lower mass defect limits, and;

**Even/odd *m/z*** – *m/z* values can be filtered based on whether they are even, odd or both.

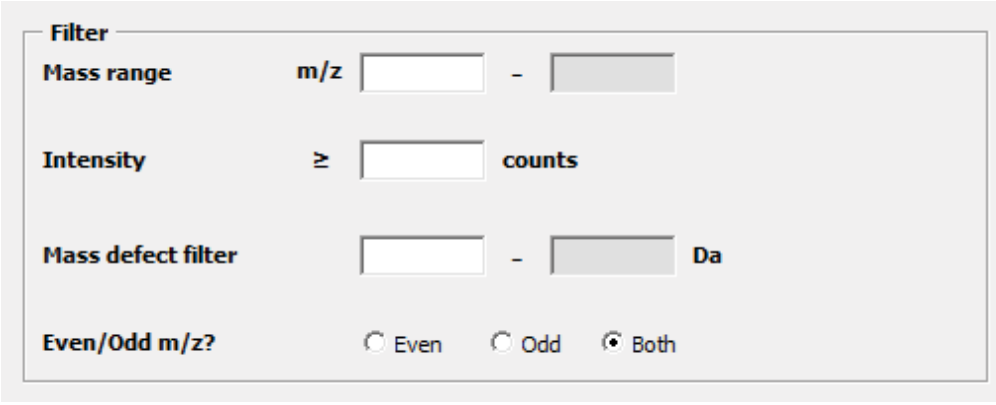


**Figure 2.11** Filtering parameters including mass range, intensity, mass defect and even/odd m/z.

An IS *m/z* value can be specified in order to evaluate the accuracy and representativeness of the results (Figure 2.12). The *m/z* value can be either for an IS analyte or a persistent background ion that is constantly observed, however, it needs to be within the filtering parameters used. Visualisation of the processed data can be customised by sorting the results based on increasing/decreasing intensity or *m/z* values. In addition, only KMD matched results or all filtered results can be displayed (Figure 2.13).

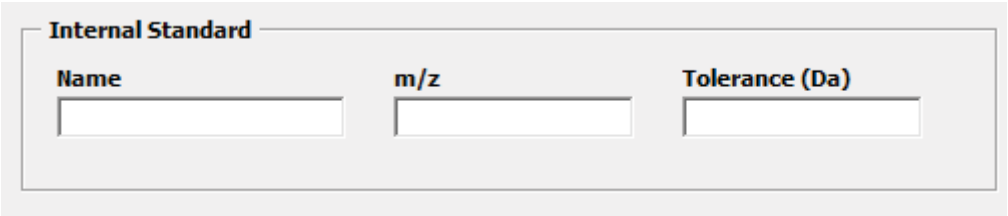


**Figure 2.12** Internal standard parameters.

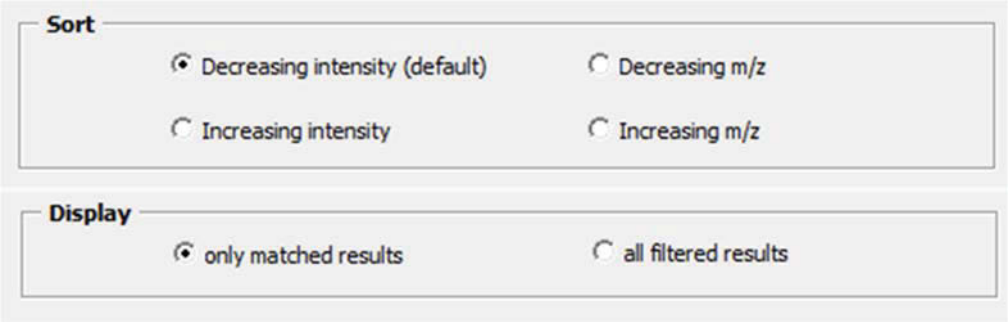


**Figure 2.13** Results visualisation options.

At the conclusion of the data processing procedure, a results worksheet is created at the start of the workbook and populated with all of data processing parameters which can be used for future reference (Figure 2.14). The filtered results from each file are then sequentially placed underneath each other. A 'Main Menu' button appears which redirects users back to the main menu where the data can be reprocessed using different

parameters. Additionally the data can be cleared in order to import different files.

The program was optimised and validated for systematic errors using acquired data from blank and fortified biological matrices extracted using SPE and analysed using LC-QTOF-MS. The IS *m/z* value was highlighted in all nine samples indicating that the results were accurate and reliable. The only other matched results in the fortified matrices correctly corresponded to the precursor ions of MDPV (*m/z* 276.1599) and 25H-NBOMe (*m/z* 302.1756) indicating that the analysis was selective even when simultaneously monitoring eight KMD values.

For the blank samples, only the IS was matched. It was also noticed that there were significant discrepancies between the raw and averaged intensities of the fortified analytes. It should be considered that due to the use of averaging algorithms to generate mass spectra there will be a subsequent decrease of analyte intensities from raw to averaged spectra. The raw intensities and averaged intensities were compared for the MDPV and 25H-NBOMe (Table 2.6) with averaged intensities typically one-hundredth of the raw intensities obtained from the native data processing software. This decrease is dependent, however, on the number of scans averaged (i.e. the retention time range) with shorter retention time ranges providing higher analyte intensities. As a result appropriate intensity threshold values would need to be optimised due to the different sensitivities of different assays and HRMS instruments. This can be achieved by determining averaged intensities for LOD concentrations of known NPS analogues. While this technique offers the rapid analysis of numerical mass spectral data, there are several limitations of the DefectDetect that need to be addressed. Firstly, since only eight KMD values can be simultaneously monitored at once, multiple analyses may need to be conducted in order to cover other NPS classes.

| | | | | | | |
|---|---|---|---|---|---|---|
| Parameters | | Internal Standard | | | | |
| Mass-to-charge (m/z) range | No filter selected | m/z 186.2221 | 186.2221 ± 0.001 | | | |
| Intensity threshold (counts) | 1000 | | | | | |
| Mass defect filter (Da) | No filter selected | Traditional Cathinones | 0.9227 - 0.9247 (min. m/z = 150) | Alkyl 2C-X | 0.913 - 0.915 (min. m/z = 182) | |
| Even/Odd m/z | Even | Methylenedioxy cathinones | 0.8632 - 0.8652 (min. m/z = 194) | Thioalkyl 2C-X | 0.8492 - 0.8512 (min. m/z = 228) | |
| Kendrick tolerance (Da) | ± 0.001 | Pyrroldino cathinones | 0.909 - 0.911 (min. m/z = 204) | Alkyl NBOMe | 0.836 - 0.838 (min. m/z = 302) | |
| Kendrick Normalisation | Methyl (-CH2) | MDpyrrolidino cathinones | 0.8497 - 0.8517 (min. m/z = 248) | Thioalkyl NBOMe | 0.7723 - 0.7743 (min. m/z = 348) | |
| **File Name** | **EQ P 25H-NBOMe** | | | | | |
| Mass-to-charge ratio (m/z) | Intensity (counts) | Even m/z? | Mass defect (Da) | Kendrick Mass | Kendrick Mass Defect | |
| 186.2220 | 8451 | TRUE | 0.2220 | 186.0134 | 0.0134 | |
| 302.1761 | 2362 | TRUE | 0.1761 | 301.8376 | 0.8376 | |
| **File Name** | **EQ P Blank** | | | | | |
| Mass-to-charge ratio (m/z) | Intensity (counts) | Even m/z? | Mass defect (Da) | Kendrick Mass | Kendrick Mass Defect | |
| 186.2221 | 8891 | TRUE | 0.2221 | 186.0135 | 0.0135 | |
| **File Name** | **EQ P MDPV** | | | | | |
| Mass-to-charge ratio (m/z) | Intensity (counts) | Even m/z? | Mass defect (Da) | Kendrick Mass | Kendrick Mass Defect | |
| 186.2221 | 6881 | TRUE | 0.2221 | 186.0135 | 0.0135 | |
| 276.1604 | 2497 | TRUE | 0.1604 | 275.8511 | 0.8511 | |

**Figure 2.14** An example of the results sheet containing the specified data processing parameters and sequentially listed results from imported files.

**Table 2.6** Comparison of raw and averaged intensities for MDPV and 25H-NBOMe.

| Matrix | Analyte | Raw intensity [counts] | Averaged intensity [counts] | Intensity reduction [%] |
|---|---|---|---|---|
| Equine Plasma | MDPV | 287,171 | 2,497 | 99.13 |
| | 25H-NBOMe | 283,606 | 2,362 | 99.16 |
| Equine Urine | MDPV | 813,379 | 7,430 | 99.09 |
| | 25H-NBOMe | 658,626 | 5,441 | 99.17 |
| Human urine | MDPV | 822,157 | 7,524 | 99.08 |
| | 25H-NBOMe | 1,018,885 | 9,460 | 99.07 |

It is reasoned, however, that monitoring a comprehensive list of KMD values may result in increases of matched *m/z* values, therefore, making interpretation difficult. It is recommended that the KMD values are prioritised based on commonly encountered analogues. Secondly, due to the fact that the input data consists of only *m/z* and intensity values for averaged mass spectra over a retention time range, there is no indication of whether matched *m/z* values are chromatographic with a discrete retention time or persistent background ions. Therefore, matched *m/z* values should be used to generate EICs in native data processing software to verify if the matched *m/z* values produce chromatographic peaks. To reduce the number of matched values due to background ions, averaged mass spectra can undergo a background subtraction prior to importation using the retention time ranges on either side of the selected retention time range. In addition, data mining software to identify chromatographic peaks can be used with the results subsequently imported into DefectDetect. Lastly, not all classes of NPS have analogues which predominantly differ by $–CH_2$ groups and, therefore, some analogues cannot be classified by a single KMD value like synthetic cathinones and hallucinogenic phenethylamines. This is evident for synthetic

cannabinoids which have significant structural difference within subclasses resulting in numerous different KMD values.

### 2.3.4 Conclusion

Calculation of KMD values normalised to $CH_2$ revealed that synthetic cathinones and phenethylamines derivatives could be categorised into KMD values corresponding to different subclasses due to the large number of $CH_2$ homologues. A Microsoft Office Excel-based program, DefectDetect, was developed as a vendor-agnostic tool to interrogate numerical mass spectral data for KMD values of interest. It was successfully and rapidly applied to samples fortified with NPS derivatives demonstrating proof-of-concept for the rapid detection of NPS analogues using KMD analysis. Future improvements of DefectDetect may involve the ability to use multiple normalisations simultaneously to monitor different substitutions. There is also scope to transfer the program to a conventional GUI which can support the importation of mass spectrometry data formats such as mzXML allowing for samples to be interrogated in DefectDetect without needing to return to the native data processing software increasing its data mining capabilities

## 2.4 References

1. Sleno L. The use of mass defect in modern mass spectrometry. *J Mass Spectrom*. 2012;47:226-36.
2. Grabenauer M, Krol WL, Wiley JL, Thomas BF. Analysis of synthetic cannabinoids using high-resolution mass spectrometry and mass defect filtering: implications for nontargeted screening of designer drugs. *Anal Chem*. 2012;84:5574-81.
3. Xie T, Liang Y, Hao H, A J, Xie L, Gong P, Dai C, Liu L, Kang A, Zheng X, Wang G. Rapid identification of ophiopogonins and ophiopogonones in Ophiopogon japonicus extract with a practical technique of mass defect filtering based on high resolution mass spectrometry. *J Chromatogr A*. 2012;1227:234-44.
4. Tian T, Jin Y, Ma Y, Xie W, Xu H, Zhang K, Zhang L, Du Y. Identification of metabolites of oridonin in rats with a single run on UPLC-Triple-TOF-MS/MS system based on multiple mass defect filter data acquisition and multiple data

processing techniques. *J Chromatogr B*. 2015;1006:80-92.
5. Liu M, Zhao S, Wang Z, Wang Y, Liu T, Li S, Wang C, Wang H, Tu P. Identification of metabolites of deoxyschizandrin in rats by UPLC–Q-TOF-MS/MS based on multiple mass defect filter data acquisition and multiple data processing techniques. *J Chromatogr B*. 2014;949:115-26.
6. Liang Y, Xiao W, Dai C, Xie L, Ding G, Wang G, Meng Z, Zhang J, Kang A, Xie T, Liu Y, Zhou Y, Liu W, Zhao L, Xu J. Structural identification of the metabolites for strictosamide in rats bile by an ion trap-TOF mass spectrometer and mass defect filter technique. *J Chromatogr B*. 2011;879:1819-22.
7. Kendrick E. A Mass Scale Based on CH2 = 14.0000 for High Resolution Mass Spectrometry of Organic Compounds. *Anal Chem*. 1963;35:2146-54.
8. van Loon A, Genuit W, Pottasch C, Smelt S, Noble P. Analysis of old master paintings by direct temperature-resolved time-of-flight mass spectrometry: Some recent developments. *Microchem J*. 2016;126:406-14.
9. Lee H, An HJ, Lerno Jr LA, German JB, Lebrilla CB. Rapid profiling of bovine and human milk gangliosides by matrix-assisted laser desorption/ionization Fourier transform ion cyclotron resonance mass spectrometry. *Int J Mass Spectrom*. 2011;305:138-50.
10. Bowman DT, Jobst KJ, Ortiz X, Reiner EJ, Warren LA, McCarry BE, Slater GF. Improved coverage of naphthenic acid fraction compounds by comprehensive two-dimensional gas chromatography coupled with high resolution mass spectrometry. *J Chromatogr A*. 2017. doi:10.1016/j.chroma.2017.07.017
11. Eyheraguibel B, Traikia M, Fontanella S, Sancelme M, Bonhomme S, Fromageot D, Lemaire J, Lauranson G, Lacoste J, Delort AM. Characterization of oxidized oligomers from polyethylene films by mass spectrometry and NMR spectroscopy before and after biodegradation by a Rhodococcus rhodochrous strain. *Chemosphere*. 2017;184:366-74.
12. He H, Emmett MR, Nilsson CL, Conrad CA, Marshall AG. High mass accuracy and resolution facilitate identification of glycosphingolipids and phospholipids. *Int J Mass Spectrom*. 2011;305:116-9.
13. Kourtchev I, O'Connor IP, Giorio C, Fuller SJ, Kristensen K, Maenhaut W, Wenger JC, Sodeau JR, Glasius M, Kalberer M. Effects of anthropogenic emissions on the molecular composition of urban organic aerosols: An ultrahigh resolution mass spectrometry study. *Atmos Environ*. 2014;89:525-32.
14. Vallverdú-Queralt A, Meudec E, Eder M, Lamuela-Raventos RM, Sommerer N, Cheynier V. Targeted filtering reduces the complexity of UHPLC-Orbitrap-HRMS data to decipher polyphenol polymerization. *Food Chem*. 2017;227:255-63.
15. Ubukata M, Jobst KJ, Reiner EJ, Reichenbach SE, Tao Q, Hang J, Wu Z, Dane AJ, Cody RB. Non-targeted analysis of electronics waste by comprehensive two-dimensional gas chromatography combined with high-resolution mass spectrometry: Using accurate mass information and mass defect analysis to explore the data. *J Chromatogr A*. 2015;1395:152-9.
16. Baduel C, Mueller JF, Rotander A, Corfield J, Gomez-Ramos M-J. Discovery of novel per- and polyfluoroalkyl substances (PFASs) at a fire fighting training ground and preliminary investigation of their fate and mobility. *Chemosphere*. 2017. doi:10.1016/j.chemosphere.2017.06.096

## 2.5 PUBLICATION: The potential for complementary targeted/non-targeted screening of novel psychoactive substances in equine urine using Liquid Chromatography-High Resolution Accurate Mass spectrometry (doi: 10.1039/C6AY00156D)

### 2.5.1 Foreword

The following manuscript was accepted for publication in *Analytical Methods* (published by The Royal Society of Chemistry) and investigates the use of differential analysis software, SIEVE® (Thermo Fisher Scientific), for the detection of hallucinogenic phenethylamines in equine urine. The publication was authored by Dr. Adam Cawley, Mr. Daniel Pasin, Ms. Namuun Ganbat, Ms. Laura Ennis, Ms. Corrine Smart, Ms. Candace Greer, Mr. John Keledjian, Associate Professor Shanlin Fu and Mr. Alex Chen. Experimental work was performed by N Ganbat with optimisation of the SIEVE® parameters performed by D Pasin. The draft manuscript was prepared by A Cawley and D Pasin with edits provided by S Fu. Technical support crucial to the success of this manuscript was provided L Ennis, C Smart, C Greer, J Keledjian and A Chen.

The previously mentioned mass defect-based detection strategies do not take into account that candidate components may be endogenous to the biological matrix, therefore, resulting in potential "false-positive" components. Differential analysis has been identified as a technique to determine compounds that are independent of the sample matrix which can then be prioritised for further interrogation. NOTE: Figure and table caption numbers have been adjusted to align with the chronology of this thesis and may not reflect those published in the actual article.

# The potential for complementary targeted/non-targeted screening of novel psychoactive substances in equine urine using Liquid Chromatography-High Resolution Accurate Mass spectrometry

**SHORT TITLE: LC-HRAM SCREENING OF NPS IN EQUINE URINE**

Adam Cawley * [a], Daniel Pasin [b], Namuun Ganbat [b], Laura Ennis [a], Corrine Smart [a], Candace Greer [a], John Keledjian [a], Shanlin Fu [b] , Alex Chen [c].

a. Australian Racing Forensic Laboratory, Racing NSW, Sydney, NSW, Australia.
b. School of Chemistry and Forensic Science, University of Technology Sydney, NSW, Australia.
c. Thermo Fisher Scientific, Scoresby, VIC, Australia

* Corresponding Author:

Adam Cawley

Australian Racing Forensic Laboratory, Racing NSW

Level 11, 51 Druitt Street Sydney, NSW 2000, Australia.

Email: acawley@racingnsw.com.au

Phone: +61 2 83445000

Fax: +61 2 95517712

### 2.5.2 Abstract

The potential for liquid chromatography-high resolution accurate mass (LC-HRAM) spectrometry to identify 'unknown' compounds using non-targeted screening methods provides a potential advantage in the fight against doping in sport. This innovation comes with the requirement for assessment to support its use in the medico-legal context. A method for the LC-HRAM detection of 2,5-dimethoxy-*N*-(2-methoxybenzyl)phenethylamine (NBOMe) compounds in equine urine was validated in order to assess the capabilities of a workflow developed for non-targeted analysis using the SIEVE® differential analysis software platform. Six NBOMe compounds (25B, 25C, 25D, 25E, 25H and 25I) were studied to develop and optimize the proposed non-targeted screening workflow before two additional candidates (25N and 25T2) were used as blind controls for verification. Chromatographic alignment and the integration threshold were found to be the most critical parameters for successful identification of 'unknown' responses. The proposed workflow serves as an example for anti-doping laboratories to implement fit-for-purpose non-targeted screening methods.

### 2.5.3 Keywords

Anti-doping, Novel psychoactive substances, NBOMe, Liquid chromatography-high resolution accurate mass spectrometry, Differential analysis.

### 2.5.4 Introduction

Novel psychoactive substances (NPS) are chemical modifications of currently controlled substances that have similar pharmacological effects and chemically designed to circumvent legislation [1]. In 2012, Casale and Hays [2] reported the characterization of eleven 2,5-dimethoxy-*N*-(2-methoxybenzyl)phenethylamine (NBOMe) compounds considered to be more potent serotonin 5-$HT_{2A}$ receptor agonists than their 2,5-dimethoxyphenethylamine ("2C") precursors [3-5]. Since this time there have been multiple reports concerning adverse health effects [6-13]. Misuse of this drug class generally occurs with a single administration of approximately 0.1 g to achieve hallucinations and a varying degree of stimulation [13]. In response to a medico-legal requirement the validation of analytical methods used to detect NBOMe compounds in biological matrices have been reported by forensic toxicology laboratories [8-10]. Furthermore, metabolism studies in human and rat urine have been recently performed [14].

While there are no reports describing the effect of these compounds in horses, there is concern about the potential for misuse of NPS such as NBOMe compounds in equine athletes where handlers may have made the assumption that these compounds are undetectable by horseracing laboratories. The availability of these compounds presents a serious threat to the integrity of equine sports and to the welfare of the horse. NBOMe compounds are therefore prohibited for use by the International Federation of Horseracing Authorities [15].

Analytical methods utilizing the sensitivity and specificity of liquid chromatography-high resolution accurate mass (LC-HRAM) spectrometry applied to forensic toxicology [16-18], and more specifically to horseracing laboratories [19], have been reported in recent years. The potential for LC-HRAM technology to detect 'unknown'

compounds using non-targeted screening methods provides a potential advantage in the fight against doping in sport.

Differential analysis is a tool used in studies with large data sets that require the comparison of pre-treatment control samples of biological origin with samples collected following a treatment (such as exposure to particular stimuli) in order to detect and elucidate biomarkers correlating to the treatment response. The control and treatment samples are compared by statistical means resulting in the generation of a list of targets that are independent of the control sample. For the past 10 to 15 years, differential analysis techniques have been widely used for the assessment of microarray data [20, 21]. More recently following the development of software for MS-based applications, there is considerable potential for differential analysis in analytical chemistry [22]. Depending on the software used standard outputs may include retention time, mass-to-charge (*m/z*) ratio and the statistical probability (*p*-value) of the two samples being statistically different. From this information, a targeted approach can be applied such as tandem mass spectrometry ($MS^2$) to identify unknown compounds. This strategy is preferred over conventional visual assessment of chromatographic data since it can detect compounds that coelute or have low abundances obscured by background noise. In addition, differential analysis applied to full-scan MS provides an advantage over other chemometric approaches for biomarker detection by not excluding raw data. With the rapid proliferation of NPS such strategies have the potential to detect new compounds that have not been previously defined in published targeted methods or databases.

The aim of the study described herein was to develop and validate a method for the detection of six NBOMe compounds (Figure 2.15) in equine urine using LC-HRAM spectrometry to support integrity in horseracing. Furthermore, the applicability of

using a differential analysis software package such as SIEVE® (Statistical Iterative Exploratory Visualization Environment, Thermo Fisher Scientific) [23] was evaluated for the non-targeted screening and putative identification of two additional NBOMe compounds that were unknown to the analyst under 'blind' testing conditions.

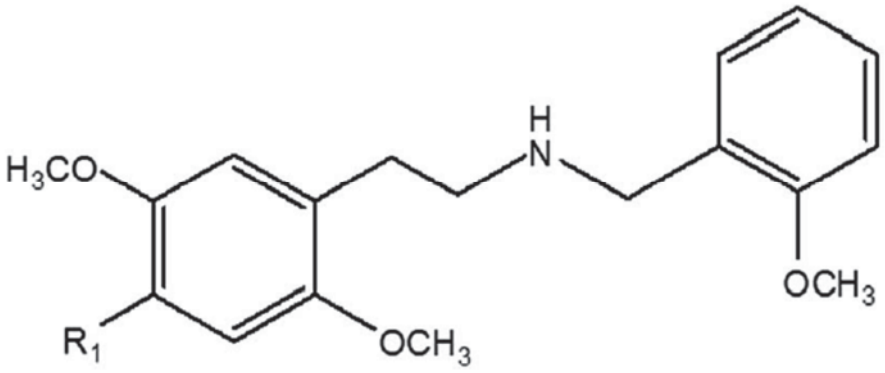


**Figure 2.15** General NBOMe structure ($R_1$: Br = 25B, Cl = 25C, $CH_3$ = 25D, $C_2H_5$ = 25E, H = 25H, I = 25I).

## 2.5.5 Materials and methods

### *2.5.5.1 Reference materials, chemicals and reagents*

Hydrochloride salts of the NBOMe compounds [2-(4-bromo-2,5-dimethoxyphenyl)-*N*-(2-methoxybenzyl)ethanamine] (25B), [2-(4-chloro-2,5-dimethoxyphenyl)-*N*-(2-methoxybenzyl)ethanamine] (25C), [2-(4-methyl-2,5-dimethoxyphenyl)-*N*-(2-methoxybenzyl)ethanamine] (25D), [2-(4-ethyl-2,5-dimethoxyphenyl)-*N*-(2-methoxybenzyl)ethanamine] (25E), [2-(2,5-dimethoxyphenyl)-*N*-(2-methoxybenzyl)ethanamine] (25H), [2-(4-iodo-2,5-dimethoxyphenyl)-*N*-(2-methoxybenzyl)ethanamine] (25I), [2-(4-nitro-2,5-dimethoxyphenyl)-*N*-(2-methoxybenzyl)ethanamine] (25N) and [2-(4-methylthio-2,5-dimethoxyphenyl)-*N*-(2-methoxybenzyl)ethanamine] (25T2) manufactured by Lipomed AG (Arlesheim,

Switzerland) were purchased as 1 mg/mL (in methanol) ampoules from PM Separations (Capalaba, Queensland, Australia). Desipramine-$d_3$ was purchased from Grace (Deerfield, IL, USA). Trypsin and sodium acetate were obtained from Sigma-Aldrich (St Louis, MO, USA). β-Glucuronidase K12 from *E.coli* was purchased from Roche Diagnostics (Mannheim, Germany). Analytical grade ammonia (aqueous solution 28%) and acetic acid (glacial) together with HPLC grade solvents were purchased from Thermo Fisher Scientific (Fair Lawn, NJ, USA). Ultra-pure water was obtained using a Millipore filtration system (Bedford, MA, USA)

*2.5.5.2 Preparation of standard solutions*

Stock solutions for each NBOMe standard were prepared at 100 μg/mL by quantitatively diluting the purchased 1 mg/mL solution into 10 mL of methanol in a volumetric flask. For the method validation, a mixed NBOMe intermediate solution (1 μg/mL) containing the six candidates (25B, 25C, 25D, 25E, 25H and 25I) was prepared by diluting 100 μL of each stock into 10 mL of methanol in a volumetric flask. A mixed NBOMe working solution (100 ng/mL) was prepared by diluting 1 mL of the mixed intermediate solution into 10 mL methanol in a volumetric flask. Desipramine-$d_3$ stock solution (1 mg/mL) was prepared from dissolving 5 mg of primary standard, weighed using an analytical balance (Mettler Toledo AT261, Columbus, OH, USA), in methanol (5 mL) using a volumetric flask. The desipramine-$d_3$ working solution (2 μg/mL) was prepared by diluting 20 μL of stock in methanol (10 mL) using a volumetric flask. Methanolic solutions were stored at 4°C for up to 12 months.

### 2.5.5.3 Preparation of blank equine urine

Authentic blank urine samples were collected from three thoroughbred gelding horses by spontaneous voiding with carrot reward following approval from the Racing NSW Animal Care and Ethics Committee (RP72). These horses were known to have not been administered any pharmaceutical agent for at least two weeks prior to sample collection. Urine samples from the three horses were pooled to provide a profile considered to be representative of the racehorse population for proof-of-concept concerning differential analysis.

### 2.5.5.4 Sample preparation

Equine urine samples (3 mL) were fortified with desipramine-$d_3$ (2 μg/mL, 50 μL) internal standard before addition of pH 5.0 acetate buffer (0.2 M, 4 mL) followed by enzyme hydrolysis with β-glucuronidase K12 from *E.coli* (20 μL) and trypsin solution (625 μg/sample) overnight at 37°C. The basic organic fraction was isolated by solid phase extraction (SPE) using a mixed-mode C8/strong cation exchange XTRACKT® column (200 mg, 3 cc, UCT, Bristol, PA, USA). The cartridge was conditioned with methanol (2 mL) and water (2 mL) before loading the urine sample and washing with acetic acid (0.1M, 2 mL) followed by methanol (2 mL). The cartridge was dried using $N_2$ gas under positive pressure before elution with ethyl acetate/ammonia/methanol (100:3:0.5, 3 mL). HCl/methanol (0.1 M, 20 μL) was added to extracts before evaporation to dryness under nitrogen at 60°C. Residues were reconstituted in methanol (50 μL) and pH 4 ammonium acetate (10 mM, 100 μL) for LC-HRAM analysis.

*2.5.5.5 LC-HRAM analysis*

LC-HRAM spectrometry was undertaken using an Ultimate 3000 HPLC coupled to a QExactive benchtop orbitrap mass spectrometer (Thermo Fisher Scientific, Bremen, Germany). LC separation was performed using a Gemini® C18 column (50 x 2.1 mm, 5 um; Phenomenex, Torrence, CA, USA) operating at 35°C with a 10 µL injection volume. The mobile phase consisted of A: pH 9 ammonium acetate (10 mM) and B: 0.1% acetic acid/acetonitrile. Gradient elution was performed with a flow rate of 0.5 mL/min according to the following program: 1% B for 2 min, increased to 80% B linearly during the period between 2 and 8.5 min, before returning to 1% B at 8.6 min and held until 11.2 min. HRAM detection was performed using positive mode heated electrospray ionization (HESI) in full scan at a resolution of 70,000 (full width at half maximum, FWHM) acquiring a mass range of *m/z* 50 to 650 at 3 Hz. Mass calibration was performed prior to analysis using Pierce® ESI positive (P/N 88323) calibration solution (Thermo Fisher Scientific, Bremen, Germany) but no lock mass was used. Source temperature, spray voltage, sheath gas (high purity $N_2$) and auxiliary gas (ultra-high purity $N_2$) were set at 350°C, +4000 V, 63.74 and 10.30 arbitrary units, respectively. $MS^2$ data was acquired with a normalized collision energy of 25 arbitrary units, automatic gain control target of $2x10e^5$ and *m/z* isolation window of 0.5 to support confirmation of identity according to criteria prescribed by the Association of Official Racing Chemists (AORC) [24]. Instrument control and data processing (±5 ppm) were performed using Xcalibur® software (version 2.2 SP1) from Thermo Fisher Scientific (San Jose, CA, USA).

*2.5.5.6 Method validation*

Method parameters were assessed according to NATA Technical Note–17 [25] to support the ILAC-G7:06/2009 document for horse racing laboratories [26].

Quantitative results were obtained from full scan acquisition of $[M+H]^+$ for each analyte provided in Table 2.7. The limit of detection (LOD) and lower limit of quantification (LLOQ) for the six candidate NBOMe compounds were determined from replicate (n = 7) analyses of spiked equine urine samples achieving a signal-to-noise (*S/N*) ratio of greater than 3 and 10, respectively. Intra- and inter-assay precision (expressed as percentage relative standard deviation, %RSD), together with accuracy, were determined from the ratio of peak areas for the analyte and desipramine-$d_3$ for seven replicates of 1 ng/mL and 10 ng/mL each analysed seven days over a period of two weeks. The same spiked sample matrix was used to assess recovery with comparison to urine samples fortified at 1 ng/mL and 10 ng/mL post-extraction. In turn, matrix effect was assessed using this set of post-extraction fortified urine samples compared to neat standards reconstituted in LC mobile phase at 1 ng/mL and 10 ng/mL. Long-term stability trials were performed on additional replicates (n = 3) of spiked samples stored at 4°C, -20°C and -80°C for one-, two- and three-month intervals. Short-term stability freeze/thaw trials were conducted on three consecutive days using additional replicates (n = 3) of spiked samples stored at -20°C.

#### *2.5.5.7 Non-targeted screening*

Differential analysis of full scan ($MS^1$) data was performed using SIEVE® version 2.0.180. Data files acquired from duplicate sample injections were processed against duplicate matrix blank injections representing the control, the second of which was assigned as the reference file for chromatographic alignment. Recursive-base-peak-framing was used over the entire chromatographic run time (11.2 min) between *m/z* 50 and 500 to reflect the retention time and mass range of NPS. The default *Peak Intensity Threshold* of $1.27 \times 10^8$ resulted in the generation of 5,000 frames while the optimized *Peak Intensity Threshold* of $1 \times 10^6$ resulted in the generation of 2,000 frames, each

with a chromatographic time range of 2.5 min and *m/z* width of 10 ppm. Statistical output from SIEVE® provides a *Ratio* value between sample and control with an associated *p-value* for each putative substance.

Analysis of $MS^2$ data to investigate dissociation schemes and apply precursor ion fingerprinting was performed using Mass Frontier™ 7.0 SR1. Each of these software packages were purchased from Thermo Fisher Scientific (San Jose, CA, USA).

### 2.5.6 Results and discussion

#### *2.5.6.1 Targeted method validation*

The limited LC selectivity displayed by the six candidate NBOMe compounds is shown in Table 1 with retention times within 0.8 min, including coelution of 25C and 25D. Nevertheless, specificity was achieved from differences in mass for this group of non-isomeric NBOMe compounds. The mass error (Δ) for the six candidate NBOMe compounds was found to be within 2.0 ppm, which is within the accepted value of 5.0 ppm [24].

This included the $[M+H+2]^+$ isotopes for 25B and 25C due to the presence of bromine and chlorine atoms in their respective structures. Robustness in specificity was demonstrated by stability in mass accuracy without the use of a lock mass. Using caffeine ($[M+H]^+$ = *m/z* 195.0877) as the most representative compound of NPS contained in the calibration mix, the intra-assay standard deviation was within 0.05 ppm. For the six-month duration of the study, the inter-assay standard deviation was within 0.1 ppm.

**Table 2.7** Specificity for six candidate NBOMe compounds using LC-HRAM

| NBOMe | Retention time [min] | Formula | Experimental $[M+H]^+$ | Theoretical $[M+H]^+$ [a] | Mass Error [Δ ppm] |
|---|---|---|---|---|---|
| 25H | 5.72 | $C_{18}H_{23}NO_3$ | 302.1745 | 302.1751 | 2.0 |
| 25B | 6.20 | $C_{18}H_{22}NO_3Br$ | 380.0850<br>382.0829 | 380.0856<br>382.0835 | 1.6<br>1.6 |
| 25C | 6.10 | $C_{18}H_{22}NO_3Cl$ | 336.1355<br>338.1325 | 336.1361<br>338.1331 | 1.8<br>1.8 |
| 25D | 6.10 | $C_{19}H_{25}NO_3$ | 316.1902 | 316.1907 | 1.6 |
| 25E | 6.48 | $C_{20}H_{27}NO_3$ | 330.2059 | 330.2064 | 1.5 |
| 25I | 6.37 | $C_{18}H_{22}NO_3I$ | 428.0712 | 428.0717 | 1.2 |

[a]Determined by isotope simulation tool in the Xcalibur® operating software

Quantitative validation results are provided in Table 2.8, which shows the LOD to be 0.1 ng/mL for 25B, 25E, 25H and 25I, and 0.5 ng/mL for 25C and 25D. The LLOQ for all six candidate NBOMe compounds was 1 ng/mL. Linearity was achieved between this LLOQ and 200 ng/mL with coefficient of determination ($R^2$) ≥ 0.995 to establish the calibration range performed in duplicate at the following concentrations: 1, 2, 5, 10, 20, 50, 100 and 200 ng/mL.

Intra- and inter-assay precision was assessed at a spiking level of 1 ng/mL to be within 8.7% (<10%) and 13.2% (<15%), respectively. At 10 ng/mL these were within 4.0% (<10%) and 10.9% (<15%), respectively. Suitability of the SPE sample preparation method was demonstrated by excellent recoveries (88% to 97%) from 10 ng/mL spiked equine urine samples, supporting accuracy between 93 ± 4% and 113 ± 6% (between 80% and 120%). Matrix effects were determined to be negligible from the results that were within 20% of the expected value. Samples were stable after 3 freeze/thaw cycles and stable for up to 3 months at 4°C, -20°C and -80°C.

**Table 2.8** Quantitative validation results for the six candidate NBOMe compound

| Parameter | 25B | 25C | 25D | 25E | 25H | 25I |
|---|---|---|---|---|---|---|
| LOD [ng/mL] | 0.1 | 0.5 | 0.5 | 0.1 | 0.1 | 0.1 |
| LLOQ [ng/mL] | 1.0 | 1.0 | 1.0 | 1.0 | 1.0 | 1.0 |
| Linearity [ng/mL, $R^2 \geq 0.995$] | 1-200 | 1-200 | 1-200 | 1-200 | 1-200 | 1-200 |
| Intra-assay at 1 ng/mL [%RSD] | 6.9 | 8.5 | 7.3 | 6.2 | 8.7 | 5.7 |
| Intra-assay at 10 ng/mL [%RSD] | 5.2 | 5.4 | 6.1 | 4.0 | 7.3 | 3.5 |
| Inter-assay at 1 ng/mL [%RSD] | 6.7 | 7.5 | 10.5 | 13.2 | 11.8 | 8.6 |
| Inter-assay at 10 ng/mL [%RSD] | 5.3 | 7.6 | 5.9 | 5.0 | 10.9 | 6.2 |
| Accuracy [%±SD, at 10 ng/mL] | 93 ± 4 | 109 ± 5 | 108 ± 5 | 106 ± 4 | 107 ± 7 | 113 ± 6 |
| Recovery [%, at 10 ng/mL] | 93 | 97 | 96 | 97 | 91 | 88 |

### 2.5.7 Non-targeted analysis using differential analysis

Individual components of the SIEVE® software workflow were assessed; chromatographic alignment, peak detection, statistical analysis and identification.

#### *2.5.7.1 Chromatographic alignment*

Since SIEVE® can compare between two or more samples simultaneously, it is important that the sample chromatograms are first aligned for the peak detection process to provide accurate results. The ChromAlign algorithm corrects for inherent chromatographic variability by calculating optimal correlations between full-scan spectra in separate data files [27]. Retention time results for the six candidate NBOMe compounds and desipramine-$d_3$ internal standard ($[M+H]^+$ = *m/z* 198.1065) obtained from the precision validation matrix were compared to assess variation that may reduce the robustness of the alignment algorithm used by SIEVE®. The suitability of LC

parameters was demonstrated by relative standard deviations of less than 0.1% determined from seven 10 ng/mL replicates over seven sets of analyses conducted within two weeks. Using the example of 25B spiked at 100 ng/mL, Figure 2.16 demonstrates proof-of-concept for SIEVE® to provide visual identification of an abnormal response.

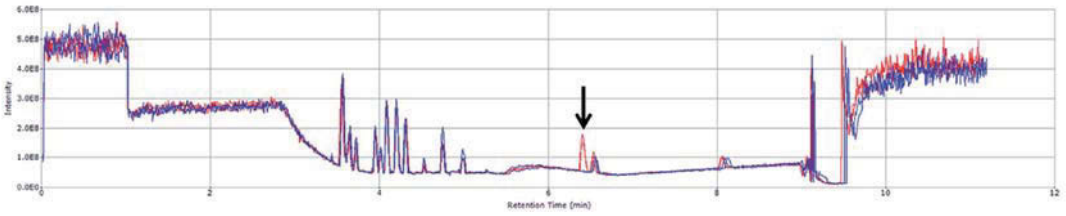


**Figure 2.16** SIEVE® total ion chromatogram (TIC) alignment showing the presence of 25B (annotated with ↓) spiked at 100 ng mL-1 in equine urine by comparison to a blank equine urine sample.

### *2.5.7.2 Peak detection*

Following chromatographic alignment, spectral data is plotted in three-dimensional space with retention time, *m/z* and relative intensity on the x-, y- and z-axes, respectively. Peaks in the control and treatment sample are detected using an algorithm called recursive-base-peak-framing where spectral data from both samples in the experiment are grouped together by relative intensity. Once the common base peak is known, a frame is established according to user-defined retention time, *m/z* and intensity tolerances [28]. The *Peak Intensity Threshold* is the lowest intensity for which a spectral data point will be framed and is recommended to be one that is representative of the LOD for the respective class.

The default *Peak Intensity Threshold* setting of $1.27 \times 10^8$ analyzing 5000 frames provided detection of the six candidate NBOMe compounds at concentrations between

20 and 100 ng/mL. While sufficient for proof-of-concept that differential analysis was applicable to the method, these levels were considered too high for routine application. Optimization of the *Peak Intensity Threshold* to $1x10^6$ analyzing 2000 frames resulted in detection levels between 0.5 ng/mL and 10 ng/mL that are considered fit-for-purpose.

*2.5.7.3 Statistical analysis*

At the conclusion of the peak detection process, the mean peak intensity values for peaks in each frame from sample and control replicates are compared using paired *t*-tests for determination of significant differences. The generated frame report contains the associated *p-value* for verification by the user. For simplicity, the frame report also contains a *Ratio* parameter which provides the user with direct comparison of mean peak intensities that can be filtered to identify compounds of interest. By convention, the maximum *Ratio* and minimum *p-value* is 99999.90 and $1.00x10^{-5}$, which implies the compound in the treatment sample is completely independent to the control sample. In addition to numerical statistical evaluation, the data can be reviewed as volcano plots, scores plots from principal component analysis (PCA) or scatter plots to visualize correlation between *Ratio* and *p-value*.

For this study, compounds exhibiting a *Ratio* > 10 and *p-value* < 0.001 were deemed compounds of interest. Figure 2.17 shows the frame report for 25B spiked at 5 ng/mL with maximum *Ratio* values of 99999.90 for *m/z* 380.0852 ($[M+H]^+$, Δ=1.1 ppm) and 2657.679 for *m/z* 382.0830 ($[M+H+2]^+$, Δ = 1.3 ppm), together with 99999.90 for their $^{13}C$ isotope responses *m/z* 381.0887 and *m/z* 383.0866, respectively. The *p-value* associated with the maximum possible *Ratio* values was $1.00x10^{-5}$, while that for *m/z* 382.0830 with a lower yet clearly high *Ratio* value was $2.44x10^{-3}$. Interestingly, these *m/z* values only differ by approximately 1 Da yet they are all associated with

different frames. For example *m/z* 380.0852, 381.0887, 382.0830 and 383.0866 are associated with frames 515, 1775, 537 and 1726 and respectively.

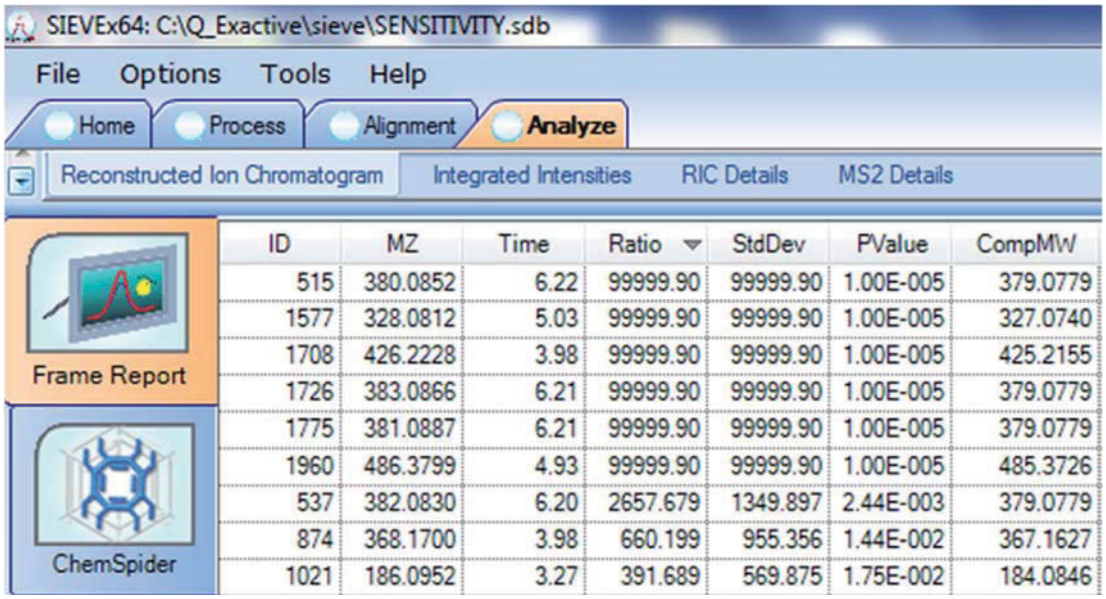


| ID | MZ | Time | Ratio | StdDev | PValue | CompMW |
|---|---|---|---|---|---|---|
| 515 | 380.0852 | 6.22 | 99999.90 | 99999.90 | 1.00E-005 | 379.0779 |
| 1577 | 328.0812 | 5.03 | 99999.90 | 99999.90 | 1.00E-005 | 327.0740 |
| 1708 | 426.2228 | 3.98 | 99999.90 | 99999.90 | 1.00E-005 | 425.2155 |
| 1726 | 383.0866 | 6.21 | 99999.90 | 99999.90 | 1.00E-005 | 379.0779 |
| 1775 | 381.0887 | 6.21 | 99999.90 | 99999.90 | 1.00E-005 | 379.0779 |
| 1960 | 486.3799 | 4.93 | 99999.90 | 99999.90 | 1.00E-005 | 485.3726 |
| 537 | 382.0830 | 6.20 | 2657.679 | 1349.897 | 2.44E-003 | 379.0779 |
| 874 | 368.1700 | 3.98 | 660.199 | 955.356 | 1.44E-002 | 367.1627 |
| 1021 | 186.0952 | 3.27 | 391.689 | 569.875 | 1.75E-002 | 184.0846 |

**Figure 2.17** SIEVE® frame report for 25B spiked at 25 ng/mL in equine urine.

### *2.5.7.4 Identification*

Comparison of retention times for responses corresponding to an isotope distribution that record high *Ratio* values (>10) and low *p-values* (<1.00x10$^{-3}$) enabled a presumptive finding to be made. Figure 2.17 shows the retention time range (6.20 to 6.22 min) for the four responses attributable to 25B at 5 ng/mL in equine urine. The component molecular weight (*CompMW*) for these responses at 379.0779 Da was input to the elemental composition table of the Xcalibur® operating software for generation of chemical formula using defined parameters. The elements selected were C, H, N, O, F, Cl, Br, I and S with a mass tolerance of ±10 ppm and double-bond equivalents (DBE) range of 4.0 to 10.0. The second of ten results (in order of increasing Δ) was $C_{18}H_{22}NO_3Br$ with Δ=0.4 ppm and DBE=8.0. This could be selected

as the correct candidate based on two assessments; known DBE for NBOMe compounds of 8.0 due to the presence of two benzene rings and the simulated spectral comparison feature of Xcalibur®.The latter provides a visual comparison of experimental and theoretical isotope patterns for the given chemical formula as shown by Figure 2.18 for the example of 25B at 5 ng/mL in equine urine. Accuracy in the provision of *CompMW* of 25B (379.0779 Da) from SIEVE® was assessed by Δ to be -0.3 ppm. With the molecular weight and chemical formula proposed for an 'unknown' compound using SIEVE® and Xcalibur®, respectively, the identification process can proceed using $MS^2$ studies. For this purpose Mass Frontier™ spectral interpretation software was used to interrogate targeted $MS^2$ data uploaded from Xcalibur®. Mass Frontier™ software can predict product-ion structures and provide dissociation pathways for user-defined compounds.

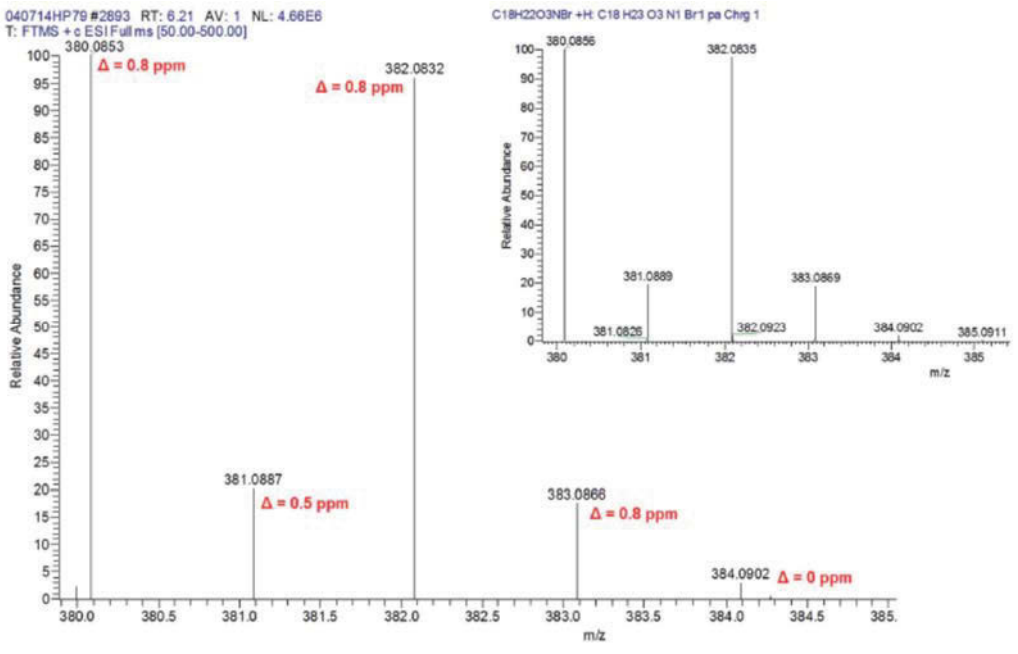


**Figure 2.18** Xcalibur® simulated isotope pattern for 25B spiked at 5 ng/mL in equine urine (with annotated D) and theoretical pattern for $C_{18}H_{22}O_3NBr$ (right inset).

Precursor ion fingerprinting was investigated as a means for using structurally-related product ions to identify the precursor [29]. $MS^2$ studies of the six candidate NBOMe compounds revealed a common dissociation pathway resulting in the cleavage of benzyl moiety to produce *m/z* 121.0651 (±1.2 ppm) and detection of the tropylium ion (*m/z* 91.0548, ±1.8 ppm). These diagnostic product ions can be used to confirm the NBOMe class of compounds following investigation of screening abnormalities produced from differential analysis.

### *2.5.7.5 Proposed workflow*

The results for 25B were used to propose a workflow (Figure 2.19) that could be implemented by forensic laboratories using differential analysis to perform non-targeted screening. This was successfully applied to the detection of 25C (10 ng/mL), 25D (5 ng/mL), 25E (10 ng/mL), 25H (5 ng/mL) and 25I (0.5 ng/mL) in equine urine. The proposed workflow is composed of four sections that are separated based on the software required; SIEVE®, Xcalibur®, Mass Frontier™ and database searching. At the conclusion of differential analysis by SIEVE®, the frame results can be filtered by *Ratio* (or *p-value*) and components that exhibit a *Ratio* > 10 and *p-value* < 0.001 can be selected for further interrogation. Those that do not meet these criteria can be considered as matrix contributions. Since the majority of NBOMe compounds have one (i.e. an odd number) of nitrogen atoms it would result in an even *m/z* value for the precursor ion due to the addition of a proton from the electrospray ionization process. Components that have an odd *m/z* value can also be included for interrogation since analogues containing an even number of nitrogen atoms are possible, however, odd *m/z* values can imply that the molecule contains no nitrogen atoms and would result in a larger data set for evaluation.

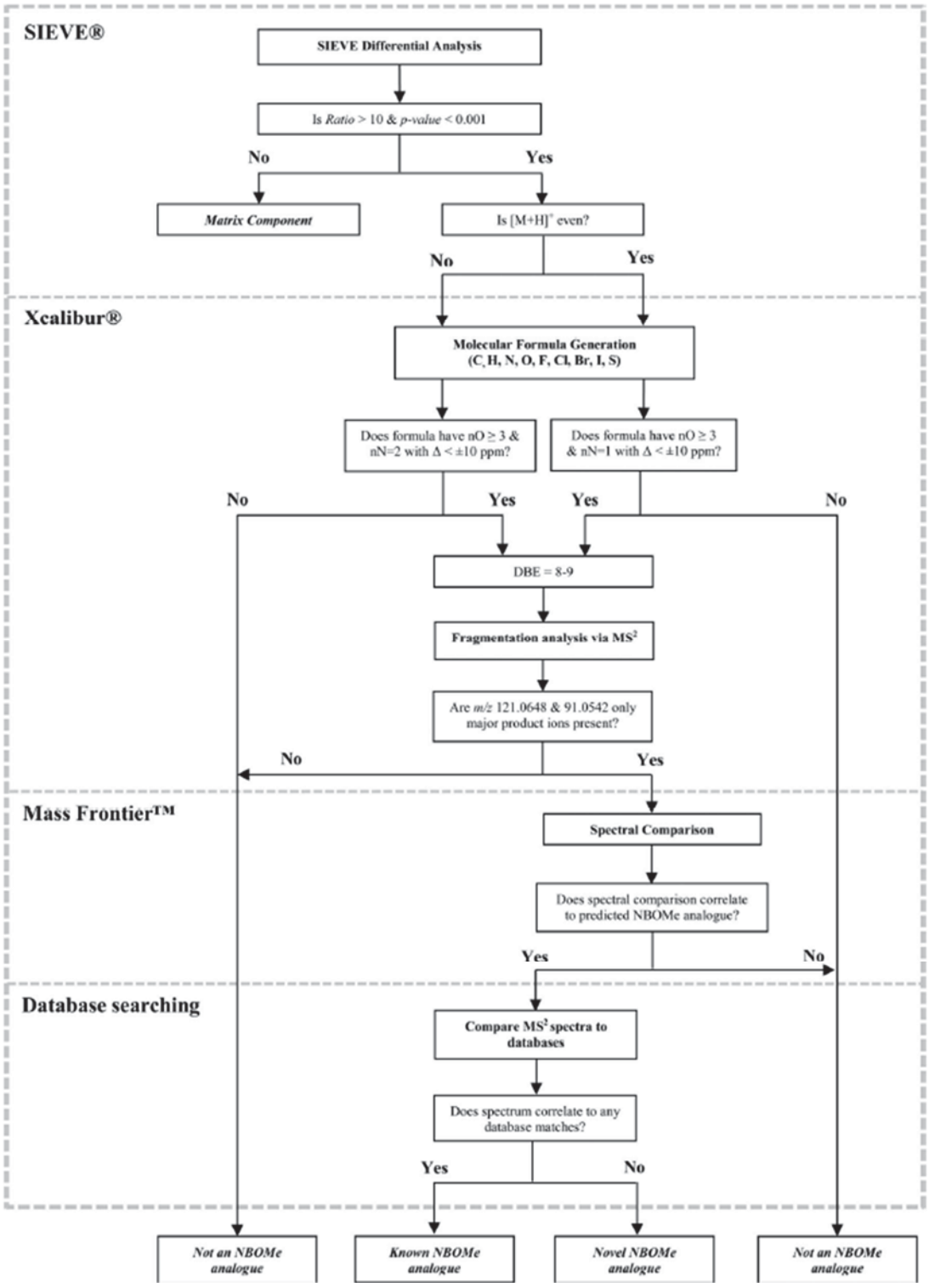


**Figure 2.19** Proposed workflow for non-targeted screening of NBOMe compounds in equine urine.

Following differential analysis, the molecular formulae for selected components can be generated in Xcalibur® using the elemental composition tool by including C, H, N, O, F, Cl, Br, I, S as elements of interest. If the formula generated for a particular component contains a single nitrogen with three oxygen atoms and a DBE = 8 it can be subjected to $MS^2$ studies. The mass error difference should be within ±10 ppm, however, this value can be modified as required by the user. The $MS^2$ data of selected components can be evaluated for the presence of only two major product ions, specifically *m/z* 121.0648 and 91.0542. The added substituent can be determined by comparing the mass difference of the target analyte and the least substituted analogue 25H-NBOMe. Once the structure has been tentatively identified the likelihood can be assessed by using structural correlation software such as Mass Frontier™ to compare the *in silico* and experimental fragmentation patterns. If they correlate, the data can then be compared to a database and if the database search yields no result the analyte of interest could be a novel NBOMe compound.

It should be considered that while the strategy outlined here is aimed explicitly at users of Thermo Fisher Scientific hardware-software configurations for screening of NBOMe compounds, the general workflow can be adapted by users of instruments manufactured by other vendors. For instance, SIEVE® is not the only differential analysis software package available to LC-HRAM practitioners; Mass Profiler Professional developed by Agilent Technologies (Santa Clara, CA, USA) and MetaboLynx™ developed by Waters Corporation. (Milford, MA, USA) are also available.

#### *2.5.7.6 Verification*

The proposed workflow was subsequently verified by two blind control tests, each performed by a separate analyst with the knowledge that a NBOMe compound was

spiked into equine urine at 100 ng/mL but not which particular compound it was.

Test Case 1:

In conjunction with the tabulated frame report, a scatter plot of *Ratio* versus *p-value* is provided by SIEVE® for rapid visual inspection of differential analysis results. Selection of an outlier with a *Ratio* of 416.063 and *p-value* of $1.16 \times 10^{-2}$ had a corresponding *m/z* entry with 347.1596 at a retention time of 6.07 min. In addition, a $^{13}C$ isotopic response with a *Ratio* of 15.252 and *p-value* $1.01 \times 10^{-2}$ was found with *m/z* 348.1631 at the same retention time and *CompMW* of 346.1524 Da. Simulated spectral comparison provided good agreement ($\Delta$ = 1.4 ppm and $\Delta$ = 1.1 ppm) between the two ions detected by SIEVE® and the theoretical *m/z*, respectively. While the *p-value* for both ions was relatively high (i.e. $>1 \times 10^{-3}$), the retention time alignment of these responses with high *Ratio* values was considered sufficient evidence for entry into Xcalibur® to determine the chemical formula as $C_{18}H_{22}N_2O_5$ with $\Delta$ = 0.2 ppm and DBE = 9.0. Mass Frontier™ analysis of $MS^2$ data revealed *m/z* 91.0545 and *m/z* 121.0646 belonging to the diagnostic fragments of an NBOMe compound. The above information was used to identify the unknown compound as the nitro-NBOMe compound, 25N with comparison to literature data reported by Casale and Hays [2]. The DBE value found in this case was 9.0 instead of 8.0 found for other NBOMe compounds, thereby providing a characteristic feature of the $NO_2$-analogue.

Test Case 2:

A second analyst selected an outlier with a *Ratio* of 194.980 and *p-value* of $6.38 \times 10^{-3}$ that had a corresponding *m/z* entry with 363.1814 at a retention time of 6.64 min. A second entry at 6.64 min with *m/z* 362.1779 had a *Ratio* of 86.715 and *p-value* of $9.43 \times 10^{-4}$ with the *CompMW* for both entries at 361.1706 Da. Xcalibur® determined

the chemical formula to be $C_{20}H_{27}NO_3S$ with $\Delta$ = -0.04 ppm and DBE = 8.0. The simulated spectral comparison revealed excellent agreement for *m/z* 362.1781 (100% rel. int., $\Delta$ = 0.8 ppm), *m/z* 363.1816 (20% rel. int., $\Delta$ = 0.6 ppm), *m/z* 364.1736 (5% rel. int., $\Delta$ = 1.6 ppm) and *m/z* 365.1771 (1% rel. int., $\Delta$ = 1.4 ppm). Precursor ion fingerprinting of $MS^2$ data confirmed the NBOMe class before web searching of the chemical formula provided the putative identification to be 25T2 [30, 31].

Illicit administration of NPS such as NBOMe compounds to racehorses is expected to be in response to surveillance of conventional amphetamine-type substances by laboratories. This requires accredited racing laboratories to implement testing methods for substances that become readily available on the black market in order to deter and prosecute licensed persons who are tempted to administer non-approved drugs without knowledge of adverse health effects to an animal. Since 2013, the Australian Racing Forensic Laboratory (ARFL) has no reported findings for NBOMe compounds in equine urine.

The challenge of screening for an ever-increasing number of target compounds, many of which may be 'unknown' to a laboratory or for which no reference material is available, necessitates the use of hardware-software technology combinations that can assist in identifying abnormal responses in a biological sample for further investigation. To this end, the advantages of HRAM instrumentation in racing laboratories can be further enhanced by incorporating differential analysis software such as SIEVE® investigated in this study.

The individual components of the SIEVE® software workflow were assessed to identify critical control points that could be optimized for a proposed non-targeted analysis workflow in forensic laboratories. The importance of mass accuracy for confidence in determining unknowns should not be understated. Following the

assessment of this parameter to document specificity in method validation, successful differential analysis was shown by this study to be dependent on robustness of chromatographic alignment and optimization of the *Peak Intensity Threshold* to achieve the required sensitivity. Recursive-base-peak-framing provides retention time, *m/z*, *Ratio*, *p-value* and *CompMW* that can be reviewed to determine an abnormal finding. While the processing time (approximately 1 min) for differential analysis per sample is reasonable, further work is required to enable batch processing of multiple sample files for more efficient translation of this workflow to routine testing. Regardless, the proposed workflow was used in conjunction with routine targeted analysis of 95 equine urine samples over a three-week period during a major racing carnival. No abnormalities requiring further investigation have yet been reported, however, work continues to increase the coverage of samples analyzed by this method.

The *CompMW* can be used by the instrument operating software (Xcalibur®) to provide a putative chemical formula within defined parameters for elemental composition, which is critical to ensure sufficient coverage of NPS that may include halogen and sulfur substituents. In addition, DBE was found to be a useful discriminator of NPS classes, with 8 or 9 (in the case of 25N) being characteristic of NBOMe compounds. Subsequent $MS^2$ data was interrogated using Mass Frontier™ to enable precursor ion fingerprinting where diagnostic product ions could identify the NBOMe present. The major limitation of this study was the reliance on conventional literature sources to facilitate the final stage of compound identification from $MS^2$ data. Further work is required to investigate the possibility that *pseudo*-$MS^3$ (using in-source collision-induced dissociation; CID) studies of small molecules such as NBOMe compounds could provide the means for *in silico* structural elucidation. This would allow collaborative approaches such as *mzCloud* [32], a $MS^n$ spectral database, to be

incorporated into the workflow.

An additional limitation is the focus on parent NBOMe compounds without taking into account the likely presence of metabolites following NBOMe administration as recently reported for 25I by Caspar *et al.* [14] Metabolism of NBOMe and other NPS compounds will undoubtedly be important to consider as the research into non-targeted screening strategies continues, however, the focus of this study was to use parent NBOMe compounds as model analytes for the development of non-targeted screening strategies.

Consideration must also be given to the presence of isobaric compounds such as structural isomers that are not resolved using HRAM technology. Investigation and subsequent confirmation of such compounds will require greater LC selectivity than the generic screen presented here.

Notwithstanding the limitations of the method, putative identification of a NBOMe compound using the presented screening strategy can enable an abnormality to be recorded against a sample in order for further investigation to take place. Subsequent confirmation would require the procurement of an authentic reference material but this should not preclude the method from being useful to circumvent the nexus that anti-doping laboratories find themselves in terms of targeted analysis.

### 2.5.8 Conclusion

The use of LC-HRAM spectrometry has demonstrated the capability for laboratories to combat the misuse of NPS in horseracing. Specific to this study, the presented method for the targeted detection and quantification of NBOMe compounds in equine urine was validated. In addition, proof-of-concept use of differential analysis with SIEVE® was performed for non-targeted screening to putatively identify two NBOMe

compounds, 25N and 25T2 with scope to extend this study to $MS^n$ data for *in silico* elucidation of novel compounds.

### 2.5.9 References


1. Collins M. Some new psychoactive substances: precursor chemicals and synthesis-driven end-products. *Drug Test Anal*. 2011;3:404-16.
2. Casale J, Hays P. Characterization of eleven 2,5-dimethoxy-N-(2-methoxybenzyl) phenethylamine (NBOMe) derivatives and differentiation from their 3-and 4-methoxybenzyl analogues Part–1. *Microgram J*. 2012;9.
3. Sekuła K, Zuba D. Structural elucidation and identification of a new derivative of phenethylamine using quadrupole time-of-flight mass spectrometry. *Rapid Commun Mass Spectrom*. 2013;27:2081-90.
4. Zuba D, Sekuła K. Analytical characterization of three hallucinogenic N-(2-methoxy)benzyl derivatives of the 2C-series of phenethylamine drugs. *Drug Test Anal*. 2013;5:634-45.
5. Zuba D, Sekuła K, Buczek A. 25C-NBOMe – New potent hallucinogenic substance identified on the drug market. *Forensic Sci Int*. 2013;227:7-14.
6. Rose SR, Poklis JL, Poklis A. A case of 25I-NBOMe (25-I) intoxication: a new potent 5-HT2A agonist designer drug. *Clin Toxicol*. 2013;51:174-7.
7. Hill SL, Doris T, Gurung S, Katebe S, Lomas A, Dunn M, Blain P, Thomas SHL. Severe clinical toxicity associated with analytically confirmed recreational use of 25I–NBOMe: case series. *Clin Toxicol*. 2013;51:487-92.
8. Johnson RD, Botch-Jones SR, Flowers T, Lewis CA. An evaluation of 25B-, 25C-, 25D-, 25H-, 25I- and 25T2-NBOMe via LC-MS-MS: method validation and analyte stability. *J Anal Toxicol*. 2014;38:479-84.
9. Poklis JL, Clay DJ, Poklis A. High-performance liquid chromatography with tandem mass spectrometry for the determination of nine hallucinogenic 25-NBOMe designer drugs in urine specimens. *J Anal Toxicol*. 2014;38:113-21.
10. Poklis JL, Nanco CR, Troendle MM, Wolf CE, Poklis A. Determination of 4-bromo-2,5-dimethoxy-N-[(2-methoxyphenyl)methyl]-benzeneethanamine (25B-NBOMe) in serum and urine by high performance liquid chromatography with tandem mass spectrometry in a case of severe intoxication. *Drug Test Anal*. 2014;6:764-9.
11. Stellpflug S, Kealey S, Hegarty C, Janis G. 2-(4-Iodo-2,5-dimethoxyphenyl)-N-[(2-methoxyphenyl)methyl]ethanamine (25I-NBOMe): Clinical Case with Unique Confirmatory Testing. *J Med Toxicol*. 2014;10:45-50.
12. Tang MHY, Ching CK, Tsui MSH, Chu FKC, Mak TWL. Two cases of severe intoxication associated with analytically confirmed use of the novel psychoactive substances 25B-NBOMe and 25C-NBOMe. *Clin Toxicol*. 2014;52:561-5.
13. Weaver MF, Hopper JA, Gunderson EW. Designer drugs 2015: assessment and management. *Addict Sci Clin Pract*. 2015;10:8.
14. Caspar AT, Helfer AG, Michely JA, Auwärter V, Brandt SD, Meyer MR, Maurer HH. Studies on the metabolism and toxicological detection of the new psychoactive designer drug 2-(4-iodo-2,5-dimethoxyphenyl)-N-[(2-methoxyphenyl)methyl]ethanamine (25I-NBOMe) in human and rat urine using GC-MS, LC-MS(n), and LC-HR-MS/MS. *Anal Bioanal Chem*. 2015;407:6697-

719.
15. International Federation of Horseracing Authorities. Article 6 of the International Agreement on Breeding, Racing and Wagering. Accessed in May 2015. http://www.ifhaonline.org/agreementDisplay.asp#a6
16. Meyer MR, Helfer AG, Maurer HH. Current position of high-resolution MS for drug quantification in clinical & forensic toxicology. *Bioanalysis*. 2014;6:2275-84.
17. Meyer MR, Maurer HH. Current applications of high-resolution mass spectrometry in drug metabolism studies. *Anal Bioanal Chem*. 2012;403:1221-31.
18. Ojanperä I, Kolmonen M, Pelander A. Current use of high-resolution mass spectrometry in drug screening relevant to clinical and forensic toxicology and doping control. *Anal Bioanal Chem*. 2012;403:1203-20.
19. Moulard Y, Bailly-Chouriberry L, Boyer S, Garcia P, Popot M-A, Bonnaire Y. Use of benchtop exactive high resolution and high mass accuracy orbitrap mass spectrometer for screening in horse doping control. *Anal Chim Acta*. 2011;700:126-36.
20. Hatfield GW, Hung SP, Baldi P. Differential analysis of DNA microarray gene expression data. *Mol Microbiol*. 2003;47:871-7.
21. Mocellin S, Rossi CR. Principles of gene microarray data analysis. *Adv Exp Med Biol*. 2007;593:19-30.
22. Weiss JM, Simon E, Stroomberg GJ, de Boer R, de Boer J, van der Linden SC, Leonards PE, Lamoree MH. Identification strategy for unknown pollutants using high-resolution mass spectrometry: androgen-disrupting compounds identified through effect-directed analysis. *Anal Bioanal Chem*. 2011;400:3141-9.
23. Thermo Fisher Scientific. SIEVE Software for Differential Expression Analysis. Accessed in August 2015. http://planetorbitrap.com/label-free#tab:data-analysis
24. The Association of Official Racing Chemists (2015). AORC Guidelines for the Minimum Criteria for Identification by Chromatography and Mass Spectrometry Accessed in May 2015. http://www.aorc-online.org/documents/aorc-ms-criteria-jan-2015
25. National Association of Testing Authorities (2013). Guidelines for the validation and verification of quantitative and qualitative test methods.Technical Note – 17. Accessed in July 2014. http://www.nata.com.au/nata/phocadownload/publications/Guidance_information/tech-notes-information-papers/technical_note_17.pdf
26. International Laboratory Accreditation Cooperation. Accreditation requirements and operating criteria for horseracing laboratories. ILAC-G7:06/2009. Accessed in July 2014. http://ilac.org/publications-and-resources/ilac-documents/guidance-series/
27. Sadygov RG, Martin Maroto F, Hühmer AFR. ChromAlign: A Two-Step Algorithmic Procedure for Time Alignment of Three-Dimensional LC−MS Chromatographic Surfaces. *Anal Chem*. 2006;78:8207-17.
28. Askenazi M. 2006. Recursive base peak framing of mass spectrometry data. United States Patent Number 20060293861 Accessed on August 2015. http://www.freepatentsonline.com/y2006/0293861.html
29. Sheldon MT, Mistrik R, Croley TR. Determination of Ion Structures in Structurally Related Compounds Using Precursor Ion Fingerprinting. *Journal of the American Society for Mass Spectrometry*. 2009;20:370-6.
30. Lipomed AG. NBOMe Derivatives. Accessed in July 2015.

http://www.lipomed.com/media/archive1/download/2015-01-13_Flyer-NBOMe-Derivatives.pdf
31. Isomer Design. PiHKAL. Accessed in July 2015. http://isomerdesign.com/PiHKAL/explore.php?domain=pk&id=2425
32. Thermo Fisher Scientific. mzCloud - Advanced Mass Spectral Database. Accessed in September 2015. https://www.mzcloud.org/

# *CHAPTER 3:*

# *BOTTOM-UP SCREENING*

# *STRATEGIES*

## 3.1 Rationale

Due to the ability for HRMS platforms to operate in DIA modes, it is proposed that common product ions can be monitored in full scan MS/MS in order to detect possible novel analogues which share a similar core structure to known analogues. In practice, this would involve the extraction of ion chromatograms corresponding to common product ions for different NPS classes to identify the presence of aligning chromatographic peaks. Furthermore, utilisation of DDA modes may allow for monitoring of NLs using NLFs. In order to monitor common product ions and NLs for particular classes they first need to be established via CID experiments. This chapter focusses on the determination of CID pathways for hallucinogenic phenethylamines, synthetic cathinones and synthetic cannabinoids to identify key common product ions and NLs which can be monitored in routine screening for detection of novel analogues.

NOTE: The CID studies performed in this thesis are not exhaustive in nature and were only designed to identify key product ion *m/z* values and neutral losses. The proposal of product ion structures was only to support the selection of key product ions. The proposed structures may not reflect the actual structures particularly if no deuterated standard was available.

## 3.2 PUBLICATION: Characterisation of hallucinogenic phenethylamines using high-resolution mass spectrometry for non-targeted screening purposes (doi: 10.1002/dta.2171)

### 3.2.1 Foreword

The following manuscript was published in *Drug Testing and Analysis* and details the CID pathways for hallucinogenic phenethylamines such as 2,5-dimethoxyphenethylamines (2C-X), their *N*-(2-methoxybenzyl) derivatives (25X-NBOMe) and 2,5-dimethoxyamphetamines (DOX). Inclusion of the published work in this thesis has been permitted by John Wiley and Sons via Rightslink (Licence no.: 4142731317327). The publication was authored by Mr Daniel Pasin, Dr Adam Cawley, Dr Sergei Bidny and Associate Professor Shanlin Fu. The experimental work, data analysis and initial draft preparation including supporting information were performed by D. Pasin with manuscript edits provided by A. Cawley, S. Bidny and S. Fu

.

# Characterisation of hallucinogenic phenethylamines using high-resolution mass spectrometry for non-targeted screening purposes

Daniel Pasin[1], Adam Cawley[2], Sergei Bidny[3], Shanlin Fu[1*]

[1] Centre for Forensic Science, University of Technology Sydney, Broadway NSW 2007, Australia

[2] Australian Racing Forensic Laboratory, Racing NSW, Sydney NSW 2000, Australia

[3] Forensic Toxicology Laboratory, NSW Forensic and Analytical Science Service, Lidcombe, NSW 2141, Australia

*Author to whom correspondence should be addressed:

Shanlin Fu

University of Technology Sydney

15 Broadway, Sydney NSW 2007, Australia

Email : Shanlin.Fu@uts.edu.au

### 3.2.2 Abstract

Hallucinogenic phenethylamines such as 2,5-dimethoxyphenethylamines (2C-X) and their *N*-(2-methoxybenzyl) derivatives (25X-NBOMe) has seen an increase in novel analogues in recent years. These rapidly changing analogues make it difficult for laboratories to rely on traditional targeted screening methods to detect unknown new psychoactive substances (NPS). In this study, twelve 2C-X, six 2,5-dimethoxyamphetamines (DOX) and fourteen 25X-NBOMe derivatives, including two deuterated derivatives (2C-B-$d_6$ and 25I-NBOMe-$d_9$), were analysed using ultra-performance liquid chromatography coupled with quadrupole time-of-flight mass spectrometry (UPLC-QTOF-MS). Collision-induced dissociation (CID) experiments were performed using collision energies set at 10, 20 and 40 eV. For 2C-X and DOX derivatives, common losses were observed including neutral and radical losses such as $NH_3$ (17.0265 Da), $\bullet CH_6N$ (32.0500 Da), $C_2H_7N$ (45.0578 Da) and $C_2H_9N$ (47.0735 Da). 2C-X derivatives displayed common product ions at *m/z* 164.0837 ($[C_{10}H_{12}O_2]^{+\bullet}$), 149.0603 ($[C_9H_9O_2]^+$) and 134.0732 ($[C_9H_{10}O]^{+\bullet}$) while DOX derivatives had common product ions at *m/z* 178.0994 ($[C_{11}H_{14}O_2]^{+\bullet}$), 163.0754 ($[C_{10}H_{11}O_2]^+$), 147.0804 ($[C_{10}H_{11}O]^+$) and 135.0810 ($[C_9H_{11}O]^+$). 25X-NBOMe had characteristic product ions at *m/z* 121.0654 ($[C_8H_9O]^+$) and 91.0548 ($[C_7H_7]^+$) with minor common losses corresponding to 2-methylanisole ($C_8H_{10}O$, 122.0732 Da), 2-methoxybenzylamine ($C_8H_{11}NO$, 137.0847 Da) and $\bullet C_9H_{14}NO$ (152.1074 Da). Novel analogues of the selected classes can be detected by applying neutral loss filters (NLFs) and extracting the common product ions.

### 3.2.3 Keywords

Hallucinogenic phenethylamines, new psychoactive substances, high-resolution mass spectrometry, collision-induced dissociation

### 3.2.4 Introduction

Hallucinogenic phenethylamines have recently become popular due to their potent serotonergic activity, giving users a sense of euphoria and intense hallucinogenic episodes [1-3]. Their popularity is also attributed to literature such as the notable book published by Alexander Shulgin and Ann Shulgin, PiHKAL (***P****henethylamines* ***i H****ave* ***K****nown* ***A****nd* ***L****oved*) which outlines the synthesis of almost 200 ring-substituted phenethylamine derivatives and anecdotal information on the effects at certain doses from self-administration [4]. The most prevalent are the 2,5-dimethoxyphenethylamines, colloquially known as "2C's" or "2C-X", where "2C" refers to the 2 carbons atoms between the benzene ring and amine group and "X" refers to a letter or number corresponding to a possible substituent, e.g. 'B' (bromo), 'C' (chloro), and 'I' (iodo). Typically, these compounds are modified at the *para*-position by the addition of halogens, alkyl and thioalkyl groups [5]. In addition to the 2C's, PiHKAL also outlines the synthesis of 2,5-dimethoxyamphetamines or "DOX" derivatives which are structurally similar to the 2C's and only differ by the addition of an α-methyl group [4, 6, 7].

Recently, more concerning derivatives of the ring-substituted phenethylamine class are the *N*-(2-methoxybenzyl) or 25X-NBOMe derivatives of the 2C-X compounds [8]. These compounds were first synthesized by Glennon *et al.* [9] and extensively studied by Ralf Heim [10] and Martin Hansen [11] as selective serotonin 2A ($5\text{-HT}_{2A}$) agonists. Generally, 25X-NBOMe derivatives were synthesised through reductive alkylation of selected 2C-X derivatives with 2-methoxybenzaldehyde [8, 10]. The potency of these compounds has been demonstrated in literature, detailing the severe hallucinogenic episodes experienced by users of 25X-NBOMe derivatives, some of which have led to deaths as a result of their own actions [12-15]. Additionally, these

compounds have also been investigated as 5-$HT_{2A}$ and 5-$HT_{2C}$ receptor agonist radioligands for positron emission tomography (PET) [16, 17].

In the 2016 European Drug Report by the European Monitoring Centre for Drugs and Drug Addiction (EMCDDA), 98 NPS were reported for the first time to the European Union (EU) Early Warning System (EWS) in 2015 with 9 new phenethylamines (9%) reported. The number of phenethylamine analogues was lower than previous years with 14 new analogues reported out of 74 NPS in 2012 (19%) and 14 out of 81 in 2013 (17%). While phenethylamines made up only 9% of the new analogues reported in 2015, synthetic cathinones were the most prevalent with 36 new analogues (37%) and synthetic cannabinoids having 24 analogues reported (24%) [18]. PiHKAL, Heim's and Hansen's theses are freely available online, allowing clandestine laboratory operators to obtain detailed synthetic procedures which can allow them to modify these molecules at their discretion. This proliferation of NPS can potentially make it difficult for forensic laboratories to detect novel compounds using high throughput traditional targeted screening methods that typically rely on the availability of certified reference materials (CRMs) and online databases. It is, therefore, crucial that class-based detection strategies are developed, in particular the determination of common product ions and losses through collision-induced dissociation (CID) studies using high-resolution mass spectrometry (HRMS) for identification of product ion formulae.

There have been several comprehensive CID studies on synthetic cathinones [19-21] using HRMS. There has been some literature published on single and multi-analyte characterization of hallucinogenic phenethylamines [22-28] and synthetic cannabinoids [29-31] using this technique, however, there have been no publications on the comprehensive characterization of these classes with explicitly stated rules or guidelines for the detection of novel analogues in a non-targeted screening approach.

The aim of this study was to fill this current gap in research and to investigate the CID pathways of 2C-X, DOX and 25X-NBOMe derivatives using high-resolution mass spectrometry (HRMS) in order to develop a non-targeted strategy for the detection of new emerging analogues.

### 3.2.5 Experimental

#### *3.2.5.1 Chemicals and reagents*

Hydrochloride salts of 4-bromo-2,5-dimethoxyphenethylamine (2C-B), 2,5-dimethoxy-3,4-dimethylphenethylamine (2C-G), 2,5-dimethoxy-4-methylthiophenethylamine (2C-T), 2-(3,4-dimethyl-2,5-dimethoxyphenyl)-*N*-[(2-methoxyphenyl)methyl]ethanamine (25G-NBOMe), 2-(4-methylthio-2,5-dimethoxyphenyl)-*N*-[(2-methoxyphenyl)methyl]ethanamine (25T-NBOMe), 2,5-dimethoxyamphetamine (DOH/2,5-DMA), 4-bromo-2,5-dimethoxyamphetamine (DOB), 2,5-dimethoxy-4-methylamphetamine (DOM) and 2,5-dimethoxy-4-methylthioamphetamine (DOT) were purchased as powders from the National Measurement Institute (NMI, North Ryde, NSW, Australia). Hydrochloride salts of 4-chloro-2,5-dimethoxyphenethylamine (2C-C), 2,5-dimethoxy-4-methylphenethylamine (2C-D), 4-ethyl-2,5-dimethoxyphenethylamine (2C-E), 2,5-dimethoxy-4-propylphenethylamine (2C-P), 2,5-dimethoxy-4-isopropylthiophenethylamine (2C-T-4), 2,5-dimethoxy-4-propylthiophenethylamine (2C-T-7), 2-(4-bromo-2,5-dimethoxyphenyl)-*N*-[(2-methoxyphenyl)methyl]ethanamine (25B-NBOMe), 2-(4-chloro-2,5-dimethoxyphenyl)-*N*-[(2-methoxyphenyl)methyl]ethanamine (25C-NBOMe), 2-(4-methyl-2,5-dimethoxyphenyl)-*N*-[(2-methoxyphenyl)methyl]ethanamine (25D-NBOMe), 2-(4-ethyl-2,5-dimethoxyphenyl)-*N*-[(2-methoxyphenyl)methyl]ethanamine (25E-NBOMe), 2-(2,5-dimethoxyphenyl)-*N*-[(2-

methoxyphenyl)methyl]ethanamine (25H-NBOMe), 2-(4-iodo-2,5-dimethoxyphenyl)-*N*-[(2-methoxyphenyl)methyl]ethanamine (25I-NBOMe), 2-(4-nitro-2,5-dimethoxyphenyl)-*N*-[(2-methoxyphenyl)methyl]ethanamine (25N-NBOMe), 2-(4-propyl-2,5-dimethoxyphenyl)-*N*-[(2-methoxyphenyl)methyl]ethanamine (25P-NBOMe), 2-(4-ethylthio-2,5-dimethoxyphenyl)-*N*-[(2-methoxyphenyl)methyl]ethanamine (25T2-NBOMe), 2-(4-isoproprylthio-2,5-dimethoxyphenyl)-*N*-[(2-methoxyphenyl)methyl]ethanamine (25T4-NBOMe), 2-(4-propylthio-2,5-dimethoxyphenyl)-*N*-[(2-methoxyphenyl)methyl]ethanamine (25T7-NBOMe), 4-ethyl-2,5-dimethoxyamphetamine (DOET) and 4-iodo-2,5-dimethoxyamphetamine (DOI) were purchased as powders from PM Separations (Capalaba, QLD, Australia). Deuterated standards, 2C-B-$d_6$ and 25I-NBOMe-$d_9$, were purchased as 1 mg/mL methanolic solutions from PM Separations. LC-MS grade acetonitrile was purchased from Chem-Supply Pty Ltd (Gillman, SA, Australia) and LC-MS grade formic acid and AR grade ammonium formate was purchased from Sigma Aldrich (Castle Hill, NSW, Australia). Ultrapure grade water (18.2 MΩ cm) was obtained from a Sartorius arium® pro ultra-pure water system (Goettingen, Germany).

### *3.2.5.2 Sample preparation*

Standards that were obtained as 1 mg/mL methanolic solutions were transferred into 2-mL amber sample vials. Purchased powders were weighed into 1 mg portions and dissolved in 1 mL of methanol to achieve a concentration of 1 mg/mL. Working solutions were prepared by further dilution to 1 mg/L in 2-mL sample vials and capped. All samples were stored in a refrigerator (4°C) until analysis.

*3.2.5.3 Instrumental analysis*

Chromatographic separation was achieved using an Agilent Technologies 1290 Infinity series ultra-performance liquid chromatograph (UPLC), consisting of an Inifinity II high speed pump (G4220A), thermostat (FC/ALS G1330B), column compartment (G1316C, 25ºC) and autosampler compartment (G4226A, 8ºC) coupled to an Agilent Technologies 6510 quadrupole time-of-flight mass spectrometer (QTOF-MS) fitted with a dual electrospray ionization (ESI) source. Instrument control and data acquisition was performed using Agilent Technologies MassHunter LC-MS Data Acquisition Software (Version B.05.01). A sample volume of 1 µL was injected onto an Agilent Technologies Poroshell 120 C18 column (2.1 x 75 mm, 2.7 µm particle size) using a gradient elution with a flow rate of 0.4 mL/min with a total run time of 17 min. Mobile phase A consisted of 20 mM ammonium formate and mobile phase B consisted of acetonitrile containing 0.1% (% v/v) formic acid. Initial mobile phase composition was 87% A which was held for 0.5 min and then decreased linearly to 50% A over 9.5 min. It was then decreased to 5% A over 0.75 min, held for 1.5 min and then returned to the initial conditions over 0.25 min with a final hold time of 2.5 min and post-run equilibration time of 2 min.

The QTOF-MS was operated in positive electrospray ionisation (ESI+) mode using Extended Dynamic Range (2 GHz) with capillary and fragmentor voltages set to 3500 V and 180 V, respectively. An Auto-MS/MS (data-dependent) acquisition mode was used over a mass range of *m/z* 50-1000 for both MS and MS/MS experiments with scan rates of 1 and 3 spectra/s, respectively. A maximum of 3 precursors from the MS scan were selected for CID per cycle with a cycle time of 2.1 s and an abundance threshold of 200 counts. CID experiments were performed at collision energies (CE) of 10, 20 and 40 eV in separate analyses with nitrogen as the collision gas.

#### *3.2.5.4 Data analysis*

All data acquired was processed using Agilent Technologies MassHunter Qualitative Analysis Software (Version B.06.00). The Find by Auto-MS/MS function was used to generate MS and MS/MS spectra for all precursors selected for CID. Molecular formulae for product ion mass-to-charge (*m/z*) values were generated using MassHunter's molecular formula generator (MFG) algorithms with elements of interest set to $C_{(7\rightarrow25)}$, $N_{(0\rightarrow2)}$, $O_{(0\rightarrow5)}$, $H_{(7\rightarrow30)}$, $S_{(0\rightarrow1)}$, $Cl_{(0\rightarrow1)}$, $Br_{(0\rightarrow1)}$, $I_{(0\rightarrow1)}$ and $D_{(0\rightarrow9)}$.

### 3.2.6 Results and discussion

In this study, twelve 2C-X, six DOX and fourteen 25X-NBOMe analogues were analysed by UPLC-QTOF-MS in order to evaluate their CID pathways and assess the applicability of the generated product ions for non-targeted detection of novel hallucinogenic phenethylamine analogues. The panel of selected analytes also contained isotopically labelled 2C-B-$d_6$ and 25I-NBOMe-$d_9$ which were used to aid in the elucidation of product ions. Structures, retention times and precursor ion data for all analytes are listed in Table B.1 (Appendix B).

#### *3.2.6.1 Chromatographic analysis of selected hallucinogenic phenethylamines*

All selected analytes eluted within the first 10 min of the chromatographic analysis with the least substituted 2C-X derivative (2C-H) eluting first at 1.98 min and the propyl 25X-NBOMe derivative (25P-NBOMe) eluting last at 9.40 min. All 2C-X and DOX derivatives eluted within the first 6 min of analysis with the latter typically having longer retention times than the respective 2C-X derivative. For example, 2C-B eluted at 3.82 min while its α-methyl derivative, DOB, eluted later at 4.28 min due to the additional methyl group resulting in greater retention on the reversed phase Poroshell EC120 C18 column. This was also observed for 2C-E/DOET, 2C-H/DOH,

2C-I/DOI, 2C-D/DOM and 2C-T/DOT. The panel of selected analytes had several isomeric pairs that were successfully resolved in the 15 minute chromatographic analysis. For example, isomeric analytes 2C-E ($t_r$ = 4.56 min), 2C-G ($t_r$ = 4.17 min) and DOM ($t_r$ = 3.86 min) were all baseline separated. Interestingly, it can be observed that the addition of alkyl groups to the *para*-position on the 2,5-dimethoxyphenylamine moiety have a greater retaining effect compared to the substitution at the α-carbon. For example, isomeric derivatives 2C-D (*para*-methyl) and DOH (α-methyl) have retention times of 3.25 and 2.44 min, respectively. The 25X-NBOMe compounds generally eluted towards the end of the chromatographic run due to their larger structure with the least substituted derivative (25H-NBOMe) eluting first at 5.97 min and the propyl derivative (25P-NBOMe) eluting last at 9.40 min as mentioned previously.

### *3.2.6.2 CID of hallucinogenic phenethylamines*

The main advantage of using HRMS is that losses and product ions which have the same nominal mass can be differentiated to provide greater confidence in elucidating product ions structures. For example, losses of -$NH_3$ and -OH would give a nominal mass change of 17 Da but an accurate mass change of 17.0265 and 17.0027 Da, respectively, which can be differentiated by an instrument that has sufficient mass resolution.

When determining the CID pathways and elucidating the structures of product ions using ESI, it is important to consider the basic rules for CID which have been established in literature [32-34]. In addition, the 'even-electron' rule stipulates that even electron (EE) ions will typically fragment to EE ions via neutral losses (NLs) under electron ionization (EI) in gas chromatography – mass spectrometry (GC-MS). It has also been observed that odd electron (OE) ions such as radical cations ($M^{+\bullet}$) [35]

can form other OE ions through NLs but OE ions typically do not form EE ions due to radical losses other than in a limited number of examples [36]. The use of HRMS can assist in determining whether a product ion is an EE or OE ion by using information such as the chemical formula and double bond equivalents. The MFG algorithm in the MassHunter software can designate a product ion as EE or OE.

Evaluation of product ion spectra at each of the selected collision energies showed that a CE of 20 eV provided a wide range of product ions for all analytes. In some cases, the precursor ion ($[M+H]^+$) could still be observed whilst also having lower mass product ions such as the tropylium cation ($[C_7H_7]^+$, *m/z* 91.0542) observable. Therefore, all results presented herein will be based on those produced at a collision energy of 20 eV.

### *3.2.6.3 General CID of 2C-X and DOX compounds*

The product ion data for all 2C-X and DOX analytes are listed in Table B.2 and the representative product ion spectra are illustrated in Figure S1. The CID pathways for 2C-X and DOX analytes are illustrated in Figure 3.1. For all 2C-X and DOX analytes, the first product ion was generated by simple inductive cleavage of ammonia ($NH_3$, 17.0265 Da) with charge-migration fragmentation (CMF) to the α-carbon to produce the EE ion **1** ($[M-NH_3+H]^+$ or $[C_{10}H_{12}O_2R^1R^2R^3]^+$). Where $R^1$ corresponds to the "primary" or *para*-substituent (alkyl, thioalkyl, halogen), $R^2$ is the "secondary" or *meta*-substituent and $R^3$ is the α-carbon substituent ($R^3$ = H and $R^3$ = $CH_3$ for 2C-X and DOX derivatives, respectively). For DOX analytes, there is also β-cleavage of the phenethylamine chain with a NL of $C_2H_7N$ (45.0578 Da) to give product ion **2** ($[M-C_2H_7N+H]^+$ or $([C_9H_9O_2R^1R^2]^+$).

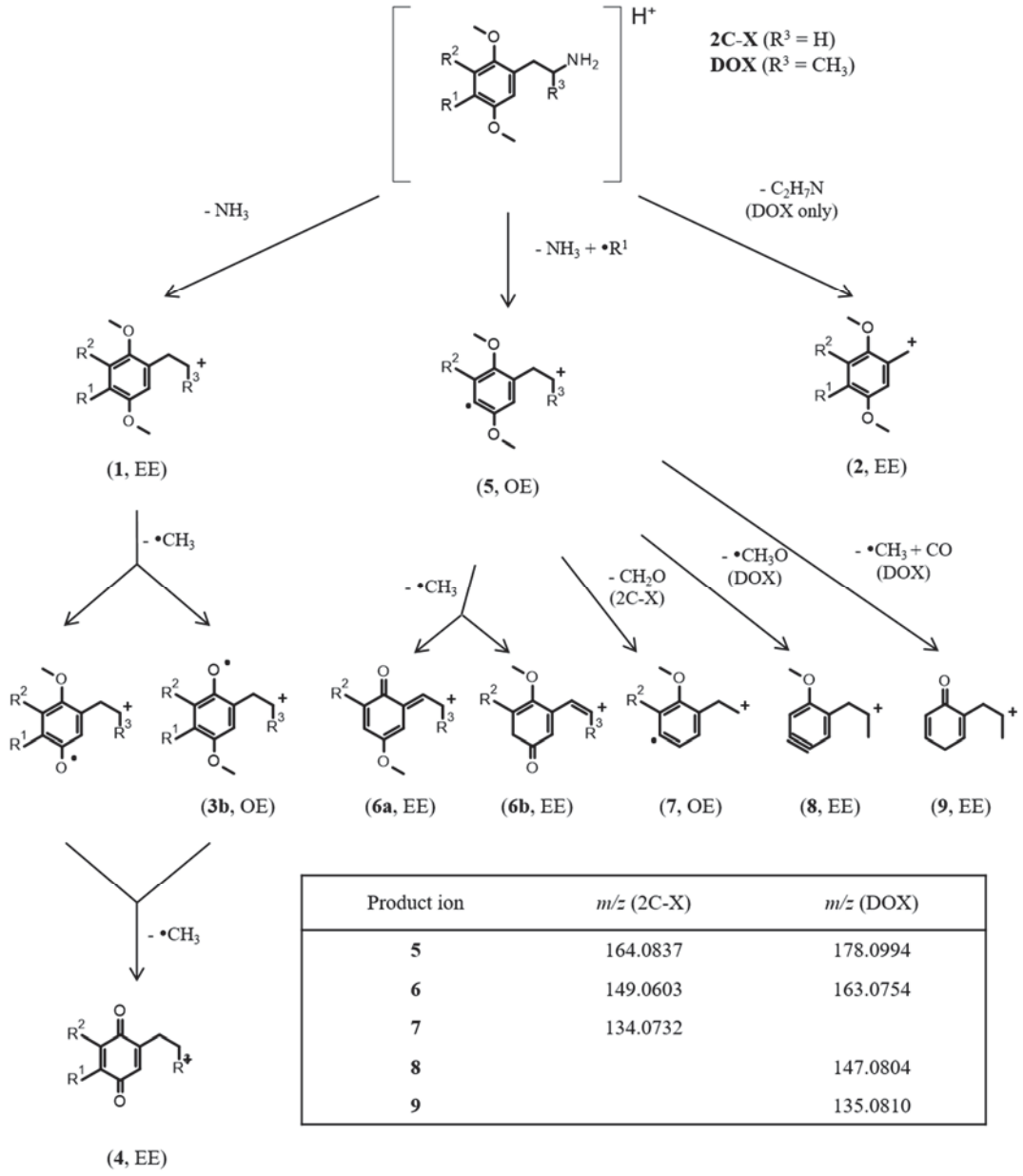


| Product ion | *m/z* (2C-X) | *m/z* (DOX) |
|---|---|---|
| **5** | 164.0837 | 178.0994 |
| **6** | 149.0603 | 163.0754 |
| **7** | 134.0732 | |
| **8** | | 147.0804 |
| **9** | | 135.0810 |

**Figure 3.1** CID pathways for 2C-X and DOX derivatives at 20 eV.

A base peak for many of the selected analytes was the loss of $NH_3$ followed by radical cleavage of the ether methyl group ($\bullet CH_3$, 15.0235 Da) to produce the distonic OE product ion **3** ($[M\text{-}CH_6N+H]^{+\bullet}$ or $[C_9H_9O_2R^1R^2R^3]^{+\bullet}$; total loss of 32.0500 Da from the precursor ion). Evaluation of the product ion spectra for 2C-B-$d_6$ (which has deuterium atoms incorporated into both methoxy groups) confirmed radical cleavage of the aromatic methoxy groups located at the 2- or 5-position. The precursor ion exhibited

a loss of 35.0689 Da as opposed to 32.0500 Da corresponding to the loss of a deuterated methyl radical (•$CD_3$, 18.0424) and $NH_3$. The formation of an OE ion from an EE ion is a violation of the previously mentioned heuristic 'even-electron' rule, however, a study by Thurman *et al.* [36] demonstrated that OE ions can be formed from EE ions under ESI by losses of stable radicals such as •$CH_3$ and •$OCH_3$ from aromatic methoxy groups. Additionally, it is postulated by Levsen *et al.* [37] that aromatic OE ions may be more stable than their EE counterparts. In this case, the location of the radical (oxygen adjacent to the aromatic ring) may stabilize the OE ion due to resonance of the radical around the aromatic ring. Subsequent radical cleavage of •$CH_3$ from the alternate methoxy group following the losses of •$CH_3$ and $NH_3$ was observed to yield product ion **4** ($[M\text{-}C_2H_9N+H]^+$ or $[C_8H_6O_2R^1R^2R^3]^+$), corresponding to a loss of 47.0735 Da. This was confirmed by the product ion spectra for 2C-B-$d_6$ which showed a loss of 53.1114 Da from the precursor ion corresponding to $NH_3$ and two •$CD_3$ radicals. A study by Karni *et al.* [35] stated that subsequent radical losses can occur if a state of aromaticity can be achieved. In this case, the formation of **4** would initially result in an EE diradical cation ($M^{+\bullet\bullet}$) intermediate but it is postulated that radical migration would occur in order to generate an aromatic EE cation. The order of radical cleavage could not be investigated in this study and would need to be confirmed by isotopically labelled analytes of which only one methoxy group contained deuterium atoms.

Product ions **1**-**4** resulted from NLs producing different *m/z* values for selected analytes excluding isomeric compounds, however, there are some product ions which are common to the majority of analytes. There is an OE product ion (**5**) observed at *m/z* 164.0837 ($[C_{10}H_{12}O_2]^{+\bullet}$) and *m/z* 178.0994 ($[C_{11}H_{14}O_2]^{+\bullet}$) for 2C-X and DOX analytes, respectively, corresponding to the loss of $NH_3$ and radical cleavage of the

*para*-substituent ($\bullet R^1$). The loss of $\bullet R^1$ was also confirmed by the absence of the $[M+2+H]^+$ isotope for the bromo and chloro derivatives 2C-B/DOB and 2C-C, respectively. It was also observed that the *meta*-substituent ($R^2$) is retained with 2C-G ($R^2 = CH_3$) having a product ion at *m/z* 178.1009 ($[C_{11}H_{14}O_2]^{+\bullet}$, +8.4 ppm) rather than *m/z* 164.0837. A subsequent loss of $\bullet CH_3$ following the losses of $NH_3$ and $\bullet R^1$ produced the diradical EE product ion at *m/z* 149.0603 ($[C_9H_9O_2]^+$) for 2C-X derivatives and *m/z* 163.0754 ($[C_{10}H_{11}O_2]^+$) for DOX derivatives and 2C-G. It is likely the resulting diradical cations underwent radical migration to form cations **6a** and **6b** corresponding to cleavages at the 2- and 5-methoxy groups, respectively.

For 2C-X analytes only, a product ion corresponding the to the NL of formaldehyde ($CH_2O$) following the loss of $NH_3$ and $\bullet R^1$ to yield the OE ion **7** at *m/z* 134.0732 ($[C_9H_{10}O]^{+\bullet}$) and *m/z* 148.0883 ($[C_{10}H_{12}O]^{+\bullet}$) for 2C-G. These proposed losses were supported by the product ion spectra of 2C-B-$d_6$ which had a product ion at *m/z* 138.0980 corresponding to $[C_9H_6D_4O]^+$, suggesting that there is rearrangement of a deuterium atom from the methoxy group to the aromatic ring. Based on the proposed CID pathways presented for product ions **1-4**, it could have been hypothesized that from product ion **5**, stepwise cleavage of $\bullet CH_3$ radicals would occur, however, that would have yielded an OE product ion at *m/z* 134.0368 ($[C_8H_{10}O_2]^{+\bullet}$). It is likely that this ion was not formed as it would have involved three radical cleavages, which may not be considered energetically favourable.

Similar to **7** for 2C-X analytes, there is an EE product ion observable at *m/z* 147.0804 ($[C_{10}H_{11}O]^+$) for DOX analytes which is proposed to be formed by the radical cleavages of $\bullet R^1$ and $\bullet OCH_3$ from the 5-position to yield two adjacent radicals which is proposed to form the benzyne cation **8**. Another product ion exclusive to the DOX class is the EE product ion **9** ($[C_9H_{11}O]^+$, *m/z* 135.0810) which is likely formed by the

NL of CO and radical cleavages of •$R^1$ and •$CH_3$ followed by radical rearrangement.

The isomeric thioalkyl derivatives, 2C-T-4 and 2C-T-7 ($[M+H]^+$ = *m/z* 256.1371), did not have product ions corresponding to the loss of $C_2H_9N$ present. However, both had an EE product ion at *m/z* 197.0631 ($[C_{10}H_{13}O_2S]^+$) corresponding to the loss of $C_3H_9N$ which was proposed to be from the NL of $NH_3$ followed by the loss of propene from 2C-T-4 and 2C-T-7, respectively. These product ions subsequently underwent radical cleavage (i.e. loss of •$CH_3$) of the methoxy group to yield the OE ion $[C_9H_{10}O_2S]^{+\bullet}$ (*m/z* 182.0401). The methylthio derivative, 2C-T, did not have a product ion at *m/z* 197.0631 since this ion is formed by the loss of the alkene and is not possible by a methyl derivative. Extrapolation to the ethylthio derivative (2C-T-2), which was not included in this study would suggest that it may form *m/z* 197.0631 by the loss of ethylene.

There have been studies on 2C-X compounds using GC-MS published by Theobald *et al*. [38-40], however, due to the different ionization techniques and the requirement for derivatization for GC-MS, product ion spectra can differ significantly and cannot be translated to LC-MS necessitating re-characterization. Zuba *et al*.[26] analysed 2C-E and 2C-G by LC-QTOF-MS and also observed product ions **1**,**3** and **4** at a collision energy of 15 eV. Similar to present study, they postulated that these product ions formed from the loss of $NH_3$, •$CH_6N$ and $CH_9N$ However, they did not suggest the location where the methyl radicals were lost (product ions **3** and **4)**. A study conducted by Boumrah *et al*. [22] identified that 2C-B was a metabolic product of 25B-NBOMe when analysed by HRMS. They postulated that product ion *m/z* 217.9551 was formed by the β-cleavage of the amine followed by cleavage of a methyl group from one of the aromatic methoxy groups, which contrasts to what was determined in this study. In addition, the CID pathway for *m/z* 227.9786 was not determined in this study.

A limitation of this study is that only six DOX derivatives were analysed so it is recommended that in future studies the panel would be extended to include newly available DOX CRMs to provide a more representative overview of the CID pathways for this class. In addition, there have been other ring-substituted phenethylamine derivatives that have been encountered such as the dihydrofuran derivative, 2-(4-bromo-2,3,6,7-tetrahydrofuro[2,3-f][1]benzofuran-8-yl)ethanamine (2C-B-Fly), and difuranyl derivative 1-(8-bromobenzo[1,2-*b*; 4,5-*b*']difuran-4-yl)-2-aminopropane (Bromo-DragonFLY) which could have the bromine atom replaced with other functional groups [7, 41, 42].

### *3.2.6.4 CID of NBOMe derivatives*

The product ion data for selected 25X-NBOMe analytes are listed in Table B.3 and their CID pathways are illustrated in Figure 3.2. For all 25X-NBOMe analytes, there is a base peak corresponding to the CMF of the 2,5-dimethoxyphenethylamine moiety to give the EE 2-methoxybenzyl cation **10** ($[C_8H_9O]^+$, *m/z* 121.0654) followed by the NL of $CH_2O$ to yield the EE tropylium cation **11** ($[C_7H_7]^+$, *m/z* 91.0548). In addition to these major product ions, there is to a small extent charge-retention fragmentation (CRF) through α-cleavage of the 2-methylanisole moiety ($C_8H_{10}O$, 122.0732 Da) to yield the EE product ion **12** ($[C_{10}H_{12}NO_2R^1R^2]^+$) . There is also α-cleavage of the 2-methoxybenzylamine moiety ($C_8H_{11}NO$, 137.0847 Da) to produce the EE product ion **13** ($[C_{10}H_{11}O_2R^1R^2]^+$) which then undergoes radical cleavage of $\bullet CH_3$ ($C_9H_{14}NO$, 152.1074 Da) to yield the OE product ion **14** $[C_9H_8O_2R^1R^2]^{+\bullet}$. The CID pathways for 25X-NBOMe compounds are relatively characteristic and do not fragment as extensively as their 2C-X counterparts, following mostly EE to EE transitions. Figure S2 illustrates the characteristic product ion spectra for selected 25X-NBOMe derivatives. Zuba *et al*. [43] analysed 25D-NBOMe, 25E-NBOMe and 25G-NBOMe

by LC-QTOF-MS and observed product ions **10-14** for all three analytes. Poklis *et al*. [44] utilized Direct Analysis in Real Time AccuTOF™ mass spectrometry (DART-MS) for the analysis of 25X-NBOMe derivatives on blotter paper and observed product ions **10**, **11** and **13**. In addition, they also observed the loss of iodine to produce *m/z* 302.1776 for 25I-NBOMe which was not observed in the present study.

The major product ions for the selected 25X-NBOMe analytes are the 2-methoxybenzyl cation (*m/z* 121.0654) and tropylium cation (*m/z* 91.0548) which are indicative of the *N*-substituted moiety. Therefore, it may be reasoned that reductive alkylation of a 2C-X derivative with a different benzaldehyde would produce a different product ions corresponding to the benzylic cation of the substituted benzaldehyde. There have been novel derivatives reported in literature which were produced by the reductive alkylation of 2C-X derivatives with 2 -fluorobenzaldehyde and 1,3-benzodioxole-4-carbaldehyde to produce the *N*-substituted derivatives ***N***-(2-fluorobenzyl)-2-(4-iodo-2,5-dimethoxyphenyl)ethanamine (25I-NBF) and (25I-NBMD), respectively[44, 45]. Sekula *et al*.[45] analysed 25I-NBMD by LC-QTOF-MS and found that it had a base peak corresponding to the 1,3-benzodioxole-4-methyl cation ($[C_8H_7O_2]^+$, *m/z* 135.0447) but did not observe the tropylium cation when the precursor ion was subjected to a CE of 15 eV.

Therefore, if a characteristic "25X-NBOMe-like" product ion spectra is observed which has a product ion at *m/z* 91.0548 and has a major product ion which is not *m/z* 121.0654 it may indicate the presence of a novel analogue which is not a *N*-(2-methoxybenzyl) derivative, however, this would need to be validated by characterization of different *N*-substituted derivatives.

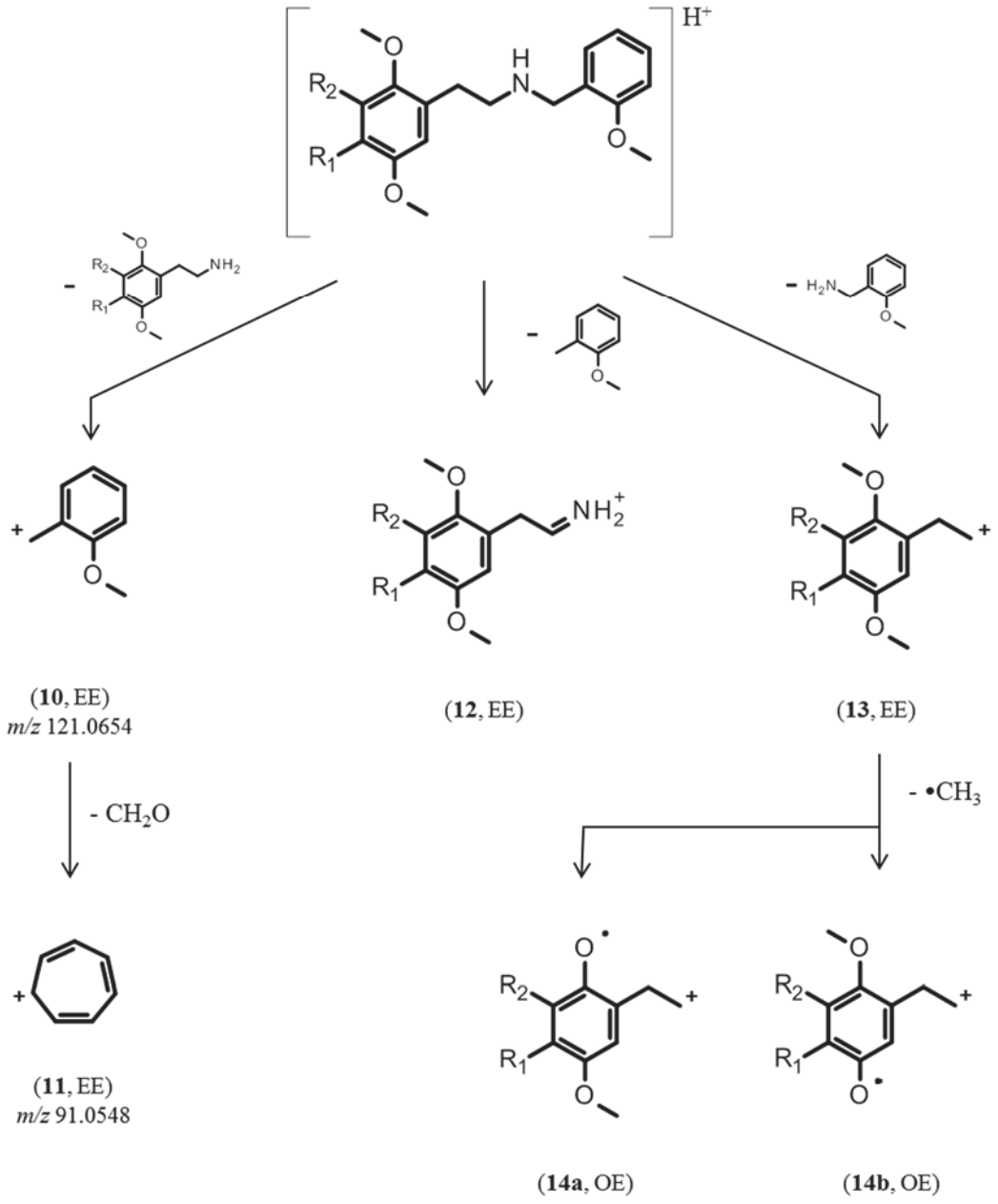


**Figure 3.2** CID pathways for 25X-NBOMe derivatives at 20 eV.

### *3.2.6.5 Non-targeted screening approach*

The recent proliferation of NPS and the lack of CRMs available for novel analogues typically results in these compounds going undetected in conventional targeted screening techniques where retention time, precursor and product ion data are collected from CRMs or databases. Therefore, a holistic or unbiased approach is required to

successfully detect and tentatively identify novel compounds so these samples of interest can be flagged and archived until suitable CRMs become available for confirmation. Non-targeted, or untargeted screening, typically refers to the method of data acquisition: data-independent acquisition (DIA) involves CID of all precursor ions whereas data-dependent acquisition (DDA) involves the CID of a limited number of precursor ions which are above user-defined thresholds. Most often this data is then compared to either in-house databases populated with retention times and mass data obtained from previous analyses of CRMs or comprehensive online databases for compound detection and identification [46, 47]. However, in the case of the work presented here, a non-targeted screening approach refers to the interrogation of DIA/DDA mass spectrometry data to detect novel analogues using class-based mass spectrometric characteristics such as common NLs and product ions which is not CRM or database-driven. This strategy is applied to MS/MS or $MS^2$ data and, therefore, its efficacy relies on the use of an appropriate data acquisition method. Both DIA and DDA can be utilized for non-targeted data acquisition purposes, however, the use of DDA, such as the technique which was used in this study (Auto MS/MS), will limit the amount of precursor ions selected for CID and, therefore, reduce the likelihood that analytes of interest will be detected, particularly if there are more abundant precursor ions from matrix components within the same scan. It can be reasoned that the number of precursors selected for CID per cycle/scan may be increased, however, the scan rate (spectra/s) is limited by the instruments data processing capabilities. DIA provides better coverage of precursor ion CID and, therefore, improves the likelihood that a novel analogue will be subjected to CID. Many instrumentation vendors have DIA options available such as All Ions MS/MS (Agilent Technologies), $MS^E$ (Waters Corporation) and broadband CID (bbCID, Bruker) that acquire data by alternating

between low and high energy channels. Additionally, a DIA method called sequential window acquisition of all theoretical mass spectra (SWATH™, AB Sciex), acquires data by sequentially allowing increments of a selected mass range through the quadrupole and into the collision cell. The major advantage of DIA is that comprehensive full scan data is acquired that can be retrospectively interrogated for new analytes of interest without the need for re-extraction and re-analysis

Detection of novel hallucinogenic phenethylamine derivatives can be achieved by the application of basic data processing techniques to acquired MS/MS data such as extracted ion chromatograms (EIC or XIC) and neutral loss filtering (NLF). The generation of NLFs and EICs was done manually in this case but MassHunter offers the ability to automate user-defined data processing steps which can be applied to multiple data files for rapid screening. NLF is typically a data processing technique which is offered in metabolomics software such as Metabolynx (Waters Corporation). Due to its usefulness in undertaking non-targeted screening of unknown compounds, NLF may find its integration into more MS data processing software in the future. Table 3.1 summarises what potential core structures may be present based on the detection of particular NLs and product ions. The presence of chromatographic peaks after NLF application of 17.0265, 32.0500 and 47.0735 Da NLFs may indicate if any 2C-X or DOX derivatives are present but will not necessarily differentiate between the two classes. However, the presence of a chromatographic peak with the NLF application of 45.0578 Da may indicate that the derivative is likely a DOX derivative. Figure 3.3 illustrates an example for the application of the precursor neutral loss chromatogram (pNLC) function in MassHunter using the isomeric analytes, 2C-D and DOH.

**Table 3.1** Potential core structures of hallucinogenic phenethylamines associated with the presence of common losses (Da) and product ions (*m/z*).

| Common losses [Da] | | | | Product ions [*m/z*] | | | | | | | | | | Potential Core Structure |
|---|---|---|---|---|---|---|---|---|---|---|---|---|---|---|
| 17.0265 | 32.0500 | 45.0578 | 47.0735 | 134.0732 | 135.0810 | 147.0804 | 148.0883 | 149.0603 | 163.0754 | 164.0837 | 178.0994 | 197.0631 | 182.0401 | |
| Y | Y | | Y | Y | | | | Y | | Y | | | | 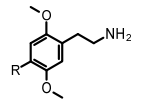 |
| Y | Y | | Y | | | | Y | | Y | | Y | | | 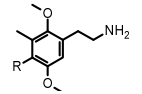 |
| Y | Y | | | Y | | | | Y | | Y | | Y | Y | 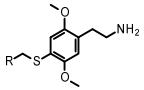 |
| Y | Y | Y | Y | | Y | Y | | | Y | | Y | | | 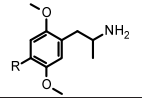 |

| Common losses [Da] | | | | | Product ions [*m/z*] | | | Potential Core Structure |
|---|---|---|---|---|---|---|---|---|
| 122.0732 | 137.0847 | 152.1074 | 136.0524[a] | 151.0633[a] | 91.0548 | 121.0654 | 135.0441[a] | |
| | | | | | Y | Y | | 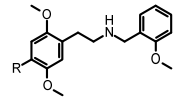 |
| U | Y | Y | | | Y | Y | | 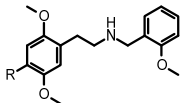 |
| | | | Y | Y | | | Y | 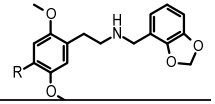 |

[a]Identified in the study by Sekuła *et al.*[45]

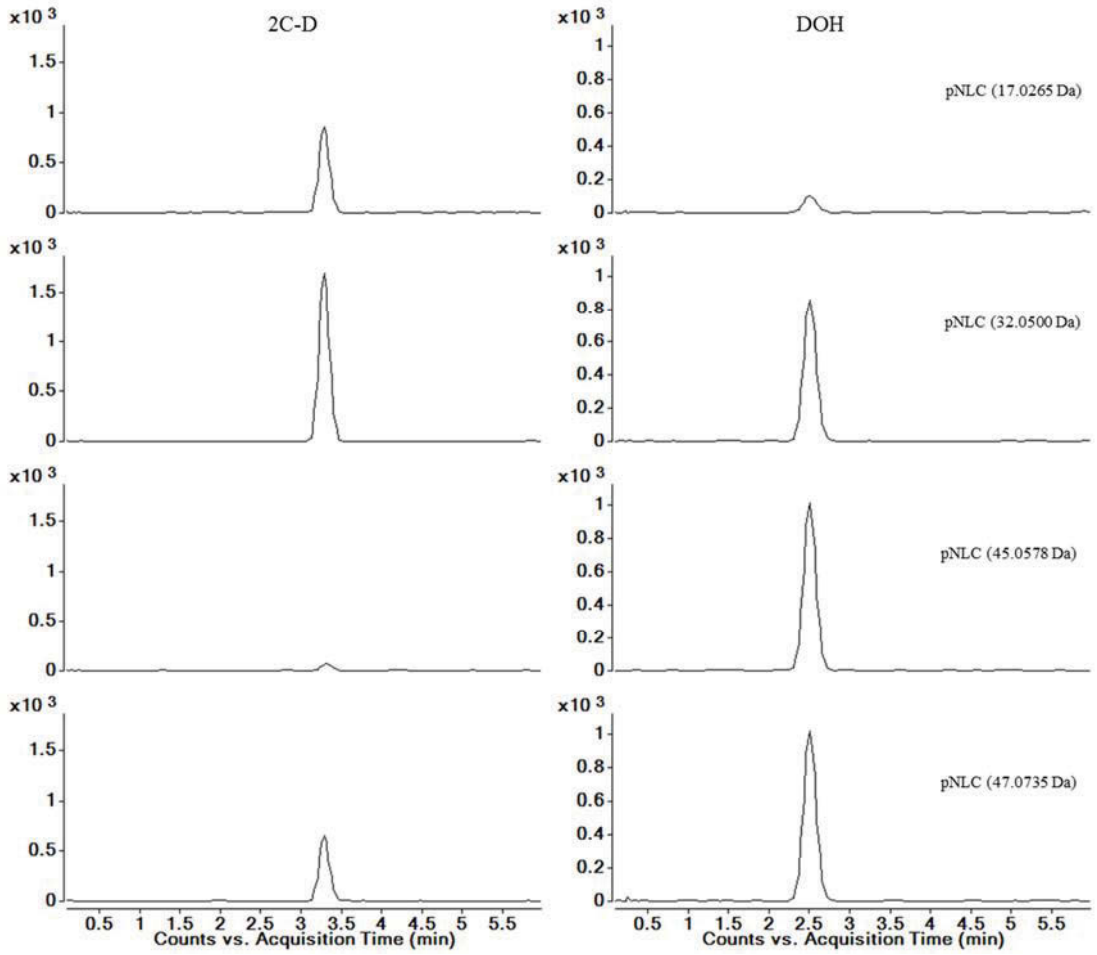


**Figure 3.3** pNLCs of 17.0265, 32.0500, 45.0576 and 47.0735 Da for 2C–D and DOH at 20 eV.

If NLF is unavailable, detection of novel analogues can be achieved by generating EICs of the common product ions such as *m/z* 164.0837, 149.0603 and 134.0732 for 2C-X derivatives and *m/z* 178.0994, 163.0754, 147.0804 and 135.0810 for DOX derivatives. However, if *m/z* 178.0994 and 163.0754 are present but *m/z* 147.0804 and 135.0810 (which are exclusive to the DOX class) are absent, it may indicate a 2C-X derivative where $R^2 = CH_3$. Additionally, presence of peaks in the 17.0265 and 32.0500 Da NLF and the EICs for *m/z* 197.0631 and 182.0401 may indicate the presence of a thio derivative. Figure 3.4 illustrates an example of the application EICs for common product ions using 2C-I and DOI.

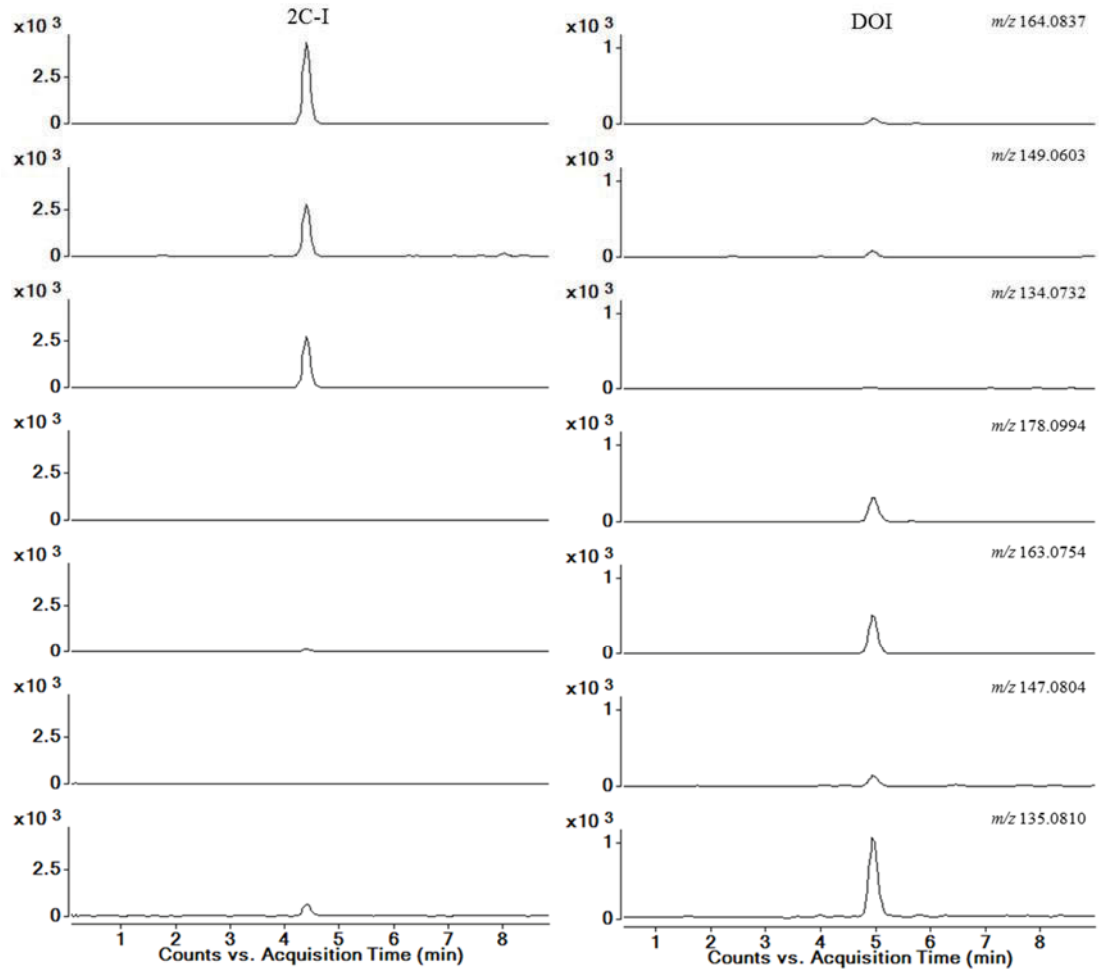


**Figure 3.4** EICs for 2C–I and DOI at *m/z* 164.0837, 149.0603, 134.0732, 178.0994, 163.0804, 147.0804 and 135.0810 at 20 eV.

Similarly, detection of 25X-NBOMe derivatives can be achieved by the application of NLFs for 122.0732, 137.0847 and 152.1074 Da, however, the absence of chromatographic peaks for some of these NLFs may not necessarily indicate a false negative as some of the product ions formed by the have low relative abundances and will depend on the sensitivity of the NLF. Detection of 25X-NBOMe derivatives would be better achieved by generating EICs for *m/z* 91.0548 and 121.0654 and checking whether the product ion spectra contains only those ions since the tropylium cation and 2-methoxybenzyl cation are not exclusive to the 25X-NBOMe hallucinogenic phenethylamines.

### 3.2.7 Conclusion

Hallucinogenic phenethylamines were successfully characterized by LC-QTOF-MS using CID at different CEs. The 2C-X and DOX derivatives had common losses of $NH_3$, $CH_6N$ and $C_2H_9N$ and common product ions at *m/z* 164.0837, 149.0603 and 134.0732 for 2C-X derivatives and *m/z* 178.0994, 163.0754, 147.0804 and 135.0810 for DOX derivatives. The 25X-NBOMe derivatives had characteristic product ion spectra with abundant ions at *m/z* 121.0654 and 91.0548, together with minor NLs corresponding to 2-methylanisole and 2-methoxybenzylamine and $C_9H_{14}NO$. Screening for these common NLs and product ions can be used in a non-targeted screening approach to detect and tentatively identify novel analogues.

### 3.2.8 Acknowledgements

The authors would like to thank NSW FASS for providing financial support though an industry scholarship top-up

### 3.2.9 References

1. Cole MD, Lea C, Oxley N. 4-Bromo-2,5-dimethoxyphenethylamine (2C-B): a review of the public domain literature. *Sci Justice*. 2002;42:223-4.
2. de Boer D, Bosman I. A new trend in drugs-of-abuse; the 2C-series of phenethylamine designer drugs. *Pharm World Sci*. 2004;26:110-3.
3. Dean B, Stellpflug S, Burnett A, Engebretsen K. 2C or Not 2C: Phenethylamine Designer Drug Review. *J Med Toxicol*. 2013;9:172-8.
4. Shulgin AT, Shulgin A. Phenethylamines I have Known and Loved: A Chemical Love Story. Berkley: Transform Press; 1991.
5. Glennon RA, Young R, Benington F, Morin RD. Behavioral and serotonin receptor properties of 4-substituted derivatives of the hallucinogen 1-(2, 5-dimethoxyphenyl)-2-aminopropane. *J Med Chem*. 1982;25:1163-8.
6. Halberstadt AL, Powell SB, Geyer MA. Role of the 5-HT2A receptor in the locomotor hyperactivity produced by phenylalkylamine hallucinogens in mice. *Neuropharmacology*. 2013;70:218-27.
7. Collins M. Some new psychoactive substances: precursor chemicals and synthesis-driven end-products. *Drug Test Anal*. 2011;3:404-16.
8. Casale J, Hays P. Characterization of eleven 2,5-dimethoxy-N-(2-methoxybenzyl) phenethylamine (NBOMe) derivatives and differentiation from their 3-and 4-methoxybenzyl analogues Part–1. *Microgram J*. 2012;9.
9. Glennon RA, Dukat M, el-Bermawy M, Law H, De los Angeles J, Teitler M,

King A, Herrick-Davis K. Influence of amine substituents on 5-HT2A versus 5-HT2C binding of phenylalkyl- and indolylalkylamines. *J Med Chem*. 1994;37:1929-35.

10. Heim R (2003), Synthese und Pharmakologie potenter 5-$HT_{2A}$-Rezeptoragonisten mit N-2-Methoxybenzyl-Partialstruktur, PhD thesis, Freie Universität Berlin.
11. Hansen M (2010), Design and Synthesis of Selective Serotonin Receptor Agonists for Positron Emission Tomography Imaging of the Brain, PhD thesis, Faculty of Pharmaceutical Sciences, University of Copenhagen.
12. Hill SL, Doris T, Gurung S, Katebe S, Lomas A, Dunn M, Blain P, Thomas SHL. Severe clinical toxicity associated with analytically confirmed recreational use of 25I–NBOMe: case series. *Clin Toxicol*. 2013;51:487-92.
13. Poklis JL, Devers KG, Arbefeville EF, Pearson JM, Houston E, Poklis A. Postmortem detection of 25I-NBOMe [2-(4-iodo-2,5-dimethoxyphenyl)-N-[(2-methoxyphenyl)methyl]ethanamine] in fluids and tissues determined by high performance liquid chromatography with tandem mass spectrometry from a traumatic death. *Forensic Sci Int*. 2014;234:e14-e20.
14. Rose SR, Poklis JL, Poklis A. A case of 25I-NBOMe (25-I) intoxication: a new potent 5-HT2A agonist designer drug. *Clin Toxicol*. 2013;51:174-7.
15. Stellpflug S, Kealey S, Hegarty C, Janis G. 2-(4-Iodo-2,5-dimethoxyphenyl)-N-[(2-methoxyphenyl)methyl]ethanamine (25I-NBOMe): Clinical Case with Unique Confirmatory Testing. *J Med Toxicol*. 2014;10:45-50.
16. Ettrup A, Hansen M, Santini M, Paine J, Gillings N, Palner M, Lehel S, Herth M, Madsen J, Kristensen J, Begtrup M, Knudsen G. Radiosynthesis and in vivo evaluation of a series of substituted 11C-phenethylamines as 5-HT2A agonist PET tracers. *Eur J Nucl Med Mol Imaging*. 2011;38:681-93.
17. Finnema SJ, Stepanov V, Ettrup A, Nakao R, Amini N, Svedberg M, Lehmann C, Hansen M, Knudsen GM, Halldin C. Characterization of [11C]Cimbi-36 as an agonist PET radioligand for the 5-HT2A and 5-HT2C receptors in the nonhuman primate brain. *NeuroImage*. 2014;84:342-53.
18. European Monitoring Centre for Drugs and Drug Abuse. European Drug Report 2016. Accessed in October 2016. http://www.emcdda.europa.eu/edr2016
19. Fornal E. Formation of odd-electron product ions in collision-induced fragmentation of electrospray-generated protonated cathinone derivatives: aryl α-primary amino ketones. *Rapid Commun Mass Spectrom*. 2013;27:1858-66.
20. Fornal E. Identification of substituted cathinones: 3,4-Methylenedioxy derivatives by high performance liquid chromatography–quadrupole time of flight mass spectrometry. *J Pharm Biomed Anal*. 2013;81–82:13-9.
21. Fornal E. Study of collision-induced dissociation of electrospray-generated protonated cathinones. *Drug Test Anal*. 2014;6:705-15.
22. Boumrah Y, Humbert L, Phanithavong M, Khimeche K, Dahmani A, Allorge D. In vitro characterization of potential CYP- and UGT-derived metabolites of the psychoactive drug 25B-NBOMe using LC-high resolution MS. *Drug Test Anal*. 2016;8:248-56.
23. Frison G, Odoardi S, Frasson S, Sciarrone R, Ortar G, Romolo FS, Strano Rossi S. Characterization of the designer drug bk-2C-B (2-amino-1-(bromo-dimethoxyphenyl)ethan-1-one) by gas chromatography/mass spectrometry without and with derivatization with 2,2,2-trichloroethyl chloroformate, liquid chromatography/high-resolution mass spectrometry, and nuclear magnetic resonance. *Rapid Commun Mass Spectrom*. 2015;29:1196-204.

24. Shevyrin V, Kupriyanova O, Lebedev AT, Melkozerov V, Eltsov O, Shafran Y, Morzherin Y, Sadykova R. Mass spectrometric properties of N-(2-methoxybenzyl)-2-(2,4,6-trimethoxyphenyl)ethanamine (2,4,6-TMPEA-NBOMe), a new representative of designer drugs of NBOMe series and derivatives thereof. *J Mass Spectrom*. 2016;51:969-79.
25. Wohlfarth A, Roman M, Andersson M, Kugelberg FC, Diao X, Carlier J, Eriksson C, Wu X, Konradsson P, Josefsson M, Huestis MA, Kronstrand R. 25C-NBOMe and 25I-NBOMe metabolite studies in human hepatocytes, in vivo mouse and human urine with high-resolution mass spectrometry. *Drug Test Anal*. 2016.
26. Zuba D, Sekuła K. Identification and characterization of 2,5-dimethoxy-3,4-dimethyl-β-phenethylamine (2C-G) – A new designer drug. *Drug Test Anal*. 2013;5:549-59.
27. Zuba D, Sekuła K, Buczek A. Identification and characterization of 2,5-dimethoxy-4-nitro-β-phenethylamine (2C-N) – A new member of 2C-series of designer drug. *Forensic Sci Int*. 2012;222:298-305.
28. Power JD, Kavanagh P, O'Brien J, Barry M, Twamley B, Talbot B, Dowling G, Brandt SD. Test purchase, identification and synthesis of 2-amino-1-(4-bromo-2, 5-dimethoxyphenyl)ethan-1-one (bk-2C-B). *Drug Test Anal*. 2015;7:512-8.
29. Kneisel S, Westphal F, Bisel P, Brecht V, Broecker S, Auwärter V. Identification and structural characterization of the synthetic cannabinoid 3-(1-adamantoyl)-1-pentylindole as an additive in 'herbal incense'. *J Mass Spectrom*. 2012;47:195-200.
30. Zaitsu K, Nakayama H, Yamanaka M, Hisatsune K, Taki K, Asano T, Kamata T, Katagai M, Hayashi Y, Kusano M, Tsuchihashi H, Ishii A. High-resolution mass spectrometric determination of the synthetic cannabinoids MAM-2201, AM-2201, AM-2232, and their metabolites in postmortem plasma and urine by LC/Q-TOFMS. *Int J Legal Med*. 2015;129:1233-45.
31. Shevyrin V, Melkozerov V, Eltsov O, Shafran Y, Morzherin Y. Synthetic cannabinoid 3-benzyl-5-[1-(2-pyrrolidin-1-ylethyl)-1H-indol-3-yl]-1,2,4-oxadiazole. The first detection in illicit market of new psychoactive substances. *Forensic Sci Int*. 2016;259:95-100.
32. Demarque DP, Crotti AEM, Vessecchi R, Lopes JLC, Lopes NP. Fragmentation reactions using electrospray ionization mass spectrometry: an important tool for the structural elucidation and characterization of synthetic and natural products. *Nat Prod Rep*. 2016;33:432-55.
33. Holcapek M, Jirasko R, Lisa M. Basic rules for the interpretation of atmospheric pressure ionization mass spectra of small molecules. *J Chromatogr A*. 2010;1217:3908-21.
34. Niessen WM. Fragmentation of toxicologically relevant drugs in positive-ion liquid chromatography-tandem mass spectrometry. *Mass Spectrom Rev*. 2011;30:626-63.
35. Karni M, Mandelbaum A. The 'even-electron rule'. *Org Mass Spectrom*. 1980;15:53-64.
36. Thurman EM, Ferrer I, Pozo OJ, Sancho JV, Hernandez F. The even-electron rule in electrospray mass spectra of pesticides. *Rapid Commun Mass Spectrom*. 2007;21:3855-68.
37. Levsen K, Schiebel HM, Terlouw JK, Jobst KJ, Elend M, Preiss A, Thiele H, Ingendoh A. Even-electron ions: a systematic study of the neutral species lost in the dissociation of quasi-molecular ions. *J Mass Spectrom*. 2007;42:1024-44.

38. Theobald DS, Maurer HH. Studies on the metabolism and toxicological detection of the designer drug 2,5-dimethoxy-4-methyl-β- phenethylamine (2C-D) in rat urine using gas chromatographic/mass spectrometric techniques. *J Mass Spectrom*. 2006;41:1509-19.
39. Theobald DS, Maurer HH. Studies on the metabolism and toxicological detection of the designer drug 4-ethyl-2,5-dimethoxy-β-phenethylamine (2C-E) in rat urine using gas chromatographic–mass spectrometric techniques. *J Chromatogr B*. 2006;842:76-90.
40. Theobald DS, Pütz M, Schneider E, Maurer HH. New designer drug 4-iodo-2,5-dimethoxy-β-phenethylamine (2C-I): studies on its metabolism and toxicological detection in rat urine using gas chromatographic/mass spectrometric and capillary electrophoretic/mass spectrometric techniques. *J Mass Spectrom*. 2006;41:872-86.
41. Andreasen MF, Telving R, Birkler RID, Schumacher B, Johannsen M. A fatal poisoning involving Bromo-Dragonfly. *Forensic Sci Int*. 2009;183:91-6.
42. Pichini S, Pujadas M, Marchei E, Pellegrini M, Fiz J, Pacifici R, Zuccaro P, Farre M, de la Torre R. Liquid chromatography-atmospheric pressure ionization electrospray mass spectrometry determination of "hallucinogenic designer drugs" in urine of consumers. *J Pharm Biomed Anal*. 2008;47:335-42.
43. Zuba D, Sekuła K. Analytical characterization of three hallucinogenic N-(2-methoxy)benzyl derivatives of the 2C-series of phenethylamine drugs. *Drug Test Anal*. 2013;5:634-45.
44. Poklis JL, Raso SA, Alford KN, Poklis A, Peace MR. Analysis of 25I-NBOMe, 25B-NBOMe, 25C-NBOMe and other dimethoxyphenyl-N-[(2-methoxyphenyl) methyl]ethanamine derivatives on blotter paper. *J Anal Toxicol*. 2015;39:617-23.
45. Sekuła K, Zuba D. Structural elucidation and identification of a new derivative of phenethylamine using quadrupole time-of-flight mass spectrometry. *Rapid Commun Mass Spectrom*. 2013;27:2081-90.
46. Baz-Lomba JA, Reid MJ, Thomas KV. Target and suspect screening of psychoactive substances in sewage-based samples by UHPLC-QTOF. *Anal Chim Acta*. 2016;914:81-90.
47. Kinyua J, Negreira N, Ibáñez M, Bijlsma L, Hernández F, Covaci A, van Nuijs ALN. A data-independent acquisition workflow for qualitative screening of new psychoactive substances in biological samples. *Anal Bioanal Chem*. 2015;407:8773-85.

## 3.3 CID studies of synthetic cathinones

As previously indicated in Section 1.1.1, synthetic cathinones can be classified into four different subclasses. Traditional cathinones typically undergo alkylation at the phenyl ring, α-carbon and amino group, however, other substitutions have been observed on the phenyl ring such as the addition of methoxy groups and halogens. Due to availability of substitution sites, traditional cathinones have the highest number of derivatives out of the four subclasses due to the different permutations possible if multiple substitutions occur. Methylenedioxy-type cathinones typically undergo alkylation at the α-carbon and amino group due to the restricted number of substitution sites on the phenyl ring, while α-pyrrolidinophenone-type cathinones are restricted to alkylation at the phenyl ring and α-carbon due to the addition of the tertiary pyrrolidino group. For methylenedioxy-α-pyrrolidinophenone-type cathinones, only alkylation at the α-carbon has been observed due to the presence of the methylenedioxy and pyrrolidine rings. The aim of this study was to investigate the CID pathways of synthetic cathinones including traditional cathinones ($n$ = 12), methylenedioxy-type ($n$ = 5), α-pyrrolidinophenone-type ($n$ = 5) and methylenedioxy-α-pyrrolidinophenone-type ($n$ = 3) cathinones using LC-QTOF-MS.

### 3.3.1 Methods and materials

#### *3.3.1.1 Chemicals and reagents*

Cathinone, 2-(methylamino)-1-phenyl-1-propanone (methcathinone), 2-ethylamino-1-phenyl-1-propanone (ethcathinone) 2-ethylamino-1-(4-methylphenyl)-1-propanone (4-methylethcathinone; 4-MEC), 2-methylamino-1-(4-methylphenyl)-1-propanone 4-methylmethcathinone (mephedrone; 4-MMC), 1-(4-fluorophenyl)-2-(methylamino)-1-propanone (4-fluoromethcathinone; flephedrone), 2-amino-1-(3,4-

methylenedioxyphenyl)-1-propanone (3,4-methylenedioxycathinone, amylone), 1-(1,3-benzodioxol-5-yl)-2-(methylamino)-1-propanone, (3,4-methylenedioxy-*N*-methylcathinone; methylone), 1-(1,3-benzodioxol-5-yl)-2-(ethylamino)-1-propanone (3,4-methylenedioxy-*N*-ethylcathinone; ethylone), 1-(1,3-benzodioxol-5-yl)-2-(methylamino)-1-butanone (butylone), 1-(4-methylphenyl)-2-(1-pyrrolidinyl)-1-pentanone (pyrovalerone), and 1-(1,3-benzodioxol-5-yl)-2-(pyrrolidin-1-yl)-1-pentanone (3,4-methylenedioxypyrovalerone, MDPV) were purchased as 1 mg/mL methanolic solutions from PM Separations (Capalaba, QLD, Australia). 1-(3,4-dimethylphenyl)-2-(methylamino)-1-propanone (3,4-dimethylmethcathinone; 3,4-DMMC), 1-(4-Methoxyphenyl)-2-(methylamino)-1-propanone (4-methoxymethcathinone, methedrone), 2-(methylamino)-1-phenyl-1-butanone (buphedrone), 1-phenyl-2-(methylamino)-1-pentanone (pentedrone), 2-(dimethylamino)-1-phenyl-1-propanone (metamfepramone) 2-(diethylamino)-1-phenyl-1-propanone (amfepramone) 1-(1,3-benzodioxol-5-yl)-2-(methylamino)-1-pentanone (pentylone), 1-phenyl-2-(1-pyrrolidinyl)-1-pentanone (α-pyrrolidinovalerophenone; α-PVP), 1-phenyl-2-(1-pyrrolidinyl)-1-propanone (α-pyrrolidinopropiophenone; PPP), 1-(1,3-benzodioxol-5-yl)-2-(1-pyrrolidinyl)-1-propanone (3,4-methylenedioxy-α-pyrrolidinopropiophenone; MDPPP), 1-(4-methylphenyl)-2-(1-pyrrolidinyl)-1-butanone (4-methyl-α-pyrrodinobutiophenone; MPBP), 1-(1,3-benzodioxol-5-yl)-2-(1-pyrrolidinyl)-1-butanone (3,4-methylenedioxy-α-pyrrolidinobutiophenone; MDPBP) were purchased in either 5 mg or 10 mg powdered portions from Cayman Chemical (Ann Arbor, MI, USA). HPLC grade methanol and Optima grade acetonitrile were purchased from Thermo Fisher Scientific (North Ryde, NSW, Australia). MS grade ammonium formate, AR grade formic acid and AR grade sodium chloride were purchased from Sigma Aldrich (Castle

Hill, NSW, Australia).

#### *3.3.1.2 Sample preparation*

Powders were weighed into 1 mg portions and dissolved in 1 mL of methanol to achieve a concentration of 1 mg/mL. Working solutions were prepared by taking 1 µL aliquots and diluting with 1 mL of methanol in sample vials. Standards obtained as 1 mg/mL methanolic solutions were diluted to achieve the same working solution concentration as described above.

#### *3.3.1.3 Instrumental analysis and data processing*

The CID studies of synthetic cathinones were performed on an Agilent Technologies 1290 LC coupled to an Agilent Technologies 6510 QTOF-MS as outlined in Section 3.2.5.3 and 3.2.5.4.

### 3.3.2 Results and discussion

#### *3.3.2.1 Chromatographic analysis of selected synthetic cathinones*

All analytes eluted within the first 5 min of the analytical run with the lowest molecular weight derivative, cathinone, eluting first at 0.99 min and the pyrrolidino-type cathinone, pyrovalerone, eluting the latest at 4.74 min. Similar to hallucinogenic phenethylamines, it could be observed that substitutions on the benzene ring had the greatest effect on retention compared to substitutions on either the α-carbon or amine group. For example, isomeric compounds (*m/z* 178.1226) ethcathinone (*N*-ethyl/α-methyl, $t_r$ = 1.45 min), buphedrone (*N*-methyl/α-ethyl, $t_r$ = 1.74 min) and mephedrone (*para*-methyl/*N*-methyl/α-methyl, $t_r$ = 2.17 min) showed increasing retention time for *N*-substituted, α-substituted and ring-substituted derivatives, however, it was also observed that methylenedioxy-type derivatives decreased retention compared to the corresponding *para*-substituted derivatives due to the addition of the highly polar

methylenedioxy ring e.g. methylone ($t_r$ = 1.34 min) and mephedrone ($t_r$ = 2.24 min). Furthermore, it was also observed that pyrrolidino-type cathinones had longer retention times than the corresponding methylenedioxy-type cathinone due to the addition of the non-polar pyrrolidine ring. Table C.1 in Appendix C summarises the formulae, structures, retention time and *m/z* data for synthetic cathinone precursor ions.

*3.3.2.2 CID of traditional cathinones*

The first major product ion for all traditional cathinones resulted from the CMF and NL of water ($H_2O$, 18.0106 Da) (Figure 3.5), typical of protonated ketones [1], to yield the EE cation **1** ($[M\text{-}H_2O+H]^+/[C_8H_4NR^1R^2R^3R^4]^+$). Following the loss of water, the next major product ion corresponded to an alkyl radical loss from the α-carbon ($\bullet R^3$) to yield the distonic OE radical cation **2a** ($[M\text{-}H_2OR^3+H]^{+\bullet}/[C_8H_4NR^1R^2R^4]^{+\bullet}$). The loss of alkyl radical from the α-carbon was confirmed by the presence of *m/z* 131.0730 for methcathinone, buphedrone and pentedrone which differ only by having an α-methyl, -ethyl and -propyl group, respectively. It is proposed that radical cation **2a** rearranges into the OE indole cation **2b**. Formation of this indole cation is likely due to the resonance stabilised aromatic structure. In addition, there is a peak corresponding to the loss of a hydrogen radical (•H, 1.0073 Da) from both **2b** to form the EE cation **3** ($[M\text{-}H_3OR^3+H]^+/ [C_8H_3NR^1R^2R^4R^5]^+$) which is indicative of methylindoles under EI-MS [2]. This rearrangement and loss of •H was also proposed by Reitzel *et al*. [3] who indicated that the EI-MS spectrum of 2,6-dimethylindole (*m/z* 145.0891) exhibited major product ions at $[M]^{+\bullet}$ and $[M\text{-}H]^+$. It was also postulated that radical loss from the amine group ($\bullet R^4$) to form the radical cation **4a** ($[M\text{-}H_2OR^4+H]^{+\bullet}/[C_8H_4NR^1R^2R^3R^5]^{+\bullet}$) may occur, however, this could not be confirmed for analytes that had both α-methyl and *N*-methyl substitutions as it would result in the same *m/z* value as product ion **2a**/**2b**.

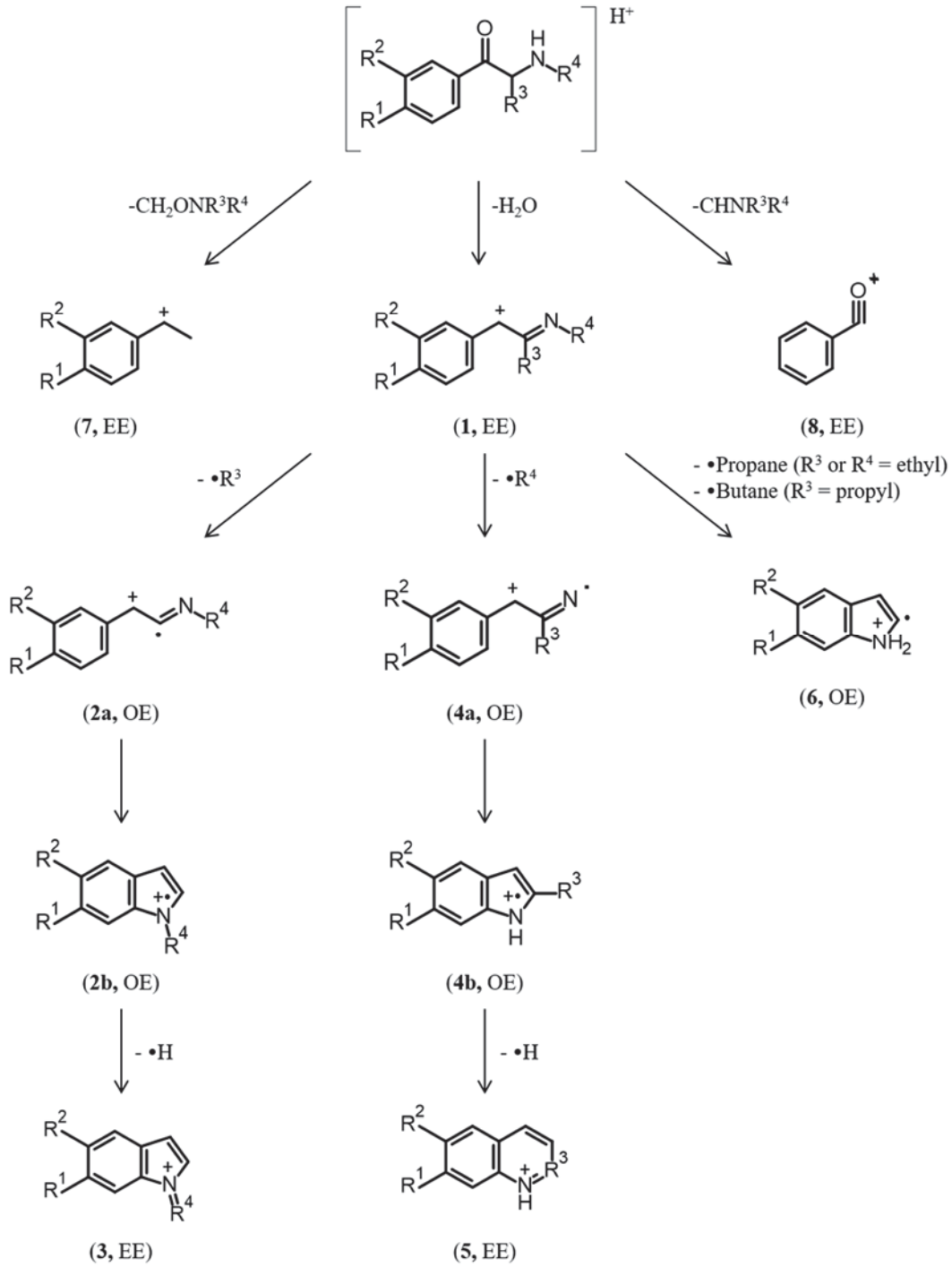


**Figure 3.5** Proposed CID pathways for traditional cathinones at 20 eV.

This postulation was supported, however, by the fact that analytes which had an *N*-ethyl substituent, such as ethcathinone and 4-MEC, had a base peak corresponding to the loss of an ethyl radical (•$CH_2CH_3$, 29.0386 Da). Furthermore, analytes with an *N*-

methyl group and α-substitutions greater than a methyl group had product ions corresponding to the loss of a methyl radical observable, however, this product ion was not as abundant indicating that the loss of long chain radicals is favoured. Similarly, the loss •H was also observed to form the EE cation **5** ([M-$H_3OR^4$+H]$^+$/[$C_8H_3NR^1R^2R^3R^5$]$^+$). Analytes which had either an $R^3$ or $R^4$ substituent greater than a methyl group exhibited radical loss of an alkane corresponding to the combination of the $R^3$ and $R^4$ substituents to yield the OE cation **6** ([$C_8H_5NR^1R^2$]$^{\bullet+}$). For example, ethcathinone (α-methyl/*N*-ethyl) exhibited the radical loss of propane (•$CH_2CH_2CH_3$, 43.0546 Da) from **1** to yield **6** ([$C_8H_7N$]$^{+\bullet}$, *m/z* 117.0573). The EE cation **7** ([$C_8H_7R^1R^2$]$^+$) was observable for analytes which had an α-methyl substituent. In 2012, Zuba [4] reported that the main CID pathways of synthetic cathinones under ESI/QTOF-MS were the losses of water followed by the loss of $R^4$, however, it was not specified whether this was due to a radical loss or NL. In contrast to the present study, cleavage of methylamine and ethylamine for *N*-methyl and *N*-ethyl derivatives, respectively was also observed, however, there was no indication of relative intensities for these product ions.

Similarly, Fornal [5] investigated the CID pathways of protonated synthetic cathinones, however, the CID pathways reported followed mostly EE to EE transitions with the loss of water, cleavage of the amine group and β-cleavage at the keto group. The formation of OE ions for synthetic cathinones was also investigated by Fornal [6] who observed the same OE ions as the present study, however, the mechanisms for the formation of these ions were not discussed and product ion structures were not postulated. Helfer *et al*. [7] studied the metabolism of 4-MEC and observed the same product ions, however, structures were not postulated. Frison *et al*. [8] analysed the *meta*-regioisomer of mephedrone, 3-methylmethcathinone (3-MMC), observing the

same product ions as those identified for mephedrone in this study indicating that regioisomers cannot be differentiated by product ion spectra. Product ion data for traditional cathinones is summarised in Table C.2

*3.3.2.3 CID of methylenedioxy-type cathinones*

Methylenedioxy-type cathinones exhibit the NL of water (Figure 3.6) to yield the EE cation **9** ($[M\text{-}H_2O+H]^+/[C_9H_6NO_2R^1R^2]^+$). Butylone and pentylone also exhibited the radical loss of $\bullet R^1$ to form the OE radical cation **10** ($[M\text{-}H_2OR^1+H]^+/[C_9H_6NO_2R^2]^+$). Unlike traditional cathinones, methylenedioxy-type cathinones did not undergo rearrangement into an indole derivative similar to cation **2b** This was supported by the absence of the *m/z* value corresponding to the loss of •H from cation **10**. The addition of the methylenedioxy ring potentially aids in resonance stabilising cation **10**. The base peak for all methylenedioxy-type cathinones corresponded to the loss of methanediol ($CH_4O_2$, 48.0211 Da) to yield the EE cation **11** ($[M\text{-}CH_4O_2+H]^+/[C_8H_2NOR^1R^2]^+$). Fornal *et al*. [5, 9] postulated that the loss of $CH_4O_2$ was due to CRF followed by rearrangement due to a series of 1,5 and 1,2 hydrogen shifts to form an oxazole cation. The formation of this cation requires that the $R_2$ substituent is a methyl group or larger in order to form the ring structure. In the present study, however, the primary amine derivative, 3,4-methylenedioxycathinone (amylone) was also investigated which showed the loss of $CH_4O_2$. This indicated that the formation of an oxazole cation is unlikely and, therefore, has been proposed to form a fused ring indole-like cation with a keto group situated on the 3-position. This product ion then exhibits the loss of carbon monoxide (CO, 27.9949 Da) to yield the EE product ion **12** ($[C_7H_4NR^1R^2]^+$). The loss of CO is believed to proceed through the opening of the 3-pyrrolidinone ring to yield a resonance stabilised cation **12a** or via ring contraction to form **12b**. The CID pathways of cyclic ketones such as lactones and diketopiperazines under ESI

conditions have been studied previously indicating that the loss of CO proceeds through a similar mechanism [10, 11]. Product ion data for methylenedioxy-type cathinones is summarised in Table C.3.

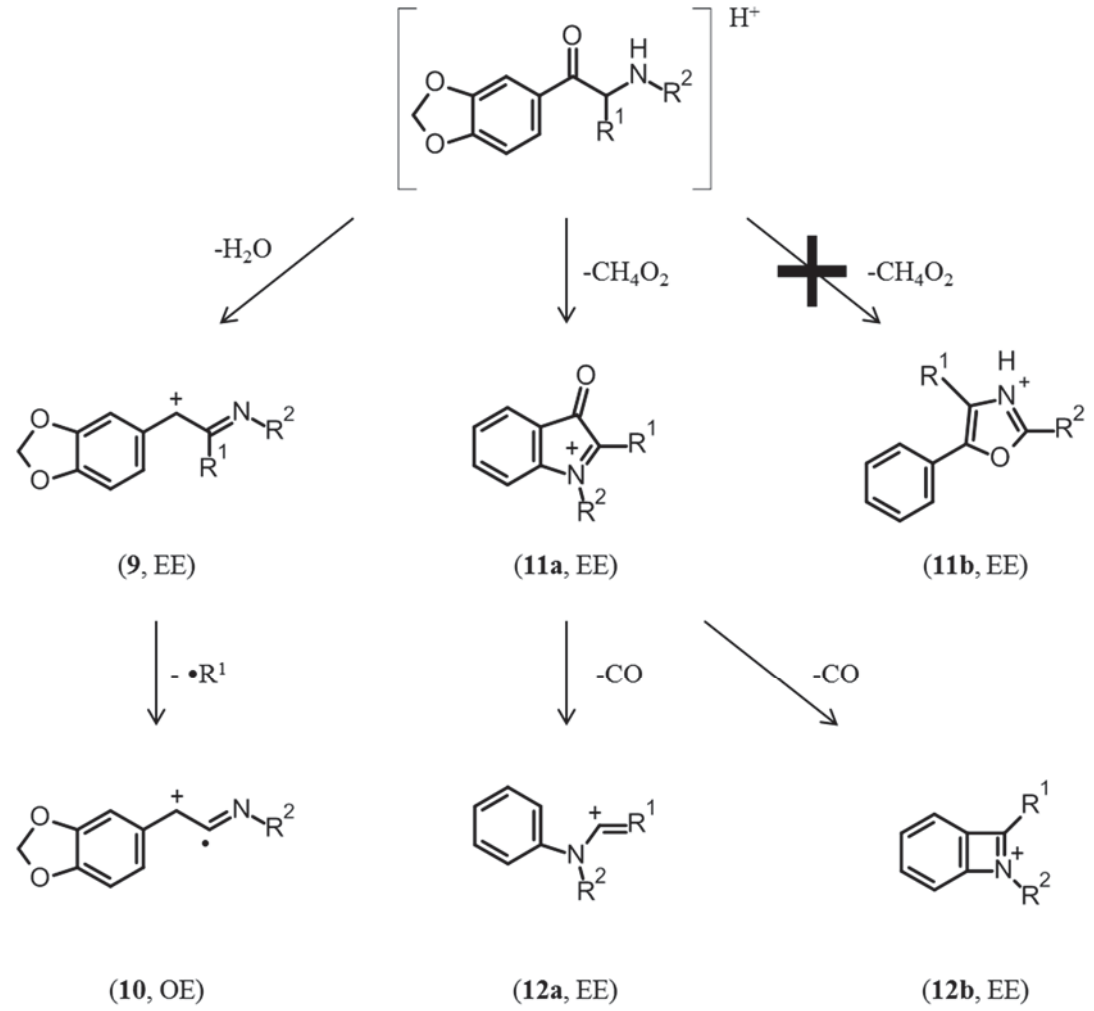


**Figure 3.6** Proposed CID pathways of methylenedioxy-type cathinones at 20 eV.

### *3.3.2.4 CID of α-pyrrolidinophenone-type cathinones*

In general, the precursor ions of α-pyrrolidinophenone-type cathinones were more stable than traditional and methylenedioxy-type cathinones at 20 eV, exhibiting relative intensities (% rel. int.) greater than 35%. The first product ion corresponded

to the CMF and NL of pyrrolidine ($C_4H_9N$, 71.0735 Da) (Figure 3.7) to yield the EE product ion **13** (**(**$[M\text{-}C_4H_9N+H]^+/[C_8H_4OR^1R^2]^+$). The loss of the amino group is indicative of tertiary amine analytes and was also observed for the traditional cathinone derivatives metamfepramone (*N*,*N*-dimethyl) and amfepramone (*N*,*N*-diethyl) which exhibited losses of dimethylamine ($((CH_3)_2NH$, 45.0578 Da) and diethylamine ($((CH_3CH_2)_2NH$, 73.0891 Da), respectively. Simple β-cleavage was also observed for MPBP, α-PVP, pyrovalerone with the formation of EE product ions **14** ($[M\text{-}C_5H_{10}NR^2+H]^+/[C_7H_4OR^1]^+$) and **15** ($[M\text{-}C_7H_4OR^1]^+/[C_5H_{10}NR^2]^+$).

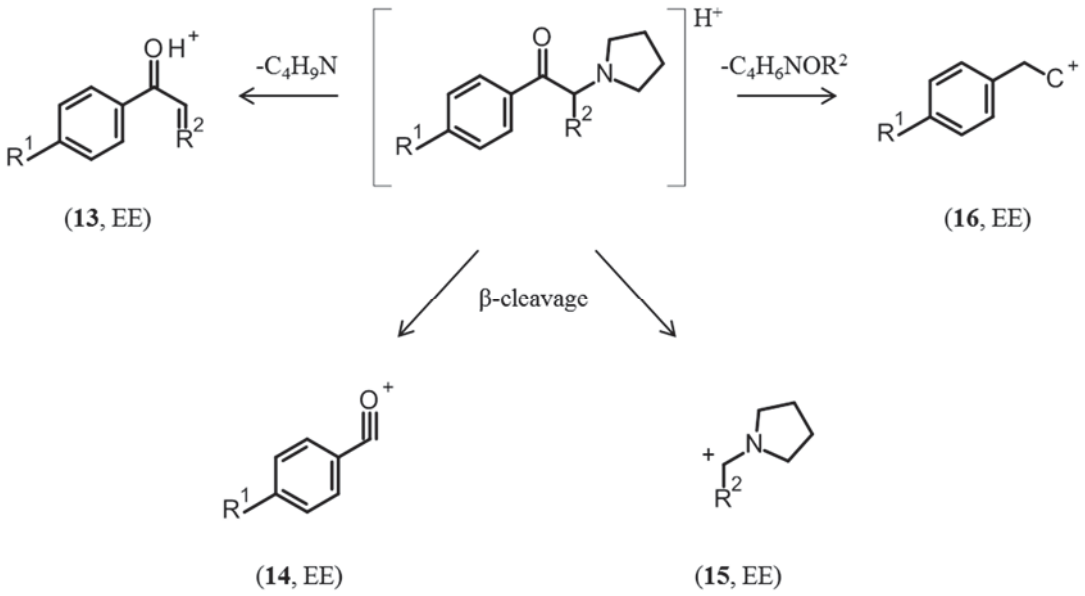


**Figure 3.7** Proposed CID pathways of α-pyrrolidinophenone-type cathinones at 20 eV.

Interestingly, for analytes which have an α-methyl group (PPP and MePPP), the formation of the benzylidyneoxonium ion (**14**) was not favoured but significant intensities were observed for the *N*-ethylpyrrolidine (**15**) cation ($[C_6H_{12}N]^+$, *m/z* 98.0964). A base peak for α-pyrrolidinophenone-type cathinones corresponded to the loss of $C_4H_6NOR^2$ to yield the product ion $[C_8H_8R^1]^+$ (**16**), however, this was not

observed for α-PVP. Swortwood *et al*. [12] investigated the CID pathways of PV8, an α-pentyl homologue of PPP, observing the loss of pyrrolidine with β-cleavage product ions corresponding to the benzylidyneoxonium (**14**) and *N*-pentylpyrrolidine (**15**) product ions. Product ion data for α-pyrrolidinophenone-type cathinones is summarised in Table C.4.

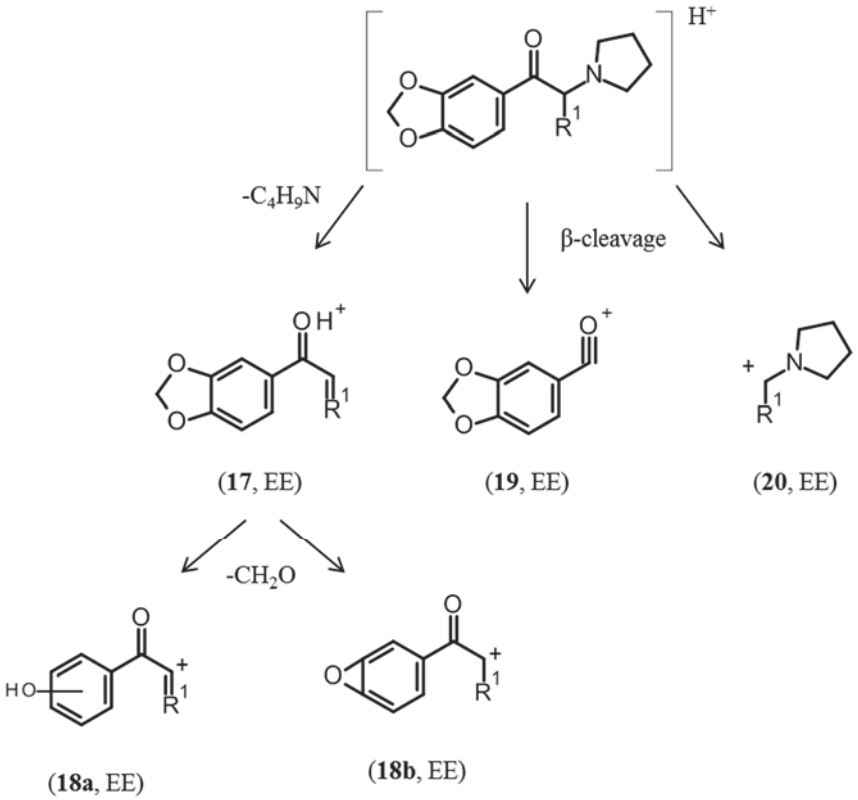


**Figure 3.8** Proposed CID pathways for methylenedioxy-α-pyrrolidinophenone-type cathinones at 20 eV.

### *3.3.2.5 CID of methylenedioxypyrrolidino-type cathinones*

Similar to α-pyrrolidinophenone-type cathinones, methylenedioxypyrrolidino-type cathinones also exhibit stable precursor ions. It was hypothesised that methylenedioxypyrrolidino-type cathinones would produce a combination of product ions as those outlined in Section 3.3.2.3 and 3.3.2.4, however, it appears that the

pathways of α-pyrrolidinophenone-type cathinones were favoured with the NL of pyrrolidine (Figure 3.8) to yield product ion **17 (**$[M\text{-}C_4H_9N+H]^+/[C_7H_4O_2R^1]^+$) observed**.**

There were product ions observable corresponding to the loss of formaldehyde ($CH_2O$, 30.0106 Da) likely from the methylenedioxy ring following the loss of pyrrolidine to yield product ion **18** ($[M\text{-}C_5H_{11}NO+H]^+/[C_8H_4O_2R^1]^+$). Mardal and Meyer [13] investigated the microbial biotransformation of MDPV indicating that this product formed by ring opening followed by to form **18a**. Similarly, Ibañez [14] investigated the metabolites of MDPV in authentic urine and postulated that the loss of $CH_2O$ proceeded via a ring contraction mechanism resulting in the formation of the bicyclic cation **18b**. β-cleavage was also observed to yield the benzylidyneoxonium (**19**) and *N*-alkylpyrrolidine (**20**) product ions. Product ion data for methylenedioxy- α-pyrrolidinophenone-type cathinones is summarised in Table C.5.

### 3.3.3 Summary of key synthetic cathinone product ions for non-targeted screening

The characteristic product ions and NLs for synthetic cathinones are summarised in Table 3.2. The presence of aligning chromatographic peaks for the product ion pair *m/z* 117.0573/105.0699 may indicate a primary amine cathinone derivative with an unsubstituted ring while the presence of *m/z* 131.0730/105.0699 indicates the presence of an unsubstituted secondary amine cathinone derivative with either an α-methyl or *N*-methyl group. Ring substituted derivatives with either α-methyl or *N*-methyl substituents can be detected by extracting product ion pairs *m/z* 145.0886/119.0855, 159.1043/133.1012, 149.0635/123.0605 and 161.0835/135.0804 for methyl, dimethyl, fluoro and methoxy substituted derivatives, respectively. It has been postulated that in addition to dimethyl substituted derivatives, aligning peaks for *m/z* 159.1043/133.1012

may also indicate the presence of a ring-substituted ethyl group, however, such analytes were not included in this study. Fornal [5] analysed 4-ethylmethcathinone (4-EMC) and 4-ethylethcathinone (4-EEC) and observed negligible abundances for *m/z* 133.1012 for both analytes, however, the CID pathway responsible for the formation of *m/z* 159.1043 was not considered in that study.

For methylenedioxycathinone-type cathinones, common product ions were typically not observed since the CID pathways involved the formation of product ions that retained the $R^1$ and $R^2$ groups. In this case, the detection of methylenedioxy derivatives would be better achieved, if possible, by monitoring common NLs via NLFs since all derivatives exhibited NLs of 18.0106 ($H_2O$), 48.0211 ($CH_4O_2$) and 76.0160 Da ($C_2H_4O_3$). In the absence of appropriate data processing software or if the data was acquired using DIA detection can be achieved by extracting the $CH_2$ homologous series of product ions such as *m/z* 146.0600, 160.0757, 174.0913, 188.1070, etc. corresponding to increases in the $R^1$ alkyl chain length.

Product ions *m/z* 105.0699 and 119.0855 were not only indicative for traditional cathinones but also for unsubstituted and methylphenyl substituted α-pyrrolidinophenone-type cathinones, respectively. The presence of *m/z* 105.0335 and 119.0491 is also indicative of this subclass. For methylenedioxy-α-pyrrolidinophenone-type cathinones, *m/z* 149.0233 was an indicative product ion. For both α-pyrrolidinophenone and methylenedioxy-α-pyrrolidinophenone the presence of *m/z* 98.0964, 112.1121 or 126.1277 and NL of 71.0735 Da is indicative of pyrrolidinophenone structure containing an $R^2$ substituent which is either a methyl, ethyl or propyl group, respectively.

**Table 3.2** Potential core structures of synthetic cathinones associated with the presence of product ions and NLs.

| Product ions [*m/z*] | Neutral losses [Da] | Potential Structure |
|---|---|---|
| 117.0573<br>105.0699 | 18.0106 | 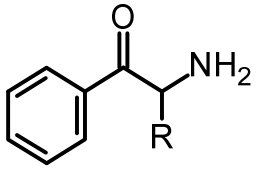 |
| 131.0730<br>105.0699 | 18.0106 | 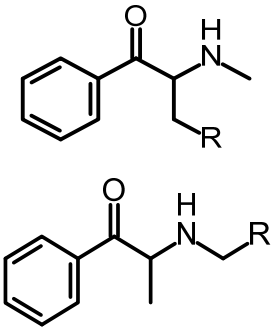 |
| 145.0886, 119.0855 ($R^1 = CH_3$, $R^2 = H$)<br>159.1043, 133.1012 ($R^1 = CH_3$, $R^2 = CH_3$)<br>149.0635, 123.0605 ($R^1 = F$, $R^2 = H$)<br>161.0835, 135.0804 ($R^1 = OCH_3$, $R^2 = H$) | 18.0106 | 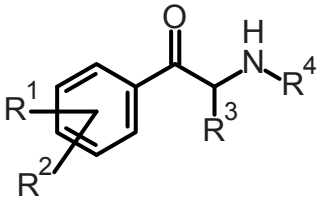 |
| 146.0600 ($R^1 = H$, $R^2 = H$)<br>160.0757 ($R^1 = H$, $R^2 = CH_3$)<br>174.0913 ($R^1 = CH_3$, $R^2 = CH_3$)<br>174.0913 ($R^1 = H$, $R^2 = CH_2CH_3$)<br>188.1070 ($R^1 = CH_2CH_3$, $R^2 = CH_3$) | 18.0106<br>48.0210<br>76.0159 | 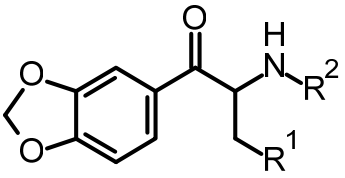 |
| 105.0699 ($R^1 = H$)<br>119.0491 ($R^1 = CH_3$)<br><br>98.0964 ($R^2 = CH_3$)<br>112.1121 ($R^2 = CH_2CH_3$)<br>126.1277 ($R^2 = CH_2CH_2CH_3$) | 71.0735 | 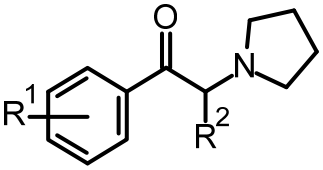 |
| 149.0233 ($R > CH_3$)<br><br>98.0964 ($R = CH_3$)<br>112.1121 ($R = CH_2CH_3$)<br>126.1277 ($R = CH_2CH_2CH_3$) | 71.0735 | 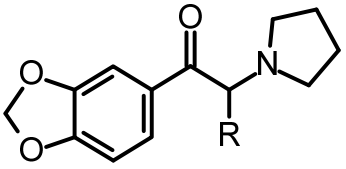 |

### 3.3.4 Conclusion

The CID pathways of synthetic cathinone derivatives were successfully elucidated using LC-QTOF-MS. Traditional cathinones exhibited common NL of water (18.0106 Da) with product ion pairs *m/z* 117.0573/105.0699, 131.0730/105.0699, 145.0886/119.0855, 159.1043/133.1012, 149.0635/123.0605 and 161.0835/135.0804 indicative of phenyl-substituted and alkylamino derivatives. Methylenedioxycathinone-type cathinones did not exhibit common product ions but instead exhibited diagnostic NLs of 18.0106 ($H_2O$), 48.0211 ($CH_4O_2$) and 76.0160 Da ($C_2H_4O_3$). The presence of *m/z* 98.0964, 112.1121 or 126.1277 and NL of 71.0735 Da is indicative of cathinone derivatives containing a pyrrolidine ring such as the α-pyrrolidinophenone-type and methylenedioxy-α-pyrrolidinophenone-type cathinones. Product ions *m/z* 105.0699 and 119.0855 were indicative of unsubstituted and 4-methylphenyl α-pyrrolidinophenone-type cathinones, respectively, while *m/z* 149.0233 was indicative of methylenedioxy-α-pyrrolidinophenone-type cathinones.

### 3.3.5 References

1. Sigsby ML, Day RJ, Cooks RG. Fragmentation of even electron ions. Protonated ketones and ethers. *Org Mass Spectrom*. 1979;14:273-80.
2. Powers JC. Mass spectrometry of simple indoles. *J Org Chem*. 1968;33:2044-50.
3. Reitzel LA, Dalsgaard PW, Müller IB, Cornett C. Identification of ten new designer drugs by GC-MS, UPLC-QTOF-MS, and NMR as part of a police investigation of a Danish Internet company. *Drug Test Anal*. 2012;4:342-54.
4. Zuba D. Identification of cathinones and other active components of 'legal highs' by mass spectrometric methods. *TrAC, Trends Anal Chem*. 2012;32:15-30.
5. Fornal E. Study of collision-induced dissociation of electrospray-generated protonated cathinones. *Drug Test Anal*. 2014;6:705-15.
6. Fornal E. Formation of odd-electron product ions in collision-induced fragmentation of electrospray-generated protonated cathinone derivatives: aryl α-primary amino ketones. *Rapid Commun Mass Spectrom*. 2013;27:1858-66.
7. Helfer AG, Turcant A, Boels D, Ferec S, Lelievre B, Welter J, Meyer MR, Maurer HH. Elucidation of the metabolites of the novel psychoactive substance 4-methyl-N-ethyl-cathinone (4-MEC) in human urine and pooled liver

microsomes by GC-MS and LC-HR-MS/MS techniques and of its detectability by GC-MS or LC-MS(n) standard screening approaches. *Drug Test Anal*. 2015;7:368-75.

8. Frison G, Frasson S, Zancanaro F, Tedeschi G, Zamengo L. Detection of 3-methylmethcathinone and its metabolites 3-methylephedrine and 3-methylnorephedrine in pubic hair samples by liquid chromatography-high resolution/high accuracy Orbitrap mass spectrometry. *Forensic Sci Int*. 2016;265:131-7.
9. Fornal E. Identification of substituted cathinones: 3,4-Methylenedioxy derivatives by high performance liquid chromatography–quadrupole time of flight mass spectrometry. *J Pharm Biomed Anal*. 2013;81–82:13-9.
10. Crotti AEM, Fonseca T, Hong H, Staunton J, Galembeck SE, Lopes NP, Gates PJ. The fragmentation mechanism of five-membered lactones by electrospray ionisation tandem mass spectrometry. *Int J Mass Spectrom*. 2004;232:271-6.
11. Furtado NAJC, Vessecchi R, Tomaz JC, Galembeck SE, Bastos JK, Lopes NP, Crotti AEM. Fragmentation of diketopiperazines from Aspergillus fumigatus by electrospray ionization tandem mass spectrometry (ESI-MS/MS). *J Mass Spectrom*. 2007;42:1279-86.
12. Swortwood MJ, Ellefsen KN, Wohlfarth A, Diao X, Concheiro-Guisan M, Kronstrand R, Huestis MA. First metabolic profile of PV8, a novel synthetic cathinone, in human hepatocytes and urine by high-resolution mass spectrometry. *Anal Bioanal Chem*. 2016;408:4845-56.
13. Mardal M, Meyer MR. Studies on the microbial biotransformation of the novel psychoactive substance methylenedioxypyrovalerone (MDPV) in wastewater by means of liquid chromatography-high resolution mass spectrometry/mass spectrometry. *Sci Total Environ*. 2014;493:588-95.
14. Ibanez M, Pozo OJ, Sancho JV, Orengo T, Haro G, Hernandez F. Analytical strategy to investigate 3,4-methylenedioxypyrovalerone (MDPV) metabolites in consumers' urine by high-resolution mass spectrometry. *Anal Bioanal Chem*. 2016;408:151-64.

## 3.4 CID studies of synthetic cannabinoids

Synthetic cannabinoids can be considered to consist of four key parts including a tail, core, linker and head-group (Figure 3.9). For most synthetic cannabinoids the core consists of either an indole, 2-methylindole or indazole ring, although, more recently the use of indazole rings has become more prevalent. While the use of bicyclic aromatic rings is common, pyrrole and 2-(2-fluorophenyl)pyrrole, rings have been observed in a limited number of analytes. For earlier generation synthetic cannabinoids, such as the JWH- and AM-series, the core and head group were typically connected via carbonyl or acetyl linker at the 3-position of the indole ring, however, ester and carboxamide linkers have been observed for newer generation synthetic cannabinoids with both indole and indazole rings. The tail group is bonded at the 1-position (*N*-position) of the indole or indazole ring and have typically been alkyl chains, predominantly pentyl and 5-fluorpentyl chains, however, other chain lengths have been observed ranging from propyl to heptyl chains. More recently, the tail has typically been comprised of 1-cyclohexylmethyl (CHMICA/CHMINACA-type) and 1-(4-fluorobenzyl) (FUBICA/FUBINACA-type) ring systems. The head group has predominantly consisted of ring-substituted groups such as naphthalene and its substituted derivatives, 2,2,3,3-tetramethylcyclopropyl (TCMP) and adamantyl rings. The aim of this study was to investigate the CID pathways of synthetic cannabinoids using LC-QTOF-MS.

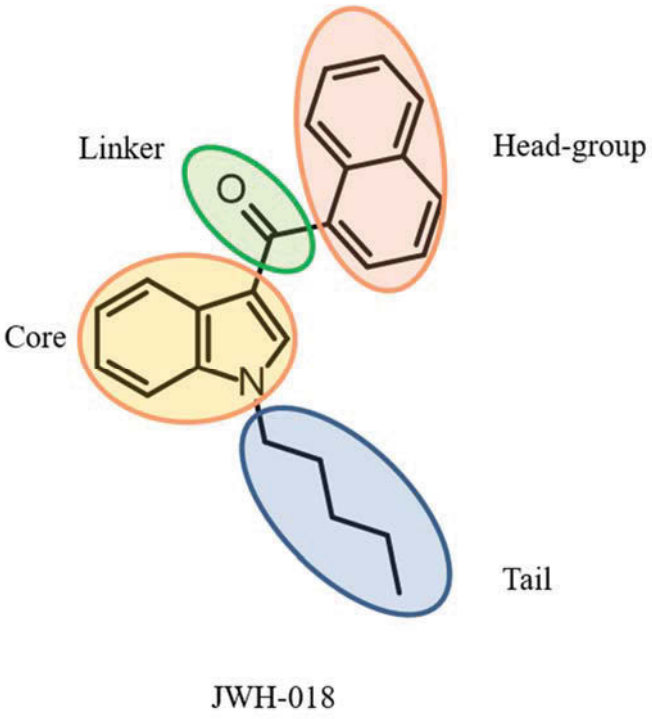


**Figure 3.9** An example of the four parts that make up the synthetic cannabinoid structure for JWH-018.

## 3.4.1 Materials and methods

### *3.4.1.1 Chemicals and reagents*

JWH-007, JWH-015, JWH-016, JWH-018, JWH-019, JWH-020, JWH-030, JWH-073, JWH-081, JWH-098, JWH-122, JWH-200, JWH-203, JWH-210, JWH-250, JWH-307, AM-694, AM-1241, AM-1248, AM-2201, AM-2233, UR-144, XLR-11, FUB-144, BB-22, 5F-PB-22, FUB-NPB-22, NM-2201, APICA, 5F-APICA, ADBICA, 5F-ADBICA, 5F-MMB-PICA, AB-PINACA, 5F-AB-PINACA, 5F-MMB-PINACA, 5F-MDMB-PINACA, 5F-CUMYL-PINACA, MDMB-CHMICA, AB-CHMINACA, ADB-CHMINACA, AB-FUBINACA, ADB-FUBINACA, MMB-FUBINACA MDMB-FUBINACA were purchased from Cayman Chemical, Lipomed AG (Arlseheim, Switzerland), LGC Standards (Teddington, UK), Cerilliant (Round Rock, TX, USA) and NMI as either 0.1, 1 and 5 mg/mL methanolic solutions or

powdered portions. The IUPAC names for all selected synthetic cannabinoids are listed in Table D.1 in Appendix D.

#### *3.4.1.2 Sample preparation*

Analytes obtained in ampoules were diluted to 100 mg/L in 10-mL volumetric flask with methanol. Similarly, powders were dissolved in methanol to achieve a stock solution of 1 mg/mL which were further diluted to 100 mg/L. Working solutions were prepared at 1 mg/L by dilution of 100 mg/L stock solutions.

#### *3.4.1.3 Instrumental analysis*

Chromatographic separation was performed using a Waters Corporation (Milford, MA, USA) ACQUITY HPLC coupled to a Waters Corporation XEVO QTOF-MS according to previously published methods [1, 2]. Briefly, samples were injected (1 µL) onto a Waters Corporation ACQUITY HSS C18 column (150 × 2.1 mm, 1.8 µm particle size) with a gradient elution at a flow rate of 0.4 mL/min for a total analytical runtime of 15 min. Mobile phase composition consisted of A: 5 mM ammonium formate (pH =3) and B: acetonitrile containing 0.1 % (v/v) formic acid. The QTOF-MS was operated in positive electrospray ionisation mode with capillary and cone voltages set to 0.80 kV and 20 V, respectively. Data was acquired over a *m/z* range of 50-1000 using data-independent $MS^E$ with two functions: function 1 at 6 eV and function 2 at a collision energy ramp of 10-40 eV.

#### *3.4.1.4 Data processing*

Acquired data was processed using Waters Corporation MassLynx 4.0. Theoretical precursor ions were extracted in both the function 1 and function 2. The "Combine Spectra" function was used with a peak separation value set to 0.001 Da to subtract background product ions from the analyte product ions. Molecular formulae for

product ion *m/z* values were generated using the MassLynx's Elemental Composition Tool algorithm with elements of interest set to $C_{(0\rightarrow30)}$, $N_{(0\rightarrow5)}$, $O_{(0\rightarrow5)}$, $H_{(0\rightarrow40)}$, $F_{(0\rightarrow1)}$, $Cl_{(0\rightarrow1)}$ and $I_{(0\rightarrow1)}$

### 3.4.2 Results and discussion

The method used in this study has been developed for routine screening of almost 200 pharmaceuticals and drugs of abuse and, therefore, not specifically developed for chromatographic separation of synthetic cannabinoids. The majority of synthetic cannabinoids eluted within a very narrow retention time window in the high organic content wash-out phase towards the end of the analytical run. Due to the highly conjugated structures of synthetic cannabinoid the precursor ions appeared to be relatively stable and provided a limited number of product ions compared to those observed in the CID studies for hallucinogenic phenethylamines and synthetic cathinones even when subjected to a collision energy ramp of 10-40 eV. Furthermore, the CID data presented (Table D.1 in Appendix D) in this study are from spectra that have been averaged over the collision energy ramp, rather than a specific collision energy.

#### *3.4.2.1 General CID pathways of synthetic cannabinoids*

Synthetic cannabinoids exhibited mostly EE to EE transitions typically involving the β-cleavage at the carbonyl linker resulting in the formation of a linker-head cation (**1**) and linker-core-tail cation (**2**) (Figure 3.10). In addition, the alternative β-cleavage products involving the formation of head-group cation (**3**) was also observed for ring-substituted head groups. Cleavage of tail and head-groups were also observed with the formation of linker-core cations (**4**) were also observed to a smaller extent.

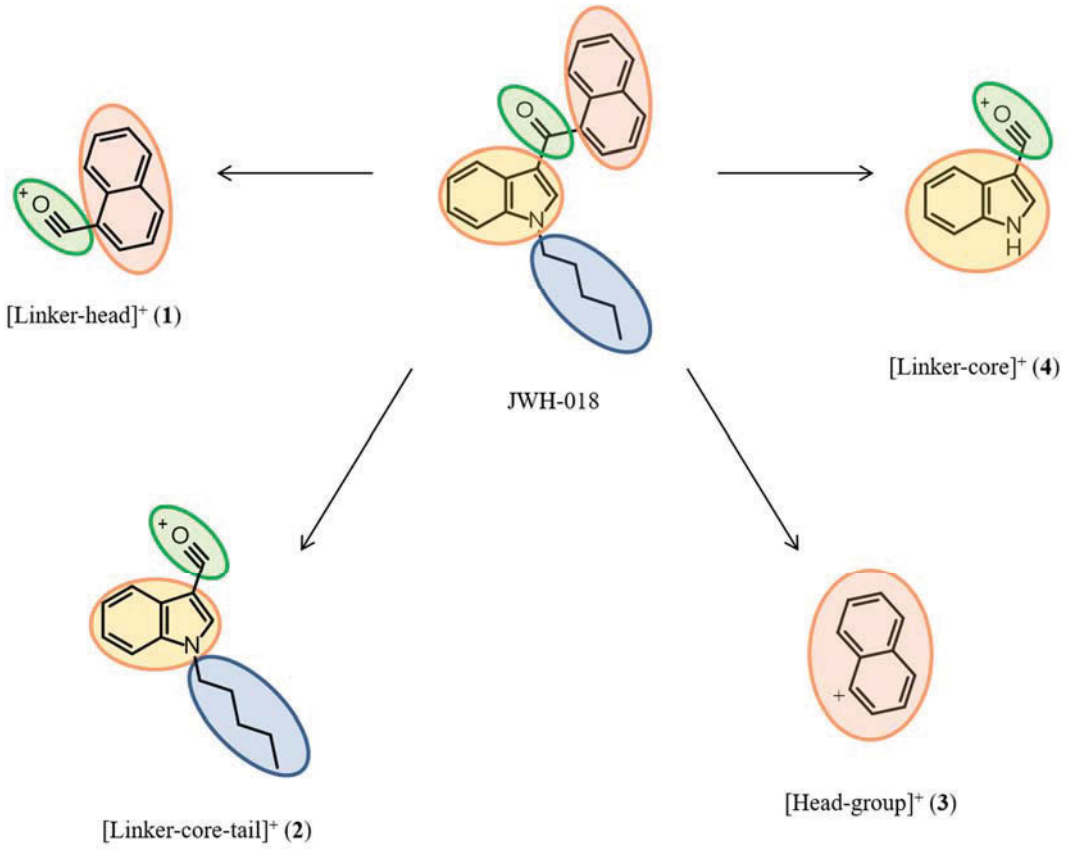


**Figure 3.10** General CID pathways of synthetic cannabinoids.

The linker-head cation was a major product ion for many of the selected synthetic cannabinoids that contained either saturated or unsaturated ring head-groups, however, for derivatives that had an acetyl linker, the formation of the head-group cation was favoured. Similarly, newer generation synthetic cannabinoids with non-cyclic head-groups did not produce linker-head or head-group cations. The formation of the linker-core-tail and linker-core cations were observed for majority of selected analytes while head-group cations were only observed for some ring-substituted derivatives such as those containing naphthyl, 2-substituted benzyl and adamantyl ring substituents. Lastly, NLs of ammonia and carboxamide were observed for AB and ADB-type derivatives and methylformate for MMB and MDMB-type derivatives.

### *3.4.2.2 Key linker-head cations*

Naphthoylindole-type synthetic cannabinoids, such as the JWH series, exhibited major product ions corresponding to the naphthoyl cation **1a (**$[C_{11}H_6OR]^+$) where R was either H (*m/z* 155.0491), $CH_3$ (*m/z* 169.0648), $CH_2CH_3$ (*m/z* 183.0804) or $OCH_3$ (*m/z* 185.0597). Analogues containing a TMCP head group, such as XLR-11, UR-144 and FUB-144, exhibited product ion **1b** ($[C_8H_{13}O]^+$, *m/z* 125.0961). Lastly, the 2-iodobenzoylindole derivatives, such as AM-694 and AM-2233, exhibited the product ion **1b** ($[C_7H_4IO]^+$, *m/z* 230.9301), however, for 2-iodo-5-nitrobenzoylindole derivative, AM-1241, the linker-head cation ($[C_7H_3INO_3]^+$, 275.9152) was weakly abundant. The key linker-head product ions are illustrated in Figure 3.11.

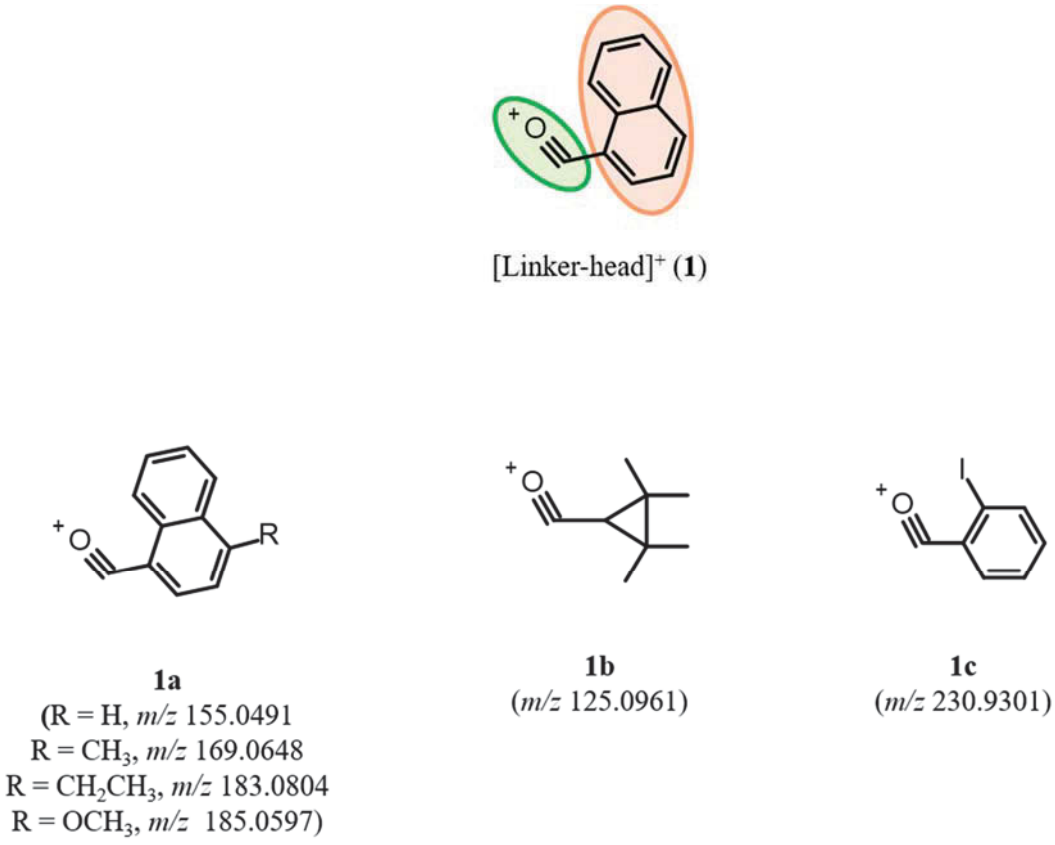


**Figure 3.11** Key linker-head product ions observed at a collision energy ramp of 10-40 eV.

*3.4.2.3 Key linker-core-tail cations*

In most cases, this corresponded to the formation of a substituted indole or indazole oxonium cation. A product ion at *m/z* 214.1226 ($[C_{14}H_{16}NO]^+$, **2a**) was indicative of a 1-pentylindole derivative while a product ion at *m/z* 232.1132 ($[C_{14}H_{15}FNO]^+$, **2b**) was indicative of 1-(5-fluoropentyl)indole. Similarly product ions at *m/z* 215.1179 ($[C_{13}H_{15}N_2O]^+$, **2c**) and 233.1085 ($[C_{13}H_{14}FN_2O]^+$, **2d**) were indicative for 1-pentylindazole (PINACA-type) and 1-(5-fluoropentyl)indazole (5F-PINACA-type), respectively. Furthermore, product ions at *m/z* 240.1383 ($[C_{16}H_{18}NO]^+$, **2e**) 241.1335 ($[C_{15}H_{17}N_2O]^+$, **2f**), 252.0819 ($[C_{16}H_{11}FNO]^+$, **2g**) 253.0772 ($[C_{15}H_{10}FN_2O]^+$, **2h**) corresponded to 1-(cyclohexylmethyl)indole (CHMICA), 1-(cyclohexylmethyl)indazole (CHMINACA), 1-(4-fluorobenzyl)indole (FUBICA) and 1-(4-fluorobenzyl)indazole (FUBINACA) derivatives, respectively. The key linker-core-tail product ions are illustrated in Figure 3.12**.**

*3.4.2.4 Key head-group cations*

While not as abundant as naphthoyl cation ($[C_{10}H_7]^+$), the substituted naphthalene cations ($[C_{10}H_6R]^+$, **3a**) were also observed for naphthoylindole-type synthetic cannabinoids. Interestingly, however, some analogues favoured the formation of head-group instead of the linker-head cations. This was evident for the phenacetylindole-type synthetic cannabinoids, JWH-203 and JWH-250, which exhibited the formation of the 2-substituted benzyl cations (**3b**) ($[C_7H_6Cl]^+$, *m/z* 125.0153) and 2-methoxybenzyl ($[C_8H_9O]^+$, *m/z* 121.0648) cations, respectively. In addition, adamantyl-linked analogues such as AM-1248, APICA and 5F-APICA exhibited a product ion (**3c**) corresponding to the adamantyl cation ($[C_{10}H_{15}]^+$, *m/z* 135.1168). The key head-group cations are illustrated in Figure 3.13.

**Figure 3.12** Key linker-core-tail product ions observed at a collision energy ramp of 10-40 eV.

*3.4.2.5 Key core-linker cations*

The formation of core linker product ions such as the indole ($[C_9H_6NO]^+$, *m/z* 144.0444, **4a**), 2-methylindole ($[C_{10}H_8NO]^+$, *m/z* 158.0600, **4b**) and indazole ($[C_8H_5N_2O]^+$, *m/z* 145.0402, **4c**) acylium cations were observed to a small extent for the majority of analytes except for JWH-030 and JWH-307 which have a pyrrole and 2-(2-flurophenyl)pyrrole core, respectively. The key linker-core-tail product ions are illustrated in Figure 3.14.

### 3.4.3 Conclusion

The CID pathways of synthetic cannabinoids were successfully elucidated using LC-QTOF-MS. Substituted naphthoylindole derived synthetic cannabinoids exhibited key major product ions at *m/z* 155.0491, 169.0648, 183.0804 and *m/z* 185.0597 while 2-iodobenzoylindole and TMCP derivatives exhibited the product ion *m/z* 230.9301 and *m/z* 125.0961, respectively. Key product ions corresponding to the linker-core-tail structure were observed at *m/z* 214.1226 (PICA), 232.1132 (5F-PICA), 215.1179 (PINACA), 233.1085 (5F-PINACA), 240.1383 (CHMICA), 241.1335 (CHMINACA), 252.0819 (FUBICA) and 253.0772 (FUBINACA). Furthermore, the presence of *m/z* 144.0444, 158.0600 and 145.0402 were indicative of the indole, 2-methylindole and indazole acylium cations. These product ions can be utilised to detect most known and novel synthetic cannabinoids if at least one part of the structure is unmodified and instrument sensitivity is adequate.

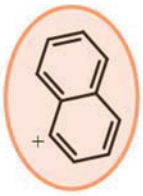

[Head-group]$^+$ (**3**)

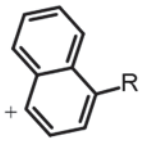

**3a**
(R = H, *m/z* 127.0542
R = $CH_3$, *m/z* 141.0699
R = $CH_2CH_3$, *m/z* 155.0855
R = $OCH_3$, *m/z* 157.0648)

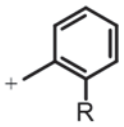

**3b**
(R = $OCH_3$, *m/z* 121.0648
R = Cl, *m/z* 125.0153)

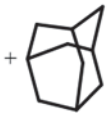

**3c**
(*m/z* 135.1168)

**Figure 3.13** Key head-group product ions observed at a collision energy ramp of 10-40 eV.

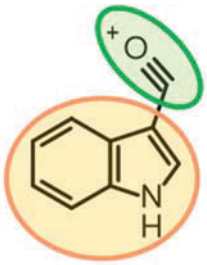

[Linker-core]$^+$ (**4**)

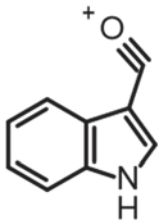

**4a**
(*m/z* 144.0444)

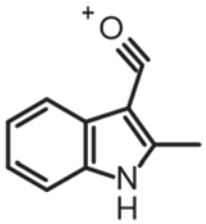

**4b**
(*m/z* 158.0600)

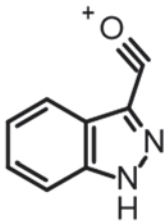

**4c**
(*m/z* 145.0402)

**Figure 3.14** Key linker-core product ions observed at a collision energy ramp of 10-40 eV.

### 3.4.4 References

1. Bidny S, Gago K, Chung P, Albertyn D, Pasin D. Simultaneous Screening and Quantification of Basic, Neutral and Acidic Drugs in Blood Using UPLC-QTOF-MS. *J Anal Toxicol*. 2017;41:181-95.
2. Pasin D, Bidny S, Fu S. Analysis of new designer drugs in post-mortem blood using high-resolution mass spectrometry. *J Anal Toxicol*. 2015;39:163-71.

# *CHAPTER 4:*

# *APPLICATION TO FORENSIC CASEWORK*

## 4.1 Rationale

In order to evaluate the efficacy of the aforementioned top-down and bottom-up screening strategies, they were applied to three authentic toxicological forensic casework samples previously confirmed to contain NPS. These samples were received by the Australian Racing Forensic Laboratory (ARFL, Sydney, NSW, Australia) and the Forensic Toxicology Laboratory at the New South Wales Forensic and Analytical Science Service (NSW FASS, Lidcombe, NSW, Australia) between 2013 and 2016. In one of the cases, the strategies were applied retrospectively to already acquired full scan data as samples were unavailable for re-analysis, however, in the two more recent cases the samples were still accessible and could be re-analysed using different acquisition methods.

## 4.2 Sample preparation and instrumental analysis methods

The samples were received as human urine as part of routine anti-doping testing by ARFL and human whole blood as part of post-mortem toxicological analysis by NSW FASS. Subsequently, these samples were prepared and analysed using different routine methods.

### 4.2.1 Analysis of human urine

#### *4.2.1.1 Sample preparation*

Urine samples were prepared using SPE as previously outlined in Section 2.5.5.4.

#### *4.2.1.2 Instrumental analysis*

Sample extracts were analysed using an Agilent Technologies 1290 Infinity II series UPLC consisting of High Speed Pump (G7120A), Thermostatted Column Compartment (G1316A) and Infinity II Multisampler (G7167A) coupled to an Agilent

Technologies 6545 QTOF-MS fitted with a Dual Agilent Jet Stream Electrospray Ionisation (AJS ESI) source.

Urine extracts were injected (3 µL) and separated using either an (1) Agilent Technologies Poroshell 120 C18 column (2.1 × 75 mm, 2.7 µm particle size) with a mobile phase composition consisting of 20 mM ammonium formate (A) and acetonitrile containing 0.1% (v/v) formic acid (B) or a (2) Phenomenx Gemini C18 column (2 × 50 mm, 5 µm particle size) with a mobile phase composition consisting of 10 mM ammonium acetate (A) and acetonitrile containing 0.1% (v/v) acetic acid (B). A gradient elution was used at a flow rate of 0.5 mL/min with an initial composition of 99% A which was held for 2 min, decreased linearly to 20% A over 6.5 min then returned to the initial conditions over 2 min. The QTOF-MS was operated in ESI+ using All Ions DIA with a fragmentor voltage at 100 V and collision energies set to 10, 20 and 40 eV over a *m/z* range 50-1000.

In order to perform differential analysis, samples were also analysed using a Thermo Fisher Scientific Ultimate 3000 HPLC coupled to a Thermo Fisher Scientific Q Exactive™ orbitrap MS according to Section 2.5.5.5.

### 4.2.2 Analysis of human whole blood

The analysis of human whole blood was performed using SALLE and LC-QTOF-MS according to previously published methods [1, 2]

#### *4.2.2.1 Sample preparation*

Whole blood (100 µL) was mixed with a saturated solution (300 µL) of sodium chloride (NaCl) containing methadone-$d_3$ (0.2 mg/L) as an IS in a 7-mL polypropylene round-bottom tube. The tubes were firstly vortexed for 20 s and ultrasonicated for 15 min followed by the addition of 3 mL acetonitrile, capped, vortexed (1 min), placed

on an Intellimixer for 20 min and finally centrifuged (10 min, 6000 rpm, 6520 × *g*). The upper organic layer was transferred to 5-mL flat-bottomed tubes, evaporated to dryness under a gentle stream of nitrogen at room temperature and reconstituted with 200 µL of methanol: 5 mM ammonium formate (pH 3, 1:1).

#### *4.2.2.2 Instrumental analysis*

Extracts (1 µL) were analysed using a Waters Corporation ACQUITY UPLC coupled to a Waters Corporation XEVO QTOF-MS. Separation was achieved with a Waters Corporation ACQUITY UPLC HSS C18 column (150 mm × 2.1 mm, 1.8 µm particle size, 50°C) using a gradient elution with 5 mM ammonium formate and acetonitrile containing 0.1% (v/v) formic acid at a flow rate of 0.4 mL/min. The initial mobile phase conditions were 87% A which was held for 0.5 min, linearly decreased over 9.5 min to 50% A then decreased to 5% A over 0.75 min, held for 1.5 min and returned to 87% A over 0.25 min with an equilibration time of 2.5 min.

The QTOF-MS was operated in ESI+ with a capillary voltage of 0.80 kV and sampling cone voltage of 20 V. DIA was performed using $MS^E$ with a function 1 collision energy at 6 eV and a function 2 collision energy ramp of 10-40 eV over a *m/z* range of 50-1000.

### 4.2.3 Data analysis

In general, all samples were subjected to KMD analysis over their respective elution ranges, followed by extraction of key product ions. For the KMD analysis, a total of eight KMD values were monitored corresponding to traditional cathinones (T), methylenedioxy cathinones (MD), α-pyrrolidinophenone cathinones (PP), methylenedioxy-α-pyrrolidinophenone cathinones (MDPP), alkyl 2C-X, bromo 2C-X, iodo 2C-X and alkyl 25X-NBOMe derivatives. Sample-specific intensity and

threshold values will be provided in the Results and Discussion.

## 4.3 Results and discussion

### 4.3.1 Case 1: 2C-B in human urine

A human urine sample previously confirmed to contain 2C-B via GC-MS was extracted according to the SPE procedures outlined in Section 2.5.5.4 and analysed using Method 1 according to Section 4.2.1.2. Averaged MS spectra were obtained over a retention time range of 1.0-9.0 min and 2.5-6.5 min, the latter focussing on the known elution range for that chromatographic method. In addition, background subtracted average spectra to remove persistent *m/z* values were also obtained by subtracting the averaged spectra generated on either side of the specified chromatographic period.

The datasets were firstly screened to ensure that the IS, desipramine-$d_3$ (*m/z* 270.2044), could be detected and also to select appropriate intensity threshold and KMD tolerance values. Desipramine-$d_3$ was detected in all four datasets with averaged intensities ranging between 1803-3110 counts and a mass error of +1.6 mDa. Considering that the concentration of desipramine-$d_3$ in urine was 33 ng/mL, the KMD analysis was performed with an intensity threshold of 100 counts to account for analytes at much lower concentrations. In addition, the KMD tolerance value was set to 0.0020 Da to account for variations in accurate mass measurement. The results for the KMD analysis are summarised in Table 4.1.

**Table 4.1** Summary of results from the KMD analysis for the human urine sample containing 2C-B.

| Retention time range [min] | Background subtracted | Dataset size [*m/z* values] | Positive hits | Reduction of dataset [%] |
|---|---|---|---|---|
| 1.0-9.0 | N | 2,966 | 12 | 99.60 |
| | Y | 2,770 | 12 | 99.57 |
| 2.5-6.5 | N | 2,311 | 20 | 99.13 |
| | Y | 1,953 | 20 | 98.98 |
| | MFE[a] | 1,909 | 8 | 99.58 |

[a] Intensity threshold > 1000 counts

For the results of the KMD analysis, a total of 12 positive hits were identified over a retention time range of 1-9 min (8 min window) and 20 positive hits for 2.5-6.5 min (4 min window), corresponding to > 99% reduction in dataset size. For the background subtracted datasets, there was a decrease in the number of *m/z* values, however, the same number of hits were observed, indicating that none of the positive hits were due to persistent background ions. Interestingly, it was observed that the shorter retention time range yielded a higher number of positive hits, although, it was reasoned that due to the decreased amount of scans (approximately half) used to generate the averaged spectra it would increase the averaged intensities of *m/z* values. Consequently, some *m/z* values which had intensities below the intensity threshold value for the 8 min window spectrum now had > 100 counts for the 4 min window spectrum. Additionally, it was observed that the intensities of *m/z* values for the 2.5-6.5 spectrum were approximately double that of the 1.0-9.0 spectrum.

In addition, the use of an intermediate data mining software prior to KMD analysis was investigated using the MFE function in MassHunter over the 2.5-6.5 min retention time range where peak extraction was limited to peaks with height ≥ 1000 counts.

The compound *m/z* values and heights for the resulting compounds were copied to a MS Office excel workbook and saved as a .csv file. Since the intensity values used in this scenario are the raw intensity values, an IS screen was performed to determine an appropriate intensity threshold. An approximate intensity of 120,000 counts was observed for desipramine-$d_3$, therefore, an intensity threshold of 10,000 counts was used for the KMD analysis. An increased number of positive hits ($n$ = 30) were observed compared to those obtained using the averaged mass spectra, however, there were a significant amount of duplicate *m/z* results likely due to multiple chromatographic peaks over the chromatographic ranges. The removal of duplicate *m/z* values resulted in a revised total of 8 positive hits that corresponded to those identified in the averaged spectra datasets.

The positive hits for the KMD analysis are listed in Table 4.2 for all datasets. Many of the *m/z* values corresponded to the different cathinone subclasses and alkyl 2C-X derivatives with single *m/z* values corresponding to the analyte of interest (bromo 2C-X) and PP derivative. It was observed that the averaged intensity values had negligible change when subtraction algorithms were used.

The top 10 positive hit *m/z* values were used to generate EICs in MassHunter in order to observe distinct chromatographic peaks. The majority of EICs did not exhibit distinct chromatographic peaks, specifically for *m/z* 164.1076, 178.1238, 192.1393 and 222.1145 indicating that those precursor ions were present over most of the chromatographic period. The only positive hit that provided distinct chromatographic peaks was the analyte of interest, *m/z* 260.0294 at 4.45 and 4.70 min.

**Table 4.2** Matched m/z values from the results of the KMD analysis for the human urine sample containing 2C-B.

| No. | *m/z* | Class | Intensity [counts] | | | | |
|---|---|---|---|---|---|---|---|
| | | | 1.0-9.0 min | 1.0-9.0 min subtracted | 2.5-6.5 min | 2.5-6.5 min subtracted | 2.5-6.5 MFE |
| 1 | 182.1187 | Alkyl 2C-X | 2,203 | 2,206 | 4,394 | 4,390 | 120,468 |
| 2 | 196.1349 | Alkyl 2C-X | 1,049 | 1,047 | 2,079 | 2,068 | |
| 3 | 150.0918 | T | 1,027 | 1,028 | 2,043 | 2,040 | 256,587 |
| 4 | 164.1076 | T | 563 | 564 | 1,124 | 1,124 | 54,711 |
| 5 | 210.1503 | Alkyl 2C-X | 440 | 440 | 862 | 857 | 16,578 |
| 6 | 208.0983 | MD | 418 | 418 | 816 | 805 | 15,943 |
| 7 | 260.0294 | Bromo-2C-X | 402 | 403 | 800 | 800 | 65,180 |
| 8 | 192.1393 | T | 450 | 407 | 746 | 644 | |
| 9 | 222.1144 | MD | 314 | 313 | 602 | 598 | |
| 10 | 178.1236 | T | 310 | 310 | 598 | 594 | 14,539 |
| 11 | 248.1306 | MDPP | | | 476 | 476 | |
| 12 | 236.1272 | MD | | | 379 | 332 | |
| 13 | 224.1663 | Alkyl 2C-X | 148 | 149 | 298 | 298 | |
| 14 | 194.0821 | MD | 163 | 163 | 300 | 288 | 11,589 |
| 15 | 430.3321 | MDPP | | | 176 | 171 | |
| 16 | 432.3480 | MD | | | 165 | 165 | |
| 17 | 238.1827 | Alkyl 2C-X | | | 139 | 139 | |
| 18 | 206.1562 | T | | | 141 | 127 | |
| 19 | 278.1778 | MD | | | 128 | 127 | |
| 20 | 204.1392 | PP | | | 104 | 104 | |

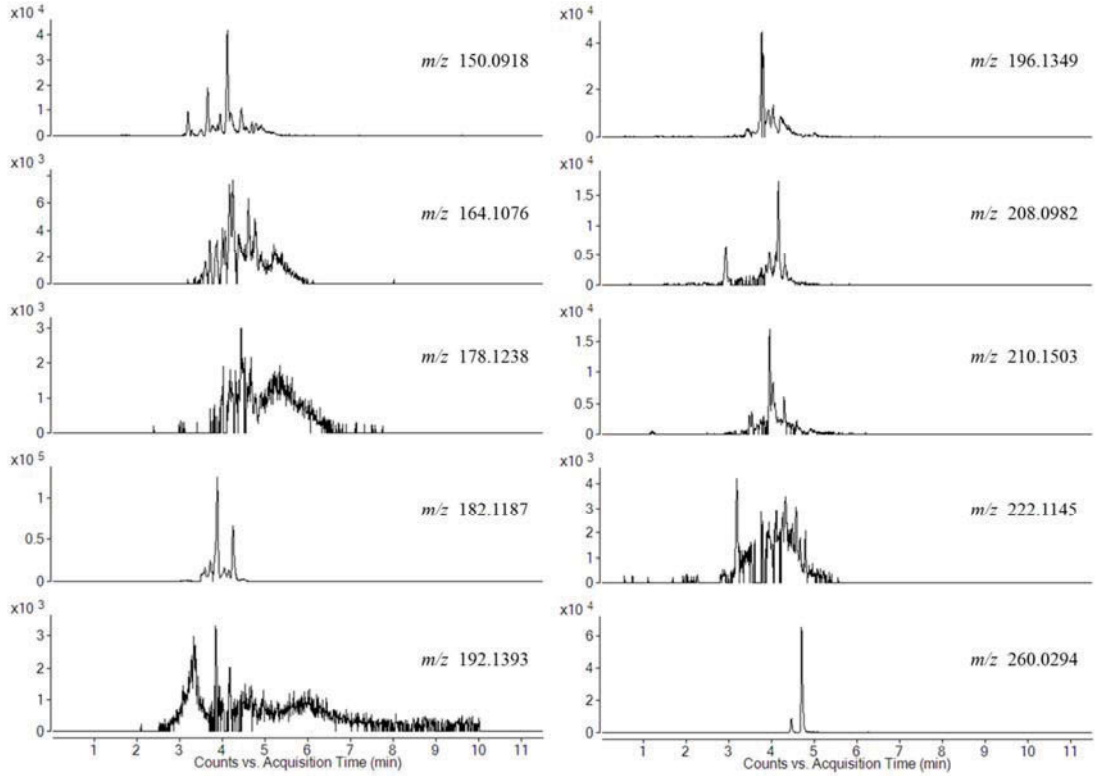


**Figure 4.1** EICs of the top ten abundant *m/z* values from the KMD analysis of human urine containing 2C-B.

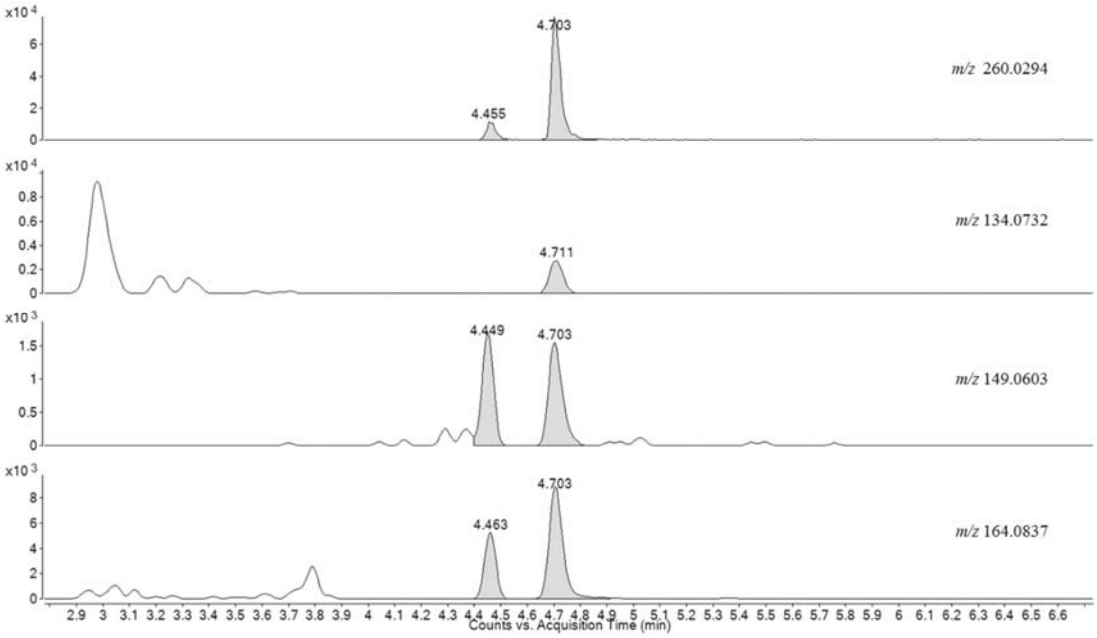


**Figure 4.2** EIC for *m/z* 260.0294 at 0 eV and EICs for common product ions of 2C-X derivatives at 20 eV (*m/z* 164.0637 and 149.0603) and 40 eV (*m/z* 134.0732).

To confirm the potential presence of a bromo-2C-X analogue, EICs for common product ions for 2C-X phenethylamines (according to Section 3.2.6.5) were generated (Figure 4.2). Interestingly, two chromatographic peaks could be observed in the EICs of common product ions *m/z* 165.0837 and 149.0603 at 20 eV at the same retention times observed for *m/z* 260.0294, however, only *m/z* 134.0732 (40 eV) was observed at 4.71 min indicating that this peak was likely due to a bromo-2C-X derivative. The spectra of both chromatographic peaks were generated at 20 eV (Figure 4.3). The spectrum for the peak at 4.46 min contained a significant amount of background ions and was subsequently difficult to interpret. Product ions corresponding to the characteristic losses of $NH_3$ (*m/z* 243.0017, -1.51 ppm) and $\bullet CH_3NH_3$ (*m/z* 227.9783, -1.28 ppm) for 2C-X derivatives could be observed in the spectrum for the peak at 4.71 min, however, their relative abundances are low due to the presence of background ions *m/z* 167.0737 and 182.0987. The spectra also highlighted the limitations of DIA due to the presence of all product ions from all precursor ions. If only the bottom-up strategy was applied, it would be difficult to determine what precursor ion was responsible for the product ions, demonstrating the importance of their complementary use.

### 4.3.2 Case 2: MDMC in human urine

A human urine sample previously confirmed to contain 2,3-methylenedioxymethcathinone (MDMC) via LC-QTOF-MS was extracted according to the SPE procedures outlined in Section 2.5.5.4 and analysed using Method 2 according to Section 4.2.1.2. Data processing was performed in a similar manner as for Case 1. Firstly, KMD analysis was performed over a retention time range of 2.5-6.5 min with background subtraction with an intensity threshold > 100 counts and KMD tolerance of 0.002 Da with a total of 28 hits observed.

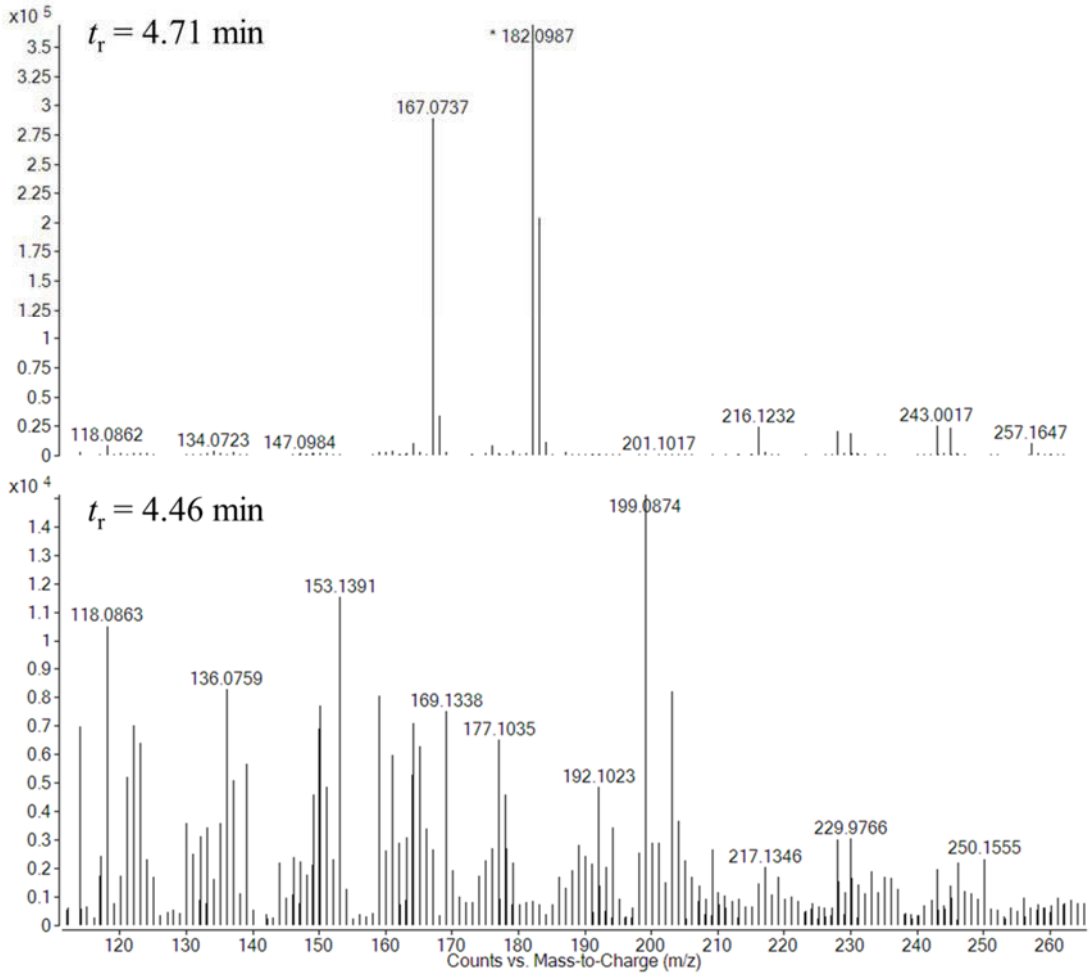


**Figure 4.3** Mass spectra for chromatographic peaks at 4.71 and 4.46 min at 20 eV.

The dataset for this sample contained more than ten-times the number (29,988 values) of *m/z* values compared to those observed for the datasets in Case 1 and is likely due to the different chromatographic method. For some of the more abundant positive hits, it was observed that the *m/z* values corresponded to analytes resulting from a significant amount of alkylation. For example, the most abundant positive hit corresponded to a MD cathinone derivative with *m/z* 432.3496, indicating that this analogue was due to the addition of seventeen $CH_2$ subunits to the base structure, methylenedioxycathinone (*m/z* 194.0817). Subsequently, unrealistic positive hits were removed resulting in a revised number of positive hits of 14 (Table 4.3). It was also

observed that many of the *m/z* values observed in this sample were similar to Case 1 indicating that these ions may be due to the sample, however, since these *m/z* values may correspond to potential analogues they cannot be disregarded. The top ten *m/z* values were then used to generate EICs which are illustrated in Figure 4.4. Similar to Case 1, many of the *m/z* values did not correspond to distinct chromatographic peaks, particularly *m/z* 178.1227, 182.1191 and 196.1385. An abundant and distinct chromatographic peak was observed for *m/z* 208.0981 corresponding to the analyte of interest, MDMC, at 4.5 min.

**Table 4.3** Results of the KMD analysis for the human urine sample containing MDMC.

| No. | *m/z* | Class | Intensity [counts] |
|---|---|---|---|
| 1 | 276.1598 | MDPP | 15,436 |
| 2 | 164.1074 | T | 7480 |
| 3 | 178.1227 | T | 4833 |
| 4 | 192.1385 | T | 3679 |
| 5 | 210.1479 | Alkyl 2C-X | 2452 |
| 6 | 208.0981 | MD | 1485 |
| 7 | 196.1332 | Alkyl 2C-X | 1360 |
| 8 | 182.1191 | Alkyl 2C-X | 1126 |
| 9 | 238.1818 | T | 615 |
| 10 | 234.1851 | T | 479 |
| 11 | 204.1388 | MDPP | 432 |
| 12 | 302.1767 | Alkyl-NBOMe | 407 |
| 13 | 224.1657 | Alkyl 2C-X | 346 |
| 14 | 194.0804 | MD | 181 |

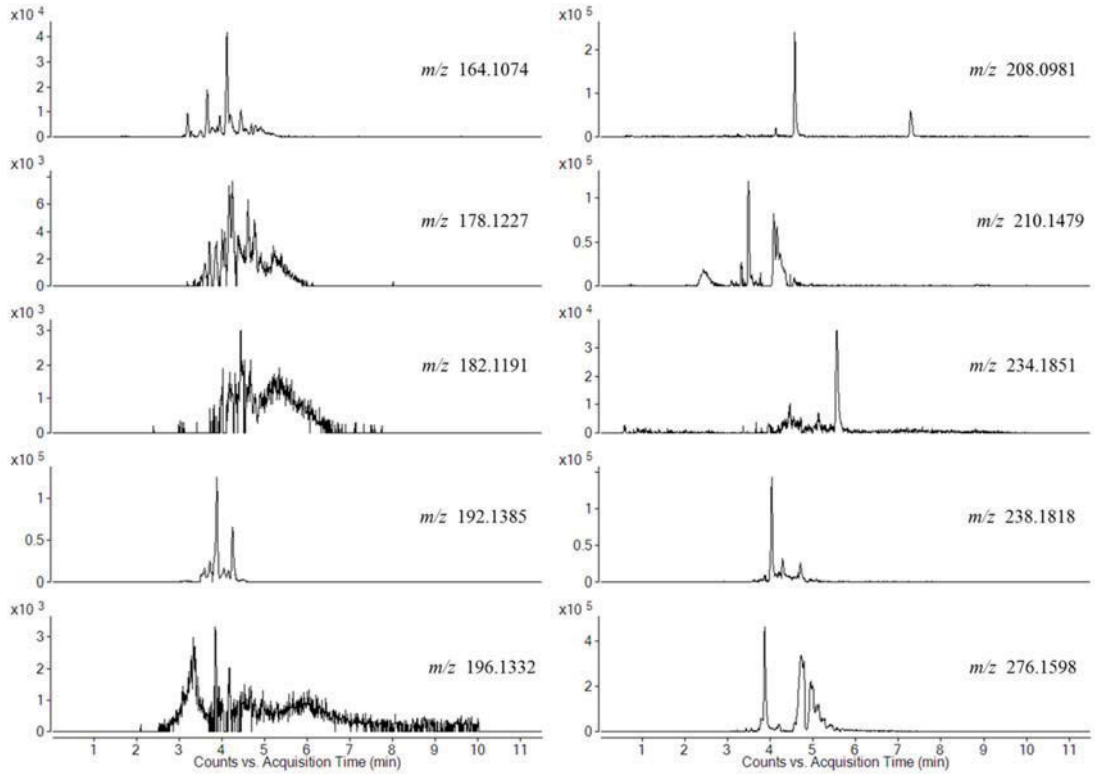


**Figure 4.4** EICs of the top ten abundant *m/z* values from the KMD analysis of human urine containing MDMC.

As previously mentioned, MD cathinones do not exhibit common product ions that can be monitored in bottom-up screening strategies, therefore, in this case homologous series of ions corresponding to the base peak product ion observed in Section 3.3.2.3 were extracted (Figure 4.5). Interestingly, distinct chromatographic peaks were observed for *m/z* 146.0600 and 174.0914, however, no distinct aligning peak was observed for the product ion corresponding to the analyte of interest (*m/z* 160.0757). Since it is more applicable to monitor NLs for MD cathinones, the sample was reanalysed using targeted MS/MS acquisition at *m/z* 208.0986. Generation of pNLCs was performed using the MassHunter Qualitative data analysis software for NLs of 18.0106, 48.0210 and 78.0159 Da (Figure 4.6). The aligning peaks for the pNLCs strongly indicates that *m/z* 208.0981 is a MD cathinone.

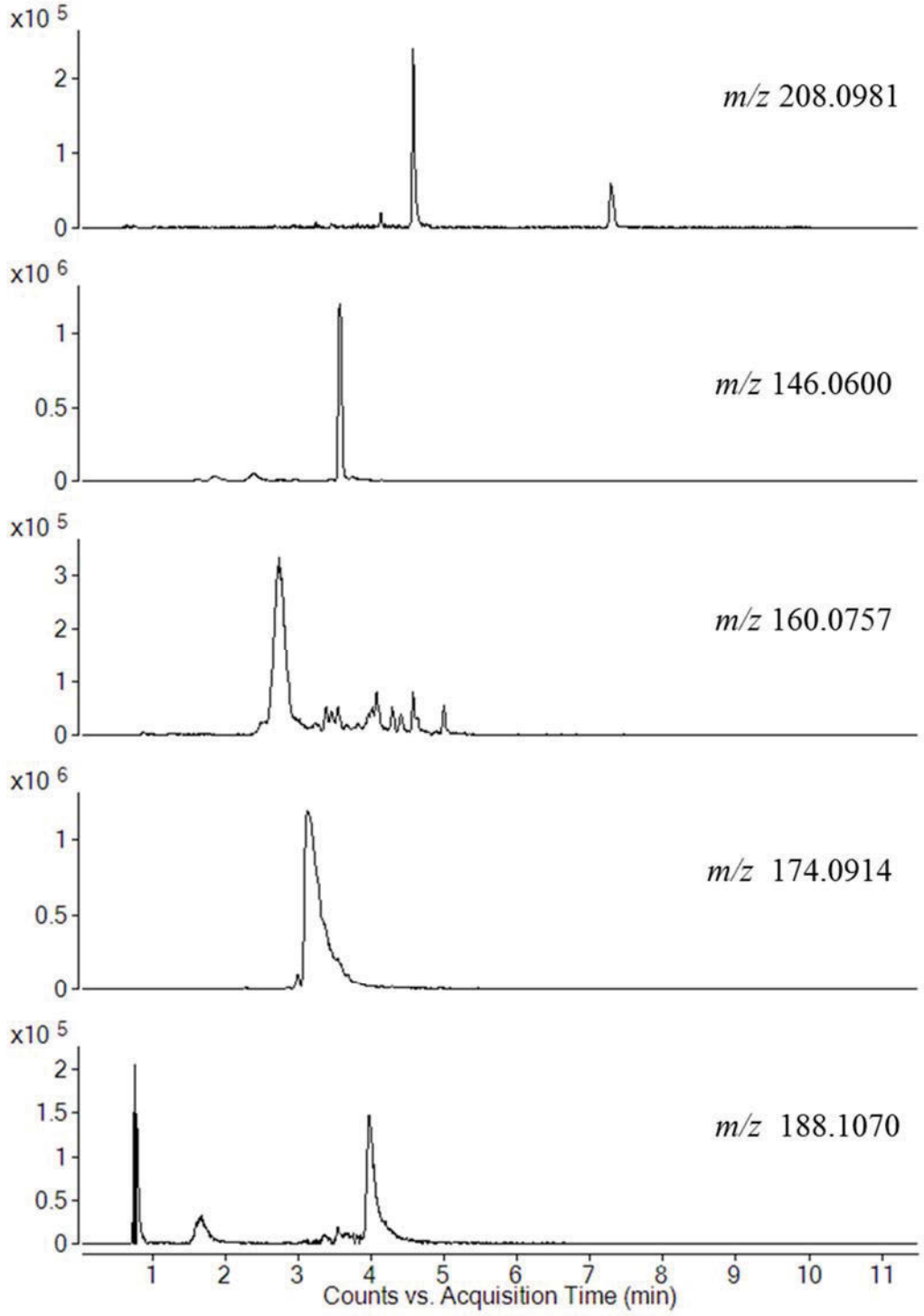


**Figure 4.5** EICs for characteristic product ions of methylenedioxy-type cathinones at 20 eV.

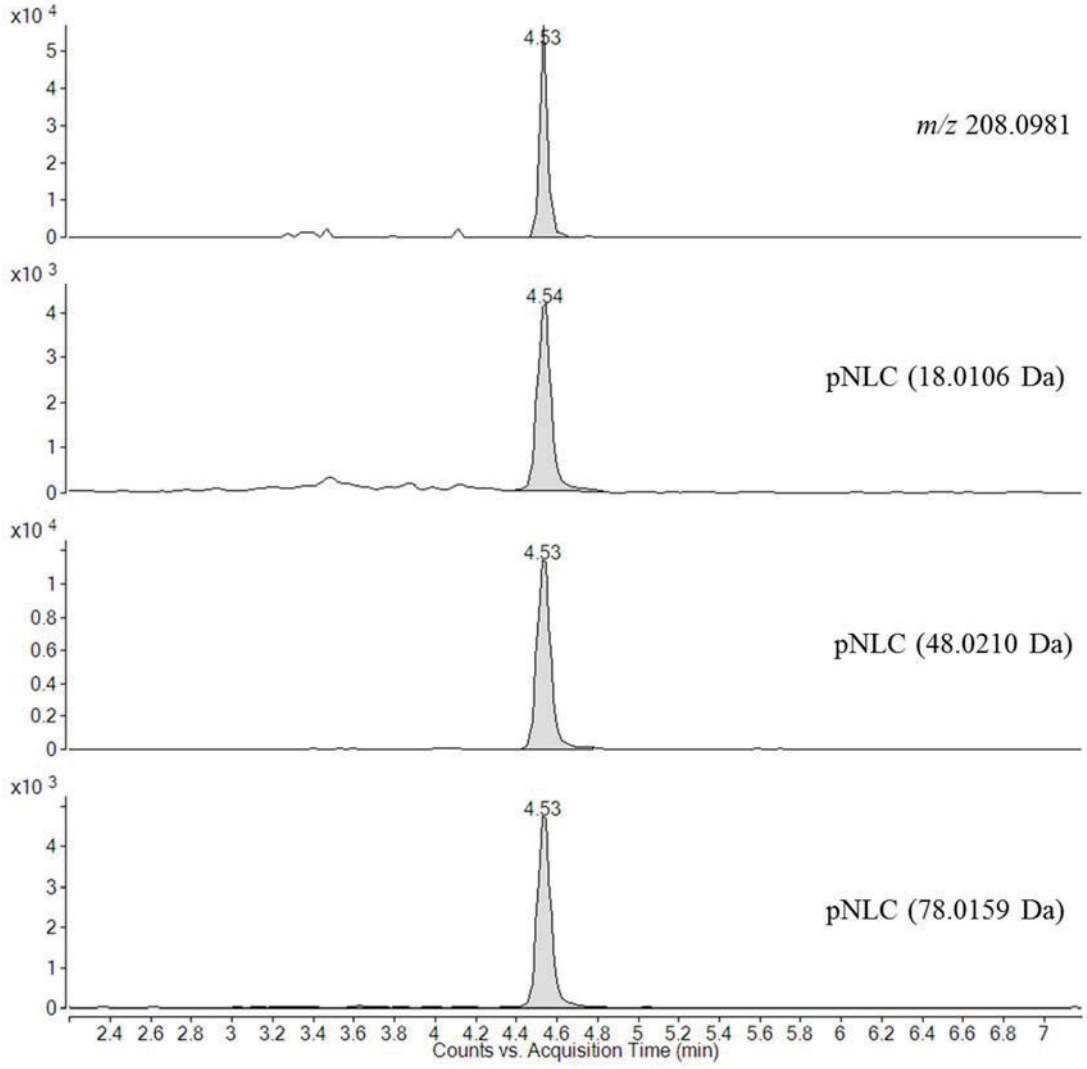


**Figure 4.6** pNLCs corresponding to the characteristic NLs of methylenedioxy-type cathinones at 20 eV.

### 4.3.3 Case 3: MDPV in human whole blood

Authentic human whole blood previously confirmed to contain MDPV via LC-QTOF-MS was extracted according to the procedures outlined in Section 4.2.2.1 and analysed using LC-QTOF-MS according to Section 4.2.2.2. Background subtracted spectra were obtained over a 9 minute chromatographic window (1-10 min) by using the 'Combine Spectra' function in MassLynx with a peak separation value of 0.001 Da. The resulting dataset comprised of 194,778 *m/z* values, which was significantly higher

compared to those datasets acquired in Case 1 and Case 2. This is due to a number of reasons, including the fact that the chromatographic period was longer. In addition, the averaged spectra were generated from function 1 which has a collision energy of 6 eV, therefore, resulting in the generation of product ions and increasing the number of *m/z* values. KMD analysis was performed with an intensity threshold > 500 counts. Considering the significantly larger dataset size, only four positive hits were identified corresponding to two MD cathinones (*m/z* 208.0937 and 222.1130), a MDPP cathinone (*m/z* 276.1590) and an alkyl-2C-X derivatives (Table 4.4).

**Table 4.4** Results of the KMD analysis for human whole blood containing MDPV.

| No. | *m/z* | Class | Intensity [counts] |
|---|---|---|---|
| 1 | 222.1130 | MD | 4850 |
| 2 | 276.1590 | MDPP | 2910 |
| 3 | 208.0973 | MD | 968 |
| 4 | 210.1491 | Alkyl-2C-X | 721 |

EICs were generated for the four positive hits with the only distinct chromatographic peaks observed for the *m/z* value corresponding to the analyte of interest, MDPV (*m/z* 276.1590) at 4.74 min (Figure 4.7). To confirm that the chromatographic peak was due to the presence of a MDPP cathinone, common product ions were extracted in function 2 (10-40 eV). Firstly, EICs corresponding to the major homologous MDPP product ions *m/z* 98.0960, 112.1120 and 126.1280 were generated to determine the α-carbon substituent (Figure 4.8). A chromatographic peak for *m/z* 126.1280 was observed at the same retention time as *m/z* 276.1590 supporting the presence of a MDPP cathinone with an α-propyl chain. Secondly, an EIC for the common product ion of MDPP cathinones, *m/z* 149.0230, was generated yielding a less abundant peak (Figure 4.9).

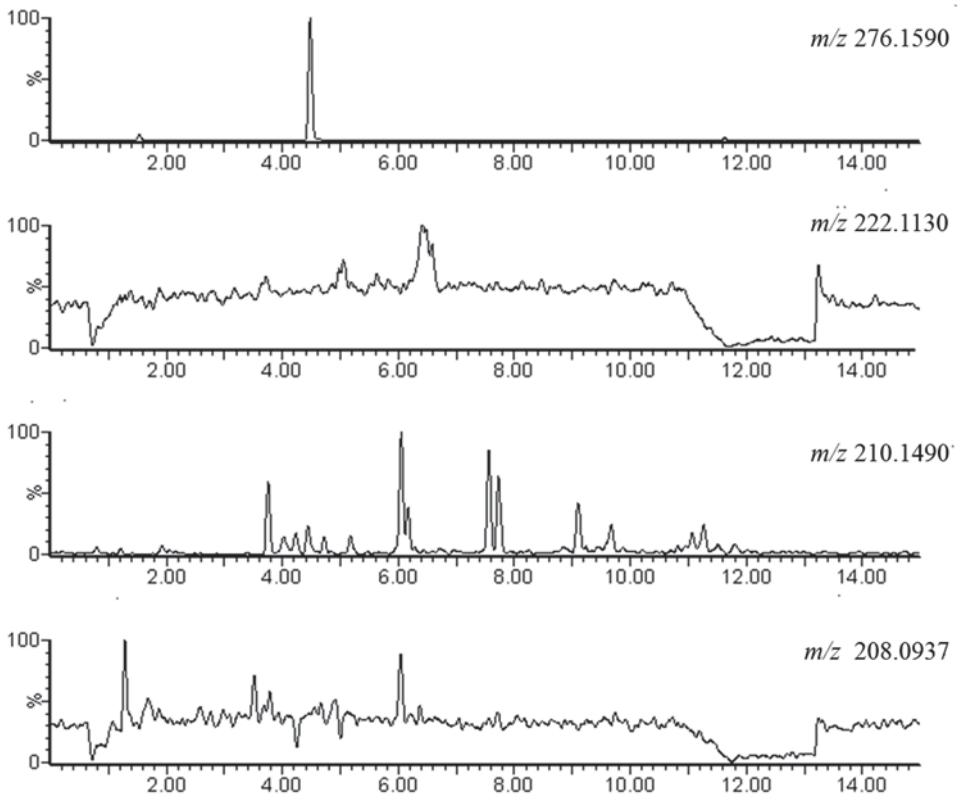


**Figure 4.7** EICs for the KMD analysis results for human whole blood containing MDPV.

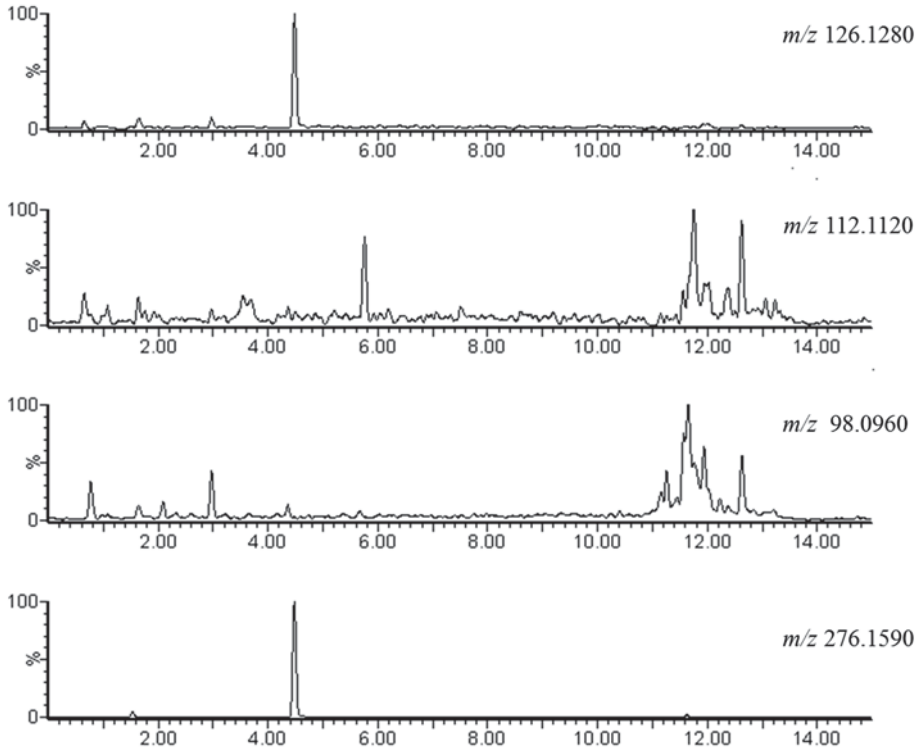


**Figure 4.8** EICs for common product ions for pyrrolidine-type cathinones at a collision energy ramp of 10-40 eV.

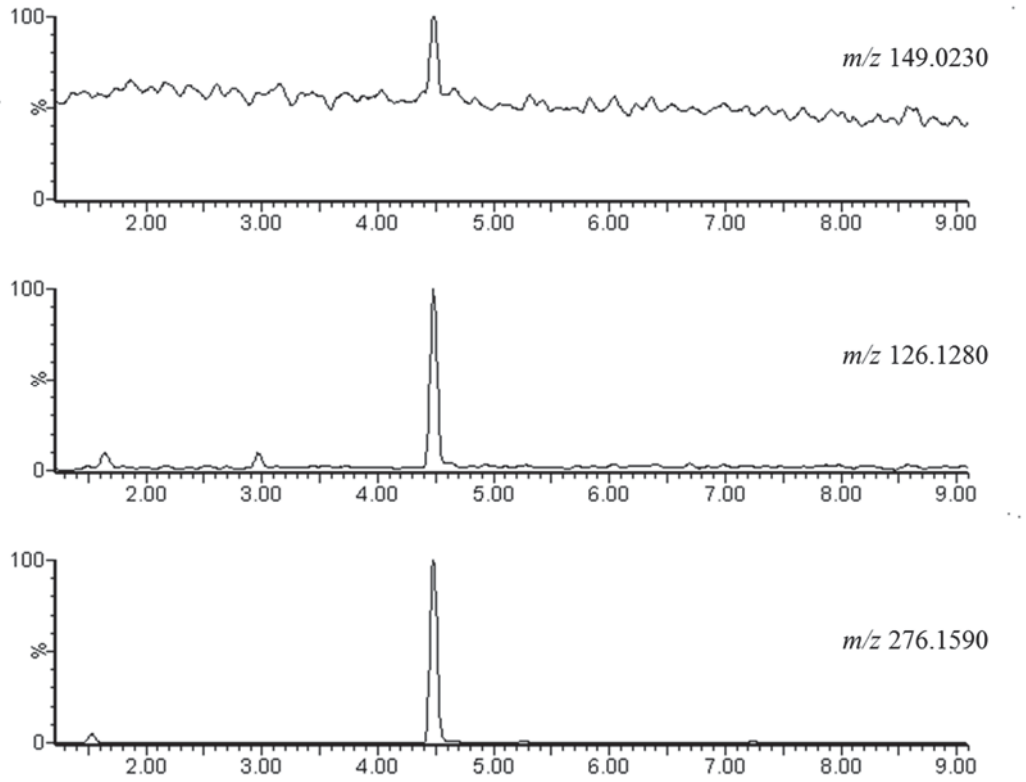


**Figure 4.9** EICs for common product ions for methylenedioxy-α-pyrrolidinophenone cathinones at a collision energy ramp of 10-40 eV.

## 4.4 Conclusion

A combination of top-down and bottom-up screening strategies were applied retrospectively to samples containing NPS acquired using DIA. Analytes of interest in all three samples were successfully detected independent of chromatographic methods and HRMS platform even when present at low concentrations (approximately 1 ng/mL for Case 1 and Case 2). KMD analysis provided rapid detection of precursor ions with analytes within the top ten positive hits for all samples. In addition, KMD analysis performed on compound lists generated from data mining algorithms reduced the number of positive hits and removed *m/z* values attributed to background noise with higher intensity values. Extraction of common product ions for bottom-up screening strategies also showed positive results for Case 1 and 3 with product ion

chromatographic peaks aligned with the precursor ion. For Case 2, however, negative results were observed for the extraction of common product ions for methylenedioxy-type cathinones and required reanalysis using targeted MS/MS to confirm the presence of characteristic NLs. This highlighted the fact that top-down and bottom-up screening strategies should be complementary techniques and cannot operate independently of each other. Furthermore, targeted MS/MS should be performed on *m/z* values that generate distinct chromatographic peaks after the application of these techniques to obtain analyte-specific spectra for structural elucidation followed by confirmation with a CRM if available.

## 4.5 References

1. Bidny S, Gago K, Chung P, Albertyn D, Pasin D. Simultaneous Screening and Quantification of Basic, Neutral and Acidic Drugs in Blood Using UPLC-QTOF-MS. *J Anal Toxicol*. 2017;41:181-95.
2. Pasin D, Bidny S, Fu S. Analysis of new designer drugs in post-mortem blood using high-resolution mass spectrometry. *J Anal Toxicol*. 2015;39:163-71.

# *CHAPTER 5:*

# *CONCLUSIONS AND*

# *RECOMMENDATIONS*

The recent proliferation of NPS has become problematic for forensic drug chemistry and toxicology laboratories that rely on the use of conventional targeted methods due to the lack of appropriate CRMs or mass spectral libraries. Biased non-targeted screening strategies involving the detection of novel analogues using HRMS based on the characteristics of known analogues has been identified as a potential technique to overcome the issues with detecting novel NPS.

Evaluation of mass defect-related top-down screening strategies revealed that the mass defect ranges of major NPS classes were comparable. Application of an Agilent Technologies post-acquisition MDF demonstrated that the efficacy of MDF was dependent on chromatographic conditions with fast elution gradients producing poor results due to inadequate chromatographic resolution whilst slow elution gradients produced optimal results. Therefore, the use of MDF should be restricted to samples acquired using slow elution gradients and, therefore, samples of interest may require a supplementary analysis with a non-routine method using appropriate conditions. Furthermore, the procedures detailed in this thesis are limited to use by laboratories which acquire data using an Agilent Technologies QTOF instrument due to the inconsistent functionality or absence of MDF in other vendor data processing software. Consequently, further research into the application of MDF for the detection of NPS is limited by the available data processing software. However, highlighting the potential of MDF to simplify HRMS data may prompt vendors to include or update MDF software to provide a more universally applicable technique that includes the ability to generate multiple MDFs simultaneously.

In addition to MDF, application of KMD theory to major NPS classes with a $CH_2$ normalisation produced characteristic KMD values specifically for subclasses where $CH_2$ homologues are prevalent. The in-house KMD analysis program, DefectDetect,

was developed as a proof-of-concept tool to interrogate numerical mass spectral data for KMD values of interest. The program was capable of rapidly interrogating numerical MS data from multiple files acquired by major HRMS platform vendors. The program's simple workflow and vendor-agnostic feature allows it to be used universally with minimal training. Furthermore, the numerical input format also allows this program to be applied to any sample regardless of chromatographic conditions, contrasting with MDF. Future developments such as the translation of DefectDetect to a conventional GUI that can import MS data, allow for the selection of multiple normalisations and utilise KMD value databases can provide a powerful data mining tool.

Evaluation of the differential analysis program, SIEVE® (Thermo Fisher Scientific, Bremen, Germany) demonstrated proof-of-concept for the detection of anomalous signals in authentic samples by comparison with control samples. In this case, however, the same matrix source was used for the preparation of controls and fortified samples providing near-identical samples which is unlikely in routine scenarios. For the analysis of authentic samples, the control sample should be a representative pooled biological matrix which may not be available. Similar to MDF, application of this technique may require supplementary software, typically at a cost. Since this type of software is typically intended for metabolomics purposes, identifying toxicologically relevant compounds in the quantity of data generated may be difficult.

Key product ions and NLs for hallucinogenic phenethylamines, synthetic cathinones and synthetic cannabinoids for bottom-up screening strategies using were established using LC-QTOF-MS. 2C-X and DOX derivatives exhibited common losses of $NH_3$, $CH_6N$ and $C_2H_9N$ and common product ions at *m/z* 164.0837, 149.0603 and 134.0732 for 2C-X derivatives and *m/z* 178.0994, 163.0754, 147.0804 and 135.0810 for DOX

derivatives. The 25X-NBOMe derivatives had characteristic product ion spectra with abundant ions at *m/z* 121.0654 and 91.0548, together with minor NLs corresponding to 2-methylanisole and 2-methoxybenzylamine and $C_9H_{14}NO$.

Traditional cathinones exhibited common losses of water (18.0106 Da) with product ion pairs *m/z* 117.0573/105.0699, 131.0730/105.0699, 145.0886/119.0855, 159.1043/133.1012, 149.0635/123.0605 and 161.0835/135.0804 indicative of phenyl-substituted and alkylamino derivatives. Methylenedioxycathinone-type cathinones did not exhibit common product ions but instead exhibited diagnostic NLs of 18.0106 ($H_2O$), 48.0211 ($CH_4O_2$) and 76.0160 Da ($C_2H_4O_3$). The presence of *m/z* 98.0964, 112.1121 or 126.1277 and NL of 71.0735 Da is indicative of cathinone derivatives containing a pyrrolidine ring such as the α-pyrrolidinophenone-type and methylenedioxy-α-pyrrolidinophenone-type cathinones. Product ions *m/z* 105.0699 and 119.0855 were indicative of unsubstituted and 4-methylphenyl α-pyrrolidinophenone-type cathinones, respectively, while *m/z* 149.0233 was indicative of methylenedioxy-α-pyrrolidinophenone-type cathinones.

Substituted naphthoylindole derived synthetic cannabinoids exhibited major product ions at *m/z* 155.0491, 169.0648, 183.0804 and *m/z* 185.0597 while 2-iodobenzoylindole and TMCP derivatives exhibited the product ion *m/z* 230.9301 and *m/z* 125.0961, respectively. Product ions corresponding to the linker-core-tail combination were observed at *m/z* 214.1226 (PICA), 232.1132 (5F-PICA), 215.1179 (PINACA), 233.1085 (5F-PINACA), 240.1383 (CHMICA), 241.1335 (CHMINACA), 252.0819 (FUBICA) and 253.0772 (FUBINACA). Furthermore, the presence of *m/z* 144.0444, 158.0600 and 145.0402 were indicative of the indole, 2-methylindole and indazole acylium cations.

Application of KMD analysis and bottom-up screening strategies were successfully

applied to three authentic forensic casework samples that were previously confirmed to contain NPS derivatives at low concentrations. KMD analysis provided rapid detection of precursor ions with analytes within the top ten positive hits for all samples Extraction of common product ions for bottom-up screening also showed positive results for Case 1 and 3 with product ion chromatographic peaks aligned with the precursor ion. For Case 2, however, negative results were observed for the extraction of common product ions for methylenedioxy-type cathinones and required reanalysis using targeted MS/MS to confirm the presence of characteristic NLs. It is recommended that the application of top-down and bottom-up screening strategies should be complementary, where the results of bottom-up strategies can support the results of top-down strategies and vice versa. If possible, samples should be re-analysed using DDA to elucidate possible NPS candidates.

The strategies developed here are proof-of-concept and provide foundation for further development of non-targeted screening for NPS. Due to the evolution of novel NPS analogues or classes, the development of non-targeted screening strategies is an on-going effort and should extend to other novel analogues of traditional NPS classes or other NPS classes such as synthetic opioids. Furthermore, this work focusses on the detection of parent molecules, however, it should be considered that metabolites are often targeted, particularly in assays performed using urine. Therefore, future research should also extend to the non-targeted screening of NPS metabolites, however, the CID pathways of known metabolites would need to be established and the metabolic pathways of new NPS would need to be investigated.

Another consideration is that particular NPS classes are known to exist at low concentrations in biological matrices, such as synthetic cannabinoids. Consequently, the detection of these analytes is limited by instrument sensitivity and often requires

the use of LRMS instrumentation which cannot perform non-targeted screening. It is believed that with advances in HRMS technology, the sensitivity of HRMS instruments will match sensitivities typical of LRMS instruments.

# *APPENDICES*

# APPENDIX A

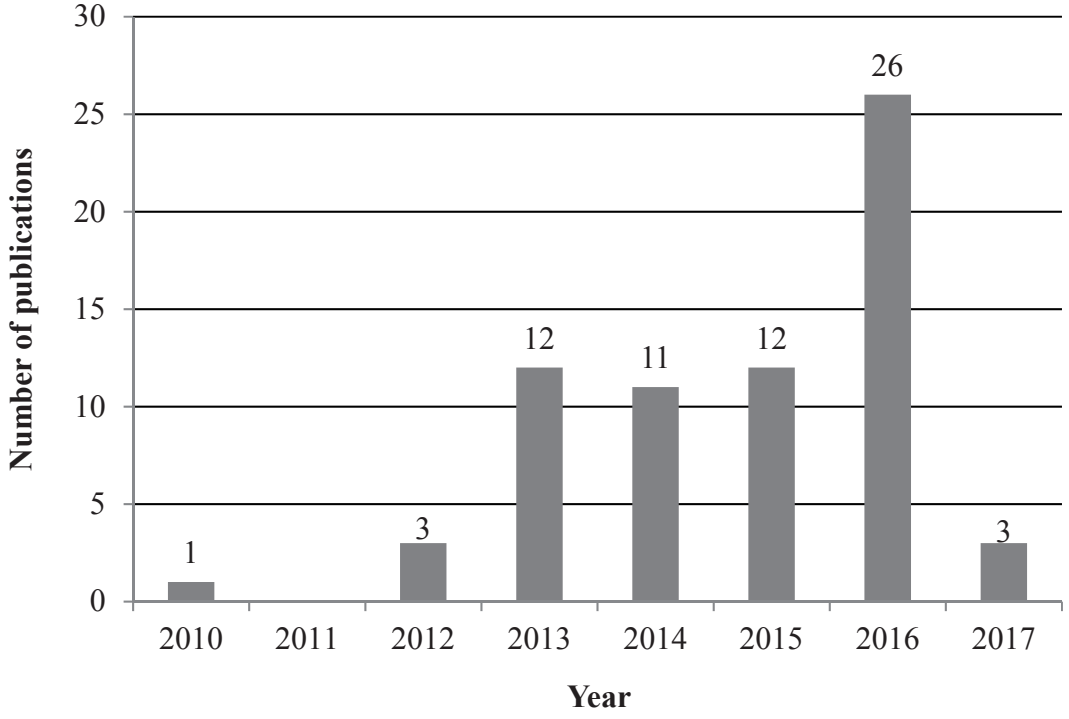


**Figure A.1** Number of original research articles related to the analysis of NPS using HRMS by publication year (sources: PubMed and ScienceDirect, accessed 01/02/2017).

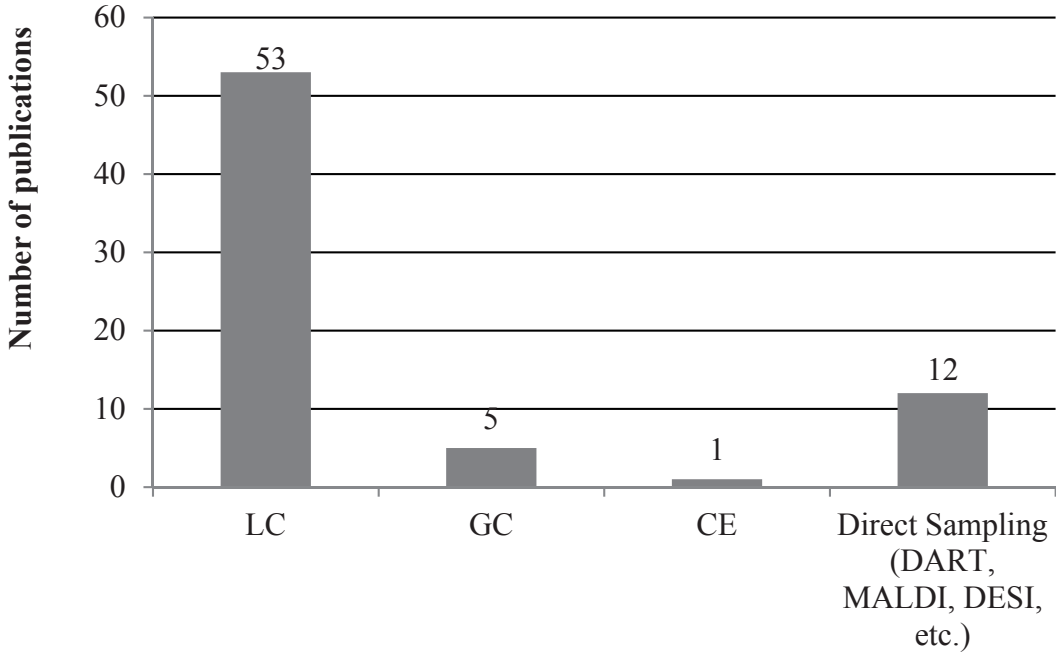


**Figure A.2** Number of original research articles reporting different chromatographic and direct sampling techniques. Note: some articles may have reported more than one separation or direct sampling technique (sources: PubMed and ScienceDirect, accessed 01/02/2017).

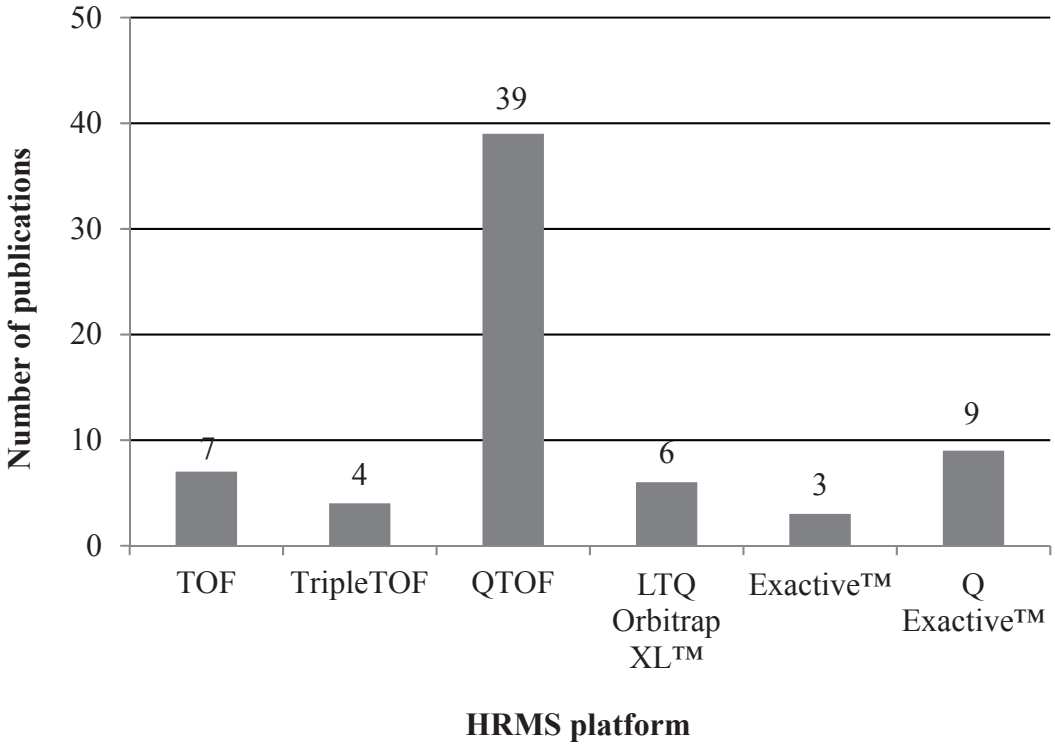


**Figure A.3** Number of original research articles reporting different HRMS platforms (sources: PubMed and ScienceDirect, accessed 01/02/2017).

**Table B.1** Formulae, structures, retention time, precursor ion data and mass error for selected hallucinogenic phenethylamines.

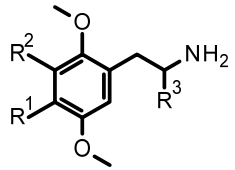


| Class | Analyte | Formula | $R^1$ | $R^2$ | $R^3$ | Retention time [min] | Monoisotopic Mass [M+H]+ | Experimental Mass [M+H]+ | Mass error [mDa (ppm)] |
|---|---|---|---|---|---|---|---|---|---|
| 2C-X | 2C-B | $C_{10}H_{15}BrNO_2$ | Br | H | H | 3.78 | 260.0281 | 260.0283 | 0.2 (0.9) |
| | 2C-B-$d_6$ [a] | $C_{10}H_9D_6BrNO_2$ | Br | H | H | 3.73 | 266.0657 | 266.0660 | 0.3 (-1.0) |
| | 2C-C | $C_{10}H_{15}ClNO_2$ | Cl | H | H | 3.41 | 216.0786 | 216.0790 | 0.4 (1.9) |
| | 2C-D | $C_{11}H_{18}NO_2$ | $CH_3$ | H | H | 3.29 | 196.1337 | 196.1331 | -0.6 (-3.1) |
| | 2C-E | $C_{12}H_{20}NO_2$ | $CH_2CH_3$ | H | H | 4.56 | 210.1494 | 210.1490 | -0.4 (-1.9) |
| | 2C-G | $C_{12}H_{20}NO_2$ | $CH_3$ | $CH_3$ | H | 4.17 | 210.1494 | 210.1492 | -0.2 (-1.0) |
| | 2C-H | $C_{10}H_{16}NO_2$ | H | H | H | 1.93 | 182.1181 | 182.1176 | -0.5 (-2.7) |
| | 2C-I | $C_{10}H_{15}INO_2$ | I | H | H | 4.42 | 308.0147 | 308.0149 | 0.2 (0.6) |
| | 2C-P | $C_{13}H_{22}NO_2$ | $CH_2CH_2CH_3$ | H | H | 5.83 | 224.1650 | 224.1650 | 0.0 (0.0) |
| | 2C-T | $C_{11}H_{18}NO_2S$ | $SCH_3$ | H | H | 3.37 | 228.1058 | 228.1054 | -0.4 (-1.8) |
| | 2C-T-4 | $C_{13}H_{22}NO_2S$ | $SCH(CH_3)_2$ | H | H | 5.23 | 256.1371 | 256.1360 | -1.1 (-4.3) |
| | 2C-T-7 | $C_{13}H_{22}NO_2S$ | $SCH_2CH_2CH_3$ | H | H | 5.63 | 256.1371 | 256.1353 | -0.8 (-3.1) |
| DOX | DOH | $C_{11}H_{18}NO_2$ | H | H | $CH_3$ | 2.48 | 196.1337 | 196.1338 | 0.1 (0.5) |
| | DOB | $C_{11}H_{17}BrNO_2$ | Br | H | $CH_3$ | 4.28 | 274.0442 | 274.0440 | -0.2 (-0.7) |
| | DOET | $C_{13}H_{22}NO_2$ | $CH_2CH_3$ | H | $CH_3$ | 5.09 | 224.1650 | 224.1655 | 0.5 (2.2) |
| | DOI | $C_{11}H_{17}INO_2$ | I | H | $CH_3$ | 4.89 | 322.0304 | 322.0304 | 0.0 (0.0) |
| | DOM | $C_{12}H_{20}NO_2$ | $CH_3$ | H | $CH_3$ | 3.86 | 210.1494 | 210.1492 | -0.2 (-1.0) |
| | DOT | $C_{12}H_{20}NO_2S$ | $SCH_3$ | H | $CH_3$ | 3.88 | 242.1214 | 242.1217 | 0.3 (1.2) |

[a] Deuterium located at the 2,5-methoxy groups (-$OCD_3$) for 2C-B-$d_6$

**Table B.1 (Cont'd)** Formulae, structures, retention time, precursor ion data and mass error for selected hallucinogenic phenethylamines.

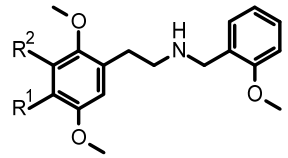

| Class | Analyte | Formula | $R^1$ | $R^2$ | Retention time [min] | Monoisotopic Mass $[M+H]^+$ | Experimental Mass $[M+H]^+$ | Mass error [mDa (ppm)] |
|---|---|---|---|---|---|---|---|---|
| 25X-NBOMe | 25B-NBOMe | $C_{18}H_{23}BrNO_3$ | Br | H | 7.45 | 380.0861 | 380.0862 | 0.1 (0.3) |
| | 25C-NBOMe | $C_{18}H_{23}ClNO_3$ | Cl | H | 7.18 | 336.1366 | 336.1368 | 0.2 (0.6) |
| | 25D-NBOMe | $C_{19}H_{26}NO_3$ | $CH_3$ | H | 7.18 | 316.1912 | 316.1914 | 0.2 (0.6) |
| | 25E-NB3OMe | $C_{20}H_{28}NO_3$ | $CH_2CH_3$ | H | 8.35 | 330.2069 | 330.2068 | -0.1 (-0.3) |
| | 25G-NBOMe | $C_{20}H_{28}NO_3$ | $CH_3$ | $CH_3$ | 7.92 | 330.2069 | 330.207 | 0.1 (0.3) |
| | 25H-NBOMe | $C_{18}H_{24}NO_3$ | H | H | 5.97 | 302.1756 | 302.1756 | 0.0 (0.0) |
| | 25I-NBOMe | $C_{18}H_{23}INO_3$ | I | H | 8.00 | 428.0722 | 428.0721 | -0.1 (-0.2) |
| | 25I-NBOMe-$d_9$ [b] | $C_{18}H_{14}D_9INO_3$ | I | H | 7.98 | 437.1289 | 437.1286 | -0.3 (-0.7) |
| | 25N-NBOMe | $C_{18}H_{23}N_2O_5$ | $NO_2$ | H | 6.18 | 347.1607 | 347.1608 | 0.1 (0.3) |
| | 25P-NBOMe | $C_{21}H_{30}NO_3$ | $CH_2CH_2CH_3$ | H | 9.4 | 344.2225 | 344.2225 | 0.0 (0.0) |
| | 25T-NBOMe | $C_{19}H_{26}NO_3S$ | $SCH_3$ | H | 7.11 | 348.1633 | 348.1634 | 0.1 (0.3) |
| | 25T2-NBOMe | $C_{20}H_{28}NO_3S$ | $SCH_2CH_3$ | H | 7.92 | 362.1790 | 362.1791 | 0.1 (0.3) |
| | 25T4-NBOMe | $C_{21}H_{30}NO_3S$ | $SCH(CH_3)_2$ | H | 8.73 | 376.1946 | 376.1947 | 0.1 (0.3) |
| | 25T4-NBOMe | $C_{21}H_{30}NO_3S$ | $SCH(CH_3)_2$ | H | 8.73 | 376.1946 | 376.1947 | 0.1 (0.3) |
| | 25T7-NBOMe | $C_{21}H_{30}NO_3S$ | $SCH_2CH_2CH_3$ | H | 8.99 | 376.1946 | 376.1943 | -0.3 (-0.8) |

[b] Deuterium located at the 2,5-methoxy groups and the 2-methoxy group (-$OCD_3$) of the *N*-(2-methoxybenzyl) moeity for 25I-NBOMe-$d_9$

**Table B.2** Product ion *m/z* values, chemical formulae/eliminated mass, mass error and intensity (% relative abundance) for selected 2C-X and DOX analytes.

| | **[M-NH$_3$+H]$^+$ (1, EE)** | | | | **[M-C$_2$H$_7$N+H]$^+$ (2, EE)** | | | | **[M-CH$_6$N+H]$^{+\bullet}$ (3, OE)** | | | |
|---|---|---|---|---|---|---|---|---|---|---|---|---|
| Analyte | *m/z* | Formula | Error [mDa (ppm)] | Intensity [%] | *m/z* | Formula | Error [mDa (ppm)] | Intensity [%] | *m/z* | Formula | Error [mDa (ppm)] | Intensity [%] |
| 2C-B | 243.0034 | $C_{10}H_{12}Br_2$ | 1.3 (5.3) | 85.2 | | | | | 227.9776 | $C_9H_9BrO_2$ | -1.0 (-4.4) | 94.2 |
| 2C-B-$d_6$ [a] | 249.0392 | $C_{10}H_6D_6BrO_2$ | -0.7 (-2.8) | 95.2 | | | | | 230.9966 | $C_9H_6D_3BrO_2$ | -0.9 (-3.9) | 43.7 |
| 2C-C | 199.0528 | $C_{10}H_{12}ClO_2$ | 0.2 (1.0) | 47.4 | | | | | 184.0286 | $C_9H_9ClO_2$ | -0.5 (-2.7) | 100 |
| 2C-D | 179.1082 | $C_{11}H_{15}O_2$ | 1.0 (5.6) | 50.5 | | | | | 164.0855 | $C_{10}H_{12}O_2$ | 1.8 (11.0) | 100 |
| 2C-E | 193.1235 | $C_{12}H_{17}O_2$ | 0.6 (3.1) | 62.6 | | | | | 178.0995 | $C_{11}H_{14}O_2$ | 0.1 (0.6) | 100 |
| 2C-G | 193.1233 | $C_{12}H_{17}O_2$ | 0.4 (2.1) | 5.1 | | | | | 178.1009 | $C_{11}H_{14}O_2$ | 1.5 (-8.4) | 100 |
| 2C-H | 165.0905 | $C_{10}H_{13}O_2$ | -1.1 (-6.7) | 21.2 | | | | | 150.0674 | $C_9H_{10}O_2$ | -1.0 (-4.7) | 100 |
| 2C-I | 290.9903 | $C_{10}H_{12}IO_2$ | 2.1 (7.2) | 100 | | | | | 275.9666 | $C_9H_9IO_2$ | 1.9 (6.9) | 96.7 |
| 2C-P | 207.1420 | $C_{13}H_{19}O_2$ | 3.5 (16.9) | 87.7 | | | | | 192.1188 | $C_{12}H_{16}O_2$ | 3.8 (19.8) | 100 |
| 2C-T | 211.0813 | $C_{11}H_{15}O_2S$ | 2.0 (-9.5) | 100 | | | | | 196.0579 | $C_{10}H_{12}O_2S$ | 2.1 (10.7) | 63.9 |
| 2C-T-4 | 239.1102 | $C_{13}H_{19}O_2S$ | -0.4 (-1.7) | 23.2 | | | | | 224.0883 | $C_{12}H_{16}O_2S$ | 1.2 (5.4) | 8.6 |
| 2C-T-7 | 239.1097 | $C_{13}H_{19}O_2S$ | -0.9 (-3.8) | 100 | | | | | 224.0871 | $C_{12}H_{16}O_2S$ | -0.8 (3.6) | 21.7 |
| DOH | 179.1079 | $C_{11}H_{15}O_2$ | 0.7 (3.9) | 17.1 | 151.0762 | $C_9H_{11}O_2$ | 0.3 (2.0) | 100 | 164.0844 | $C_{10}H_{12}O_2$ | 0.7 (4.3) | 79.1 |
| DOB | 257.0192 | $C_{11}H_{14}BrO_2$ | 1.5 (5.8) | 29.6 | 228.9872 | $C_9H_{10}BrO_2$ | 0.8 (3.5) | 73.7 | 241.9975 | $C_{10}H_{11}BrO_2$ | 3.2 (13.2) | 27.4 |
| DOET | 207.1370 | $C_{13}H_{19}O_2$ | -1.5 (-7.2) | 22.1 | 179.1072 | $C_{11}H_{15}O_2$ | -0.7 (-3.9) | 48.6 | 192.1135 | $C_{12}H_{16}O_2$ | -1.5 (-7.8) | 60.1 |
| DOI | 305.0017 | $C_{11}H_{14}IO_2$ | -2.2 (-7.2) | 13.1 | 276.9713 | $C_9H_{10}IO_2$ | -1.3 (-4.7) | 45.4 | 289.9793 | $C_{10}H_{11}IO_2$ | -1.1 (-3.8) | 41.6 |
| DOM | 193.1233 | $C_{12}H_{17}O_2$ | 0.4 (2.1) | 16.5 | 165.0900 | $C_{10}H_{13}O_2$ | -1.6 (-9.7) | 47.9 | 178.0973 | $C_{11}H_{14}O_2$ | -2.1 (-11.8) | 59.0 |
| DOT | 225.0966 | $C_{12}H_{17}O_2S$ | 1.7 (7.6) | 18.1 | 197.0614 | $C_{10}H_{13}O_2S$ | -2.2 (-11.2) | 19.5 | 210.0706 | $C_{11}H_{14}O_2S$ | 0.1 (0.5) | 26.3 |

[a] 2C-B-$d_6$ – [M-$CH_3D_3N$+H]$^{+\bullet}$(**3**, **OE**)

**Table B.2 (Cont'd)** Product ion *m/z* values, chemical formulae/eliminated mass, mass error and intensity (% relative abundance) for selected 2C-X and DOX analytes.

| | **$[M\text{-}C_2H_9N]^+$ (4, EE)** | | | | **$[M\text{-}NH_3R^1\text{+}H]^{+\bullet}$ (5, OE)** | | | | **$[M\text{-}CH_6NR^1\text{+}H]^+$ (6, EE)** | | | |
|---|---|---|---|---|---|---|---|---|---|---|---|---|
| Analyte | *m/z* | Formula | Error [mDa (ppm)] | Intensity [%] | *m/z* | Eliminated mass | Error [mDa (ppm)] | Intensity [%] | *m/z* | Eliminated mass | Error [mDa (ppm)] | Intensity [%] |
| 2C-B | 212.9533 | $C_8H_6BrO_2$ | -1.8 (-8.5) | 34.3 | 164.0838 | 95.9449 | 0.1 (0.6) | 50.0 | 149.0594 | 110.9683 | -0.9 (-6.0) | 30.8 |
| 2C-B-$d_6$ [b] | 212.9554 | $C_8H_6BrO_2$ | 0.3 (1.4) | 5.2 | 170.121 | 95.9449 | 0.2 (1.2) | 66.0 | 152.0784 | 113.9872 | -0.1 (-0.7) | 15.4 |
| 2C-C | 169.0059 | $C_8H_6ClO_2$ | 0.3 (0.6) | 22.9 | 164.0828 | 51.9954 | -0.9 (-5.5) | 28.2 | 149.0591 | 67.0188 | -1.2 (-8.1) | 8.1 |
| 2C-D | 149.0623 | $C_9H_9O_2$ | 2.1 (11.4) | 21.0 | 164.0855 | 32.0500 | 1.8 (11.0) | 100 | 149.0623 | 47.0734 | 2.1 (11.4) | 21.0 |
| 2C-E | 163.0769 | $C_{10}H_{11}O_2$ | 1.0 (3.7) | 21.3 | 164.0816 | 46.0657 | -2.1 (-12.8) | 3.7 | 149.0619 | 61.0891 | 1.6 (10.7) | 1.4 |
| 2C-G | 163.0776 | $C_{10}H_{11}O_2$ | 1.7 (8.0) | 28.7 | 178.1009 | 46.0657 | 1.5 (-8.4) | 100 | 163.0776 | 46.0657 | 1.7 (10.4) | 1.1 |
| 2C-H | 135.0452 | $C_8H_7O_2$ | 0.6 (1.5) | 25.6 | | | | | | | | |
| 2C-I | 260.9458 | $C_8H_6IO_2$ | 4.6 (16.1) | 18.9 | 164.0853 | 143.931 | 1.6 (9.8) | 28.7 | 149.0629 | 158.9544 | 2.6 (17.4) | 16.6 |
| 2C-P | 177.0922 | $C_{11}H_{13}O_2$ | 0.7 (1.7) | 7.0 | 164.0849 | 60.0813 | 1.2 (7.3) | 3.6 | 149.0621 | 75.1047 | 1.8 (12.1) | 3.3 |
| 2C-T | 181.0339 | $C_9H_9O_2S$ | 1.6 (6.6) | 24.6 | 164.0844 | 64.0221 | 0.7 (4.3) | 27.7 | 149.0608 | 79.0455 | 0.5 (3.4) | 9.5 |
| 2C-T-4 | | | | | 164.0834 | 92.0534 | -0.3 (1.8) | 12.9 | 149.0612 | 107.0768 | 0.9 (6.0) | 2.9 |
| 2C-T-7 | | | | | 164.0832 | 92.0534 | -0.5 (-3.0) | 16.9 | 149.0599 | 107.0768 | -0.4 (-2.7) | 4.3 |
| DOH | 149.0608 | $C_9H_9O_2$ | 0.6 (1.3) | 28.8 | | | | | | | | |
| DOB | 226.9707 | $C_9H_8BrO_2$ | 3.2 (14.1) | 6.3 | 178.1014 | 95.9448 | 2.0 (11.2) | 100 | 163.0766 | 33.0583 | 1.2 (7.4) | 21.0 |
| DOET | 177.0902 | $C_{11}H_{13}O_2$ | -1.3 (-9.6) | 100 | 178.0959 | 46.0657 | -3.5 (-19.7) | 24.9 | 163.0761 | 110.9688 | 0.7 (4.3) | 19.1 |
| DOI | 274.9547 | $C_9H_8IO_2$ | -2.2 (-9.5) | 49.6 | 178.0991 | 143.931 | -0.3 (-1.7) | 34.1 | 163.0744 | 61.0896 | -1.0 (-6.1) | 58.3 |
| DOM | 163.0749 | $C_{10}H_{11}O_2$ | -1.0 (-6.1) | 47.9 | 178.0973 | 32.0500 | -2.1 (-11.8) | 59.0 | 163.0749 | 158.955 | -1.0 (-6.1) | 47.9 |
| DOT | 195.0476 | $C_{10}H_{11}O_2S$ | -0.1 (-0.5) | 47.2 | 178.099 | 64.0220 | -0.4 (-2.2) | 63.6 | 163.0759 | 47.0740 | -0.3 (-1.2) | 61.1 |

[b] 2C-B-$d_6$ – $[M\text{-}C_2H_3D_6N]^+$ (**4**, **EE**), $[M\text{-}CH_3D_3NR^1\text{+}H]^+$ (**6**, **EE**)

**Table B.2 (Cont'd)** Product ion *m/z* values, chemical formulae/eliminated mass, mass error and intensity (% relative abundance) for selected 2C-X and DOX analytes.

| | **$[M\text{-}CH_5NOR^1+H]^{+\cdot}/[C_9H_9OR^2]^{+\bullet}$ (7, OE)** | | | | **$[C_{10}H_{11}O]^+$ (8, EE)** | | | | **$[C_9H_{11}O]^+$ (9, EE)** | | | |
|---|---|---|---|---|---|---|---|---|---|---|---|---|
| Analyte | *m/z* | Eliminated mass [Da] | Error [mDa (ppm)] | Intensity [%] | *m/z* | Eliminated mass [Da] | Error [mDa (ppm)] | Intensity [%] | *m/z* | Eliminated mass [Da] | Error [mDa (ppm)] | Intensity [%] |
| 2C-B | 134.0736 | 125.956 | 0.4 (3.0) | 26.3 | | | | | | | | |
| 2C-B-$d_6$ [c] | 138.0980 | 127.968 | 0.3 (2.2) | 12.3 | | | | | | | | |
| 2C-C | 134.0715 | 82.0065 | -1.7 (-12.7) | 6.5 | | | | | | | | |
| 2C-D | 134.0759 | 62.0611 | 2.7 (20.1) | 7.0 | | | | | | | | |
| 2C-E | 134.0715 | 76.0768 | -1.7 (-12.7) | 2.9 | | | | | | | | |
| 2C-G | 148.0907 | 62.0611 | 2.4 (16.4) | 4.2 | | | | | | | | |
| 2C-H | | | | | | | | | | | | |
| 2C-I | 134.0748 | 173.9421 | 1.6 (11.9) | 17.1 | | | | | | | | |
| 2C-P | 134.0770 | 90.0924 | 3.8 (28.3) | 1.7 | | | | | | | | |
| 2C-T | 134.0744 | 94.0332 | 1.2 (9.0) | 32.9 | | | | | | | | |
| 2C-T-4 | 134.0736 | 122.0645 | 0.4 (3.0) | 4.7 | | | | | | | | |
| 2C-T-7 | 134.0710 | 122.0645 | -2.2 (-16.4) | 11.0 | | | | | | | | |
| DOH | | | | | 147.0815 | 49.0533 | 1.1 (7.5) | 2.8 | | | | |
| DOB | | | | | 147.0826 | 126.9638 | 2.2 (15.0) | 2.5 | 135.0807 | 138.9632 | -0.3 (-2.2) | 6.3 |
| DOET | | | | | 147.0806 | 77.0846 | 0.2 (1.4) | 21.9 | 135.0791 | 89.0840 | -1.9 (-14.1) | 31.9 |
| DOI | | | | | 147.0789 | 174.9500 | -1.5 (-10.2) | 9.0 | 135.0804 | 186.9494 | -0.6 (-4.4) | 100 |
| DOM | | | | | 147.0802 | 63.0690 | -0.2 (-1.4) | 7.5 | 135.0802 | 75.0684 | -0.8 (-5.9) | 74.0 |
| DOT | | | | | 147.0800 | 95.0410 | -0.4 (-2.7) | 34.6 | 135.0808 | 107.0404 | -0.2 (-1.5) | 100 |

[c] 2C-B-$d_6$ – $[M\text{-}CH_3D_2NOR^1+H]^{+\bullet}/[C_9H_6D_4O]^{+\bullet}$ (**7**, **OE**)

**Table B.3** Product ion *m/z* values, chemical formulae/eliminated mass, mass error and intensity (% relative abundance) for selected 25X-NBOMe analytes.

| | **$[C_8H_9O]^+$ (10, EE)** | | | | | **$[C_7H_7]^+$ (11, EE)** | | | | |
|---|---|---|---|---|---|---|---|---|---|---|
| Analyte | *m/z* | Eliminated formula | Eliminated mass [Da] | Error [mDa (ppm)] | Intensity [%] | *m/z* | Eliminated formula | Eliminated mass [Da] | Error [mDa (ppm)] | Intensity [%] |
| 25B-NBOMe | 121.0647 | $C_{10}H_{14}BrNO_2$ | 259.0213 | -0.7 (-5.8) | 100 | 91.0544 | $C_{11}H_{16}BrNO_3$ | 289.0319 | -0.4 (-4.4) | 12.7 |
| 25C-NBOMe | 121.0649 | $C_{10}H_{14}ClNO_2$ | 215.0718 | 0.1 (0.8) | 100 | 91.0545 | $C_{11}H_{16}ClNO_3$ | 245.0824 | 0.3 (3.3) | 18.1 |
| 25D-NBOMe | 121.0654 | $C_{11}H_{17}NO_2$ | 195.1264 | 0.0 (0.0) | 100 | 91.0552 | $C_{12}H_{19}NO_3$ | 225.137 | 0.4 (4.4) | 16.4 |
| 25E-NBOMe | 121.0663 | $C_{12}H_{19}NO_2$ | 209.1421 | 1.5 (12.4) | 100 | 91.0577 | $C_{13}H_{21}NO_3$ | 239.1527 | 3.5 (38.4) | 10.5 |
| 25G-NBOMe | 121.0663 | $C_{12}H_{19}NO_2$ | 209.1421 | 0.9 (7.4) | 100 | 91.0577 | $C_{13}H_{21}NO_3$ | 239.1527 | 0.9 (9.9) | 14.0 |
| 25H-NBOMe | 121.0644 | $C_{10}H_{15}NO_2$ | 181.1108 | -1.0 (-8.3) | 100 | 91.0554 | $C_{11}H_{17}NO_3$ | 211.1214 | 0.6 (6.6) | 18.7 |
| 25I-NBOMe | 121.0661 | $C_{10}H_{14}INO_2$ | 307.0074 | 0.7 (5.8) | 100 | 91.056 | $C_{11}H_{16}INO_3$ | 337.018 | 1.2 (13.2) | 13.8 |
| 25I-NBOMe-$d_9$ [a] | 124.0841 | $C_{10}H_8D_6INO_2$ | 313.0446 | 0.5 (3.9) | 100 | 92.0616 | $C_{11}H_8D_8INO_3$ | 345.0677 | 1.1 (12.0) | 52.9 |
| 25N-NBOMe | 121.0673 | $C_{10}H_{14}N_2O_3$ | 226.0959 | 1.9 (15.7) | 100 | 91.0562 | $C_{11}H_{16}N_2O_5$ | 256.1065 | 1.4 (15.4) | 17.4 |
| 25P-NBOMe | 121.0663 | $C_{13}H_{21}NO_2$ | 223.1577 | 1.7 (7.7) | 100 | 91.0556 | $C_{14}H_{23}NO_3$ | 253.1683 | 0.8 (8.8) | 15.1 |
| 25T-NBOMe | 121.065 | $C_{11}H_{17}NO_2S$ | 227.0985 | -0.4 (-3.3) | 100 | 91.0543 | $C_{12}H_{19}NO_3S$ | 257.1091 | -0.5 (-5.5) | 14.4 |
| 25T2-NBOMe | 121.0636 | $C_{12}H_{19}NO_2S$ | 241.1142 | -1.8 (-14.9) | 100 | 91.0537 | $C_{13}H_{21}NO_3S$ | 271.1248 | -1.1 (-12.1) | 12.0 |
| 25T4-NBOMe | 121.0634 | $C_{13}H_{21}NO_2S$ | 255.1298 | -2.0 (-16.5) | 100 | 91.0532 | $C_{14}H_{23}NO_3S$ | 285.1404 | -1.6 (-17.6) | 10.3 |
| 25T7-NBOMe | 121.0641 | $C_{13}H_{21}NO_2S$ | 255.1298 | -1.3 (-14.3) | 100 | 91.0535 | $C_{14}H_{23}NO_3S$ | 285.1404 | -1.3 (-14.3) | 10.8 |

[a] 25I-NBOMe-$d_9$ – $[C_8H_6D_3O]^+$ (**10**, **EE**), $[C_7H_6D]^+$ (**11**, **EE**)

**Table B.3 (Cont'd)** Product ion m/z values, chemical formulae/eliminated mass, mass error and intensity (% relative abundance) for selected 25X-NBOMe analytes.

| | $[C_{10}H_{12}NO_2R^1R^2]^+$ (12, EE) | | | $[C_{10}H_{11}O_2R^1R^2]^+$ (13, EE) | | | $[C_9H_8O_2R^1R^2]^{+\bullet}$ (14, OE) | | |
|---|---|---|---|---|---|---|---|---|---|
| Analyte | *m/z* | Error [mDa (ppm)] | Intensity [%] | *m/z* | Error [mDa (ppm)] | Intensity [%] | *m/z* | Error [mDa (ppm)] | Intensity [%] |
| 25B-NBOMe | 258.0130 | 0.1 (0.4) | 0.3 | 243.0011 | -0.3 (-1.2) | 0.4 | 227.9782 | -0.5 (-5.8) | 0.2 |
| 25C-NBOMe | 214.0618 | -1.6 (-7.5) | 0.2 | 199.0512 | -1.3 (-6.5) | 0.8 | 184.0292 | 0.2 (1.1) | 0.3 |
| 25D-NBOMe | 194.1180 | 0.5 (2.6) | 1.4 | 179.1066 | 1.4 (7.8) | 8.5 | 164.0833 | -0.5 (-3.0) | 2.5 |
| 25E-NBOMe | 208.1357 | 2.0 (9.6) | 1.4 | 193.1242 | 1.4 (7.2) | 11.2 | 178.1008 | 1.3 (7.3) | 4.2 |
| 25G-NBOMe | 208.1349 | 1.2 (5.8) | 1.3 | 193.1232 | 1.0 (5.2) | 2.5 | 178.1005 | 1.0 (5.6) | 6.4 |
| 25H-N2.BOMe | | | | | | | | | |
| 25I-NBOMe | 305.9990 | 1.8 (5.9) | 0.5 | 290.9875 | 1.5 (5.2) | 1.0 | 275.9688 | 4.0 (14.5) | 0.4 |
| 25I-NBOMe-$d_9$ | | | | | | | | | |
| 25N-NBOMe | | | | | | | | | |
| 25P-NBOMe | 222.1510 | 1.7 (7.7) | 1.4 | 207.1399 | 2.1 (10.1) | 11.9 | 192.1162 | 1.1 (5.7) | 3.7 |
| 25T-NBOMe | 226.0901 | 1.5 (6.6) | 0.8 | 211.0799 | 1.3 (6.2) | 11.5 | 196.0566 | 0.7 (3.6) | 1.2 |
| 25T2-NBOMe | 240.1046 | -1.2 (-5.0) | 0.8 | 225.0943 | -1.0 (-4.4) | 14.3 | 210.0716 | -2.6 (-12.4) | 1.6 |
| 25T4-NBOMe | 254.1183 | -3.1 (-12.2) | 0.9 | 239.1085 | -1.4 (-5.9) | 10.6 | 224.0849 | -2.3 (10.3) | 0.6 |
| 25T7-NBOMe | 254.1250 | 3.6 (14.2) | 0.8 | 239.1093 | -0.6 (-2.5) | 15.1 | 224.0872 | 0.9 (4.0) | 0.6 |

**Table C.1** Formulae, structures, retention time, precursor ion data and mass error for selected hallucinogenic phenethylamines.

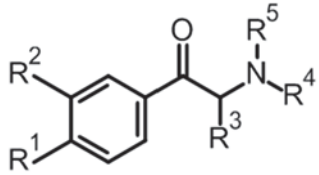


| Analyte | Precursor ion formula | $R^1$ | $R^2$ | $R^3$ | $R^4$ | $R^5$ | Retention time [min] | Monoisotopic mass $[M+H]^+$ | Experimental mass $[M+H]^+$ | Mass error [mDa (ppm)] |
|---|---|---|---|---|---|---|---|---|---|---|
| Cathinone | $C_9H_{12}NO$ | H | H | H | H | H | 0.99 | 150.0913 | 150.0918 | 0.5 (3.8) |
| Methcathinone | $C_{10}H_{14}NO$ | H | H | $CH_3$ | $CH_3$ | H | 1.17 | 164.1070 | 164.1074 | 0.4 (2.5) |
| Ethcathinone | $C_{11}H_{16}NO$ | H | H | $CH_3$ | $CH_2CH_3$ | H | 1.81 | 178.1226 | 178.1230 | 0.4 (2.0) |
| Mephedrone | $C_{11}H_{16}NO$ | $CH_3$ | H | $CH_3$ | $CH_3$ | H | 2.24 | 178.1226 | 178.1228 | 0.2 (0.9) |
| Buphedrone | $C_{11}H_{16}NO$ | H | H | $CH_2CH_3$ | $CH_3$ | H | 1.77 | 178.1226 | 178.1230 | 0.4 (2.0) |
| Pentedrone | $C_{12}H_{18}NO$ | H | H | $CH_2CH_2CH_3$ | $CH_3$ | H | 2.81 | 192.1383 | 192.1386 | 0.3 (1.6) |
| Flephedrone | $C_{10}H_{13}FNO$ | F | H | $CH_3$ | $CH_3$ | H | 1.44 | 182.0976 | 182.0980 | 0.4 (2.4) |
| Methedrone | $C11H_{16}NO_2$ | $OCH_3$ | H | $CH_3$ | $CH_3$ | H | 2.55 | 194.1176 | 194.1179 | 0.3 (1.8) |
| 4-MEC | $C_{12}H_{18}NO$ | $CH_3$ | H | $CH_3$ | $CH_2CH_3$ | H | 2.55 | 192.1383 | 192.1381 | -0.2 (-1.0) |
| 3,4-DMMC | $C_{12}H_{18}NO$ | $CH_3$ | $CH_3$ | $CH_3$ | $CH_3$ | H | 3.32 | 192.1383 | 192.1386 | 0.3 (1.6) |
| Metamfepramone | $C_{11}H_{16}NO$ | H | H | $CH_3$ | $CH_3$ | $CH_3$ | 1.24 | 178.1226 | 178.1228 | 0.2 (0.9) |
| Amfepramone | $C_{13}H_{20}NO$ | H | H | $CH_3$ | $CH_2CH_3$ | $CH_2CH_3$ | 1.87 | 206.1539 | 206.1541 | 0.2 (0.8) |

**Table C.1** Formulae, structures, retention time, precursor ion data and mass error for selected hallucinogenic phenethylamines.

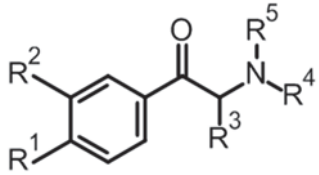


| Analyte | Precursor ion formula | $R^1$ | $R^2$ | $R^3$ | $R^4$ | $R^5$ | Retention time [min] | Monoisotopic mass $[M+H]^+$ | Experimental mass $[M+H]^+$ | Mass error [mDa (ppm)] |
|---|---|---|---|---|---|---|---|---|---|---|
| Amylone | $C_{10}H_{12}NO_3$ | $OCH_2O$ | | $CH_3$ | H | H | 0.90 | 194.0812 | 194.0814 | 0.2 (1.2) |
| Methylone | $C_{11}H_{14}NO_3$ | $OCH_2O$ | | $CH_3$ | $CH_3$ | H | 1.34 | 208.0968 | 208.0975 | 0.7 (3.3) |
| Ethylone | $C_{12}H_{16}NO_3$ | $OCH_2O$ | | $CH_3$ | $CH_2CH_3$ | H | 1.61 | 222.1125 | 222.1127 | 0.2 (1.0) |
| Butylone | $C_{12}H_{16}NO_3$ | $OCH_2O$ | | $CH_2CH_3$ | $CH_3$ | H | 2.01 | 222.1125 | 222.1132 | 0.7 (3.3) |
| Pentylone | $C_{13}H_{18}NO_3$ | $OCH_2O$ | | $CH_2CH_3CH_3$ | $CH_3$ | H | 3.08 | 236.1281 | 236.1286 | 0.5 (2.0) |
| PPP | $C_{13}H_{18}NO$ | H | H | $CH_3$ | $(CH_2)_4$ | | 1.67 | 204.1383 | 204.1382 | -0.1 (-0.5) |
| MePPP | $C_{14}H_{20}NO$ | $CH_3$ | H | $CH_3$ | $(CH_2)_4$ | | 2.88 | 218.1539 | 218.1540 | -0.1 (-0.3) |
| MPBP | $C_{15}H_{22}NO$ | $CH_3$ | H | $CH_2CH_3$ | $(CH_2)_4$ | | 3.62 | 232.1696 | 232.1697 | 0.1 (0.5) |
| α-PVP | $C_{15}H_{22}NO$ | H | H | $CH_2CH_3CH_3$ | $(CH_2)_4$ | | 3.35 | 232.1696 | 232.1698 | 0.2 (0.9) |
| Pyrovalerone | $C_{16}H_{24}NO$ | $CH_3$ | H | $CH_2CH_3CH_3$ | $(CH_2)_4$ | | 4.76 | 246.1852 | 246.1852 | 0.0 (0.0) |
| MDPPP | $C_{14}H_{18}NO_3$ | $OCH_2O$ | | $CH_3$ | $(CH_2)_4$ | | 1.94 | 248.1281 | 248.1284 | 0.3 (1.1) |
| MDPBP | $C_{15}H_{20}NO_3$ | $OCH_2O$ | | $CH_2CH_3$ | $(CH_2)_4$ | | 2.61 | 262.1438 | 262.1448 | 1.0 (3.9) |
| MDPV | $C_{16}H_{22}NO_3$ | $OCH_2O$ | | $CH_2CH_3CH_3$ | $(CH_2)_4$ | | 3.69 | 276.1594 | 276.1602 | 0.8 (2.8) |

**Table C.2** Product ion m/z values, mass error and intensity (% relative abundance) for selected traditional cathinones.

| | **[M-$H_2O$+H]$^+$ (1, EE)** | | | **[M-$H_2OR_3$+H]$^{+\bullet}$ (2, OE)** | | | **[M-$H_3OR_3$+H]$^+$ (3, EE)** | | | **[M-$H_2OR_4$+H]$^{+\bullet}$ (4, OE)** | | |
|---|---|---|---|---|---|---|---|---|---|---|---|---|
| Analyte | *m/z* | Error [mDa (ppm)] | Intensity [%] | *m/z* | Error [mDa (ppm)] | Intensiy [%] | *m/z* | Error [mDa (ppm)] | Intensity [%] | *m/z* | Error [mDa (ppm)] | Intensity [%] |
| Cathinone | 132.0806 | -0.2 (-1.3) | 51.7 | 117.0568 | -0.5 (-4.3) | 100 | | | | | | |
| Methcathinone | 146.0966 | 0.2 (1.2) | 41.7 | 131.0724 | -0.6 (-4.2) | 100 | 130.0654 | 0.3 (2.1) | 19.1 | | | |
| Ethcathinone | 160.1114 | -0.7 (-4.2) | 39.0 | 145.0925 | 3.9 (22.3) | 6.5 | 144.0777 | -3.1 (-21.5) | 3.0 | 131.0735 | 0.5 (4.2) | 100.0 |
| Mephedrone | 160.1121 | 0.0 (0.0) | 63.6 | 145.0890 | 0.4 (2.8) | 100 | 144.0806 | -0.2 (-1.2) | 20.5 | | | |
| Buphedrone | 160.1124 | 0.3 (2.0) | 41.9 | 131.0725 | -0.5 (-3.5) | 100 | 130.0654 | 0.3 (2.1) | 19.0 | | | |
| Pentedrone | 174.1275 | -0.2 (-1.3) | 33.1 | 131.0745 | 1.5 (11.9) | 25.5 | 130.0649 | -0.2 (-1.8) | 9.7 | | | |
| Flephedrone | 164.0876 | 0.6 (3.7) | 59.0 | 149.0637 | 0.2 (1.2) | 100 | 148.0570 | 1.3 (8.8) | 12.8 | | | |
| Methedrone | 176.1073 | 0.3 (1.8) | 62.0 | 161.0836 | 0.1 (0.5) | 100 | 160.0773 | 1.6 (10.0) | 4.0 | | | |
| 4-MEC | 174.1270 | -0.7 (-4.2) | 50.2 | 159.1037 | -0.6 (-3.5) | 29.8 | 158.0957 | -0.7 (-4.6) | 2.7 | 145.0880 | -0.6 (-4.2) | 100.0 |
| 3,4-DMMC | 174.1280 | 0.3 (1.6) | 44.5 | 159.1046 | 0.3 (2.2) | 100 | 158.0964 | 0.0 (0.0) | 14.8 | | | |
| Metamfepramone | | | | | | | | | | | | |
| Amfepramone | | | | | | | | | | | | |

| | **[M-$H_3OR_4$+H]$^+$ (5, EE)** | | | **[$C_8H_5NR_1R_2$]$^{+\bullet}$ (6, OE)** | | | **[$C_8H_7R_1R_2$]$^+$ (7, EE)** | | | **[$C_7H_5O$]$^+$ (8, EE)** | | |
|---|---|---|---|---|---|---|---|---|---|---|---|---|
| Cathinone | | | | | | | 105.0699 | 0.0 (0.0) | 49.4 | 105.0314 | -2.1 (-20.0) | 2.4 |
| Methcathinone | | | | | | | 105.0696 | -0.3 (-2.7) | 22.9 | 105.0304 | -3.1 (-29.5) | 1.3 |
| Ethcathinone | 130.0655 | 0.4 (2.9) | 29.1 | 117.0591 | 1.8 (15.5) | 49.5 | 105.0714 | 1.5 (14.6) | 27.1 | 105.0321 | -1.4 (-13.4) | 7.5 |
| Mephedrone | | | | | | | 119.0840 | -1.5 (-12.9) | 20.0 | | | |
| Buphedrone | | | | 117.0568 | -0.5 (-4.3) | 9.8 | | | | 105.0334 | -0.1 (-0.9) | 8.0 |
| Pentedrone | | | | 117.0587 | 1.4 (12.0) | 10.5 | | | | 105.0342 | 0.7 (6.8) | 6.8 |
| Flephedrone | | | | | | | 123.0604 | -0.1 (-0.5) | 19.7 | | | |
| Methedrone | | | | | | | 135.0817 | 1.3 (9.4) | 25.4 | | | |
| 4-MEC | 144.0805 | -0.3 (-1.9) | 45.3 | 131.0746 | 1.7 (12.7) | 25.4 | 119.0852 | -0.3 (-2.7) | 32.7 | | | |
| 3,4-DMMC | | | | | | | 133.1010 | -0.2 (-1.3) | 8.1 | | | |
| Metamfepramone | | | | | | | 105.0702 | 0.3 (3.1) | 100 | | | |
| Amfepramone | | | | | | | 105.0700 | 0.1 (1.2) | 100 | | | |

**Table C..3** Product ion m/z values, mass error and intensity (% relative abundance) for selected 3,4-methylenedioxy-type cathinones.

| | **[M-$H_2O$+H]$^+$ (9, EE)** | | | **[M-$H_2OR^1$+H]$^+$ (10, EE)** | | | **[M-$CH_4O_2$+H]$^+$ (11, EE)** | | | **[M-$C_2H_4O_3$+H]$^+$ (12, EE)** | | |
|---|---|---|---|---|---|---|---|---|---|---|---|---|
| Analyte | *m/z* | Error [mDa (ppm)] | Intensity [%] | *m/z* | Error [mDa (ppm)] | Intensity [%] | *m/z* | Error [mDa (ppm)] | Intensity [%] | *m/z* | Error [mDa, (ppm)] | Intensity [%] |
| Amylone | 176.0699 | -0.7 (-4.0) | 6.8 | | | | 146.0597 | -0.3 (-2.4) | 100 | 118.0654 | 0.3 (2.3) | 95.3 |
| Methylone | 190.0186 | -0.6 (-3.2) | 9.6 | 175.0627 | -0.1 (-0.5) | 4.4 | 160.0755 | -0.2 (-1.2) | 100 | 132.0807 | -0.1 (-0.6) | 40.9 |
| Ethylone | 204.1020 | 0.1 (0.1) | 18.6 | 189.0785 | 0.1 (0.4) | 5.0 | 174.0914 | 0.1 (0.3) | 100 | 146.0959 | -0.5 (-3.6) | 21.8 |
| Butylone | 204.1015 | -0.4 (2.0) | 16.6 | 175.0626 | -0.2 (1.0) | 31.0 | 174.0913 | 0.0 (0.0) | 100 | 146.0958 | -0.6 (-4.3) | 23.8 |
| Pentylone | 218.1168 | -0.8 (-3.5) | 21.5 | 175.0678 | 5.0 (28.6) | 40.3 | 188.1064 | -0.6 (-3.2) | 100 | 160.1112 | -0.9 (-5.5) | 15.4 |

**Table C.4** Product ion m/z values, mass error and intensity (% relative abundance) for selected pyrrolidino-type cathinones.

| | **[M-$C_4H_9N$+H]$^+$ (13, EE)** | | | **[$C_7H_4OR^1$]$^+$ (14, EE)** | | | **[$C_5H_9NR^2$]$^+$ (15, EE)** | | | **[$C_8H_8R^1$]$^+$ ( (16, EE)** | | |
|---|---|---|---|---|---|---|---|---|---|---|---|---|
| Analyte | *m/z* | Error [mDa (ppm)] | Intensity [%] | *m/z* | Error [mDa (ppm)] | Intensity [%] | *m/z* | Error [mDa (ppm)] | Intensity [%] | *m/z* | Error [mDa (ppm)] | Intensity [%] |
| PPP[a] | 133.0646 | -0.2 (-1.5) | 45.8 | | | | 98.0972 | 0.8 (8.0) | 46.1 | 105.0699 | 0.0 (0.0) | 100 |
| MePPP[b] | 147.0801 | -0.3 (-2.3) | 78.0 | | | | 98.0971 | 0.7 (6.9) | 52.4 | 119.0851 | -0.4 (-3.6) | 100 |
| MPBP[c] | 161.0955 | -0.6 (-3.7) | 57.5 | 119.0488 | -0.3 (-2.9) | 24.4 | 112.1117 | -0.4 (-3.4) | 36.3 | 105.0697 | -0.2 (-1.7) | 100 |
| Alpha-PVP[d] | 161.0958 | -0.3 (-1.8) | 44.8 | 105.0336 | 0.1 (1.0) | 44.3 | 126.1274 | -0.3 (-2.6) | 54.9 | | | |
| Pyrovalerone[e] | 175.1108 | -0.9 (-5.4) | 41.4 | 119.0485 | -0.6 (-5.4) | 25.9 | 126.1268 | -0.9 (-7.4) | 28.4 | 105.0695 | -0.4 (-3.6) | 100 |
| Precursor % rel. int. (a) 72.2 (b) 63.4 (c) 42.5 (d) 100 (e) 37.4 | | | | | | | | | | | | |

**Table C.5** Product ion m/z values, mass error and intensity (% relative abundance) for selected 3,4-methylenedioxypyrrolidino-type cathinones.

| | **[M-$C_4H_9N$+H]$^+$ (17, EE)** | | | **[$C_8H_5O_2R^1$]$^+$ (18, EE)** | | | **[$C_8H_5O_3$]$^+$ (19, EE)** | | | **[$C_5H_9NR^1$]$^+$ (20, EE)** | | |
|---|---|---|---|---|---|---|---|---|---|---|---|---|
| Analyte | *m/z* | Error [mDa (ppm)] | Intensity [%] | *m/z* | Error [mDa (ppm)] | Intensity [%] | *m/z* | Error [mDa (ppm)] | Intensity [%] | *m/z* | Error [mDa (ppm)] | Intensity [%] |
| MDPPP[a] | 177.0547 | 0.1 (0.5) | 29.4 | 147.0441 | 0.0 (0.0) | 73.2 | | | | 98.0966 | 0.2 (1.8) | 100 |
| MDPBP[b] | 191.0698 | -0.5 (-2.5) | 65.5 | 161.0597 | 0.0 (0.0) | 100 | 149.0228 | -0.5 (-3.5) | 34.6 | 112.1119 | -0.2 (-1.6) | 93.6 |
| MDPV[c] | 205.0858 | -0.1 (-0.6) | 69.2 | 175.0751 | -0.3 (-1.5) | 89.8 | 149.0231 | -0.2 (-1.5) | 41.7 | 126.1275 | -0.2 (-1.8) | 100 |
| Precursor % rel. int. (a) 77.9 (b) 74.5 (c) 88.8 | | | | | | | | | | | | |

## APPENDIX D

**Table D.1** Abbreviations and IUPAC names for selected synthetic cannabinoids.

| Abbreviation | IUPAC Name |
|---|---|
| 5F-AB-PINACA | *N*-(1-amino-3-methyl-1-oxo-2-butanyl)-1-(5-fluoropentyl)-1*H*-indazole-3-carboxamide |
| 5F-ADBICA | *N*-(1-amino-3,3-dimethyl-1-oxo-2-butanyl)-1-(5-fluoropentyl)-1*H*-indole-3-carboxamide |
| 5F-APICA | *N*-(1-adamantanyl)-1-(5-fluoropentyl)-1*H*-indole-3-carboxamide |
| 5F-CUMYL-PINACA | 1-(5-fluoropentyl)-*N*-(2-phenyl-2-propanyl)-1*H*-indazole-3-carboxamide |
| 5F-MMB-PICA | Methyl *N*-{[1-(5-fluoropentyl)-1*H*-3-indolyl]carbonyl}valinate |
| 5F-MMB-PINACA | Methyl *N*-{[1-5-fluoropentyl)-1*H*-3-indazolyl]carbonyl}valinate |
| 5F-PB-22 | 8-quinolinyl 1-(5-fluoropentyl)-1*H*-indole-3-carboxylate |
| AB-CHMINACA | *N*-(1-amino-3-methyl-1-oxo-2-butanyl)-1-(cyclohexylmethyl)-1*H*-indazole-3-carboxamide |
| AB-FUBINACA | *N*-(1-amino-3-methyl-1-oxo-2-butanyl)-1-(4-fluorobenzyl)-1*H*-indazole-3-carboxamide |
| AB-PINACA | *N*-(1-amino-3-methyl-1-oxo-2-butanyl)-1-pentyl-1*H*-indazole-3-carboxamide |
| ADB-CHMINACA | *N*-(1-amino-3,3-dimethyl-1-oxo-2-butanyl)-1-(cyclohexylmethyl)-1*H*-indazole-3-carboxamide |
| ADB-FUBINACA | *N*-(1-amino-3,3-dimethyl-1-oxo-2-butanyl)-1-(4-fluorobenzyl)-1*H*-indazole-3-carboxamide |
| ADBICA | *N*-(1-amino-3,3-dimethyl-1-oxo-2-butanyl)-1-pentyl-1*H*-indole-3-carboxamide |
| AM-1241 | (2-iodo-5-nitrophenyl){1-[(1-methyl-2-piperidinyl)methyl]-1*H*-3-indolyl}methanone |
| AM-1248 | 1-adamantanyl{1-[(1-methyl-2-piperidinyl)methyl]-1*H*-3-indolyl}methanone |
| AM-2201 | [1-(5-fluoropentyl)-1*H*-3-indolyl](1-naphthyl)methanone |
| AM-2233 | (2-iodophenyl){1-[(1-methyl-2-piperidinyl)methyl]-1*H*-3-indolyl}methanone |
| AM-694 | [1-(5-fluoropentyl)-1*H*-3-indolyl](2-iodophenyl)methanone |
| APICA | *N*-(1-adamantanyl)-1-pentyl-1*H*-indole-3-carboxamide |
| BB-22 | 8-quinolinyl 1-(cyclohexylmethyl)-1*H*-indole-3-carboxylate |
| FUB-144 | [1-(4-fluorobenzyl)-1*H*-3-indolyl](2,2,3,3-tetramethylcyclopropyl)methanone |
| FUB-NPB-22 | 8-quinolinyl 1-(4-fluorobenzyl)-1*H*-indazole-3-carboxylate |

**Table D.1 (Cont'd)** Abbreviations and IUPAC names for selected synthetic cannabinoids.

| Abbreviation | IUPAC Name |
|---|---|
| JWH-007 | (2-methyl-1-pentyl-1*H*-3-indolyl)(1-naphthyl)methanone |
| JWH-015 | (2-methyl-1-propyl-1*H*-3-indolyl)(1-naphthyl)methanone |
| JWH-016 | (1-butyl-2-methyl-1*H*-3-indolyl)(1-naphthyl)methanone |
| JWH-018 | 1-naphthyl(1-pentyl-1*H*-3-indolyl)methanone |
| JWH-019 | (1-hexyl-1*H*-3-indolyl)(1-naphthyl)methanone |
| JWH-020 | (1-heptyl-1*H*-3-indolyl)(1-naphthyl)methanone |
| JWH-030 | 1-naphthyl(1-pentyl-1*H*-3-pyrrolyl)methanone |
| JWH-073 | (1-butyl-1*H*-3-indolyl)(1-naphthyl)methanone |
| JWH-081 | (4-methoxy-1-naphthyl)(1-pentyl-1*H*-3-indolyl)methanone |
| JWH-098 | (4-methoxy-1-naphthyl)(2-methyl-1-pentyl-1*H*-3-indolyl)methanone |
| JWH-122 | (4-methyl-1-naphthyl)(1-pentyl-1*H*-3-indolyl)methanone |
| JWH-200 | {1-[2-(4-morpholinyl)ethyl]-1*H*-3-indolyl}(1-naphthyl)methanone |
| JWH-203 | 2-(2-chlorophenyl)-1-(1-pentyl-1*H*-3-indolyl)ethanone |
| JWH-210 | (4-ethyl-1-naphthyl)(1-pentyl-1*H*-3-indolyl)methanone |
| JWH-250 | 2-(2-methoxyphenyl)-1-(1-pentyl-1*H*-3-indolyl)ethanone |
| JWH-307 | [5-(2-fluorophenyl)-1-pentyl-1*H*-3-pyrrolyl](1-naphtyl)methanone |
| MDMB-CHMICA | Methyl *N*-{[1-(cyclohexylmethyl)-1*H*-3-indolyl]carbonyl}-3-methyl-L-valinate |
| MDMB-FUBINACA | Methyl *N*-{[1-(4-fluorobenzyl)-1*H*-3-indazolyl]carbonyl}-3-methylvalinate |
| MDMB-PINACA | Methyl *N*-[(1-pentyl-1*H*-3-indazolyl)carbonyl]-3-methylvalinate |
| MMB-FUBINACA | Methyl *N*-{[1-(4-fluorobenzyl)-1*H*-3-indazolyl]carbonyl}valinate |
| UR-144 | (1-pentyl-1*H*-3-indolyl)(2,2,3,3-tetramethylcyclopropyl)methanone |
| XLR-11 | [1-(5-fluoropentyl)-1*H*-3-indolyl](2,2,3,3-tetramethylcyclopropyl)methanone |